

# Rh(II)-catalyzed Cyclopropanation of Aromatic Heterocycles and its Application to the Total Synthesis of Natural Product Derivatives

Dissertation

Zur Erlangung des Doktorgrades

Dr. rer. nat.

der Fakultät für Chemie und Pharmazie

der Universität Regensburg



vorgelegt von

**Verena Lehner**

aus Viechtach

**Regensburg 2017**

Die Arbeit wurde angeleitet von:

Prof. Dr. O. Reiser

Promotionsgesuch eingereicht am:

30.08.2017

Promotionskolloquium am:

28.09.2017

Prüfungsausschuss:

Vorsitz: Prof. Dr. Jörg Heilmann

1. Gutachter: Prof. Dr. Oliver Reiser

2. Gutachter: PD Dr. Sabine Amslinger

3. Gutachter: Prof. Dr. Arno Pfitzner

Der experimentelle Teil der vorliegenden Arbeit wurde in der Zeit von November 2013 bis Januar 2017 unter der Leitung von Prof. Dr. O. Reiser am Lehrstuhl für Organische Chemie der Universität Regensburg und von Januar 2014 bis April 2014 an der Emory University (USA) bei Prof. Dr. H. M. L. Davies angefertigt.

Herrn Prof. Dr. Oliver Reiser möchte ich herzlich für die Themenstellung, die anregenden Diskussionen, die stete Unterstützung, sowie die Ermöglichung des Auslandsaufenthaltes in Atlanta danken.





*Für meine Oma*



# Table of contents

<b>A Introduction .....</b>	<b>1</b>
1 Introduction - Applications of aromatic heterocycles .....	1
2 Applications of cyclopropanated furan derivatives .....	3
3 Applications of cyclopropanated pyrrole derivatives .....	6
4 Applications of cyclopropanated indole derivatives.....	9
5 References .....	12
<b>B Main part.....</b>	<b>17</b>
1 Cyclopropanation of aromatic heterocycles .....	17
1.1 Introduction – Classification of diazo ester .....	17
1.2 Chiral rhodium(II) tetracarboxylates catalysts - Synthesis and Application .....	22
1.3 Asymmetric cyclopropanation of methyl furan-2-carboxylate ( <b>19</b> ) .....	24
1.4 Asymmetric cyclopropanation of furan derivatives and thiophene .....	32
1.5 Asymmetric cyclopropanation of pyrroles.....	35
1.6 Asymmetric cyclopropanation of <i>N</i> -tosyl pyrrole ( <b>113c</b> ).....	41
1.7 Asymmetric cyclopropanation of <i>N</i> -tosyl indole <b>125</b> .....	44
1.8 Conclusion and outlook .....	46
2 Cyclopropane <b>119c</b> as precursor for the synthesis of a homo- $\beta$ -proline analogue.....	47
2.1 Introduction – Pyrrolidines as catalysts and bioactive compounds .....	47
2.2 Enantioselective synthesis of homo- $\beta$ -proline – State of the art.....	49
2.3 Synthesis of homo- $\beta$ -proline analogue <b>147</b> .....	51
2.4 Conclusion and Outlook .....	54
3 Cyclopropanes <b>98a/b</b> as precursors for the synthesis of paraconic acid derivatives.....	55
3.1 Introduction – $\gamma$ -Butyrolactone: a privileged motif in natural products and drugs.....	55
3.2 Literature syntheses of paraconic acids – Utilization of donor-acceptor cyclopropanes .....	57
3.3 Preliminary studies on the synthesis of paraconic acid derivatives <b>176a</b> and <b>179a</b> ...	59
3.4 Synthesis of novel paraconic acid derivatives .....	62
3.5 Biological evaluation .....	64
3.6 Conclusion .....	66
4 References .....	67
<b>C Summary .....</b>	<b>76</b>
<b>D Zusammenfassung .....</b>	<b>78</b>
<b>E Experimental part.....</b>	<b>80</b>

1 General information.....	80
2 Synthesis of starting materials and catalysts .....	81
3 Synthesis of Cyclopropanes.....	83
3.1 General procedures .....	83
3.2 Synthesis of cyclopropane <b>98a</b> with 0.001 mol% Rh <sub>2</sub> ( <i>S</i> -TCPTTL) <sub>4</sub> .....	84
3.3 Characterization .....	85
3.4 Kinetic resolution experiments .....	99
4 Synthesis of homo-β-proline derivative <b>147</b> .....	101
5 Synthesis of paraconic acid derivatives .....	104
5.1 Enantioselective synthesis of paraconic acid derivatives <b>176a</b> and <b>179a</b> .....	104
5.2 Racemic synthesis of paraconic acid derivatives <b>179b</b> , <b>180a</b> and <b>181b</b> .....	109
6 References .....	113
<b>F Appendix.....</b>	<b>114</b>
1 <sup>1</sup> H and <sup>13</sup> C NMR spectra .....	114
2 Chiral HPLC data .....	145
3 X-ray crystallography data .....	168
4. Curriculum vitae .....	219
<b>G. Acknowledgments – Danksagung .....</b>	<b>221</b>
<b>H. Declaration.....</b>	<b>223</b>

## Abbreviations

Å	angstrom	EWG	electron-withdrawing group
Ac	acetyl	g	gram(s)
AIBN	aza- <i>isobutyronitrile</i>	GABA	$\gamma$ -aminobutyric acid
Ar	aryl	h	hour(s)
atm.	Atmosphere	HPLC	high-performance liquid chromatography
BAIB	(bisacetoxyiodo)benzene	HRMS	high-resolution mass spectrometry
Boc	<i>tert</i> -butoxycarbonyl	Hz	Hertz
brine	saturated NaCl solution	<i>i</i> Pr	<i>iso</i> -propyl
Bu	butyl	IR	infrared
BuLi	butyl lithium	L	liter; ligand
°C	degrees Celsius	M	molar
calcd.	calculated	$\mu$	micro
cm <sup>-1</sup>	wavenumber(s)	max	maximum
d	day(s)	Me	methyl
DBU	1,8-diazabicyclo[5.4.0]undec-7-ene	MeOH	methanol
DCM	dichloromethane	MHz	megahertz
DMF	dimethyl formamide	min	minute(s)
DMS	dimethyl sulfide	mL	milliliter
DMSO	dimethylsulfoxide	mm	millimeter
<i>dr</i>	diastereomeric ratio	mmol	millimole(s)
ed.	edition	mp	melting point
EDG	electron-donating group	Ms	mesyl
<i>ee</i>	enantiomeric excess	NBS	<i>N</i> -bromosuccinimide
e.g.	<i>exempli gratia</i> , for example	NMR	nuclear magnetic resonance
eq	equation	Nu	nucleophile
equiv	equivalent(s)	Pg	protection group
ESI	electrospray ionization	pH	proton log units
Et	ethyl	Ph	phenyl
<i>et al.</i>	and others (co-authors)	ppm	part per million
etc.	and so forth	Piv	pivaloyl
Et <sub>3</sub> N	trimethylamine		

quant	quantitative
rac	racemic
recryst.	recrystallized
R <sub>f</sub>	retention factor (in chromatography)
rt	room temperature
sat.	saturated
<i>t</i> Bu	<i>tert</i> -butyl
TEMPO	2,2,6,6-Tetramethyl-piperidine 1-oxyl
Tf	triflate
TFA	trifluoroacetic acid
THF	tetrahydrofuran
TIPS	triisopropylsilyl
TLC	thin layer chromatography
TON	turnover number
TOF	turnover frequency
t <sub>R</sub>	retention time
Ts	tosyl
TsN <sub>3</sub>	tosyl azide
<i>vs</i>	versus
UV	ultraviolet
wt%	weight percent

## A Introduction

### 1 Introduction - Applications of aromatic heterocycles

Aromatic heterocycles are ubiquitous in our daily life. A great number of essential biochemical processes rely upon systems derived from biological molecules containing heteroaromatic compounds as key building blocks. The side groups of DNA and RNA, the fundamental components of all living cells, are based on aromatic heterocycles. Furthermore, they are major constituents of essential amino acids, important vitamins, coenzymes, as well as plant and animal hormones, to name just a few. In addition to their import role in living organisms, heteroaromatic compounds are applied as herbicides, dyes, food additives, cosmetics, and perfumery ingredients among myriad other areas of modern life and industry.<sup>1</sup> However, the most important contribution of aromatic heterocycles to improve the quality of human life is probably their utilization in medicine. A great number of biologically active natural products and pharmaceuticals contain heteroaromatic building blocks. Some representatives are shown below (figure 1).<sup>2</sup>

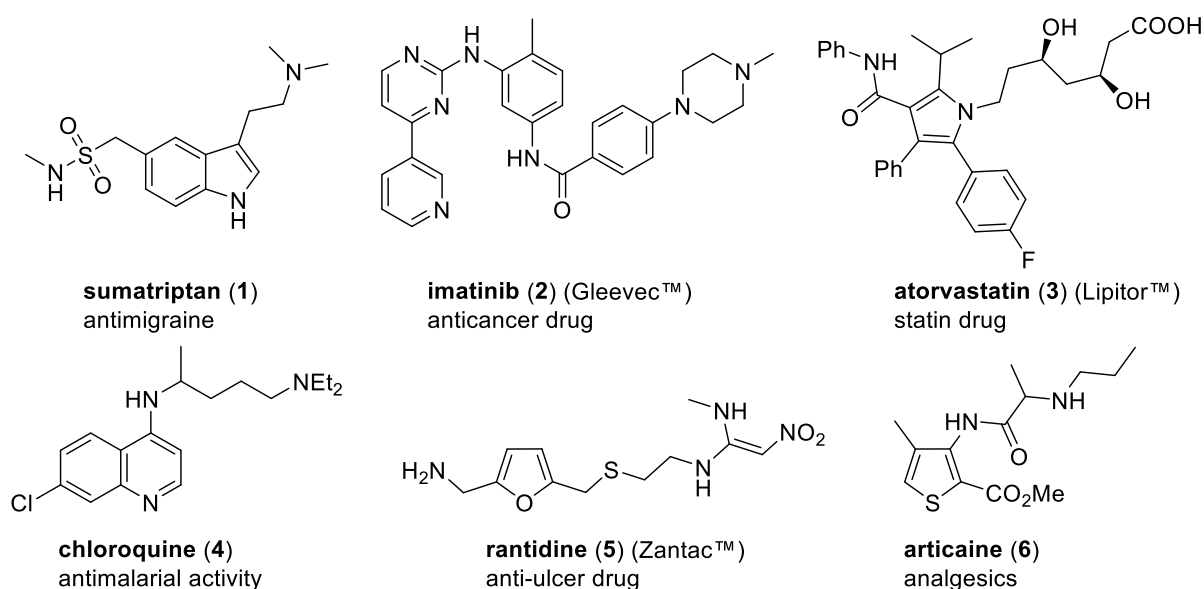


**Figure 1.** Pharmaceuticals based on a heteroaromatic scaffold.<sup>2</sup>

Sumatriptan (**1**), a selective serotonin 5-HT<sub>1B/1D</sub> agonist, is effective in the treatment of migraine, a disease that affects approximately 15% of the world's population. In the fight against cancer, imatinib (**2**) and other tyrosine kinase inhibitors are used as drugs in the therapy of gastrointestinal stromal tumors and chronic myeloid leukemia. Cardiovascular diseases along

with cancer have become the two major causes of death in industrialized countries. Drugs like atorvastatin (**3**), an especially successful representative of the so-called statins, were developed to reduce the risk of myocardial infarction by lowering cholesterol and triglycerides levels in the blood. As a potent medication against parasitic diseases, chloroquine (**4**) may be exemplified, which is used to prevent and to treat malaria. Another widespread health problem are gastric ulcers, which are caused by a disorder in the production of gastric hydrochloric acid. Ranitidine (**5**) can reduce this production by blocking the histamine H<sub>2</sub> receptors. An example of a drug that can act as an analgesic is articaine (**6**), which is usually applied as a local dental anesthetic.<sup>2</sup>

Since a large number of synthetic as well as natural pharmaceuticals are constructed on an aromatic heterocyclic scaffold, it is not surprising, that methods to functionalize heteroaromatic compounds are still of continuing interest in organic chemistry. Furthermore, simple aromatic heterocycles are frequently used as intermediates for the synthesis of natural products and other high complexity targets.<sup>3,4,5</sup> An attractive approach to utilize aromatic heterocycles for the generation of versatile intermediates is the [2+1] addition of carbenes.<sup>6</sup> Applying this reaction to furan, pyrrole and indole derivatives gives access to valuable building blocks with the general substructure of **7**.<sup>4</sup> This report will focus on the transformation of cyclopropanes **7** into natural products, analogues, and other synthetically useful compounds. Some accessible target<sup>7-13</sup> compounds are shown in figure 2 and details on their synthesis will be described together with a variety of other applications in the following chapters.

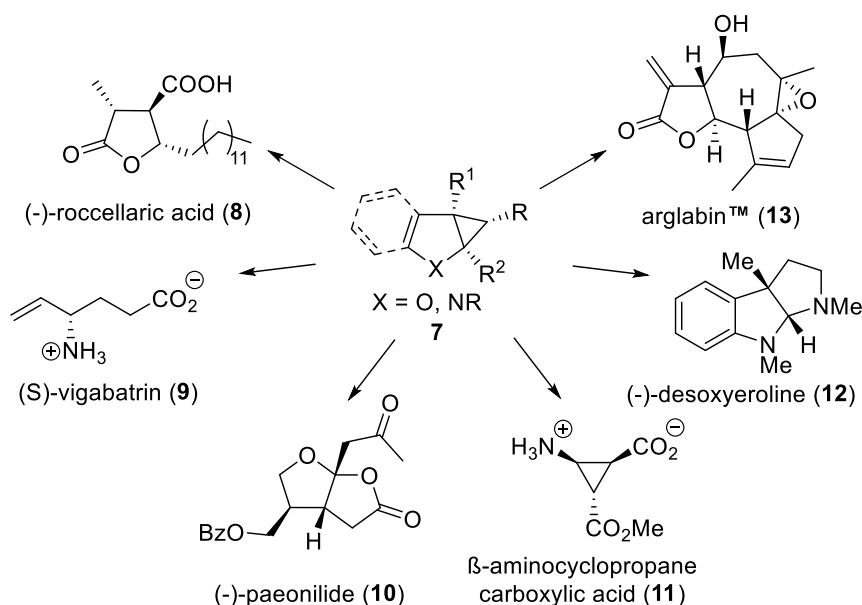


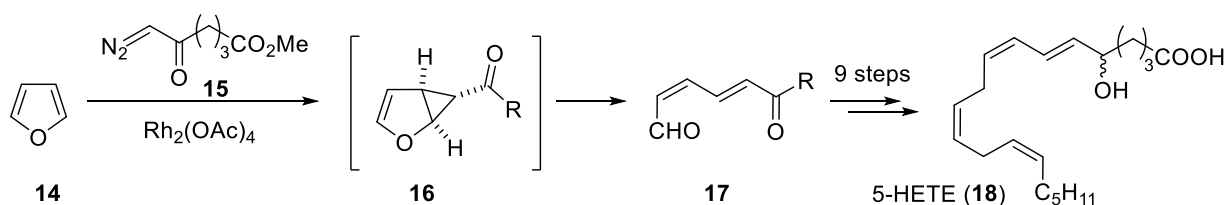
**Figure 2.** Examples of accessible compounds from cyclopropanes **7**.<sup>7-13</sup>



## 2 Applications of cyclopropanated furan derivatives

Furan and its derivatives are probably the most frequently used aromatic heterocycles for organic synthesis.<sup>3</sup> A possible reason for this might be their accessibility from lignocellulose, being the most abundant biomass resource on earth, via furfural as an intermediate.<sup>14</sup> Furthermore, their versatile reactivity analogous to arenes as well as masked alkenes and dienes, makes them excellent starting materials for the synthesis of complex targets like natural products.<sup>4</sup>

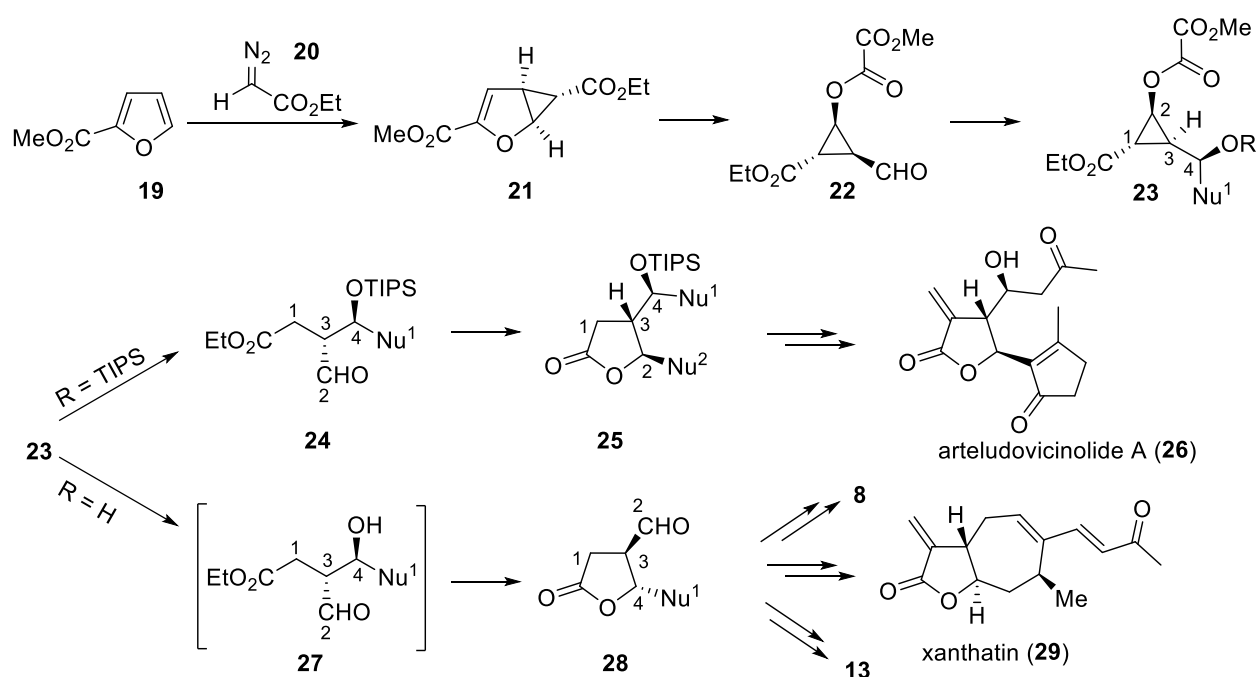
In 1983, *Rokach* and co-workers<sup>15,16</sup> presented a method to utilize furan for the synthesis of racemic 5-HETE **18** (5-hydroxyeicosatetraenoic acid) by taking advantage of the cyclopropane ring unraveling strategy introduced earlier by *Wenkert et al.*<sup>17</sup> Rhodium(II)-catalyzed cyclopropanation of furan **14** with diazo ketone **15** followed by ring opening of intermediate **16** gave access to diene **17**, which was transformed into **18** in 9 additional steps (scheme 1). In subsequent years, this unraveling strategy was also successfully applied by *Fitzsimmons*<sup>18</sup> for the synthesis of racemic 12-HETE (12-hydroeicosatetraenoic acid) and by *Wenkert*<sup>19</sup> for the synthesis of corticocin, whereas an intramolecular variation of this strategy was utilized by *Doyle et al.*<sup>20</sup> for the construction of macrocyclic lactones and ketones.



**Scheme 1.** Synthesis of 5-HETE **13** by *Rokach* and co-workers.<sup>15,16</sup>

An efficient methodology for the enantioselective construction of *anti*-4,5-disubstituted  $\gamma$ -butyrolactones starting from inexpensive furan **19** was developed by *Reiser* and co-workers.<sup>9</sup> One of the key steps is the Cu(I)-catalyzed cyclopropanation of **19** with diazo ester **20**, which enables the introduction of three new stereocenters (see chapter B.1.1 for details). Ozonolysis of cyclopropane **21** followed by reductive workup gave rise to aldehyde **22**, which was subjected to a nucleophilic addition in the next step. Depending on the nucleophile that is applied, this reaction forms the Felkin-Ahn<sup>21–23</sup> or the Cram-Chelate<sup>24</sup> products in high diastereoselectivity, respectively.<sup>25</sup> In the next step, Felkin-Ahn product **23** was transformed to *trans*-substituted  $\gamma$ -butyrolactone **28** by a base induced hydrolysis that triggers a subsequent retroaldol/lactonization cascade (*via* **27**), whereas the corresponding *cis*-substituted  $\gamma$ -butyrolactones could be formed by applying the analog Cram-Chelate products.<sup>24</sup> These

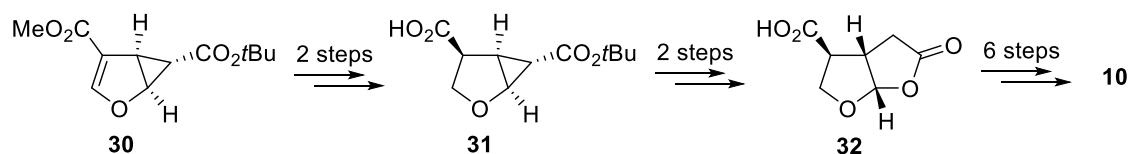
versatile building blocks were utilized to construct the core structures of xanthanolides, guaianolides, elemanolides, as well as eudesmanolides.<sup>23</sup> Furthermore, they were successfully utilized for the total synthesis of various natural products like (-)-rocellaric acid (**8**)<sup>9</sup> (among other paraconic acids,<sup>26</sup> see chapter B.3.2 for details), xanthatin (**29**)<sup>27</sup> and arglabin<sup>TM</sup> (**13**).<sup>12</sup> For the construction of both enantiomers of arteludovicinolide A (**26**)<sup>28</sup> a variation of this strategy was used. Protection of the free hydroxyl group in **23** with TIPS, followed by hydrolysis of the oxalic ester gave access to acyclic aldehyde **24**, which was further transformed to lactones of type **25** by the addition of Grignard or organolithium reagents. The synthesis of arteludovicinolide A (**26**) was accomplished in five additional steps.



**Scheme 2.** Synthesis of arteludovicinolide A (**26**), (-)-rocellaric acid (**8**), xanthatin (**29**) and arglabin<sup>TM</sup> (**13**) starting from furoate **19** by Reiser and co-workers.<sup>21–23,26–28</sup>

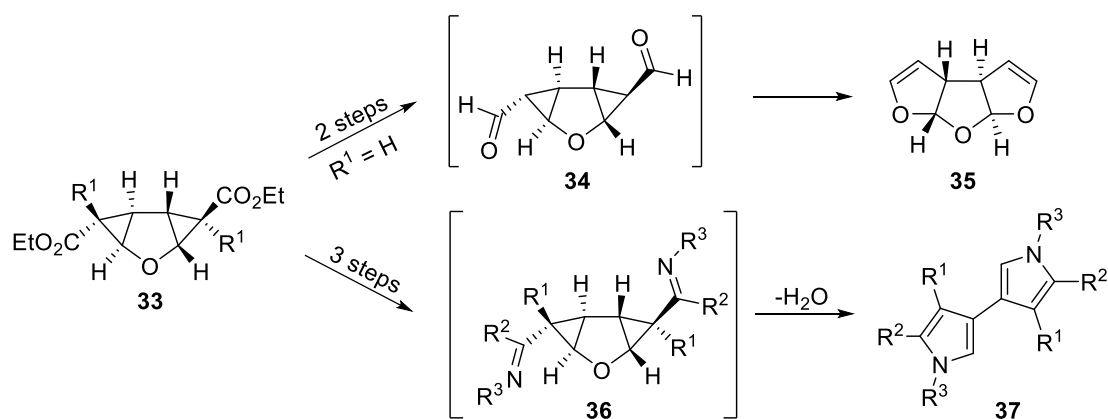
Based on the earlier work of Chandrasekaran<sup>29</sup> and Theodorakis,<sup>30</sup> an elegant method to convert cyclopropane **30** to the unnatural enantiomer **10** of paeonilide was developed by Harrar and Reiser.<sup>31</sup> Cyclopropane **30**, which was synthesized analogous to **21** (see chapter B.1.1 for details) from methyl furan-3-carboxylate, was transformed to acid **31** by ester hydrolysis and subsequent hydrogenation of the double bond occurring exclusively at the convex side of the bicycle. An acid-catalyzed ring opening and subsequent treatment with pyridine causing epimerization of the bridge-head centers, followed by an intramolecular lactonization, giving access to bicyclic lactone **32**, which was further converted to **10** in 6 steps. It is notable, that recently the enantioselective synthesis of natural (+)-paeonilide ((*ent*)-**10**) was accomplished

starting from (*ent*)-**30**.<sup>32</sup> A similar method was also utilized to construct the core nuclei of several spongiane diterpenoids like cheloviolene A and B, norrisolide and macfarlandin C.<sup>33</sup>



**Scheme 3.** Synthesis of (-)-paeonilide (**10**) by *Harrar and Reiser*.<sup>31</sup>

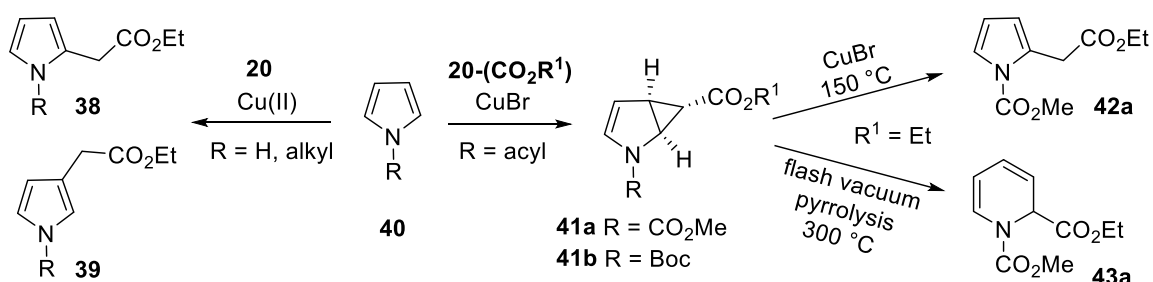
Compared to mono-cyclopropanated furans, the corresponding double-cyclopropanated representatives are less frequently used in organic synthesis. Nevertheless, some interesting transformations from tricycles **33**, which include a donor-acceptor ring enlargement strategy were reported by *Werz* and co-workers.<sup>34-37</sup> Starting materials of type **33** were synthesized by a Cu(I) or Rh(II)-catalyzed cyclopropanation of furan **14** with a variety of diazo esters. Reducing the ester groups of **33** to aldehydes in 2 steps followed by ring enlargement of intermediate **34**, gave rise to tricyclic bisacetal **35**. A similar approach was used for the synthesis of 3,3'-linked dipyrroles **37**, that includes imine formation and ring enlargement followed by the elimination of water via intermediate **36**.



**Scheme 4.** Synthesis of tricyclic bisacetal **35** and 3,3'-linked dipyrroles **37** starting from tricycles **33** by *Werz* and co-workers.<sup>34-37</sup>

### 3 Applications of cyclopropanated pyrrole derivatives

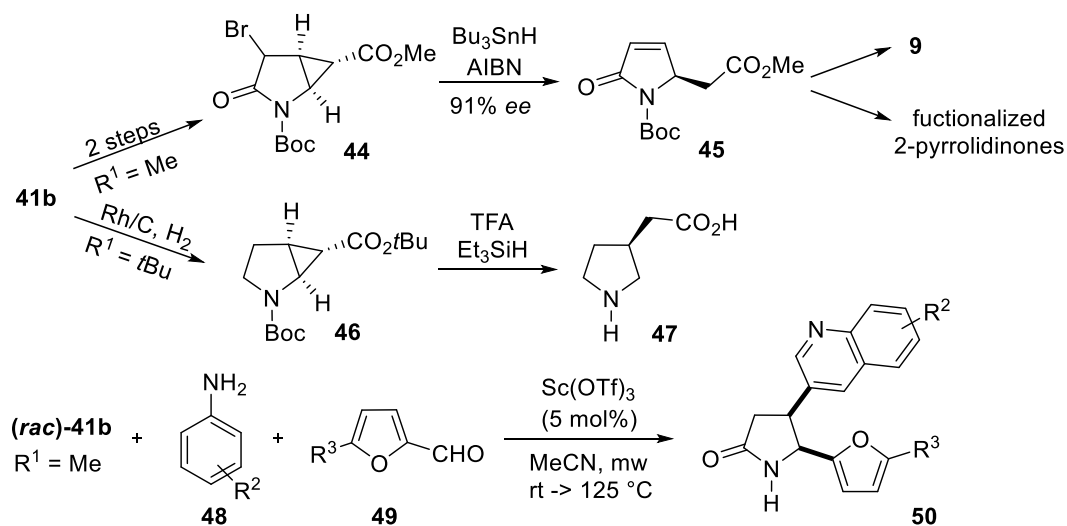
Just like furans, pyrroles offer a great range of diverse chemistry and have been utilized in numerous target-oriented syntheses.<sup>38</sup> However, in contrast to furans, the reactivity of pyrroles is influenced by the functionality on the nitrogen.<sup>39,40</sup> In the reaction with carbenoids, electron-rich *N*-H or *N*-alkyl pyrroles behave more typically like arenes, forming exclusively substitution products **38** and **39** *via* zwitterionic intermediates. The product ratio is dependent on the catalyst as well as the size of the alkyl group.<sup>41</sup> Due to the conjugation of the carbonyl group with the nitrogen lone pair, the aromatic ring of *N*-acyl pyrroles is not as electron-rich, therefore forming predominantly cyclopropanation products of type **41a** and **41b** in the reaction with carbenoids.<sup>42-44</sup> The versatile reactivity of these cyclopropanes arising from pyrroles was already shown in the pioneering work of *Fowler*.<sup>42</sup> Cyclopropane **41a** was transformed to pyrrole acetate **42a** by heating in the presence of CuBr, whereas subjection of **41a** to flash vacuum pyrolysis caused rearrangement to **43a**. Furthermore, it was demonstrated by *Tanny* and *Fowler*,<sup>45</sup> that **41a** is amenable to undergo [5+2] cycloaddition reactions with suitable dienophiles forming the corresponding bridged seven-membered rings. In contrast to the reaction of acceptor diazo ester **20** with pyrrole **40** (R = Boc), decomposition of 2-(siloxy)vinyl diazoacetate (donor-acceptor diazo ester: see chapter B.1.1 for details) in the presence of **40** (R = Boc) allowed the asymmetric formation of tropanes *via* a tandem cyclopropanation/Cope rearrangement mechanism.<sup>46</sup>



**Scheme 5.** Influence on the reactivity of pyrrole **40** by using different *N*-substituents and transformations of **41a** using different reaction conditions.<sup>39-42,44,45</sup>

An approach to utilize cyclopropane **41b** without destroying the cyclopropane moiety was realized by ozonolytic cleavage of the double bond in **41b** analog to furan **21** (scheme 2), followed by oxidation and deformylation. This method was successfully applied for the construction of conformationally constrained *cis*- as well as *trans*- $\beta$ -aminocyclopropane-carboxylic acids ( $\beta$ -ACC's).<sup>47</sup> The incorporation of this amino acids into peptides enabled the

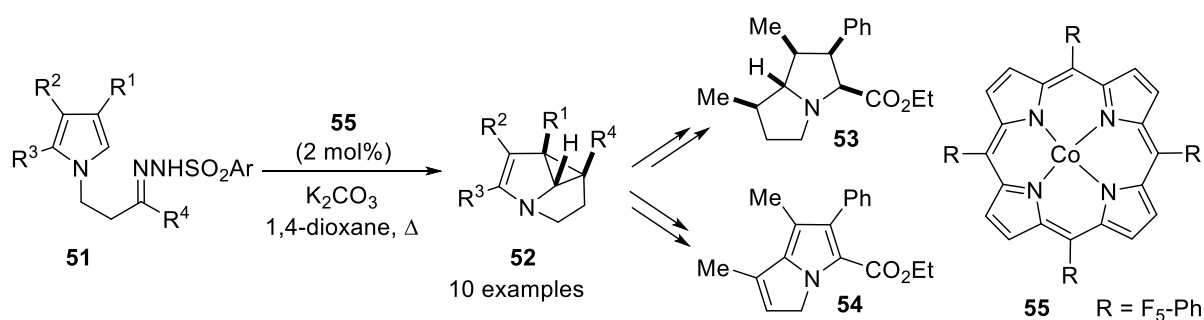
construction of novel secondary structural motifs<sup>48</sup> and was successfully utilized for the synthesis of organocatalysts<sup>49</sup> as well as biologically active ligands toward orexin,<sup>50</sup> neuropeptide Y<sup>51</sup> and calcitonin gene-related peptide receptors.<sup>52</sup>



**Scheme 6.** Possible transformations of cyclopropanated pyrroles **41b** and *(rac)*-**41b**.<sup>53–55</sup>

Furthermore, cyclopropane **41b** was successfully used as starting point for the enantioselective construction of substituted 5-membered *N*-heterocycles *via* selective ring opening of the *exo*-cyclic cyclopropane bonds (scheme 6).<sup>53–55</sup> In these approaches, the enamine double bond in **41b** had to be removed first, because otherwise products analog to **38** and **39** resulting from rearomatization of the pyrrole moiety were formed. Treatment of **41b** with NBS to form the corresponding bromohydrin followed by oxidation set the stage for cleavage of the cyclopropane bond with  $\text{Bu}_3\text{SnH}$ , giving access to 3,4-didehydropyrrohomoglutamate **45** *via* intermediate **44**. Although a slight epimerization could be obtained during the ring opening step, **45** was successfully applied for the enantioselective synthesis of (*S*)-vigabatrin (**9**) as well as a number of *anti*-substituted pyrrolidine-2-ones.<sup>53</sup> In addition, a multicomponent approach, which showed the accessibility of *cis*-4,5-disubstituted pyrrolidinones **50** by treating *(rac)*-**41b** with  $\text{Sc}(\text{OTf})_3$  (5 mol%) under microwave (mw) irradiation, was reported. This cascade sequence starts with a [4+2]-cycloaddition (Povarov reaction) of aromatic imines, which can be *in situ* formed from aldehydes **49** and anilines **48**, with the double bond of cyclopropane *(rac)*-**41b** to form the scaffold of the quinoline moiety in **50**. Carrying out the reaction at ambient temperature allows the isolation of the resulting products at this stage, whereas heating causes further transformation to **50** *via* selective cyclopropane ring opening, followed by 1,4-

shift of the furan moiety and rearomatization of the quinoline moiety, *N*-Boc hydrolysis and lactamization.<sup>54</sup> Recently, the transformation of **41b** to homo- $\beta$ -proline **47**, a structurally restricted analogue of GABA, was reported by hydrogenation of the double bond in **41b** followed by acid-catalyzed ring-opening of intermediate **47** (see chapter B.2.2 for details).<sup>55</sup> An elegant protocol for the construction of polycyclic *N*-heterocycles of type **52** starting from hydrazones **51**, which can be readily synthesized from the corresponding ketones or aldehydes with arenesulfonyl hydrazides, was developed by *Zhou, Che* and co-workers (scheme 7).<sup>56</sup> The use of *N*-hydrazones **51** as carbene precursors gave access to **52** via an intramolecular cyclopropanation catalyzed by cobalt(II)-porphyrin complex **55**. Moreover, the utility of these polycycles as intermediates for the synthesis of *N*-heterocycles like pyrrolizidine **53** and pyrrolizine **54** was shown. It is notable, that an analog transformation was possible with indoles, enabling the construction of numerous *N*-heterocycles having potential biological interest.<sup>56</sup>

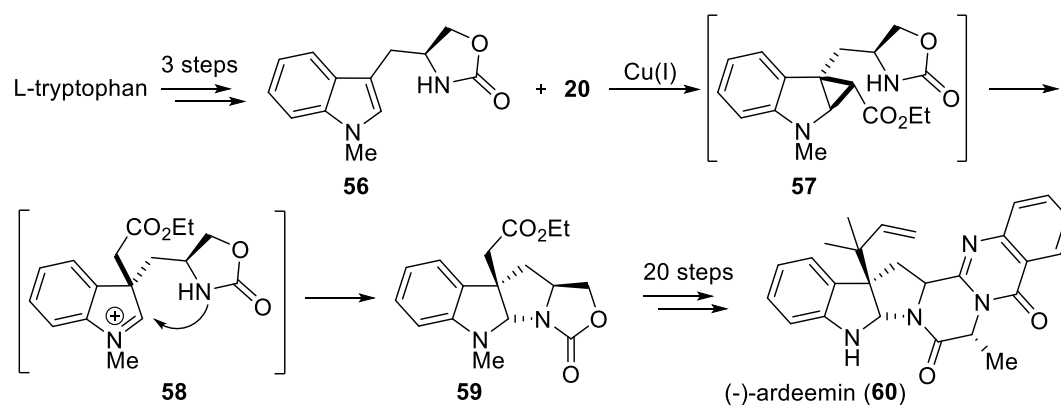


**Scheme 7.** Synthesis of polycyclic *N*-heterocycles of type **52** starting from hydrazones **51** and further transformation to pyrrolizidine **53** and pyrrolizine **54**.<sup>56</sup>

#### 4 Applications of cyclopropanated indole derivatives

Due to the great importance of the indole ring, that is present in more than ten thousand biologically active compounds, enormous efforts have been devoted to the development of synthetic methods for the preparation of this aromatic heterocycle and derivatives thereof.<sup>57</sup> Considering the complexity of several naturally occurring indole derivatives, it is not surprising, that the construction, as well as the direct functionalization of this heteroaromatic compound, has drawn great attention in organic chemistry.<sup>57,58</sup> For this purpose, the [2+1]-addition of carbenes represents a powerful and attractive tool, which was already successfully applied as inter- as well as intramolecular variant for the construction of natural products.<sup>59-61</sup> Additional strategies, establishing the indole core structure concurrent or after the formation of the cyclopropane ring, have also been described, but will not be covered in here.

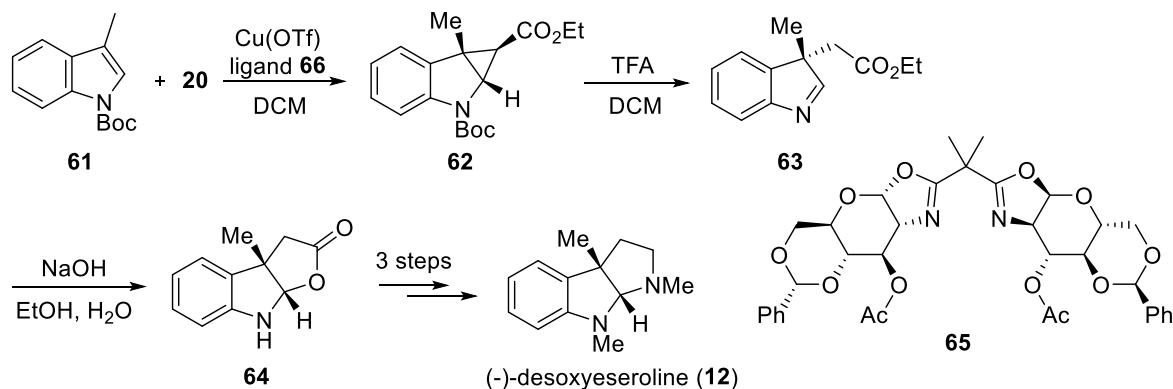
In 2006, *Qin* and co-workers reported an efficient synthetic route to chiral 3-substituted hexahydropyrroloindoline **59** starting from readily available L-tryptophan (scheme 8).<sup>62</sup> The key step in this synthesis is a Cu(I)-catalyzed one-pot-cascade reaction of oxazolidinone **56**, which is accessible in three steps starting from readily available L-tryptophan. This cascade is initiated by a cyclopropanation reaction of **56** with diazo ester **20** followed by ring opening and cyclization via intermediates **57** and **58**. Two years later, they were able to transform **59** into (-)-ardeemin (**60**) in 20 additional steps.<sup>59</sup>



**Scheme 8.** Synthesis of (-)-ardeemin (**60**) starting from L-tryptophan by *Qin* and co-workers.<sup>59,62</sup>

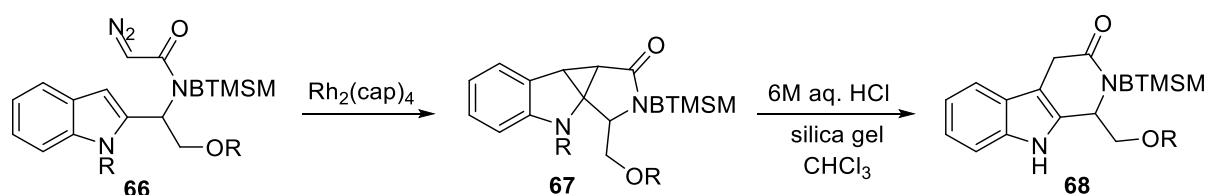
An intermolecular cyclopropanation reaction was also a crucial step in the synthesis of (-)-desoxyeseroline (**12**) (scheme 9). The reaction of indole **61** with diazo ester **20** in the presence of Cu(OTf) and glucoBox ligand **65** produced cyclopropane **62**, which was directly transformed into imine **63** via acidic removal of the Boc-group and subsequent ring-opening in 61% yield. Cleavage of the ester moiety in **63** triggers a cyclization, which gave access to

intermediate **64** in 71% yield and 96% *ee*. A protocol of *Ikeda et al.* for the racemic synthesis of esermethole<sup>63</sup> was applied successfully to transform **64** into (-)-desoxyeseroline (**12**) in 3 steps.<sup>60</sup>



**Scheme 9.** Synthesis of (-)-desoxyeseroline (**12**) starting from indole **61** by *Boysen* and co-workers.<sup>60</sup>

An intramolecular cyclopropanation was utilized as a key step in the synthesis of tetrahydro- $\beta$ -carboline **68** (scheme 10). Treatment of diazo compound **66** with Rh<sub>2</sub>(cap)<sub>4</sub> (cap = caprolactamate) gave access to intermediate **67**, whereby the *N*-BTMSM (bis(trimethylsilyl)methyl) group was crucial to suppress the formation of C-H-insertion byproducts *via* conformational control about the amide moiety. Subsequent acid catalyzed rearrangement provided tetrahydro- $\beta$ -carboline **68** in 84% yield.<sup>64</sup>

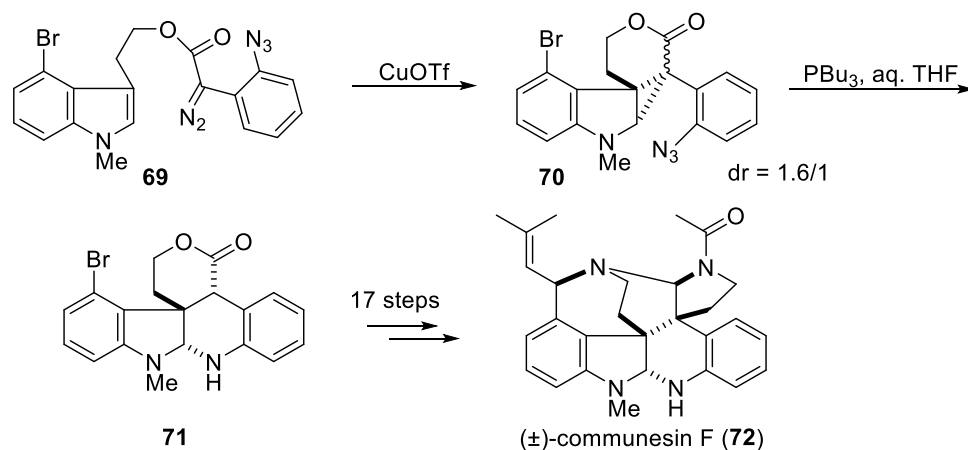


**Scheme 10.** Synthesis of tetrahydro- $\beta$ -carboline **68** *via* intramolecular cyclopropanation as a key step.<sup>64</sup>

Furthermore, intramolecular cyclopropanation has proven to be a powerful tool to create an all-carbon quaternary center at the C-3-position of substituted indoles. This strategy was successfully applied to the total synthesis of a great number of indole alkaloids (*Spino et al.*: (+)-aspidofractinine;<sup>65</sup> *Nishida et al.*: lundurine A and B (racemic);<sup>66</sup> *Qin et al.*: communesin F (racemic), minfiensine (racemic), (-)-kopsine, (-)-isokopsine, (+)-methyl chanofrucosinate, (-)-fruticosine and (-)-kopsanone).<sup>61,67</sup> The cyclopropanation as a key step and the following ring-opening strategy in the synthesis of ( $\pm$ )-communesin F are depicted in scheme 11 as an illustrative example. Reaction of  $\alpha$ -aryl- $\alpha$ -diazo ester **69** in the presence of copper(I) triflate led



to cyclopropanation product **70** as a mixture of two diastereomers in a 1.6:1 ratio. Reduction of the azide group in **70** with  $\text{PBU}_3$  in aqueous THF and subsequent ring opening followed by ring closure with *in situ* generated aniline, provided the kinetic product **71** as a single diastereomer. The resulting pentacyclic substructure **71** was transformed to ( $\pm$ )-communesin F (**72**) in 17 additional steps.<sup>61</sup>



**Scheme 11.** Synthesis of ( $\pm$ )-communesin F (**72**) starting from indole **69** by *Qin* and co-workers.<sup>61</sup>

The impressive applications of cyclopropanes **7** described here, demonstrate the great potential of this building blocks in organic chemistry. Cyclopropanation reactions were used as a key step and enabled the installation of key stereocenters in these synthetic strategies and further transformation *via* either rearrangement or ring-opening of the cyclopropanes led to a wide portfolio of accessible structures. The last example presented in this chapter utilizes a donor/acceptor carbenoid (classification of diazo compounds: see chapter B.1.1 for details) for the intramolecular cyclopropanation step in the total synthesis of ( $\pm$ )-communesin F (**72**). These type of carbenoids are stabilized by an additional donor group and thus, capable of undergoing highly chemoselective reactions.<sup>40</sup> However, in most applications presented here, simple acceptor diazo esters were used for the formation of the cyclopropanes. In the present thesis, the asymmetric, intermolecular cyclopropanation of aromatic heterocycles with donor-acceptor carbenoids was investigated to expand the scope of these useful building blocks. In the following, the utility of these cyclopropanes for the construction of natural products derivatives was explored.

## 5 References

- (1) a) Balaban, A. T.; Oniciu, D. C.; Katritzky, A. R. *Chem. Rev.* **2004**, *104*, 2777–2812; b) Quin, L. D.; Tyrell, J. A. *Fundamentals of heterocyclic chemistry: Importance in Nature and in the Synthesis of Pharmaceuticals*; Wiley, New York, 2010.
- (2) Pozharskiĭ, A. F.; Katritzky, A. R.; Soldatenkov, A. T. *Heterocycles in life and society: An introduction to heterocyclic chemistry, biochemistry, and applications*, 2nd ed., Wiley: Chichester West Sussex, 2011.
- (3) Shipman, M. *Contemp. Org. Synth.* **1995**, *2*, 1–17.
- (4) Reiser, O. *Isr. J. Chem.* **2016**, *56*, 531–539.
- (5) a) Abaev, V. T.; Plieva, A. T.; Chalikidi, P. N.; Uchuskin, M. G.; Trushkov, I. V.; Butin, A. V. *Org. Lett.* **2014**, *16*, 4150–4153; b) Bhardwaj, V.; Gumber, D.; Abbot, V.; Dhiman, S.; Sharma, P. *RSC Adv* **2015**, *5*, 15233–15266; c) Trushkov, I. V.; Uchuskin, M. G.; Butin, A. V. *Eur. J. Org. Chem.* **2015**, 2999–3016; d) Lopes, S. M. M.; Henriques, M. S. C.; Paixão, J. A.; Pinho e Melo, T. M. V. D. *Eur. J. Org. Chem.* **2015**, 6146–6151;
- (6) a) Novak, J.; Sorm, F. *Collect. Czech. Chem. Commun.* **1958**, *23*, 1126–1132; b) Rees, C. W.; Smithen, C. E. *Advan. Heterocycl. Chem.* **1964**, *3*, 57–78; c) Schenck, G. O.; Steinmetz, R. *Justus Liebigs Ann. Chem.* **1963**, 668, 19–30; d) Kulinkovich, O. G. *Cyclopropanes in organic synthesis*, 2nd ed.; Wiley, Hoboken New Jersey, 2015;
- (7) Beumer, R.; Bubert, C.; Cabrele, C.; Vielhauer, O.; Pietzsch, M.; Reiser, O. *J. Org. Chem.* **2000**, *65*, 8960–8969.
- (8) Beumer, R.; Reiser, O. *Tetrahedron* **2001**, *57*, 6497–6503.
- (9) Böhm, C.; Reiser, O. *Org. Lett.* **2001**, *3*, 1315–1318.
- (10) Gheorghe, A.; Schulte, M.; Reiser, O. *J. Org. Chem.* **2006**, *71*, 2173–2176.
- (11) Harrar, K.; Reiser, O. *Chem. Commun.* **2012**, *48*, 3457–3459.
- (12) Kalidindi, S.; Jeong, W. B.; Schall, A.; Bandichhor, R.; Nosse, B.; Reiser, O. *Angew. Chem. Int. Ed.* **2007**, *46*, 6361–6363; *Angew. Chem.* **2007**, *119*, 6478–6481.
- (13) Ozuduru, G.; Schubach, T.; Boysen, M. M. K. *Org. Lett.* **2012**, *14*, 4990–4993.
- (14) a) Dutta, S.; De, S.; Saha, B.; Alam, M. I. *Catal. Sci. Technol.* **2012**, *2*, 2025–2036; b) Higasio, Y. S.; Shoji, T. *Appl. Catal., A* **2001**, *221*, 197–207; c) Liu, B.; Zhang, Z. *ChemSusChem* **2016**, *9*, 2015–2036; d) Mariscal, R.; Maireles-Torres, P.; Ojeda, M.; Sádaba, I.; López Granados, M. *Energy Environ. Sci.* **2016**, *9*, 1144–1189; e) Xia, H.; Xu, S.; Yang, L. *RSC Adv* **2017**, *7*, 1200–1205;
- (15) Adams, J.; Rokach, J. *Tetrahedron Lett.* **1984**, *25*, 35–38.
- (16) Rokach, J.; Adams, J.; Perry, R. *Tetrahedron Lett.* **1983**, *24*, 5185–5188.

- (17) Wenkert, E.; Bakuzis, M. L. F.; Buckwalter, B. L.; Woodgate, P. D. *Synth. Commun.* **1981**, *11*, 533–543.
- (18) Leblanc, Y.; Fitzsimmons, B. J.; Adams, J.; Perez, F.; Rokach, J. *J. Org. Chem.* **1986**, *51*, 789–793.
- (19) Wenkert, E.; Guo, M.; Lavilla, R.; Porter, B.; Ramachandran, K.; Sheu, J. H. *J. Org. Chem.* **1990**, *55*, 6203–6214.
- (20) Doyle, M. P.; Chapman, B. J.; Hu, W.; Peterson, C. S.; McKerverey, M. A.; Garcia, C. F. *Org. Lett.* **1999**, *1*, 1327–1329.
- (21) Böhm, C.; Schinnerl, M.; Bubert, C.; Zabel, M.; Labahn, T.; Parisini, E.; Reiser, O. *Eur. J. Org. Chem.* **2000**, 2955–2965.
- (22) Jezek, E.; Schall, A.; Kreitmeier, P.; Reiser, O. *Synlett* **2005**, 915–918.
- (23) Nosse, B.; Chhor, R. B.; Jeong, W. B.; Bohm, C.; Reiser, O. *Org. Lett.* **2003**, *5*, 941–944.
- (24) Macabeo, A. P. G.; Kreuzer, A.; Reiser, O. *Org. Biomol. Chem.* **2011**, *9*, 3146–3150.
- (25) Mengel, A.; Reiser, O. *Chem. Rev.* **1999**, *99*, 1191–1224.
- (26) Chhor, R. B.; Nosse, B.; Soergel, S.; Boehm, C.; Seitz, M.; Reiser, O. *Chem. Eur. J.* **2003**, *9*, 260–270.
- (27) Bergmann, A.; Reiser, O. *Chem. Eur. J.* **2014**, *20*, 7613–7615.
- (28) Kreuzer, A.; Kerres, S.; Ertl, T.; Ruecker, H.; Amslinger, S.; Reiser, O. *Org. Lett.* **2013**, *15*, 3420–3423.
- (29) Haveli, S. D.; Sridhar, P. R.; Suguna, P.; Chandrasekaran, S. *Org. Lett.* **2007**, *9*, 1331–1334.
- (30) Brady, T. P.; Kim, S. H.; Wen, K.; Theodorakis, E. A. *Angew. Chem. Int. Ed.* **2004**, *43*, 739–742; *Angew. Chem.* **2004**, *116*, 757–760.
- (31) Harrar, K.; Reiser, O. *Chem. Commun.* **2012**, *48*, 3457–3459.
- (32) Gnahn, M., Enantiopure Synthesis of (+)-Paeonilide. Master Thesis, Universität Regensburg, Regensburg, **2014**.
- (33) Weisser, R.; Yue, W.; Reiser, O. *Org. Lett.* **2005**, *7*, 5353–5356.
- (34) Schneider, T. F.; Kaschel, J.; Dittrich, B.; Werz, D. B. *Org. Lett.* **2009**, *11*, 2317–2320.
- (35) Schneider, T. F.; Kaschel, J.; Awan, S. I.; Dittrich, B.; Werz, D. B. *Chem. Eur. J.* **2010**, *16*, 11276–11288.
- (36) Kaschel, J.; Schneider, T. F.; Kratzert, D.; Stalke, D.; Werz, D. B. *Org. Biomol. Chem.* **2013**, *11*, 3494–3509.
- (37) Kaschel, J.; Schneider, T. F.; Kratzert, D.; Stalke, D.; Werz, D. B. *Angew. Chem. Int. Ed.* **2012**, *51*, 11153–11156; *Angew. Chem.* **2012**, *44*, 11315–11318.

- (38) a) Gonzalez, J.; Koontz, J. I.; Hodges, L. M.; Nillson, K. R.; Neely, L. K.; Myers, W. H.; Sabat, M.; Harman, W. D. *J. Am. Chem. Soc.* **1995**, *117*, 3405–3421; b) Pavri N. P.; Trudell M. L. *Tetrahedron Lett.* **1997**, *38*, 7993–7996; c) Gribble, G. W. *J. Chem. Soc., Perkin Trans. 1* **2000**, 1045–1075; d) Antoline, J. E.; Hsung, R. P.; Huang, J.; Song, Z.; Li, G. *Org. Lett.* **2007**, *9*, 1275–1278; e) Jiang, C.; Frontier, A. J. *Org. Lett.* **2007**, *9*, 4939–4942; f) Tucker, J. W.; Narayanam, J. M. R.; Krabbe, S. W.; Stephenson, C. R. J. *Org. Lett.* **2010**, *12*, 368–371; g) Howard, J. K.; Rihak, K. J.; Bissember, A. C.; Smith, J. A. *Chem. Asian J.* **2016**, *11*, 155–167;
- (39) Davies, H. M. L.; Antoulinakis, E. G. *Org. React.* **2001**, *57*, 1–326.
- (40) Davies, H. M. L.; Hedley, S. J. *Chem. Soc. Rev.* **2007**, *36*, 1109–1119.
- (41) Maryanoff, B. E. *J. Org. Chem.* **1979**, *44*, 4410–4419.
- (42) Tanny, S. R.; Grossman, J.; Fowler, F. W. *J. Am. Chem. Soc.* **1972**, *94*, 6495–6501.
- (43) Fowler, F. W. *J. Chem. Soc. D* **1969**, 1359–1360.
- (44) Beumer, R.; Reiser, O. *Tetrahedron* **2001**, *57*, 6497–6503.
- (45) Tanny, S. R.; Fowler, F. W. *J. Org. Chem.* **1974**, *39*, 2715–2718.
- (46) Reddy, R. P.; Davies, H. M. L. *J. Am. Chem. Soc.* **2007**, *129*, 10312–10313.
- (47) a) Bubert, C.; Voigt, J.; Biasetton, S.; Reiser, O. *Synlett* **1994**, 675–677; b) Beumer, R.; Bubert, C.; Cabrele, C.; Vielhauer, O.; Pietzsch, M.; Reiser, O. *J. Org. Chem.* **2000**, *65*, 8960–8969; c) Beumer, R.; Reiser, O. *Tetrahedron* **2001**, *57*, 6497–6503; d) Gnad, F.; Reiser, O. *Chem. Rev.* **2003**, *103*, 1603–1623;
- (48) Pol, S. de; Zorn, C.; Klein, C. D.; Zerbe, O.; Reiser, O. *Angew. Chem. Int. Ed.* **2004**, *43*, 511–514; *Angew. Chem.* **2004**, *116*, 517–520.
- (49) D'Elia, V.; Zwicknagl, H.; Reiser, O. *J. Org. Chem.* **2008**, *73*, 3262–3265.
- (50) Lang, M.; Bufe, B.; Pol, S. de; Reiser, O.; Meyerhof, W.; Beck-Sickinger, A. G. *J. Pept. Sci.* **2006**, *12*, 258–266.
- (51) Koglin, N.; Zorn, C.; Beumer, R.; Cabrele, C.; Bubert, C.; Sewald, N.; Reiser, O.; Beck-Sickinger, A. G. *Angew. Chem. Int. Ed.* **2003**, *42*, 202–205; *Angew. Chem.* **2003**, *115*, 212–215.
- (52) Lang, M.; Pol, S. de; Baldauf, C.; Hofmann, H.-J.; Reiser, O.; Beck-Sickinger, A. G. *J. Med. Chem.* **2006**, *49*, 616–624.
- (53) Gheorghe, A.; Schulte, M.; Reiser, O. *J. Org. Chem.* **2006**, *71*, 2173–2176.
- (54) Roy, S.; Reiser, O. *Angew. Chem. Int. Ed.* **2012**, *51*, 4722–4725; *Angew. Chem.* **2012**, *124*, 4801–4804.
- (55) Pilsl, L. K. A.; Ertl, T.; Reiser, O. *Org. Lett.* **2017**, *19*, 2754–2757.

- (56) Reddy, A. R.; Hao, F.; Wu, K.; Zhou, C.-Y.; Che, C.-M. *Angew. Chem. Int. Ed.* **2016**, *55*, 1810–1815; *Angew. Chem.* **2016**, *128*, 1842–1847.
- (57) Dalpozzo, R. *Chem. Soc. Rev.* **2015**, *44*, 742–778.
- (58) a) Bandini, M.; Eichholzer, A. *Angew. Chem. Int. Ed.* **2009**, *48*, 9608–9644; *Angew. Chem.* **2009**, *121*, 9786–9824; b) Taber, D. F.; Tirunahari, P. K. *Tetrahedron* **2011**, *67*, 7195–7210; c) Vicente, R. *Org. Biomol. Chem.* **2011**, *9*, 6469–6480;
- (59) He, B.; Song, H.; Du, Y.; Qin, Y. *J. Org. Chem.* **2009**, *74*, 298–304.
- (60) Ozuduru, G.; Schubach, T.; Boysen, M. M. K. *Org. Lett.* **2012**, *14*, 4990–4993.
- (61) Yang, J.; Wu, H.; Shen, L.; Qin, Y. *J. Am. Chem. Soc.* **2007**, *129*, 13794–13795.
- (62) Song, H.; Yang, J.; Chen, W.; Qin, Y. *Org. Lett.* **2006**, *8*, 6011–6014.
- (63) Ikeda, M.; Matsugashita, S.; Tamura, Y. *J. Chem. Soc. Perkin Trans. 1* **1977**, 1770–1772.
- (64) Zhang, B.; Wee, A. G. H. *Chem. Commun.* **2008**, 4837–4839.
- (65) Gagnon, D.; Spino, C. *J. Org. Chem.* **2009**, *74*, 6035–6041.
- (66) Arai, S.; Nakajima, M.; Nishida, A. *Angew. Chem. Int. Ed.* **2014**, *53*, 5569–5572; *Angew. Chem.* **2014**, *126*, 5675–5678.
- (67) a) Yang, J.; Song, H.; Xiao, X.; Wang, J.; Qin, Y. *Org. Lett.* **2006**, *8*, 2187–2190; b) Shen, L.; Zhang, M.; Wu, Y.; Qin, Y. *Angew. Chem. Int. Ed.* **2008**, *47*, 3618–3621; *Angew. Chem.* **2008**, *120*, 3674–3677; c) Leng, L.; Zhou, X.; Liao, Q.; Wang, F.; Song, H.; Zhang, D.; Liu, X.-Y.; Qin, Y. *Angew. Chem. Int. Ed.* **2017**, *56*, 3703–3707; *Angew. Chem.* **2017**, *129*, 3618–3621;



## B Main part

### 1 Cyclopropanation of aromatic heterocycles

#### 1.1 Introduction – Classification of diazo ester

The cyclopropane ring is ubiquitous in nature and can be found in various structural classes of natural products including pheromones, fatty acid metabolites, terpenoids and unusual amino acids. Naturally occurring cyclopropanes, as well as several synthetic representatives, possess a broad spectrum of biological activities and thus, they are popular targets in organic synthesis.<sup>1</sup> Moreover, an impressive array of cyclopropane-based strategies to complex molecules like natural products was published.<sup>2</sup> Therefore, there is a continuing interest in developing effective methods and new catalysts for the chemo-, diastereo- and enantioselective synthesis of cyclopropanes. A powerful approach for the construction of highly functionalized cyclopropanes represents the reaction of alkenes with carbenoids, which are most readily generated by metal-catalyzed decomposition of diazo compounds.<sup>3</sup> The reactivity profile of the carbenoid is dependent on the metal-ligand system as well as the substitution pattern of the applied diazo compound.<sup>4-6</sup> According to their adjacent functionalities, metal-carbenes are categorized into three major groups: acceptor-acceptor, acceptor and donor-acceptor substituted carbenoids, whereby the terms acceptor and donor refer to the ability of the substituents to accept or donate electron density at the carbenoid center by resonance (figure 3). Electron-withdrawing groups increase the electrophilicity, and thus the reactivity of the carbenoid, whereas electron-donating substituents make the carbenoid considerably more stable and chemoselective.<sup>4-6</sup>

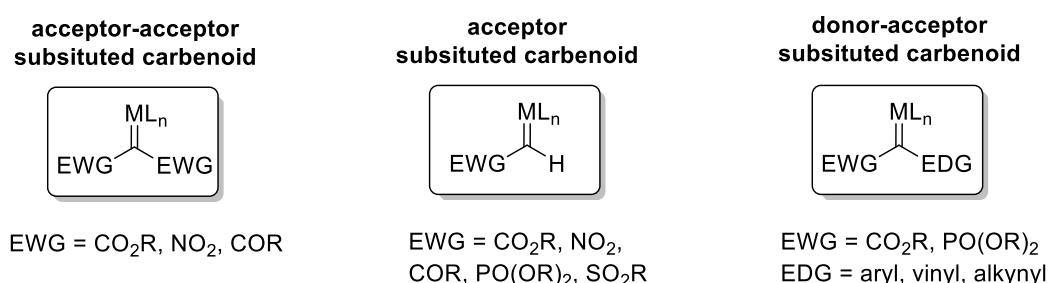
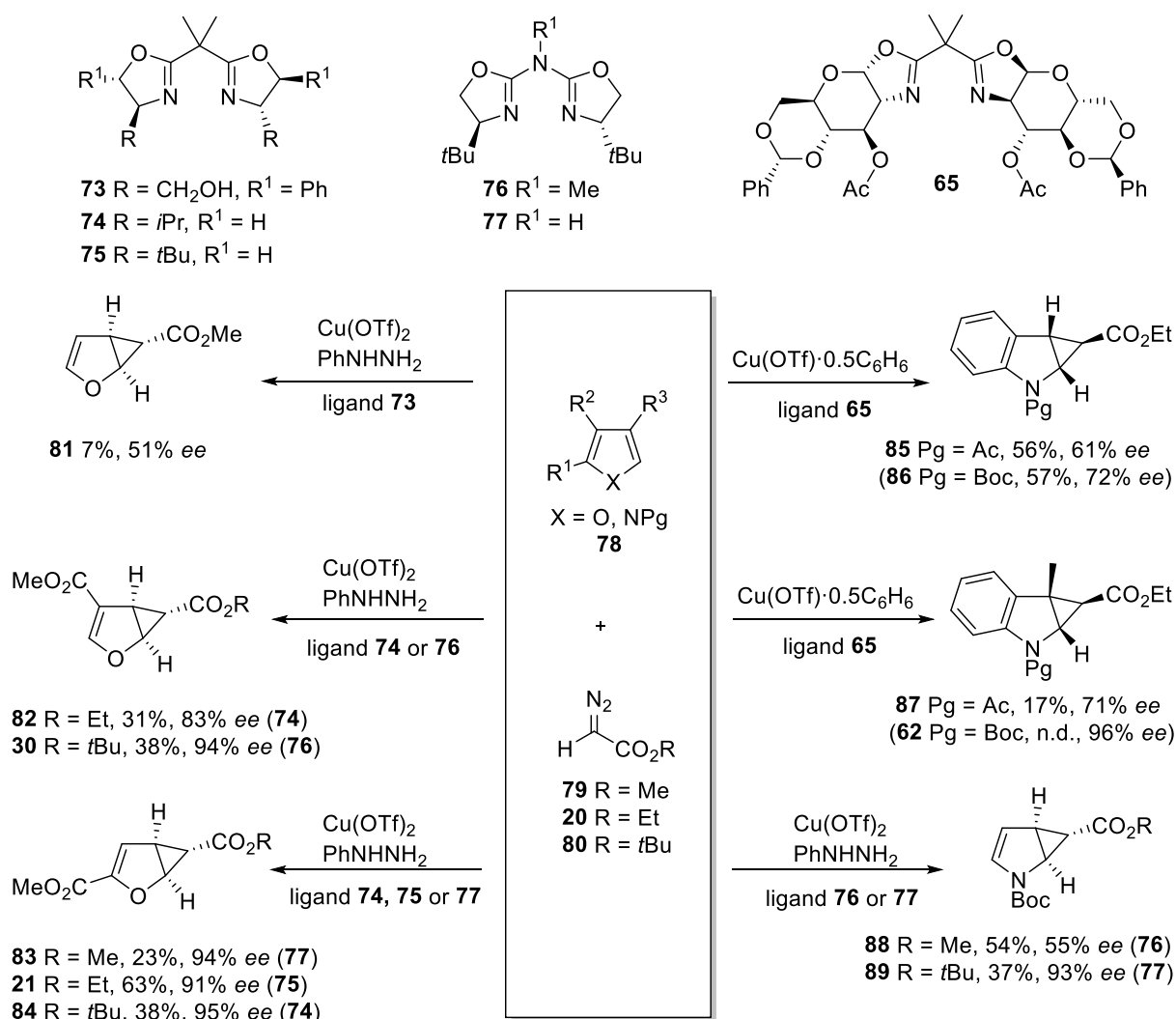


**Figure 3.** Classification of metal carbenoids (EWG = electron-withdrawing group; EDG = electron-donating group).<sup>4-6</sup>

Although a wide range of chiral catalysts was developed and successfully applied for the enantioselective cyclopropanation of electron-rich, electron-neutral and to a lesser extent electron-deficient alkenes,<sup>7,8</sup> only a few catalytic systems have been employed for the asymmetric cyclopropanation of electron-rich heterocycles.<sup>9</sup> In the following sections, current methods for the enantioselective cyclopropanation of furans, pyrroles, and indoles with acceptor diazo esters (scheme 12) and donor-acceptor diazo esters (scheme 13) are presented. The reactions of acceptor-acceptor diazo esters with aromatic heterocycles are not covered in this thesis since they tend to form substitution products rather than cyclopropanation products.<sup>10,11</sup>



**Scheme 12.** Overview of the currently most successful results regarding enantioselectivity for the monocyclopropanation of furans, pyrroles, and indoles with acceptor diazo esters **79**, **20** and **80**.<sup>12–18</sup>



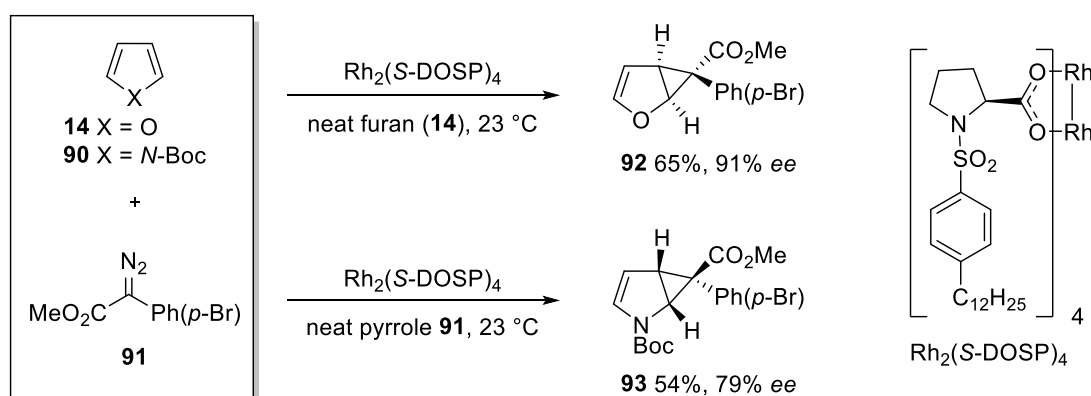
Copper(I)-complexes with C2-symmetric chiral bis(oxazoline) (box, **73-75**), carbohydrate-based bis(oxazoline) (*glucoBox*, **65**) and aza-bis(oxazoline) (azabox, **76-77**) ligands have emerged as excellent catalysts for enantioselective cyclopropanation of aromatic heterocycles (scheme 12).<sup>12-17</sup> Trifluoromethanesulfonate (OTf = triflate) is an exceptionally weak coordinating anion<sup>19</sup> and therefore, Cu(OTf) or Cu(OTf)<sub>2</sub>, which is reduced with phenylhydrazine *in situ*, were most commonly used to generate the active copper(I)-species in the presence of the chiral ligands. *Reiser* and co-workers reported that the reaction of furan with acceptor diazo esters catalyzed by copper bis(oxazoline) complexes gave only moderate enantioselectivities ( $\leq 51\%$  *ee*) and very low yields (< 20%).<sup>17</sup> The low chemical yields may be rationalized by the inherent instability of the resulting adducts, which are prone to undergo rearrangement. In contrast, employing these catalytic systems for furans containing an ester functionality in 2- or 3-position gave rise to cyclopropanes **21**, **30** and **82-84** with excellent levels of enantioselectivity (83%-95% *ee*), albeit with moderate yields (23-63%).<sup>15-17</sup> Noteworthy, these reactions proceeded regioselectively, since only the less hindered double bond was cyclopropanated, and moreover, highly diastereoselectively, forming the *exo*-products exclusively.<sup>17</sup>

Whereas box, as well as azabox ligands, were successfully applied for the enantioselective cyclopropanation of substituted furans, pyrrole turned out to be a more challenging substrate. While copper(I)-box complexes were reported to give only moderate enantioselectivities up to 46% *ee* for the reaction of *N*-Boc pyrrole,<sup>20</sup> highly increased levels of selectivity were achieved with azabox ligands by *Reiser* and co-workers.<sup>12,15</sup> Additionally, it was shown, that the reaction temperature and the residue R on the diazo ester have a crucial impact on the selectivity. Best results regarding enantioselectivity (93% *ee*) were obtained using diazo ester **80**, bearing a sterically demanding *tert*-butyl group, at -20 °C in the presence of azabox ligand **77**.<sup>12,15</sup> The stereochemical outcome of this reaction was rationalized by a model for the asymmetric cyclopropanation of olefins introduced earlier by Pfaltz<sup>21</sup> and Andersson.<sup>22</sup> It is notable, that the cyclopropanation products of substituted furans, as well as *N*-Boc pyrrole, were accessible in the enantiomerically pure form in a multi-gram quantity,<sup>12,18</sup> setting the foundation for a diverse follow-up chemistry (see chapter A.2 and A.3 for details).

The first enantioselective cyclopropanation of *N*-acyl indoles with acceptor diazo ester **20** was recently reported by *Boysen* and co-workers.<sup>14</sup> Using copper(I) triflate and *glucoBox* ligand **65**, cyclopropanes **85** and **87** were obtained in up to 71% *ee*, albeit with moderate yields (17% and 56%). Although the reactions of *N*-Boc-protected indoles led to higher levels of enantioselectivity compared to their acetylated counterparts, it was not feasible to isolate

cyclopropanes **86** and **62**, since they were not separable from byproducts derived from carbene dimerization. Nevertheless, direct transformation of **62** gave rise to hemiaminal ester **64**, a key intermediate in the synthesis of (-)-desoxyseroline (**12**), in 96% *ee* (see chapter A.4, scheme 9 for details).<sup>14</sup>

Dirhodium(II) tetracarboxylates are known to be remarkably active catalysts for reactions of donor-acceptor diazo esters.<sup>23–25</sup> Using  $\text{Rh}_2(\text{S-DOSP})_4$ ,<sup>26</sup> a well-established catalyst for various transformations of donor-acceptor diazo esters, *Davies* and co-workers<sup>9,27</sup> have systematically investigated the reactions of a variety of heterocycles with diazo ester **91** (scheme 13). This study contributed in great measure to improve our understanding of the influence of the heterocyclic structure on the enantioinduction in the rhodium-catalyzed reaction with donor-acceptor carbenoids. However, it also revealed that the construction of monocyclopropanated heterocycles is quite challenging since furan (**14**) and *N*-Boc pyrrole (**90**) are prone to form products resulting from a second cyclopropanation with donor-acceptor carbenoids.<sup>9,27</sup> This behavior contrasts with the chemistry of these heterocycles reacting with acceptor carbenoids, in which the monocyclopropane products are preferentially formed.<sup>18</sup>



**Scheme 13.** Overview of the currently most successful results regarding enantioselectivity for the monocyclopropanation of furans and pyrroles with donor-acceptor diazo ester **91**.<sup>27</sup>

The tendency to undergo a second cyclopropanation event became especially noticeable with the reaction of *N*-Boc pyrrole (**90**) and diazo ester **91**. Even when 6 equiv of **90** were used, the double cyclopropanation product was exclusively formed. In order to obtain monocyclopropane **93** as the major product, *N*-Boc pyrrole (**90**) has to be used in vast excess as solvent. Thus, **93** could be isolated in 54% yield with 79% *ee*, albeit with a significant amount of the corresponding double cyclopropanation product (34%). Employing the same conditions for the reaction of furan (**14**) with diazo ester **91** gave access to monocyclopropane **92** in 65% yield with 91% *ee*. An interesting feature of these reactions is that cyclopropanes **92** and **93** were

formed with opposite sense of asymmetric induction, although the same enantiomer of the catalyst was utilized (scheme 13).<sup>27</sup> The authors propose that the difference was caused by two possible orientations for the asynchronous concerted cyclopropanation.<sup>6,28</sup> The initial bond formation is supposed to occur at the 2-position of furan, following the expected trend for aromatic electrophilic substitution, whereas the steric influence of the *N*-Boc group and 2,5-dimethylfuran causes the initial bond formation to take place at the 3-position. Noteworthy,  $\text{Rh}_2(\text{S-DOSP})_4$  was reported to be ineffective in catalyzing the reaction of unsubstituted *N*-Boc indole with diazo ester **91**, resulting in the recovery of the starting material along with products deriving from carbene dimerization.<sup>9</sup> The reactions of vinyl diazo acetates and *N*-Boc pyrroles as well as furans proceed *via* a tandem cyclopropanation/Cope rearrangement and were elegantly exploited for the asymmetric synthesis of tropanes<sup>29,30</sup> and highly functionalized 8-oxabicyclo[3.2.1]octene derivatives<sup>31-33</sup> by *Davies et al.* However, no monocyclopropanation products were isolated in these reactions.

## 1.2 Chiral rhodium(II) tetracarboxylates catalysts - Synthesis and Application

A central part of the present thesis deals with the asymmetric cyclopropanation of aromatic heterocyclic substrates with donor-acceptor carbenoids. Since chiral rhodium(II) tetracarboxylates have emerged as very effective catalysts for the cyclopropanation chemistry of donor-acceptor carbenoids,<sup>23–25,34</sup> the following investigations were predominantly focused on the application of this type of catalysts. Figure 4 gives an overview of the catalysts that were used in these cyclopropanation studies.<sup>8,26,35–42</sup>

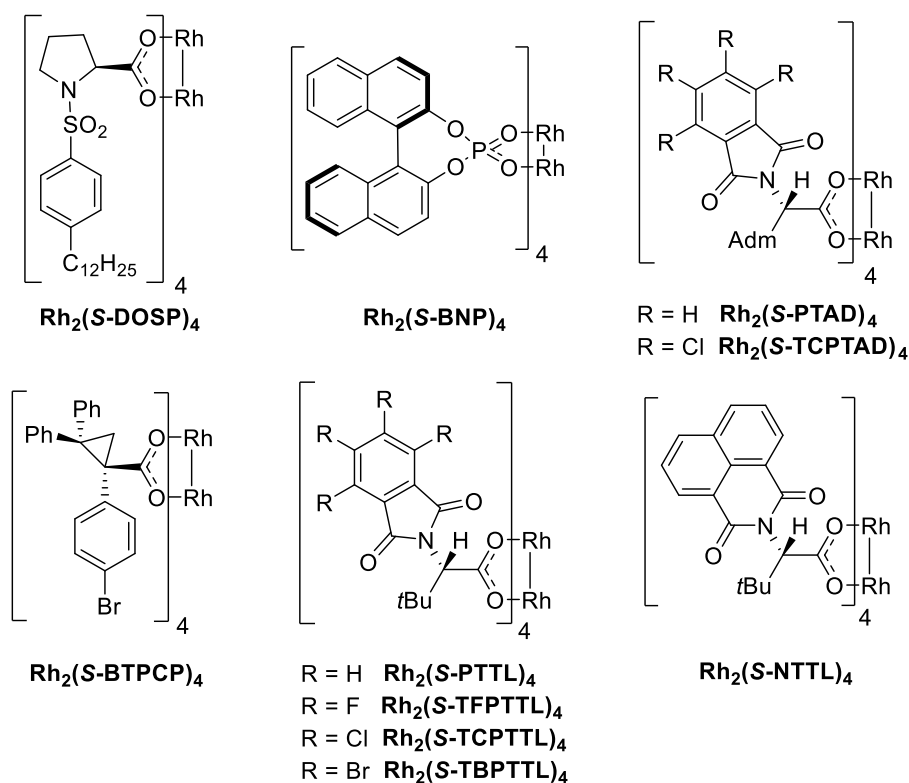
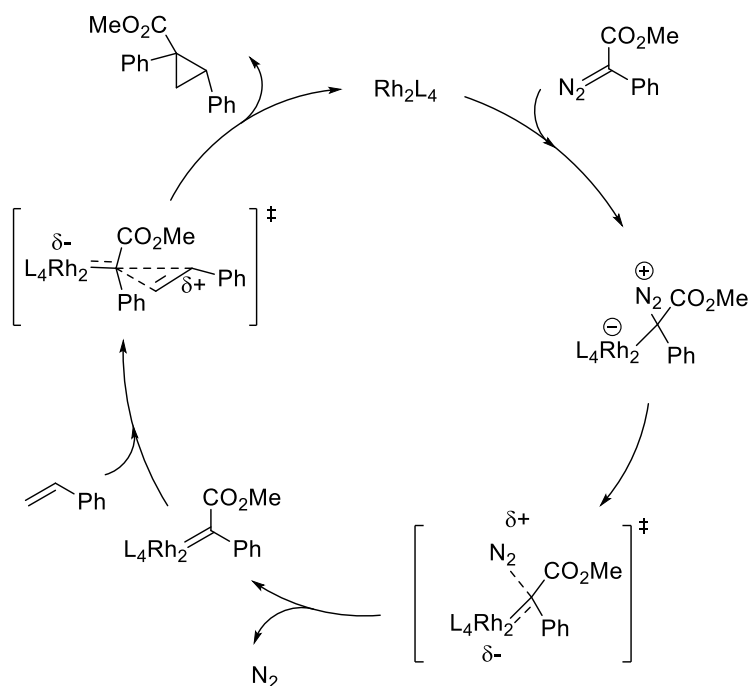


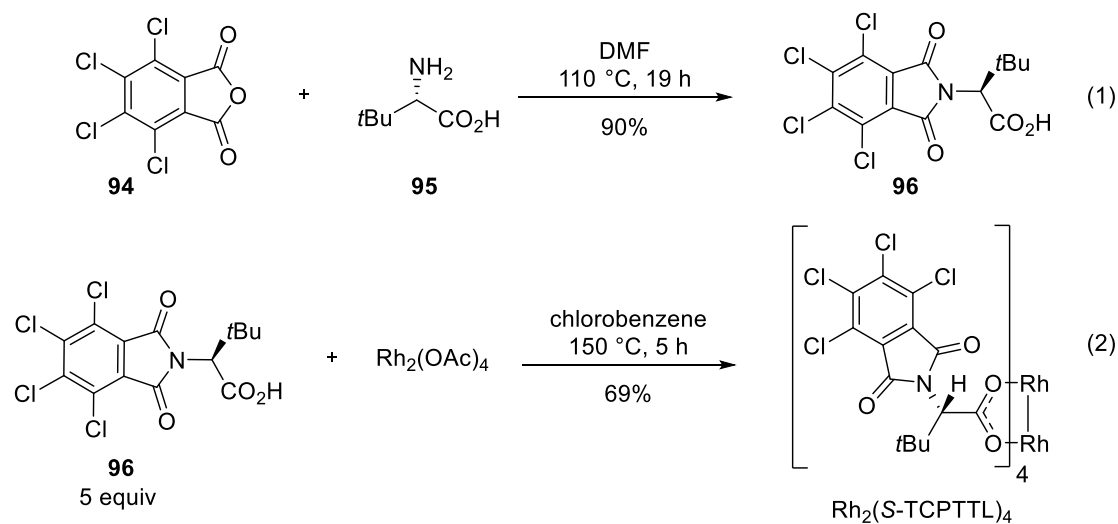
**Figure 4.** Chiral dirhodium(II) catalysts used in this study.

The currently accepted mechanism for the dirhodium(II)-catalyzed cyclopropanation with donor-acceptor diazo compounds is shown in scheme 14.<sup>43–45</sup> The reaction is initiated by nucleophilic attack of the negatively polarized carbon of the diazo ester on the coordinatively unsaturated, axial site of the Rh(II)-catalyst.<sup>44</sup> Subsequent extrusion of nitrogen generates a rhodium carbenoid that reacts with an alkene in a concerted, non-synchronous manner.<sup>43</sup>



**Scheme 14.** Currently accepted mechanism for the cyclopropanation with donor-acceptor diazo compounds.<sup>43</sup>

Chiral rhodium(II) tetracarboxylates, like  $\text{Rh}_2(\text{S-TCPTTL})_4$ , which was originally developed by *Hashimoto* and co-workers<sup>36</sup> to catalyze aromatic C-H insertion reactions of diazo ketoesters, are readily generated by high-temperature ligand exchange<sup>46</sup> (scheme 15, eq 2). Phthalimide ligands of type **96** are commonly synthesized *via* dehydrative condensation of phthalic anhydrides and chiral primary amines (scheme 15, eq 1).<sup>47</sup>



**Scheme 15.** Synthesis of  $\text{Rh}_2(\text{S-TCPTTL})_4$ .

### 1.3 Asymmetric cyclopropanation of methyl furan-2-carboxylate (**19**)\*

The Cu(I)-catalyzed reactions of methyl furan-2-carboxylate (**19**) with acceptor diazo esters create the foundation for a variety of synthetic approaches aiming at natural products and valuable, chiral intermediates (see chapter A.1.2, scheme 2).<sup>18</sup> Inspired by these versatile applications, it was envisioned that an analog transformation of **19** with donor-acceptor diazo esters would provide access to new, highly substituted, chiral monocyclopropanes, which could be used as building blocks in stereoselective synthesis. Furthermore, the steric demand of the ester group in **19** is supposed to suppress the tendency to undergo a second cyclopropanation, which has been observed in earlier studies with donor-acceptor diazo esters (see chapter B.1.1). Thus, it was decided to use **19** as the model substrate for an initial catalyst screening.

#### 1.3.1 Optimization studies

Rh<sub>2</sub>(*S*-DOSP)<sub>4</sub><sup>26</sup> shows a quite broad substrate scope in terms of both the trapping agents as well as donor groups on the carbenoid in cyclopropanation reactions,<sup>48</sup> and thus, it seemed to be an ideal catalyst for an initial test reaction. With Rh<sub>2</sub>(*S*-DOSP)<sub>4</sub> the reaction of methyl phenyldiazoacetate **97a** with **19** produced a mixture of cyclopropane **98a** and the dienone **99** in a ratio of 46:54 (table 1, entry 2). This result contrasts with our previous observations aiming at the racemic synthesis of **98a**, since an almost negligible amount of **99** was formed in the Rh<sub>2</sub>(OPiv)<sub>4</sub>-catalyzed reaction (entry 1). The formation of ring-opening product **99** is indicative that attack of the carbene is occurring at the  $\alpha$ -position of **19**, resulting in zwitterionic<sup>27</sup> intermediate **102** that can ring open to **99** (scheme 16). An electron-withdrawing substituent in 2-position was expected to have a destabilizing effect on intermediate **102**,<sup>27,31–33</sup> and thus, reduce the unraveling tendency. However, this was not in line with the observed results.

Previous studies have shown, that nonpolar solvents can have a beneficial impact on the product distribution by limiting the formation of side products derived from zwitterionic intermediates.<sup>30,49</sup> Changing the reaction solvent from dichloromethane to  $\alpha,\alpha,\alpha$ -trifluorotoluene<sup>50</sup> (table 1) gave a worse ratio of **98a**:**99** (37:63), whereas the use of hexanes resulted in a slight improvement of the product ratio (52:48). Lowering the reaction temperature to -42 °C led to an additional enhancement of the product ratio (76:24). However,

---

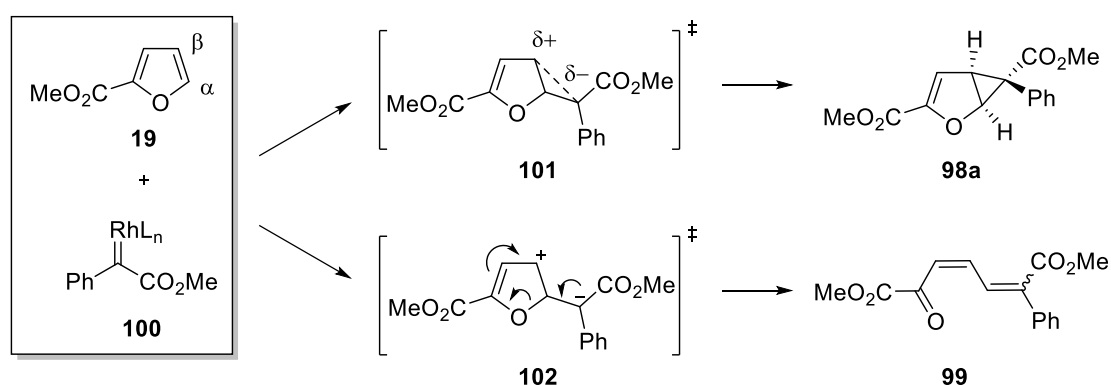
\* This chapter is partially based on Lehner, V.; Davies, H. M. L.; Reiser, O. *Rh(II)-Catalyzed Cyclopropanation of Furans and Its Application to the Total Synthesis of Natural Product Derivatives*. *Org. Lett.* **2017** (accepted)

this approach was not further pursued, since regardless of the applied solvent system and the reaction temperature substantial amounts of byproduct **99** were formed in the presence of  $\text{Rh}_2(\text{S-DOSP})_4$  and it was not feasible to isolate **98a** in pure form.

**Table 1.** Asymmetric cyclopropanation of furan-2-carboxylate (**19**) using  $\text{Rh}_2(\text{S-DOSP})_4$ .

entry <sup>a</sup>	$\text{Rh}_2\text{L}_4$	solvent	temperature (°C)	ratio <b>98a</b> : <b>99</b> <sup>c</sup>
1 <sup>b</sup>	$\text{Rh}_2(\text{OPiv})_4$	hexanes	25	> 80:1
2	$\text{Rh}_2(\text{S-DOSP})_4$	$\text{CH}_2\text{Cl}_2$	25	46:54
3	$\text{Rh}_2(\text{S-DOSP})_4$	$\text{CF}_3\text{C}_6\text{H}_5$	25	37:63
4	$\text{Rh}_2(\text{S-DOSP})_4$	hexanes	25	52:48
5 <sup>b</sup>	$\text{Rh}_2(\text{S-DOSP})_4$	hexanes	-42	76:24

<sup>a</sup>Standard reaction conditions: **97a** (1.0 equiv) in dry solvent (2 mL) was added to **19** (4.0 equiv) in dry solvent (2 mL) and  $\text{Rh}_2\text{L}_4$  (1 mol%) over 1 h. <sup>b</sup>2 equiv of **19** was used. <sup>c</sup>Determined by <sup>1</sup>H-NMR analysis of the crude mixture.

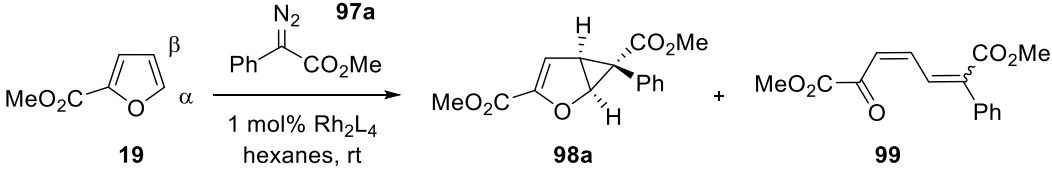


**Scheme 16.** Possible mechanisms for the formation of cyclopropane **98a** and ring-opening product **99**.

Obviously, the ligand on the rhodium catalyst has a crucial impact on the product formation (table 1, entry 1 vs. 2)<sup>30,49</sup> and thus, a systematic study with chiral dirhodium(II) catalysts was conducted (table 2). Catalysts, which are less effective at charge stabilization of the zwitterionic intermediate **102** were expected to promote the formation of **98a**. Indeed, the bulky triarylcyclopropane-carboxylate catalyst  $\text{Rh}_2(\text{S-BTPCP})_4$ ,<sup>8</sup> bearing less electron withdrawing

ligands, gave a greatly improved ratio of **98a:99** (93:7) compared to the analog transformations with  $\text{Rh}_2(\text{S-DOSP})_4$ <sup>26</sup> and  $\text{Rh}_2(\text{S-BNP})_4$ <sup>42</sup> (table 2, entry 3 vs. 1 and 2). The use of  $\text{Rh}_2(\text{S-BTPCP})_4$  allows the isolation of **98a** in high yield (84%), but with a relatively moderate level of enantioselectivity (56% *ee*). Attempts to increase the enantioinduction by modification of the reaction conditions as well as extending the substrate scope were not successful.

**Table 2.** Catalyst screening for the reaction of furan **19** with diazo ester **97a**.



entry <sup>a</sup>	Rh <sub>2</sub> L <sub>4</sub>	ratio <b>98a:99</b> <sup>b</sup>	yield <b>98a</b> <sup>c</sup> (%)	<i>ee</i> <sup>d</sup> (%)
1 <sup>e</sup>	Rh <sub>2</sub> (S-DOSP) <sub>4</sub>	55:45	n.d.	n.d.
2 <sup>f</sup>	Rh <sub>2</sub> (S-BNP) <sub>4</sub>	68:32	n.d.	n.d.
3	Rh <sub>2</sub> (S-BTPCP) <sub>4</sub>	93:7	84	56
4	Rh <sub>2</sub> (S-NTTL) <sub>4</sub>	52:48	n.d.	89
5	Rh <sub>2</sub> (S-PTAD) <sub>4</sub>	31:69	n.d.	n.d.
6	Rh <sub>2</sub> (S-TCPTAD) <sub>4</sub>	>99:1	54	83
7	Rh <sub>2</sub> (S-PTTL) <sub>4</sub>	30:70	n.d.	48
8	Rh <sub>2</sub> (S-TFP TTL) <sub>4</sub>	80:20	n.d.	46
<b>9</b>	<b>Rh<sub>2</sub>(S-TCPTTL)<sub>4</sub></b>	<b>&gt;99:1</b>	<b>81</b>	<b>91</b>
10	Rh <sub>2</sub> (S-TBP TTL) <sub>4</sub>	>99:1	79	86

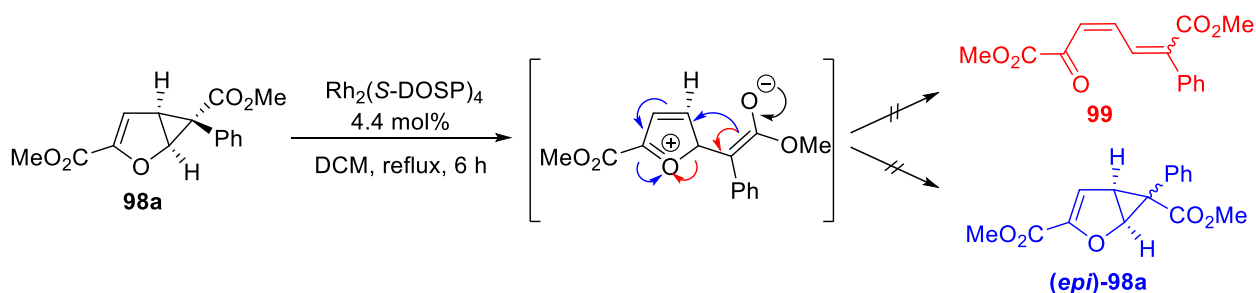
<sup>a</sup>Standard reaction conditions: **97a** (1.0 equiv) in dry hexanes (2 mL) was added to **19** in dry hexanes (2.0 equiv) and Rh<sub>2</sub>L<sub>4</sub> (1 mol%) at rt over 1 h. <sup>b</sup>Determined by <sup>1</sup>H-NMR analysis of the crude mixture. <sup>c</sup>Isolated yield. <sup>d</sup>Determined by chiral HPLC analysis. <sup>e</sup>1.5 equiv of **19** was used. <sup>f</sup>Toluene was used as a solvent.

Another generally useful series of catalysts are the phthalimido, and the naphthylimido derived catalysts.<sup>35–41</sup> Rh<sub>2</sub>(S-NTTL)<sub>4</sub><sup>41</sup> did not have a major influence on the product ratio but did result in the formation of **98a** in 89% *ee* (entry 4), whereas the Rh<sub>2</sub>(S-PTAD)<sub>4</sub><sup>40</sup> gave a worse product ratio of 31:69 (entry 5). The breakthrough came with the tetrachloro derivative Rh<sub>2</sub>(S-TCPTAD)<sub>4</sub><sup>39</sup>, which gave an extremely clean reaction, producing **98a** in 83% *ee* with no evidence for the formation of the undesired dienone **99** (entry 6). Even better results were obtained with the *tert*-leucine derived catalysts. Rh<sub>2</sub>(S-PTTL)<sub>4</sub><sup>38</sup> gave a mixture and so did the



tetrafluoro derivative  $\text{Rh}_2(\text{S-TFPTTL})_4$ <sup>37</sup> (entries 7 and 8). However, both the tetrachloro and tetrabromo catalysts  $\text{Rh}_2(\text{S-TCPTTL})_4$ <sup>36</sup> and  $\text{Rh}_2(\text{S-TBPTTL})_4$ <sup>35</sup> gave exceptionally clean reactions (entries 9 and 10). The best results were obtained with  $\text{Rh}_2(\text{S-TCPTTL})_4$ , which generated **98a** in 81% yield with 91% *ee* without any traces of byproduct **99** (entry 9). The dramatic change in product distribution with the tetrachloro- and tetrabromophthalimide catalysts indicates that these catalysts cause the carbene to react with methyl 2-furoate initially at the  $\beta$ -position.

In order to support this theory, a control experiment should demonstrate, that the formation of **99** already occurs during the reaction and not afterwards (scheme 17). Therefore, a solution of cyclopropane **98a** in DCM was refluxed in the presence of  $\text{Rh}_2(\text{S-DOSP})_4$ , which was shown to promote the ring-opening of the furan moiety in previous experiments (table 1). After six hours, no generation of **99**, as well as the corresponding epimerization products of **98a** were detectable from the crude <sup>1</sup>H-NMR. This result excludes that the ring opening process takes place after initial formation of cyclopropane **98a**.



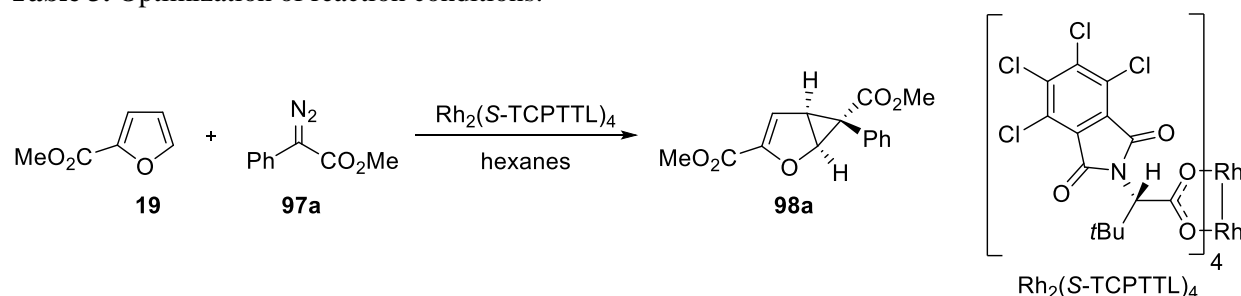
**Scheme 17.** Possible formation of diene **99** and the corresponding epimerization product (**(epi)-98a**) from cyclopropane **98a**.

## 1.3.2 Optimization of reaction conditions and catalyst loading

It is well-known that lowering the temperature can have positive effects on selectivity. Investigating this concept for the  $\text{Rh}_2(\text{S-TCPTTL})_4$ -catalyzed cyclopropanation of furan **19** with diazo ester **97a** revealed 0 °C as the optimum reaction temperature, generating **98a** with slightly improved enantioselectivity compared to room temperature (Table 3, entry 1 vs. 2, 91% *ee* vs. 96% *ee*). In contrast, a further decrease of the temperature to -40 °C led to reduced selectivity accompanied by a considerably diminished yield (entry 2 vs. 3, 96% *ee* vs. 93% *ee*).

It is well-established, that donor-acceptor carbenoids are capable of operating at low catalyst loadings.<sup>23,24</sup> Gratifyingly, decreasing the amount of  $\text{Rh}_2(\text{S-TCPTTL})_4$  from 1.0 mol% to 0.001 mol% did not greatly affect the outcome of the reaction regarding yield and enantioselectivity (entry 2 and 4-6) and **98a** was obtained in 86% yield (TON = 88000, TOF = 24/s) and with 96% *ee* (entry 6).

**Table 3.** Optimization of reaction conditions.<sup>†</sup>



entry <sup>a</sup>	temperature (°C)	catalyst load (mol%)	yield <sup>b</sup> (%)	<i>ee</i> <sup>c</sup> (%)
1	rt	1	81	91
2	0	1	88	96 <sup>d,e</sup>
3	-40	1	<48	93
4	0	0.1	88	96
5	0	0.01	92	96 <sup>f</sup>
6	0	0.001	86	96 <sup>f</sup>

<sup>a</sup>Standard reaction conditions: **97a** (1.0 equiv) in dry hexanes was added to **19** (2.0 equiv) in dry hexanes and  $\text{Rh}_2(\text{S-TCPTTL})_4$  over 1 h. <sup>b</sup>Isolated yield. <sup>c</sup>Determined by chiral HPLC analysis. <sup>d</sup>>99% *ee* after recrystallization <sup>e</sup>Absolute configuration of **98a** was determined by X-ray crystallography. <sup>f</sup>Isolation was carried out by filtration from the crude reaction mixture.

<sup>†</sup> Entry 5 is taken from the Bachelor thesis of F. Ostler, 2015, Universität Regensburg (supervised by V. Lehner)

A notable feature of this reaction is that cyclopropane **98a** already precipitates from the reaction mixture. Since furan **19**, which was used in excess, as well as  $\text{Rh}_2(\text{S-TCPTTL})_4$  are soluble in hexanes, purification of **98a** can be performed by simple filtration. The high efficiency of  $\text{Rh}_2(\text{S-TCPTTL})_4$  in combination with the ease of purification make this reaction a promising candidate for up-scaling. Notably, reactions up to 74 mmol were already successfully performed (table 3, entry 6)

A single recrystallization from methanol gave access to enantiopure **98a**, and the absolute configuration of **98a** was unambiguously assigned by X-ray crystallography (figure 5).

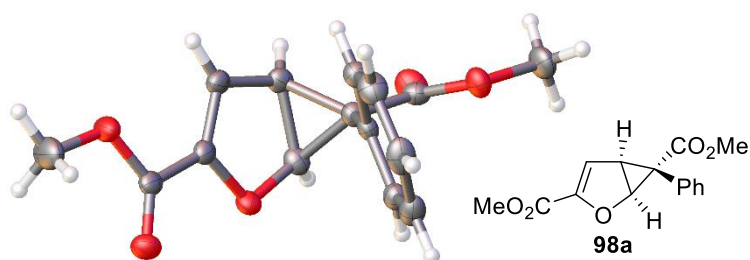
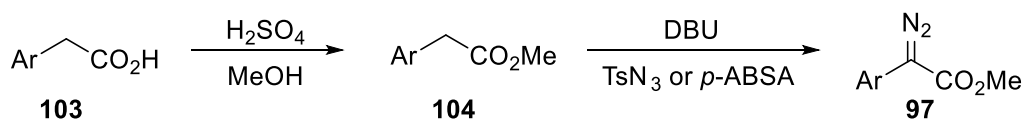


**Figure 5.** X-ray structure of cyclopropane **98a**.

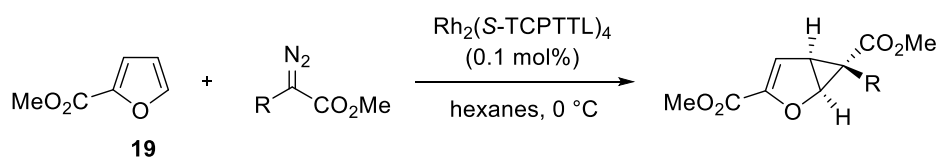
## 1.3.3. Substrate scope of aryl groups on the carbenoid

Previous reports of *Davies* and co-workers<sup>48</sup> have shown, that the nature of the aryl substituent on aryl diazoacetates strongly affect the asymmetric induction imparted by chiral Rh(II)-catalysts in cyclopropanation reactions with styrene as a model substrate. Due to the promising results, that have been obtained in the Rh<sub>2</sub>(*S*-TCPTTL)<sub>4</sub>-catalyzed cyclopropanation reaction of furan **19** with diazo ester **97a** (see chapter B.1.3.2), the effect of different aryl groups on the enantioselectivity for this reaction was investigated. Therefore, several aryl diazo esters (**97**) were synthesized according to a literature-known two-step procedure,<sup>51,52</sup> which includes an acid catalyzed esterification of starting materials **103** followed by a Regitz diazo-transfer with tosyl azide or 4-acetamidobenzenesulfonyl azide (*p*-ABSA) as diazo-transfer reagents (scheme 18).



**Scheme 18.** General method to synthesize diazo esters of type **97**.<sup>51,52</sup>

The cyclopropanation could be applied to a range of aryl diazoacetates as illustrated in table 4. Electron-rich aryl groups (entry 2 and 3) performed well, providing the cyclopropanes **98b** and **98c** in good yields (81%, 85%) and excellent levels of enantioselectivity (both 95% *ee*), respectively. The best results regarding enantioinduction were obtained by applying halo-substituted aryl groups (entry 4 and 5), giving access to cyclopropanes **98d** and **98e** in good yields (78%, 81%) and excellent levels of enantioselectivity (both 98%). Employing larger (entry 6) or strongly electron-withdrawing groups (entry 7) resulted in a considerable drop in yield (65%, 57%), generating cyclopropanes **98f** and **98g** with slightly diminished levels of enantioselectivities (87, 93%). Methyl diazoacetate (**79**), with just an acceptor group, gives poor results in the cyclopropanation (entry 8). This is routinely the case for diazoacetate cyclopropanations with the dirhodium tetracarboxyate catalysts,<sup>53</sup> but fortunately, copper(I)bis(oxazoline) catalysts give high levels of enantioselectivity (up to 94% *ee*)<sup>17</sup> with this reagent (see chapter B.1.1, scheme 12).

**Table 4.** Examination of the influence of substitution on aryl diazoacetate.<sup>a</sup>

entry	diazo ester	R	product	yield <sup>a</sup> (%)	<i>ee</i> <sup>b</sup> (%)
1	<b>97a</b>	C <sub>6</sub> H <sub>5</sub>	<b>98a</b>	88	96
2	<b>97b</b>	4-CH <sub>3</sub> OC <sub>6</sub> H <sub>4</sub>	<b>98b</b>	81	95
3	<b>97c</b>	4-CH <sub>3</sub> C <sub>6</sub> H <sub>4</sub>	<b>98c</b>	85	95
4	<b>97d</b>	4-ClC <sub>6</sub> H <sub>4</sub>	<b>98d</b>	81	98
5	<b>91</b>	4-BrC <sub>6</sub> H <sub>4</sub>	<b>98e</b>	78	98
6	<b>97f</b>	2-Naphthyl	<b>98f</b>	65	93
7	<b>97g</b>	4-NO <sub>2</sub> C <sub>6</sub> H <sub>4</sub>	<b>98g</b>	57	87
8	<b>79</b>	H	<b>83</b>	36	8

<sup>a</sup>Standard reaction conditions: diazo ester (1.0 mmol, 1.0 equiv) in dry hexanes and DCM (2 mL) was added to **19** in dry hexanes (0.5 M, 2.0 mmol, 2.0 equiv) and Rh<sub>2</sub>(S-TCPTTL)<sub>4</sub> (0.001 mmol, 0.1 mol%) at 0 °C over 1 h.

### 1.4 Asymmetric cyclopropanation of furan derivatives and thiophene<sup>‡</sup>

Having identified  $\text{Rh}_2(\text{S-TCPTTL})_4$  as an excellent catalyst for the reaction of **19** with a range of aryl diazoacetates (see chapter B.1.3.3), the cyclopropanation was then extended to other furans to determine if they would also react cleanly without unravelling of the furan moiety under previously optimized conditions (table 5).

**Table 5.** Scope of heterocycles.<sup>a,§</sup>

entry	heterocycle	product	yield (%)	ee (%)
1			73	86
2			72	74
3			91	25
4			0	-

<sup>a</sup>Standard reaction conditions: **97a** (1.0 mmol, 1.0 equiv) in dry hexanes and DCM (2 mL) was added to **19** in dry hexanes (0.5 M, 2.0 mmol, 2.0 equiv) and  $\text{Rh}_2(\text{S-TCPTTL})_4$  (0.001 mmol, 0.1 mol%) at 0 °C over 1 h.

<sup>‡</sup> This chapter is partially based on Lehner, V.; Davies, H. M. L.; Reiser, O. *Rh(II)-Catalyzed Cyclopropanation of Furans and Its Application to the Total Synthesis of Natural Product Derivatives*. *Org. Lett.* **2017** (accepted)

<sup>§</sup>Entry 1 is taken from the Bachelor thesis of F. Ostler, 2015, Universität Regensburg (supervised by V. Lehner)

The reaction with 3-methyl furoate (**105**) gave the cyclopropane **108** in 86% *ee*, whereas the reaction of furan (**14**) gave the cyclopropane **109** in 74% *ee*. No evidence of ring opening products was observed, indicating that the reaction was not being initiated at the  $\alpha$ -position of the furan (see chapter B.1.3.1, scheme 16). Recrystallization gave access to enantiopure **108** and **109**, and the absolute configurations were unambiguously assigned by X-ray crystallography (figure 6). In contrast, the reaction with benzofuran (**8**) proceeded with low levels of enantioselectivity, suggesting that distinction between  $\alpha$ - and  $\beta$ -position is not as effective here.

Thiophene (**107**) is known as a quite challenging substrate in cyclopropanation reactions.<sup>54</sup> Although  $\text{Rh}_2(\text{S-TCPTTL})_4$  is an excellent catalyst for the reaction of furans with donor-acceptor diazo esters, attempts to extend the scope of heterocycles to **107** resulted in a complex mixture of products, and none of cyclopropane **111** was formed.

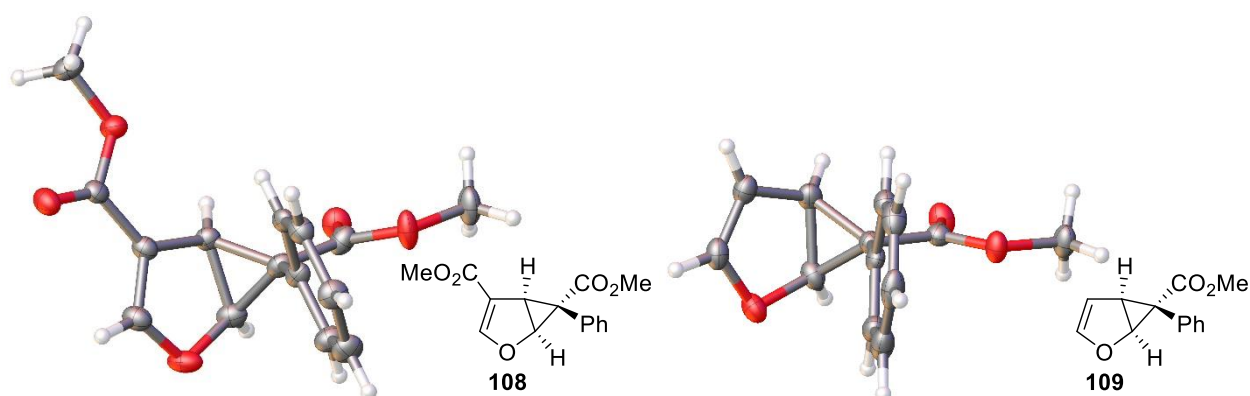
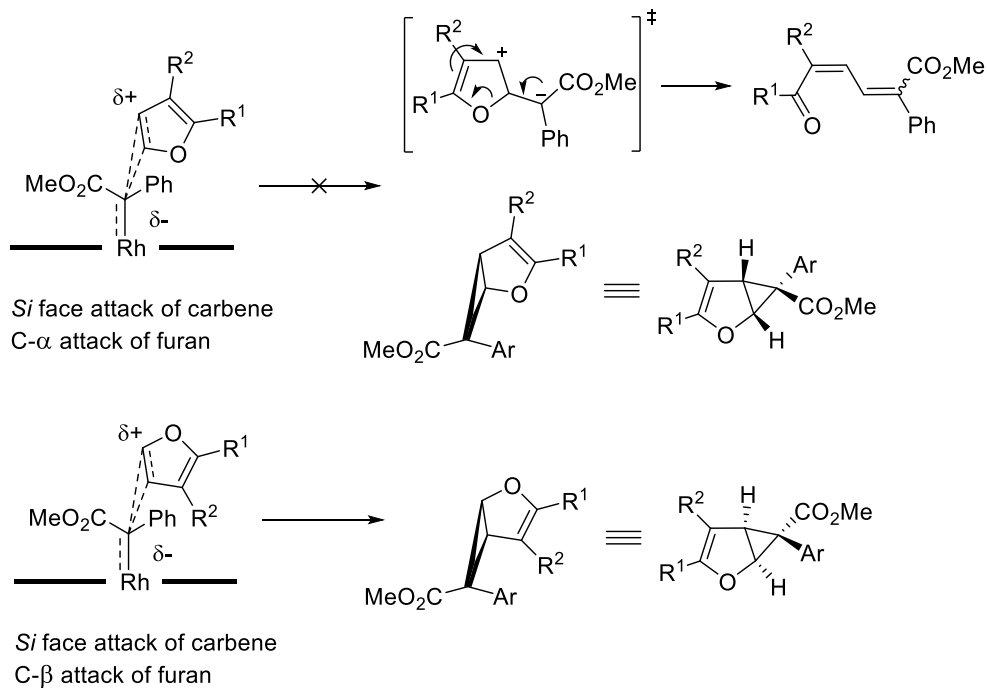


**Figure 6.** X-ray structures of cyclopropanes **108** and **109**.

The X-ray crystallographic analysis of monocyclopropanated furans **98a**, **108** and **109** revealed that all three products had been formed with the same sense of asymmetric induction (figure 5 and 6). These results are different from what had been reported in the  $\text{Rh}_2(\text{S-DOSP})_4$  catalyzed<sup>26</sup> donor/acceptor carbene reactions,<sup>27,31–33</sup> where the sense of asymmetric induction changed, depending on the structure of the furan (see chapter B.1.1).

Both experimental and computational studies have shown that  $\text{Rh}_2(\text{S-TCPTTL})_4$  and  $\text{Rh}_2(\text{S-TCPTAD})_4$  cause the reaction of the rhodium bound carbene to occur from the *si* face of the carbene.<sup>55–57</sup> Using the same orientation of attack, the observed stereochemistry is consistent with attack occurring at the  $\beta$ -position for all three furan derivatives (scheme 19). This means that  $\text{Rh}_2(\text{S-TCPTTL})_4$  and  $\text{Rh}_2(\text{S-TCPTAD})_4$  which have a well-defined “chiral bowl”<sup>56</sup> do not accommodate the approach of the furan at the  $\alpha$ -position with the oxygen of the furan pointing

towards the catalysts. Therefore, none of the ring opening products were observed with these catalysts (see also chapter B.1.3.1). The different behavior illustrates the subtle influences that the catalysts can have on the selectivity of donor/acceptor carbene reactions.



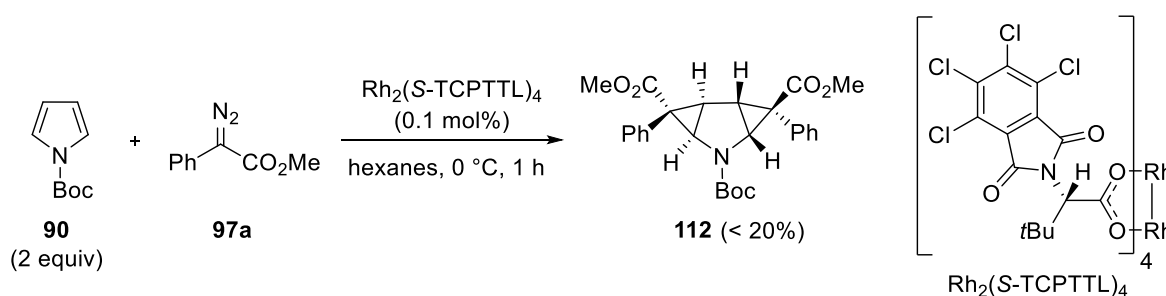
**Scheme 19.** Model for Rh<sub>2</sub>(*S*-TCPTTL)<sub>4</sub> cyclopropanation.



## 1.5 Asymmetric cyclopropanation of pyrroles

In analogy to furans, the cyclopropanation of pyrroles with acceptor diazo esters paved the road for a great range of diverse chemistry and was elegantly exploited in several target-oriented syntheses (see chapter A.3).<sup>18</sup> In contrast to furans, the reactivity of pyrrole is adjustable by means of altering the protection group on the nitrogen.<sup>9,11</sup> Very electron-rich heteroarenes like *N*-H or *N*-alkyl pyrroles are expected to favor a zwitterionic pathway since the nitrogen lone pair is highly capable of stabilizing the positive charge on the intermediate (analog to zwitterion **102**, see chapter 1.3.1, scheme 16).<sup>58</sup> However, incorporation of an electron-withdrawing group on the nitrogen atom causes the aromatic ring to be less electron-rich and thus, reduces the tendency to form zwitterionic intermediates.<sup>9,59</sup> Therefore, electron-withdrawing protection groups seemed to be the best choice for the following investigations in order to synthesize monocyclopropanes.

Due to its electron-withdrawing effect and ease of removal, Boc (*tert*-butoxycarbonyl)<sup>60,61</sup> was selected as protecting group for an initial test reaction. Under optimized conditions, attempts to extend the reaction scope to *N*-Boc pyrrole (**90**) were not very successful since almost no conversion of **90** was observable and only minor amounts of doublecyclopropanated product (< 20%) were obtained (scheme 20). This outcome was rather unexpected due to previously reported results, which showed that the reaction of pyrrole **90** in the presence of Rh<sub>2</sub>(*S*-DOSP)<sub>4</sub> generates cyclopropanes in high yields and good levels of enantioselectivity (for details see chapter B.1.1).<sup>27</sup> In regard to the low yield for cyclopropane **112**, optimization approaches aiming at the synthesis of monocyclopropanes did not promise success, and thus a new synthetic strategy was developed.



**Scheme 20.** Asymmetric cyclopropanation of *N*-Boc pyrrole (**90**).

*Charette* and co-workers<sup>57</sup> have shown that Rh<sub>2</sub>(*S*-TCPTTL)<sub>4</sub> adopts an all-up symmetry. In this conformation, one axial site is shielded by the four *tert*-butyl-groups of the ligands, whereas the reactive Rh-center is embedded in an ellipsoidal chiral pocket formed by the

tetrachlorophthaloyl moieties. It was assumed that the *N*-Boc-group in **90** might be too bulky to fit into the chiral pocket of the catalyst. In order to prove this theory, the influence of the protecting group on the nitrogen atom on the outcome of the reaction with regard to steric as well as electronic properties was investigated. The synthesis of the starting materials and the results of this study are presented in the following chapters.

### 1.5.1 Synthesis of *N*-protected pyrroles

Along with the growing interest in pyrrole chemistry due to the abundance of the pyrrolic moiety in pharmaceuticals, natural products, and new materials, a great number of protection strategies for pyrroles were developed.<sup>60</sup> With regard to the planned cyclopropanation study, a number of *N*-protected pyrroles (**113a-113e**), bearing electron-withdrawing *N*-sulfonyl or *N*-carboxyl protection groups with varying steric demands, were synthesized (figure 7).

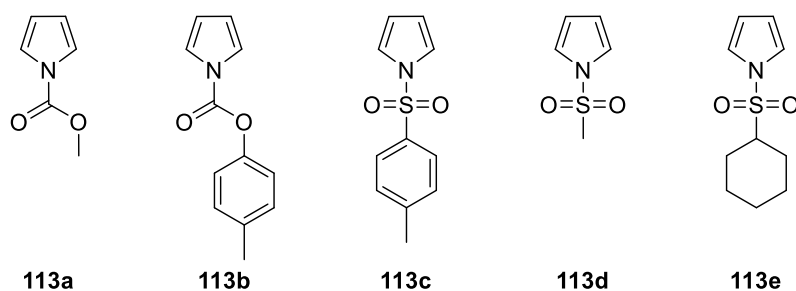
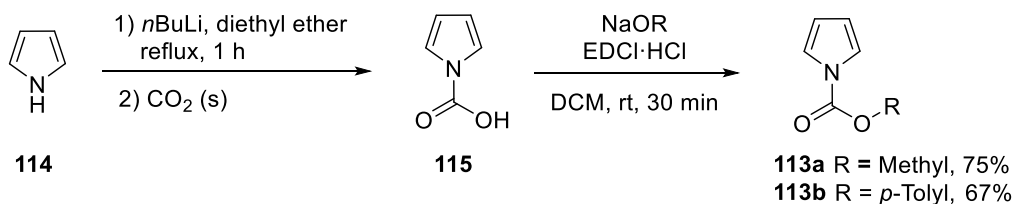


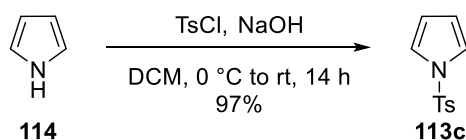
**Figure 7.** Overview of all synthesized *N*-protected pyrroles (**113a-113e**).

Deprotonation of pyrrole (**114**) with *n*-butyl lithium followed by carboxylation gave access to pyrrole-1-carboxylic acid (**115**), which served as starting point for *N*-carboxyl protected pyrroles **113a** and **113b** (scheme 21). Activation of acid **115** with carbodiimide EDCI·HCl similar to a *Steglich* esterification and subsequent treatment with the sodium salts of methanol or *p*-cresol afforded *N*-carboxyl protected pyrroles **113a** and **113b** in good yields, respectively.<sup>62</sup>



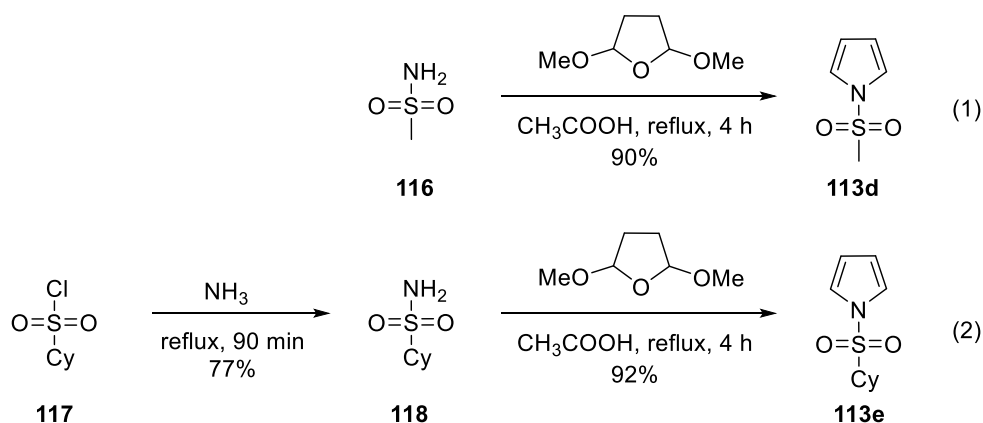
**Scheme 21.** Synthesis of *N*-protected pyrroles **113a** and **113b**.<sup>62</sup>

A quite general approach to introduce sulfonyl groups on the nitrogen of pyrrole represents the reaction of the pyrrolyl anion with sulfonyl halides. Applying this method, *N*-tosyl pyrrole **113c** has been prepared in 97% yield from 4-toluenesulfonyl chloride and the sodium anion of pyrrole (scheme 22).<sup>63</sup>



**Scheme 22.** Synthesis of *N*-protected pyrrole **113c**.<sup>63</sup>

Alternatively, condensation of 2,5-dimethoxytetrahydrofuran with a variety of sulfonamides can be utilized to synthesize *N*-sulfonyl pyrroles.<sup>64</sup> Thus, pyrroles **113d** and **113e** were readily formed from the corresponding sulfonamides **116** and **118** (scheme 23). The applied sulfonamides were either commercially available or synthesized from suitable sulfonylchloride precursor (**117**)<sup>65</sup> and liquid ammonia (scheme 23, eq 2) at reflux.



**Scheme 23.** Synthesis of *N*-protected pyrroles **113d** and **113e**.<sup>64,65</sup>

## 1.5.2 Effect of the protecting group

In order to examine, whether the poor yields for the reaction of pyrrole **90** can be traced back to the sterical demand of the *N*-Boc group, the reaction was carried out with pyrrole **113a**, bearing a less bulky methyl ester at the nitrogen. Indeed, the reaction of pyrrole **113a** generated cyclopropane **119a** at least in low yield (8%), though the corresponding double cyclopropanation product **120a** was formed in 26% yield (Table 6). Due to the poor solubility of *N*-protected pyrroles **113a-113e** in hexanes (optimized condition for furans, see chapter B.1.3), toluene was used as solvent for these experiments. The reaction of pyrrole **90** (scheme 20) was repeated using toluene as solvent, but no significant improvement in yield was observed under these modified conditions as judged by crude <sup>1</sup>H-NMR analysis.

**Table 6.** Examination of the influence of pyrrole protecting groups.\*\*

entry <sup>a</sup>	pyrrole	protecting group	product	yield <sup>b</sup> (%)	ee <sup>c</sup> (%)	product	yield <sup>b</sup> (%)
1	<b>113a</b>	Methyl ester	<b>119a</b>	8	7	<b>120a</b>	26 (52)
2	<b>113b</b>	<i>p</i> -Tolyl ester	<b>119b</b>	40	57	<b>120b</b>	27 (54)
3	<b>113c</b>	Tosyl	<b>119c</b>	61	93 <sup>d,e</sup>	<b>120c</b>	15 (31)
4	<b>113d</b>	Mesyl	<b>119d</b>	n.d.	87	<b>120d</b>	n.d.
5	<b>113e</b>	SO <sub>2</sub> -Cy	<b>119e</b>	40	94	<b>120e</b>	21 (42)

<sup>a</sup>Standard reaction conditions: **97a** (1.0 equiv) in dry toluene (2 mL) was added to **113a-e** in dry toluene (2.0 equiv) and Rh<sub>2</sub>(*S*-TCPTTL)<sub>4</sub> (0.1 mol%) at 0 °C over 1 h. <sup>b</sup>Isolated yield. <sup>c</sup>Determined by HPLC analysis. <sup>d</sup>>99% *ee* after recrystallization. <sup>e</sup>Absolute configuration was determined by X-ray crystallography.

Since the Rh<sub>2</sub>(*S*-TCPTTL)<sub>4</sub>-catalyzed cyclopropanation of **113a** with **97a** revealed to be a poor reaction in terms of enantioinduction (7% *ee*), the influence of further protecting groups on the outcome of the reaction was examined. Thus, it turned out that pyrroles with sulfonyl protection groups provided considerably higher levels of enantioselectivity compared to their ester

\*\* Results are partially taken from the Bachelor thesis of N. Wurzer, 2016, Universität Regensburg (supervised by V. Lehner)

analogues (entry 3 vs. 2, 93% *ee* vs. 57% *ee*; entry 4 vs. 1, 87% *ee* vs. 7% *ee*). Furthermore, sulfonyl protected pyrroles **113c** and **113e** favored the formation of the monocyclopropanated products **119c** and **119e** in the presence of  $\text{Rh}_2(\text{S-TCPPL})_4$ . X-ray analysis of **119c** (figure 8) revealed that the four substituents at the sulfur atom are nearly arranged in tetrahedral form, orienting the toluene group preferentially on the convex face of the bicyclic framework, and thus making a second cyclopropanation unfavorable. However, comparing the yields of **119c** and **119e** (61% vs. 40%),  $\pi$ -stacking interactions of the protecting group and the aromatic ligands of the catalyst also seem to have an impact on the product formation.

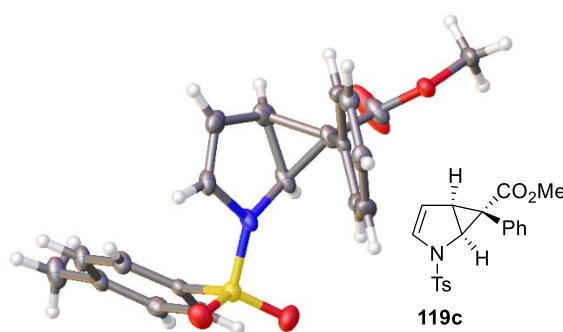
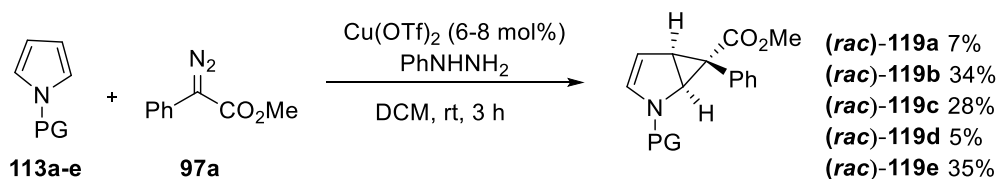


**Figure 8.** X-ray structure of cyclopropane **119c**.

Determination of the enantiomeric excess of **119a-e** necessitated prior synthesis of the analog racemic cyclopropanes. In the case of furan derivatives, this was readily achieved by using  $\text{Rh}_2(\text{OAc})_4$  or  $\text{Rh}_2(\text{OPiv})_4$ . However, pyrroles **113a-e** showed a strong tendency towards double cyclopropanation under these conditions, and thus, monocyclopropanes **119a-e** could not be observed.



**Scheme 24.** Racemic cyclopropanation of *N*-protected pyrroles **113a-e**.<sup>††</sup>

It was shown that pyrroles tend to form the monocyclopropanation products with acceptor diazo esters by using catalytic amounts of copper(II) triflate, activated by phenylhydrazine.<sup>12</sup> Applying this catalytic system for the reactions of pyrroles **113a-e** with diazo ester **97a** finally

<sup>††</sup> Results are partially taken from the Bachelor thesis of N. Wurzer, 2016, Universität Regensburg (supervised by V. Lehner)

gave access to monocyclopropanes (*rac*)-**119a-e**, albeit in low to moderate yields (5-35%) (scheme 24). Nevertheless, sufficient amounts for HPLC were obtained. It is notable that attempts to render the reaction of **113c** asymmetric under these conditions by addition of chiral box-ligand **74** failed. Hence, studies with Rh(II)-catalysts were continued.

## 1.6 Asymmetric cyclopropanation of *N*-tosyl pyrrole (**113c**)

### 1.6.1 Optimization studies

Rhodium catalysts with *N*-imidyl amino acid ligands were shown to be highly active catalysts for cyclopropanation reactions, even at  $-78\text{ }^{\circ}\text{C}$ .<sup>66</sup> In search of optimum conditions for the  $\text{Rh}_2(\text{S-TCPTTL})_4$ -catalyzed reaction of *N*-tosyl pyrrole **113c**, an examination of the temperature profile revealed that lowering the reaction temperature from  $0\text{ }^{\circ}\text{C}$  to  $-10\text{ }^{\circ}\text{C}$  resulted in a slight decrease in selectivity accompanied by considerably diminished yield (table 7, entry 1 vs 2). Hence, no further efforts were made to study the influence of the temperature on the selectivity.

**Table 7.** Optimization of reaction conditions.<sup>‡‡</sup>

entry <sup>a</sup>	temperature ( $^{\circ}\text{C}$ )	<b>113c</b> (equiv)	yield <sup>b</sup> <b>119c</b> (%)	<i>ee</i> <sup>c</sup> <b>119c</b> (%)	yield <sup>b</sup> <b>120c</b> (%)	Ratio <sup>d</sup> <b>119c/120c</b>
1	0	2	60	93 <sup>e,f</sup>	15 (31)	4.2/1
2	-10	2	45	90	11 (22)	n.d.
3	0	4	69	n.d.	8(16)	7.2/1
4	0	10	39	n.d.	-	>20/1

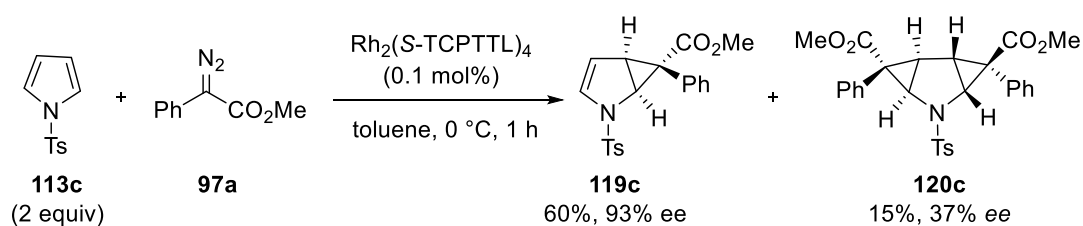
<sup>a</sup>Standard reaction conditions: **97a** (1.0 mmol, 1.0 equiv) in dry toluene was added to **113c** in dry toluene (2.0 equiv) and  $\text{Rh}_2(\text{S-TCPTTL})_4$  (0.001 mmol, 0.1 mol%) over 1 h. <sup>b</sup>Isolated yield. <sup>c</sup>Determined by HPLC analysis. <sup>d</sup>Determined by  $^1\text{H-NMR}$  analysis of the crude mixture. <sup>e</sup>>99% *ee* after recrystallization. <sup>f</sup>Absolute configuration was determined by X-ray crystallography.

With the absolute goal of synthesizing monocyclopropanes, it was supposed, that an increasing excess of pyrroles could reduce the tendency to form bicyclopropanes. Indeed, by applying a two-, four- and ten-fold excess of **113c** a clear trend with regard to product distribution was observable (table 7, entries 1, 3 and 4). However, increasing the relative amount of **113c** caused difficulties in purification, and thus led to comparatively diminished isolated yields (entry 4).

<sup>‡‡</sup> Results are partially taken from the Bachelor thesis of N. Wurzer, 2016, Universität Regensburg (supervised by V. Lehner)

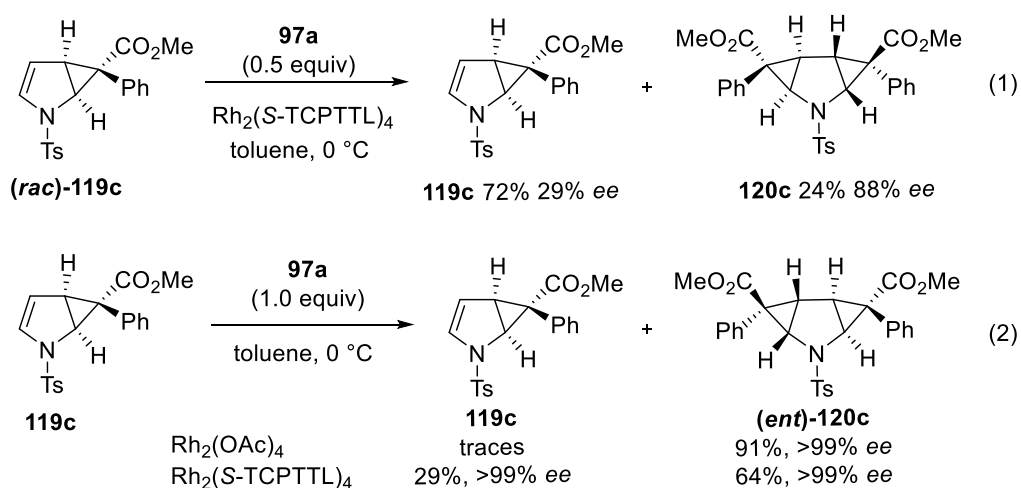
## 1.6.2 Kinetic resolution

During the course of our cyclopropanation studies with pyrrole **113c**, an interesting phenomenon was observed (scheme 25). While the initial cyclopropanation of **113c** with **97a** in the presence of  $\text{Rh}_2(\text{S-TCPTTL})_4$  provided monocyclopropane **119c** in 93% *ee*, bicyclopropane **120c** was formed with an unexpectedly low level of enantioselectivity (37% *ee*).



**Scheme 25.** Asymmetric cyclopropanation of *N*-tosyl pyrrole **113c**.

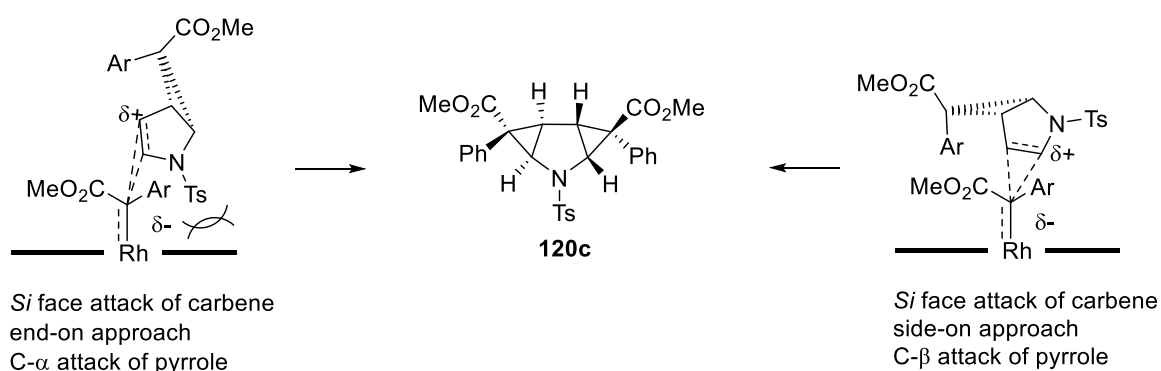
To examine, whether the second cyclopropanation event has an impact on the asymmetric induction, monocyclopropane (*rac*)-**119c** was subjected to a  $\text{Rh}_2(\text{S-TCPTTL})_4$ -catalyzed cyclopropanation reaction in the presence of **97a** (scheme 26, eq. 1). This experiment revealed that kinetic resolution occurred in this reaction since enantioenriched **119c** was recovered in 29% *ee* and 72% yield and double cyclopropanation product **120c** was formed in 88% *ee* and 24% yield.



**Scheme 26.** Kinetic resolution experiments.



Interestingly, the actually mismatched enantiomer (*ent*)-**119c** reacts preferentially in the second cyclopropanation event. Considering the model for  $\text{Rh}_2(S\text{-TCPTTL})_4$  catalyzed cyclopropanation of furans (see chapter B.1.4, scheme 19), the second cyclopropanation of (*ent*)-**119c** would be expected to initiate at the  $\beta$ -position, but this is inconsistent with the observed stereochemistry in **120c** (scheme 27). If the double bond approaches the carbenoid in an end-on manner, the initial attack has to occur at the  $\alpha$ -position to form the observed diastereomer, which is highly unfavorable due to steric as well as electronic grounds. This result indicates that a side-on approach<sup>26,67</sup> of (*ent*)-**119** is more likely, since (*ent*)-**119** would be the matched enantiomer in this case.



**Scheme 27.** Model for  $\text{Rh}_2(S\text{-TCPTTL})_4$  cyclopropanation of (*ent*)-**119c**.

If enantiopure **119c** was subjected to a second Rh(II)-catalyzed cyclopropanation reaction in the presence of **97a** (scheme 25, eq. 2), enantiopure (*ent*)-**120c** was isolated, regardless of the catalysts. This demonstrates that the enantioinduction of the second cyclopropanation event is substrate controlled and not influenced by the chiral catalyst. The absolute configuration of **119c** and (*ent*)-**120** was determined by X-ray crystallography (figure 8 and 9).

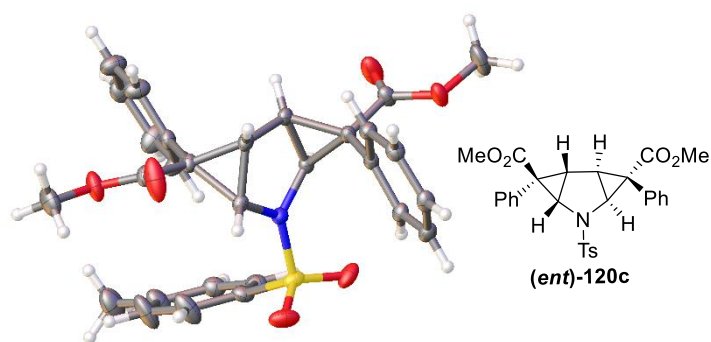
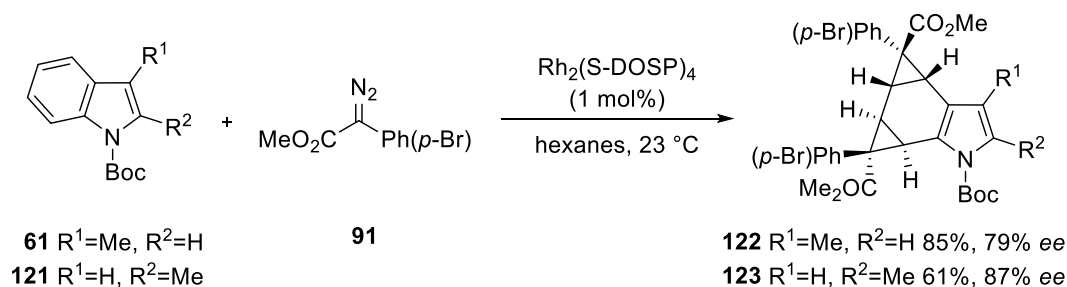


**Figure 9.** X-ray structures bicyclopentane (*ent*)-**120c**.

### 1.7 Asymmetric cyclopropanation of *N*-tosyl indole **125**

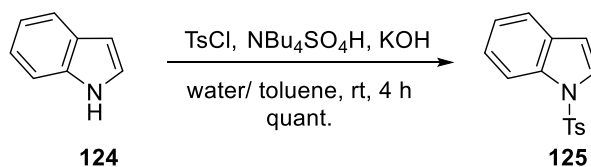
The synthesis and functionalization of indole and its derivatives have attracted great attention due to their important roles in numerous research areas, like medicinal chemistry and material science<sup>68</sup>. Although a great number of asymmetric metal-based, as well as metal-free asymmetric indole functionalization methods have been developed,<sup>69</sup> indoles have rarely been employed in asymmetric cyclopropanation reactions.<sup>9</sup> Recently, the first enantioselective intermolecular cyclopropanation of *N*-protected indoles with acceptor diazo ester **20** was reported by *Boysen* and co-workers<sup>14</sup> (for details see chapter B.1.1., scheme 12). However, the analog transformation with donor acceptor diazo esters has turned out to be challenging.<sup>9</sup>  $\text{Rh}_2(\text{S-DOSP})_4$ , an excellent catalyst for the asymmetric cyclopropanation of several electron-rich heteroarenes with aryl diazo esters, was shown to be ineffective in catalyzing the reaction of unsubstituted *N*-Boc indole, resulting in recovery of the starting material along with products deriving from carbene dimerization.<sup>27</sup> Interestingly, the analog transformation of 2- and 3-substituted indoles **61** and **121** provided bicyclopropanes **122** and **123**, arising from double cyclopropanation of the benzenoid ring (scheme 28). Studies of *Davies* and co-workers<sup>27</sup> have shown, that an initial bond formation at the pyrrole moiety of the indole core is inhibited by the sterical clash between the rhodium catalyst and either the *N*-Boc group or the benzenoid ring.



**Scheme 28.**  $\text{Rh}_2(\text{S-DOSP})_4$ -catalyzed cyclopropanation of *N*-Boc indoles **61** and **121** by *Davies et al.*<sup>27</sup>

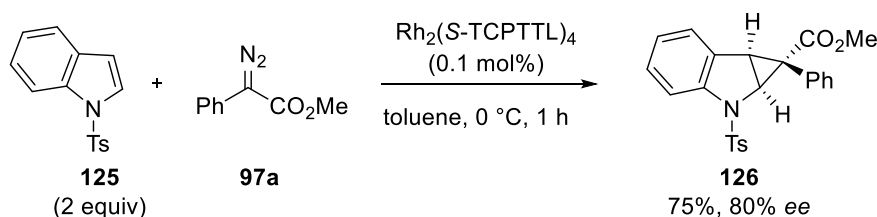
During the studies with pyrroles (see chapter B.1.5), it became obvious, that the reaction outcome is significantly influenced by the catalyst as well as the protecting group. The interplay of  $\text{Rh}_2(\text{S-TCPTTL})_4$  and *N*-tosyl protecting group was shown to be beneficial in the reaction with pyrrole. Hence, it was investigated, if the same is true for the cyclopropanation of indole.

Starting material **125** was readily prepared in quantitative yield from the potassium salt of indole and tosylchloride using tetrabutylammonium hydrogensulfate as phase transfer catalyst (scheme 29).<sup>70</sup>



**Scheme 29.** Synthesis of *N*-protected indole **125**.

Under the optimized reaction conditions, cyclopropane **126** was generated as a single diastereomer in 75% yield with 80% *ee*. It is notable that the heterocyclic ring was exclusively cyclopropanated, contrasting to previously reported results<sup>27</sup> for the asymmetric cyclopropanation of indoles with donor-acceptor diazo esters. The configuration of cyclopropane **126** was assigned by X-ray analysis.



**Scheme 28.** Asymmetric cyclopropanation of *N*-tosyl indole (**125**).<sup>§§</sup>

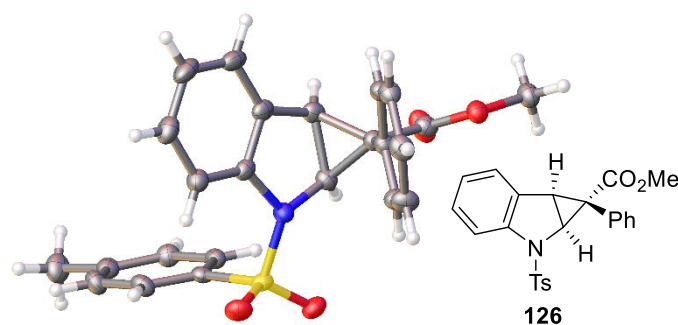


**Figure 10.** X-ray structure of cyclopropane **126**.

<sup>§§</sup> Experiment is taken from the Bachelor thesis of N. Wurzer, 2016, Universität Regensburg (supervised by V. Lehner)

## 1.8 Conclusion and outlook

In summary,  $\text{Rh}_2(\text{S-TCPTTL})_4$  was identified as an exceptionally effective catalyst in terms of catalyst loading (TON 88000 and TOF  $24 \text{ s}^{-1}$ ) and enantioinduction (up to 98% *ee*) for the generation of monocyclopropanated aromatic heterocycles. The developed protocol was applicable to furans, pyrroles, benzofurans, as well as indoles with a variety of donor-acceptor diazoesters. In the case of pyrrole, it was shown that the nature of the protecting group on the nitrogen has a great impact on the product formation (mono *vs.* doublecyclopropanation) and the best results were obtained by using the *N*-tosyl derivative (61%, 93% *ee*). Current experiments in the *Davies* group by *Jiantao Fu* are underway to extend the scope of diazoesters for the reaction of *N*-tosyl pyrrole and to also study the influence of the catalyst on the product distribution. Preliminary results indicate that by applying *N*-tosyl protected pyrrole both monocyclopropane, as well as doublecyclopropane, are selectively accessible in good yields and excellent levels of enantioselective by simply switching the catalyst.

## 2 Cyclopropane 119c as precursor for the synthesis of a homo- $\beta$ -proline analogue

### 2.1 Introduction – Pyrrolidines as catalysts and bioactive compounds

The pyrrolidine ring forms the core of various natural and unnatural compounds endowed with a host of biological activities and therapeutical properties.<sup>71,72</sup> A prominent synthetic drug containing this heterocycle as the central unit is captopril (Capoten™, **127**),<sup>73</sup> which was introduced to the market in the 1980s and has been established as a potent angiotensin converting enzyme (ACE) inhibitor (figure 11). Kanoid amino acids<sup>74</sup> (e.g. (-)- $\alpha$ -kainic acid (**130**)<sup>75</sup>, domoic acid (**128**)<sup>76</sup>) are conformationally restricted analogues of the neurotransmitter glutamic acid and have attracted considerable interest in recent years owing to their neuroexcitatory properties, as well as anthelmintic and insecticidal activities. Further examples from the about 80 known pyrrolidine alkaloids are (+)-hygrine (**129**)<sup>77</sup> and nicotine (**131**),<sup>78</sup> which have been the subject of numerous pharmacological and biological studies.<sup>79</sup>

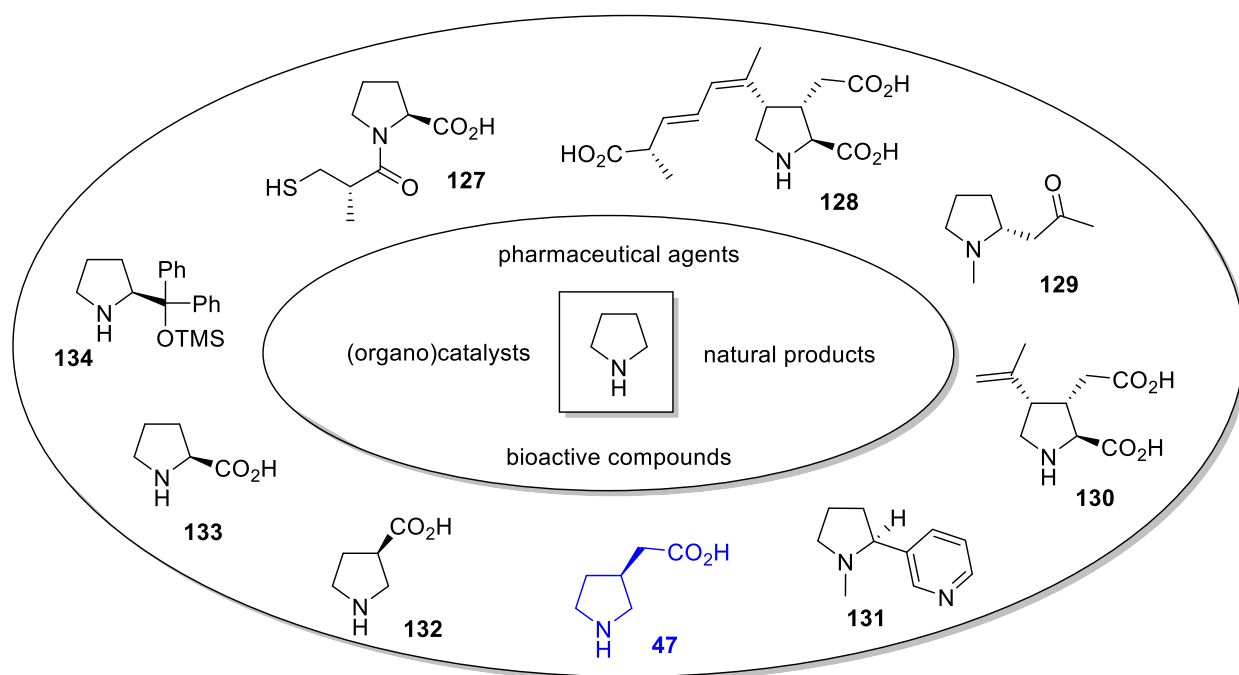


**Figure 11.** Chemical and biological interesting compounds containing the pyrrolidine ring as a central unit.

In catalysis, the pyrrolidine moiety has become ubiquitous, finding use as effective organocatalysts as well as ligands in asymmetric transition-metal catalyzed protocols.<sup>80–83</sup> In the early stage of asymmetric organocatalysis, (*S*)-proline (**133**), a non-essential amino acid, has played a key role.<sup>84</sup> Since then, an array of proline-derived catalysts have been developed

(e.g. (*R*)- $\beta$ -proline (**132**),<sup>85</sup> Hayashi-Jørgensen catalyst (**134**)<sup>86</sup>) and have expanded the scope of possible substrates and reactions. Thus, on the one hand, proline and its derivatives were demonstrated to be powerful catalysts for diverse transformations, such as epoxidation, aldol, Friedel–Crafts, Mannich and Michael reactions, etc.<sup>80–83</sup> On the other hand, functionalization and derivatization of the native proline moiety have emerged as an important tool to synthesize a myriad of naturally occurring molecules ranging from simple to highly complex compounds.<sup>79</sup> A proline derivative that has attracted considerable interest due to its structural analogy to  $\gamma$ -aminobutyric acid (GABA, **135**)<sup>87</sup> (figure 12), the most important inhibitory neurotransmitter in the mammalian brain, is (*S*)-homo- $\beta$ -proline (**47**).<sup>88</sup> GABA has been estimated to be present in 60-70% of all synapses in the central nervous system (CNS) and a number of neurological disorders, for instance, epilepsy, anxiety, pain and some forms of schizophrenia are associated with a dysfunction of the GABA system.<sup>89</sup> Several studies aiming at the evaluation of the biological potential of homo- $\beta$ -proline have shown that this conformationally restricted analogue of GABA is capable of interacting with distinct GABAergic targets. Racemic homo- $\beta$ -proline was found to be an agonist at postsynaptic GABA receptors. The (*R*)-enantiomer of homo- $\beta$ -proline binds selective to the GABA<sub>A</sub> receptor, whereas the moderate affinity for GABA<sub>B</sub> receptor sites is attributed to the (*S*)-enantiomer (**47**).<sup>90,91</sup> Furthermore, homo- $\beta$ -proline has an inhibitory effect on GABA transport proteins (GAT1), which ensure the reuptake of GABA in neuronal and astroglial cells.<sup>92</sup> The inhibitory potential of **47** was shown to be further increased by adding bulky lipophilic groups to the nitrogen (e.g. **136**), nearly reaching the potency of tiagabine (Gabitril™, **137**),<sup>92,93</sup> a GABA uptake inhibitor used for the treatment of epilepsy. Additionally, the homo- $\beta$ -proline moiety forms the core structure of a number of natural products (e.g. kanoid amino acids **128** and **130**, figure 11).<sup>74</sup> Taking into account the remarkable biological properties mentioned above, homo- $\beta$ -proline and its derivatives provide important targets in organic synthesis.

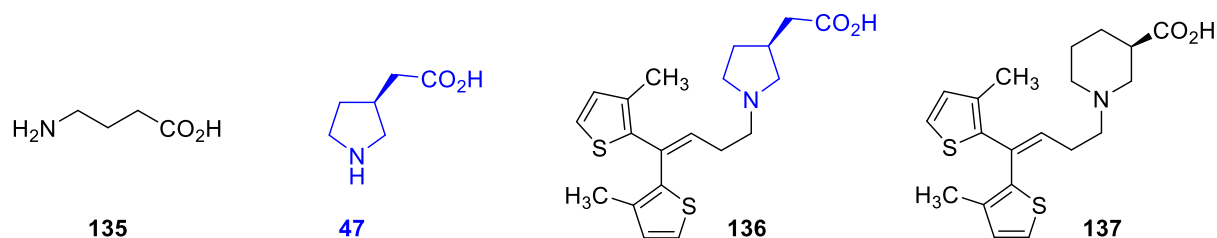
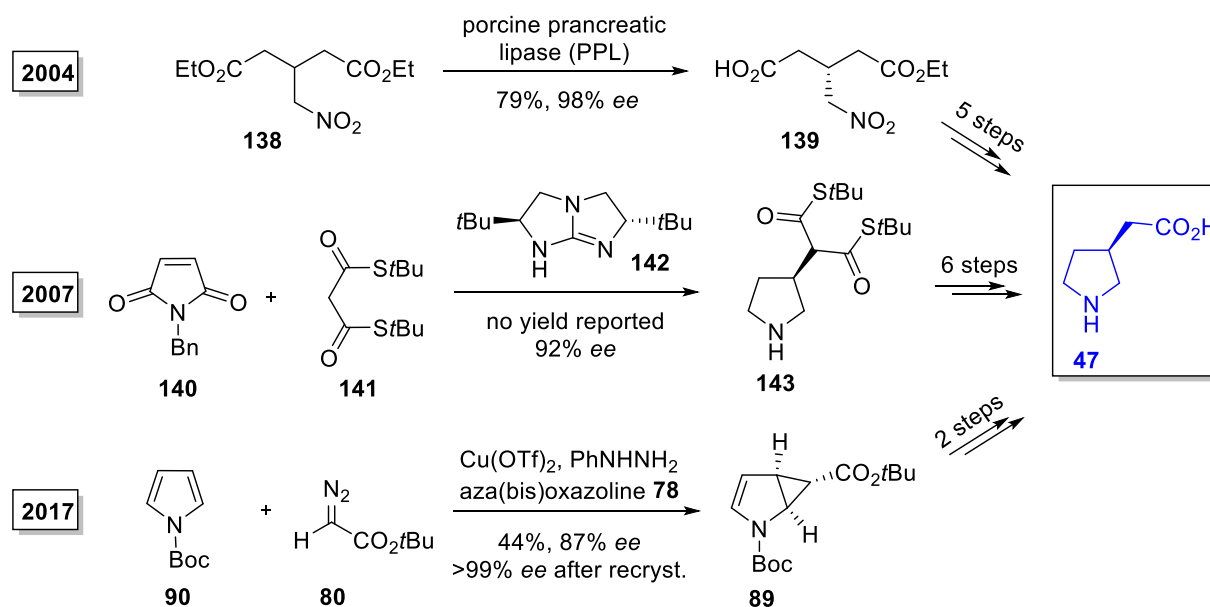


**Figure 12.** Chemical structures of GABA (**135**), GABA-related molecules (**47**, **136**) and tiagabine (**137**).

## 2.2 Enantioselective synthesis of homo- $\beta$ -proline – State of the art

A number of synthetic strategies yielding either racemic<sup>88,94</sup> or enantiopure homo- $\beta$ -proline were developed. However, most of the currently known methods to prepare (*S*)-**47** or (*R*)-**47** in enantiopure form are making use of chiral auxiliaries<sup>91,95</sup> or starting materials from the chiral pool.<sup>96</sup> Only three of these are of enantioselective nature (scheme 30).<sup>12,97,98</sup>



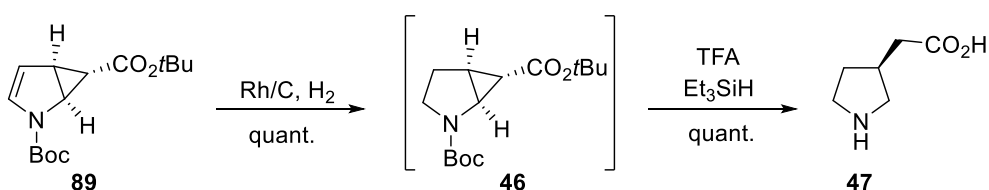
**Scheme 30.** Enantioselective synthesis of homo- $\beta$ -proline (**47**) – State of the art.<sup>12,97,98</sup>

In 2004, the first enantioselective synthesis of both enantiomers of homo- $\beta$ -proline was reported by *Felluga* and co-workers<sup>98</sup> utilizing an enzymatic transformation as key step. Desymmetrization of prochiral nitrodiester **138**, which was readily synthesized by a Michael addition of diethyl glutaconate and nitromethane, was accomplished by selective hydrolysis of the pro-*(R)* ester group of **138** in the presence of porcine pancreatic lipase (PPL). The resulting half-ester (*R*)-**139** was successfully transformed to (*S*)-homo- $\beta$ -proline (**47**) in 5 additional steps (7 steps, 38% overall yield). Alternatively, by using crude pig liver esterase (PLAP, pig liver acetone powder) instead of PPL in the desymmetrization step, (*R*)-homo- $\beta$ -proline (**(R)-47**) was accessible in 39% overall yield.

Three years later, *Tan* and co-workers<sup>97</sup> were able to develop an alternative approach to (*S*)-homo- $\beta$ -proline (**47**) in which an organocatalyzed Michael reaction was used to control the essential stereocenter. Chiral bicyclic guanidine **142** was shown to be an excellent catalyst for enantioselective Michael reactions of dithiomalonates and  $\beta$ -keto thioesters with a range of acceptors. Starting from *N*-benzyl maleimide **140** and dithiomalonate **141**, this method was

elegantly exploited for the synthesis of key intermediate **143**. Decarboxylation of one of the thioesters and functional group transformation led to (*S*)-homo- $\beta$ -proline (**47**) in 6 steps.

Recently, *Reiser* and co-workers<sup>12</sup> presented a straightforward synthetic route for (*S*)-homo- $\beta$ -proline (**47**) making use of an asymmetric Cu(I)-catalyzed cyclopropanation of *N*-Boc-pyrrole (**89**) to establish the required stereocenter in **47** (see also chapter B.1.1). Enantiomerically pure cyclopropane **89**, which was accessible in a multigram quantity by recrystallization, was transformed to **47** in a two-step sequence in quantitative yield (scheme 31). A ring-opening/ deprotection cascade finalized the synthesis of **47** and proceeded without loss of enantiopurity at 0 °C.



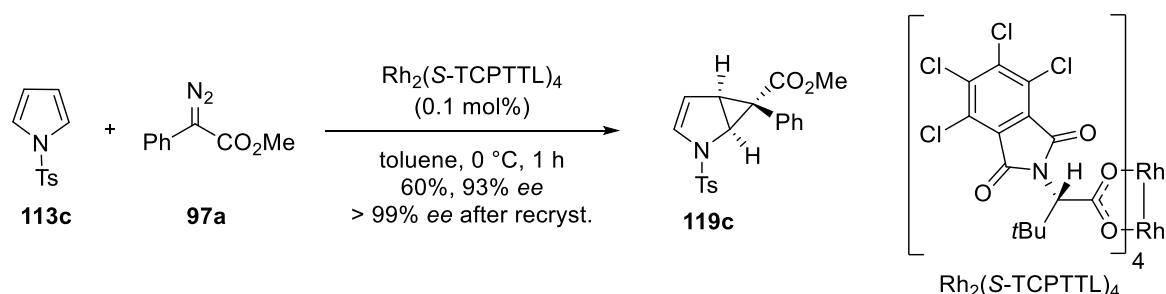
**Scheme 31.** Synthesis of (*S*)-homo- $\beta$ -proline (**47**) starting from cyclopropane **89** by *Reiser et al.*<sup>12</sup>

Inspired by this highly efficient synthetic route reported by *Reiser et al.* and encouraged by the interesting biological properties of homo- $\beta$ -proline and its derivatives (see chapter B.2.1), an analog transformation of cyclopropane **119c** aiming at the synthesis of a new, chiral homo- $\beta$ -proline analogue was investigated.



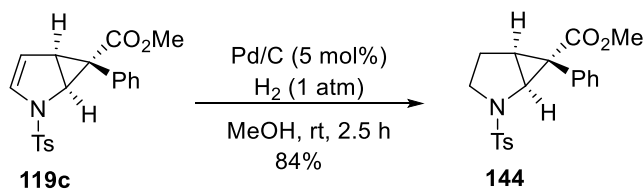
### 2.3 Synthesis of homo- $\beta$ -proline analogue **147**\*\*\*

In the previous section of this work, it was shown that monocyclopropane **119c** can be generated in good yield (60%) and excellent level of enantioselectivity (93% *ee*) from simple starting materials (scheme 32). The enantiopure material is readily accessible by a single recrystallization and low catalyst loading as well as short reaction time are required, making monocyclopropane **119c** a good starting point for further synthetic efforts. Taking the lead from the elegant work of the *Reiser* group on the employment of donor-acceptor substituted cyclopropanes derived from renewable resources,<sup>12,18</sup> the utility of cyclopropane **119c** was investigated with the synthesis of a chiral homo- $\beta$ -proline analogue.



**Scheme 32.** Enantioselective synthesis of cyclopropane **119c**.

In order to circumvent the formation of dimerization products originating from activation of the enamine moiety by protonation,<sup>12,15</sup> hydrogenation of the double bond in **119c** was performed under neutral conditions prior to acid-induced ring-opening. Performing the reaction with Pd/C at ambient pressure of hydrogen gave rise to adduct **144** in 84% yield (scheme 33).



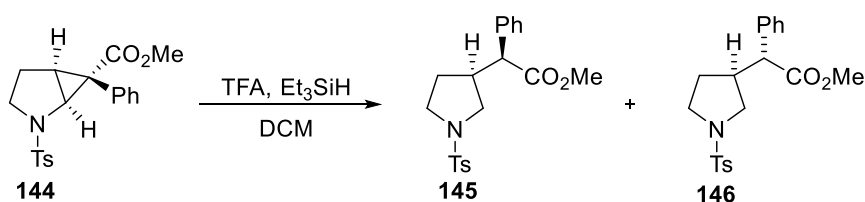
**Scheme 33.** Hydrogenation of the double bond in cyclopropane **119c**.

Utilizing the inherent properties of donor-acceptor cyclopropanes,<sup>99</sup> selective opening of the weakest bond in the cyclopropane moiety of **144** was achieved by treatment with TFA/ Et<sub>3</sub>SiH

\*\*\* Results are partially taken from the Bachelor thesis of N. Wurzer, 2016, Universität Regensburg (supervised by V. Lehner)

at room temperature (table 8, entry 2). However, under these conditions the reaction of cyclopropane **144** produced a mixture of diastereomers **145** and **146** in a ratio of 85:15, indicating that at least one of the two stereocenters is prone to epimerization. A decrease in reaction temperature had only little impact on the diastereomeric ratio (87:13 vs. 85:15) and a significantly prolonged reaction time was required to accomplish full conversion of the starting material (entry 1). Performance of the reaction at slightly elevated temperatures of 40 °C led to a decline in diastereoselectivity, forming ring-opening products **145** and **146** in a ratio of 78:22 (entry 3).

**Table 8.** Temperature dependence of ring-opening reactions with cyclopropane **144**.



entry <sup>a</sup>	temperature (°C)	time (h)	ratio <b>145/146</b> <sup>b</sup>	<i>ee</i> ( <b>145</b> ) (%) <sup>c</sup>	<i>ee</i> ( <b>146</b> ) (%) <sup>c</sup>	yield (%)
1	0	192	87:13	99	67	n.d.
2	25	48	85:15	99	37	86 <sup>d</sup>
3	40	6	78:22	96	0	n.d.

<sup>a</sup>Standard reaction conditions: TFA (2.0 equiv), Et<sub>3</sub>SiH (3.0 equiv). <sup>b</sup>Determined by <sup>1</sup>H-NMR analysis of the crude mixture. <sup>c</sup>Determined by chiral HPLC analysis. <sup>d</sup>Isolated yield: **145** (72%), **146** (14%).

Gratifyingly, separation of the diastereomers was feasible *via* column chromatography, enabling isolation of main diastereomer **145** in 72% yield with 99% *ee* and minor diastereomer **146** in 14% yield with 37% *ee* (entry 2). As can be seen from the absolute configuration of **145** that was unambiguously assigned by X-ray crystallography (figure 13), ring-opening of cyclopropane **144** occurs preferentially with retention of both stereocenters. The corresponding minor diastereomer **146** was generated in considerably diminished yields and enantioselectivity compared to **145**, indicating that each of the two stereocenters is prone to epimerization (table 8). Interestingly, while **145** was formed with uniformly high enantiomeric excess (96-99% *ee*) in all experiments, it was found, that lowering the temperature from 40 °C to 0 °C led to a significantly improved enantioselectivity of **146** (67% *ee* vs. 0% *ee*). These results

suggest that predominantly only one of the two stereocenters in **146** is influenced by modification of the reaction temperature.

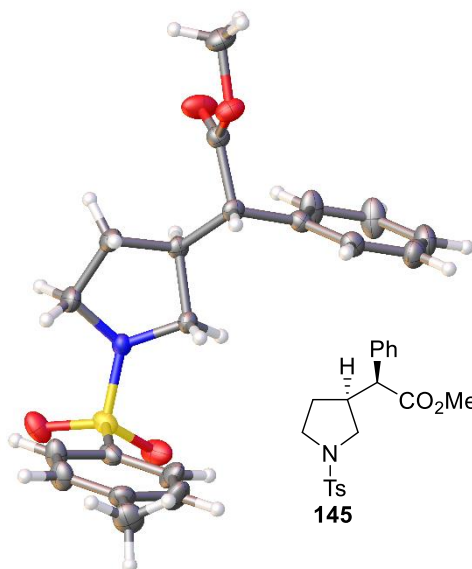
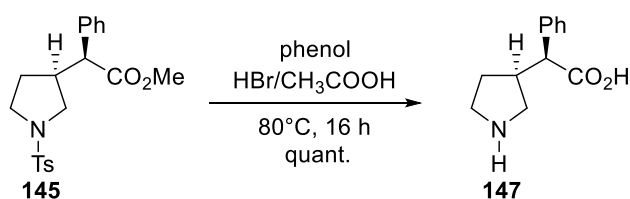


**Figure 13.** X-ray structure of ring-opening product **145** (main diastereomer).

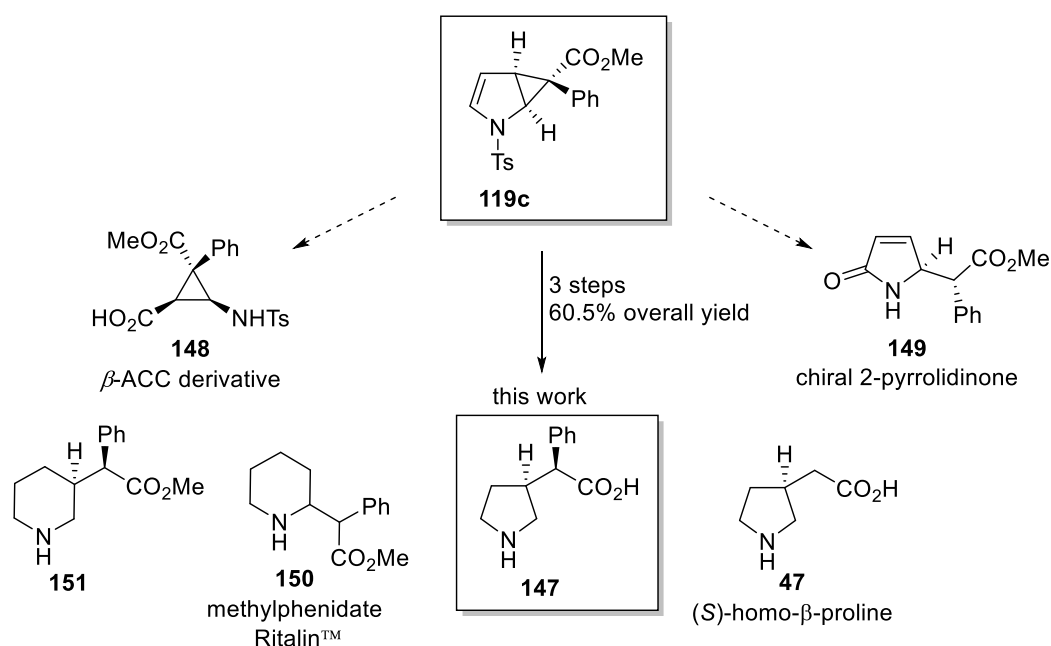
Aiming at a streamlined synthesis of chiral homo- $\beta$ -proline analogue **147**, cleavage of the two protection groups in **145** was envisioned to be accomplished in one step by following a protocol reported by *Sharpless* and co-workers.<sup>100</sup> Thus, removal of the *N*-toluenesulfonyl group and hydrolysis of the methyl ester was achieved simultaneously by treating **145** with HBr in acetic acid for 16 h at 80 °C (scheme 34). The resulting bromide salt was purified by the use of an acidic ion-exchange resin, giving rise to free amino acid **147** in quantitative yield.



**Scheme 34.** Final step in the synthesis of homo- $\beta$ -proline analogue **147**.

## 2.4 Conclusion and Outlook

In summary, the utility of cyclopropane **119c** was demonstrated with the synthesis of chiral homo- $\beta$ -proline analogue **147** (scheme 36). Starting from **119c**, the targeted pyrrolidine **147** was accessible in 3 steps and with 60.5% overall yield *via* hydrogenation, selective ring-opening and subsequent deprotection of the functional groups. Additionally, **147** can also be considered as a pyrrolidine analogue of methylphenidate (**150**, Ritalin<sup>TM</sup>),<sup>101</sup> a dopamine reuptake inhibitor used for the treatment of Attention Deficit Hyperactivity Disorder (ADHD).<sup>102</sup> A slight modification of the synthetic route in the deprotection step by using magnesium in methanol, which was reported to be capable of removing *N*-tosyl groups without affecting methyl esters,<sup>60</sup> should enable the synthesis of the corresponding methyl ester analogue of **147** (structural analogue to **150**) without the need for an additional step. Current experiments in the *Reiser* group by Alexander Röther are underway to apply this synthetic route to partially unsaturated piperidines aiming at the synthesis of the chiral 3-substituted methylphenidate derivative **151**. Taking the lead from the work of the *Reiser* group on the application of cyclopropanated pyrroles toward chiral intermediates and natural products (see chapter A.1.3 for details),<sup>18</sup> it would also be conceivable to transform **119c** into  $\beta$ -aminocyclopropanecarboxylic acid ( $\beta$ -ACC) derivative **148** or chiral 2-pyrrolidinone **149**.



**Scheme 35.** Cyclopropane **119c** as precursor and related projects.

### 3 Cyclopropanes 98a/b as precursors for the synthesis of paraconic acid derivatives

#### 3.1 Introduction – $\gamma$ -Butyrolactone: a privileged motif in natural products and drugs

The  $\gamma$ -butyrolactone ring constitutes the core structure of more than 13000 natural products spanning from simple monocycles to highly complex polycyclic scaffolds.<sup>103</sup> Along with the structural diversity,  $\gamma$ -butyrolactones display an impressive range of biological activities including antifungal, anti-inflammatory, antiviral, cytostatic, antitumor as well as antiviral properties, making them important lead structures for the development of novel therapeutic agents.<sup>104</sup> A prominent multi-target drug containing the  $\gamma$ -butyrolactone motif as central unit is spironolactone (Aldactone™, **152**),<sup>105</sup> an aldosterone agonist used for the treatment of high blood pressure and heart failure (figure 14). Mycophenolate-mofetil (CellCept™, **153**),<sup>106</sup> a prodrug of mycophenolic acid, is an effective immunosuppressive agent that is commonly used in transplant therapy to prevent allograft rejection.

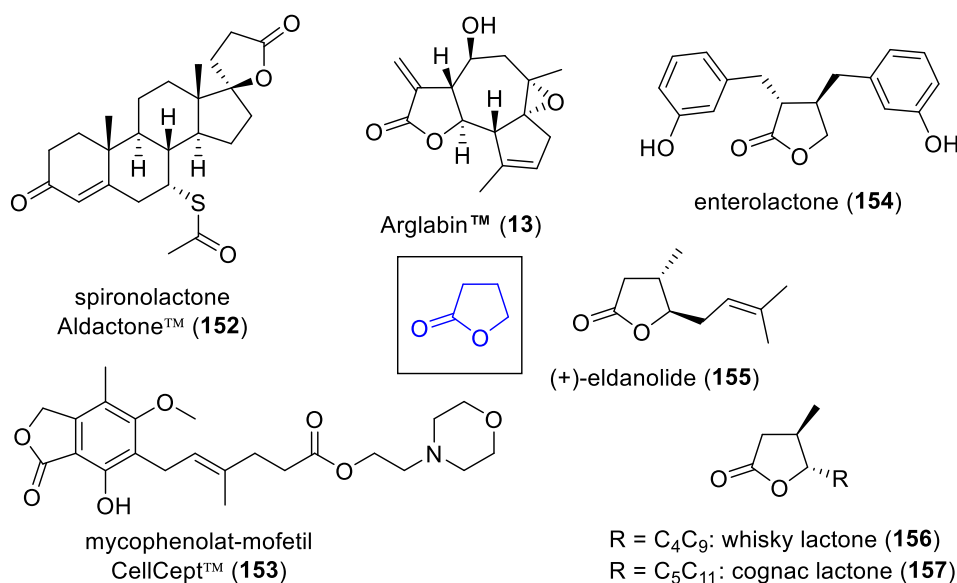


**Figure 14.** Representative examples of  $\gamma$ -butyrolactone natural products and pharmaceuticals.

A particular notable, naturally occurring  $\gamma$ -butyrolactone representative is the farnesyl transferase inhibitor Arglabin™ (**13**),<sup>107</sup> which shows promising cytotoxicity against various tumor cell lines. The water-soluble hydrochloride salt of the dimethylamino adduct of Arglabin™ is already a registered antitumor drug for the treatment of colon, ovarian, breast and lung cancers.<sup>108</sup> Enterolactone (**154**), a mammalian lignan that is formed by the metabolization of plant lignans in the colon, has been shown to possess protective properties toward breast and

prostate cancer.<sup>109</sup> Further natural disubstituted  $\gamma$ -butyrolactones are known as sex attractant pheromones (e.g. (+)-eldanolide (**155**)<sup>110</sup> and others are utilized as potential key flavor components (e.g. whisky lactone (**156**) and cognac lactone (**157**)).<sup>111</sup>

A group of chiral, trisubstituted  $\gamma$ -butyrolactones that have attracted considerable attention in recent years because of their broad biological profile including antitumor, antibiotic, antifungal, and antibacterial effects are paraconic acids.<sup>112–114</sup> This class of compounds is characterized by the presence of a carboxylic functionality at the  $\beta$ -position of the  $\gamma$ -butyrolactone ring. Naturally occurring paraconic acid derivatives, which are isolated from various species of *lichens*, *mosses* and culture filtrates of *penicillium sp.*, also bear an alkyl chain at the  $\gamma$ -carbon atom as well as a methyl or a methylene group at the  $\alpha$ -position, which is pivotal for the biological activity of the molecules.<sup>112</sup> Some representative examples are depicted in figure 15.

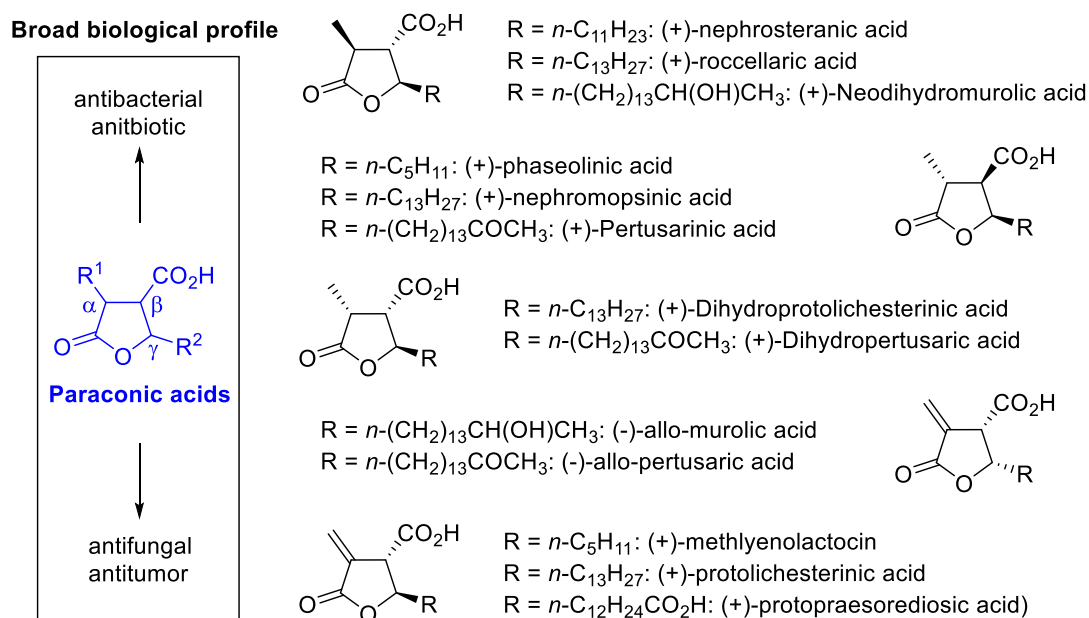
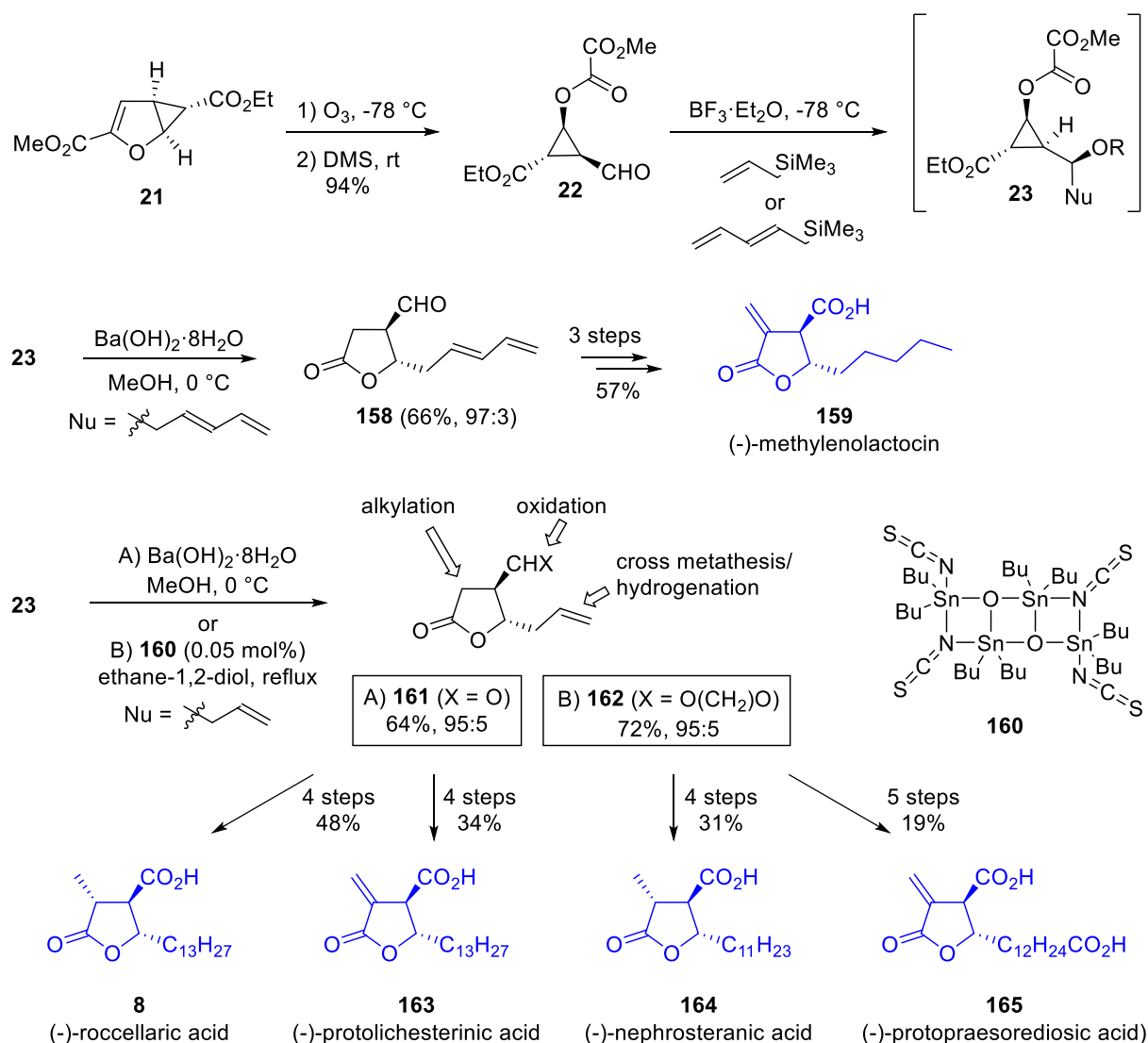


**Figure 15.** Paraconic acids.<sup>112</sup>

Inspired by the impressive structural diversity of naturally occurring  $\gamma$ -butyrolactones, synthetic chemists have developed various asymmetric strategies for assembling such challenging scaffolds in the past decades.<sup>115</sup> However, due to their broad spectrum of pharmacological and biological activities<sup>112</sup> the total synthesis of chiral  $\gamma$ -butyrolactones, especially paraconic acids and structurally related compounds, is of continuing interest.

### 3.2 Literature syntheses of paraconic acids – Utilization of donor-acceptor cyclopropanes

In addition to the various racemic approaches for assembling different members of the paraconic acid family that have been reported in the last decades,<sup>116</sup> an impressive range of strategies for the enantioselective synthesis of these natural products was developed.<sup>112</sup> These strategies include chiral pool approaches,<sup>117</sup> the use of chiral auxiliaries<sup>118</sup> or chiral synthons,<sup>119</sup> chemoenzymatic resolution,<sup>120</sup>  $\pi$ -face differentiation in chiral olefin-ketene [2 + 2] cycloaddition,<sup>121</sup> asymmetric dihydroxylation,<sup>122</sup> asymmetric epoxidation,<sup>123</sup> asymmetric reduction,<sup>124</sup> chiral conjugate addition,<sup>125</sup> as well as asymmetric allylic alkylation.<sup>103,126</sup>

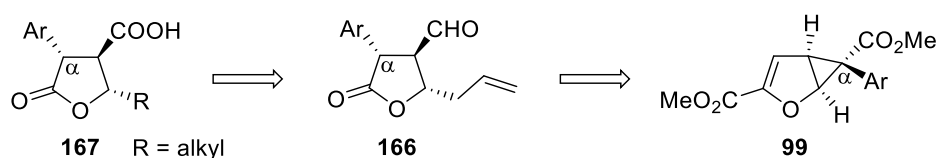


**Scheme 36.** Enantioselective synthesis of paraconic acids (blue) by Reiser and co-workers.<sup>17,127</sup>

An efficient methodology for the enantioselective construction of *anti*-4,5-disubstituted  $\gamma$ -butyrolactones **158**, **161** and **162**, which were successfully transformed to a variety of paraconic acids, was reported by *Reiser* and co-workers<sup>17,127</sup> (scheme 36). Starting from cyclopropane **21** (see chapter B.1.1), cleavage of the double *via* ozonolysis and subsequent reductive work-up gave access to aldehyde cyclopropane **22**, which was then subjected to a  $\text{BF}_3$ -mediated Hosomi-Sukurai allylation. The resulting adducts **23** that were obtained with generally high Felkin-Anh selectivity were transformed to the corresponding  $\gamma$ -butyrolactones **158** and **161** bearing a free aldehyde moiety at the  $\beta$ -position by a base induced hydrolysis that triggers a subsequent retroaldol/lactonization cascade. Alternatively, by using Otera's tin oxide catalyst (**160**) in the presence of ethane-1,2-diol, concomitant acetalization of the aldehyde group had taken place, giving access to acetal **162**.

The substitution pattern of  $\gamma$ -butyrolactones **158**, **161** and **162** set the foundation for the synthesis of several paraconic acids. Thus, (-)-methylenolactocin (**159**) was accessible from **158** in 3 steps *via* hydrogenation of the double bonds, oxidation of the aldehyde and introduction of the *exo*-methylene group. Installation of variable alkyl chains at the  $\gamma$ -carbon atom that are present in naturally occurring paraconic acids were accomplished by *Reiser* and co-workers by utilizing crossmetathesis reactions. By applying this method, the syntheses of (-)-roccellaric acid (**8**), (-)-protolichesterinic acid (**163**), (-)-nephorsteranic acid (**164**), as well as (-)-protopreosorediosic acid (**165**) were completed within 4-5 steps, respectively, starting from  $\gamma$ -butyrolactones **161** and **162**.<sup>17,127</sup>

Inspired by the protocol that was developed by the *Reiser* group for the synthesis of disubstituted  $\gamma$ -butyrolactones, it was envisioned, that an analog transformation of cyclopropanes **98** enable the construction of trisubstituted  $\gamma$ -butyrolactones **166**. The synthesis of these novel chiral building blocks **166**, and their application as precursors for the synthesis of paraconic acid derivatives bearing an aryl substituent in the  $\alpha$ -position (scheme 37) was investigated.

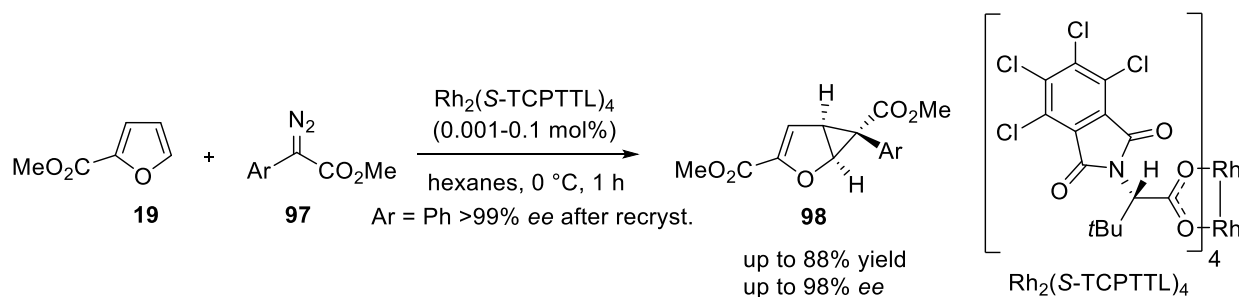


**Scheme 37.** Retrosynthetic analysis for paraconic acid derivatives **167**.



### 3.3 Preliminary studies on the synthesis of paraconic acid derivatives **176a** and **179a**<sup>†††</sup>

In chapter B.1.3 it was shown that monocyclopropanes **98** are readily generated in good yields and high levels of enantioselectivity from simple starting materials (scheme 38). Short reaction times and low catalyst loadings were generally required, and purification was realized by simple filtration. In the case of cyclopropane **98a** (Ar = Ph), reactions up to 74 mmol were already successfully performed, and enantiopure material was accessible after single recrystallization. Thus, highly functionalized cyclopropanes **98** were envisioned to be good starting points for a diverse follow-up chemistry.

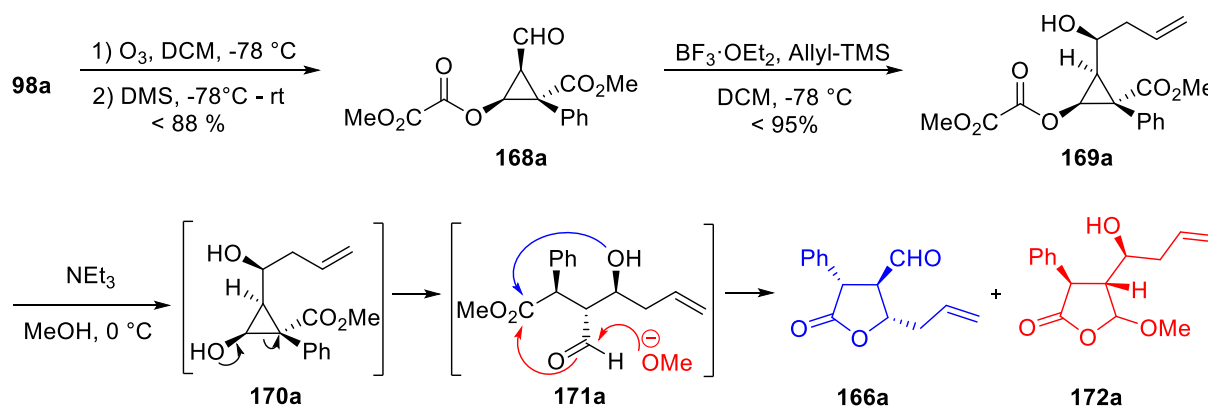


**Scheme 38.** Enantioselective synthesis of cyclopropanes **98**.

Following the protocol developed by the *Reiser* group<sup>17,127</sup> (see chapter B.3.2), cyclopropane **98a** was subjected to ozonolysis and subsequent reductive workup (scheme 39).  $\text{BF}_3$ -catalyzed allylation of the resulting cyclopropane aldehyde **168a** gave access to crude allyl alcohol **169a**. Unfortunately, it was not feasible to isolate **169a** in pure form, since it proved to be unstable during chromatographic work-up and recrystallization attempts using different solvents were unsuccessful. Thus, the configuration of the newly formed stereocenter in **169a** was assigned according to the *Felkin-Anh*-model with the prerequisite that the oxalic ester is the large substituent.<sup>128</sup> Treatment of crude **169a** with triethylamine in methanol generates unmasked donor-acceptor cyclopropane **170a** that is further transformed to  $\gamma$ -butyrolactone **166a** ( $dr = 90:5:5$ ) *via* ring opening and subsequent lactonization.

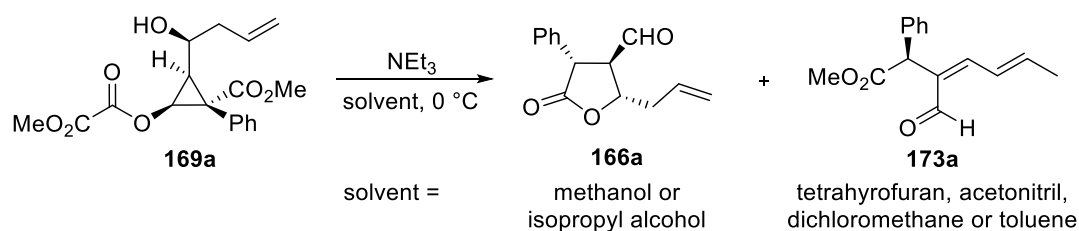
Although **166a** was obtained as the main product in this reaction, a number of byproducts resulting from elimination of the alcohol moiety, nucleophilic addition of methanol, as well as combinations thereof were formed as judged by mass spectrometry and crude  $^1\text{H-NMR}$  analysis. To prevent the formation of byproducts such as 5-methoxy  $\gamma$ -butyrolactone **172a** which derived from nucleophilic addition of methanol to the aldehyde moiety, a screening of different solvents was conducted (scheme 40).

<sup>†††</sup> Results are partially taken from the Bachelor thesis of F. Ostler, 2015, Universität Regensburg (supervised by V. Lehner)



**Scheme 39.** Synthesis of  $\gamma$ -butyrolactone **166a** starting from cyclopropane **98a**.<sup>†††</sup>

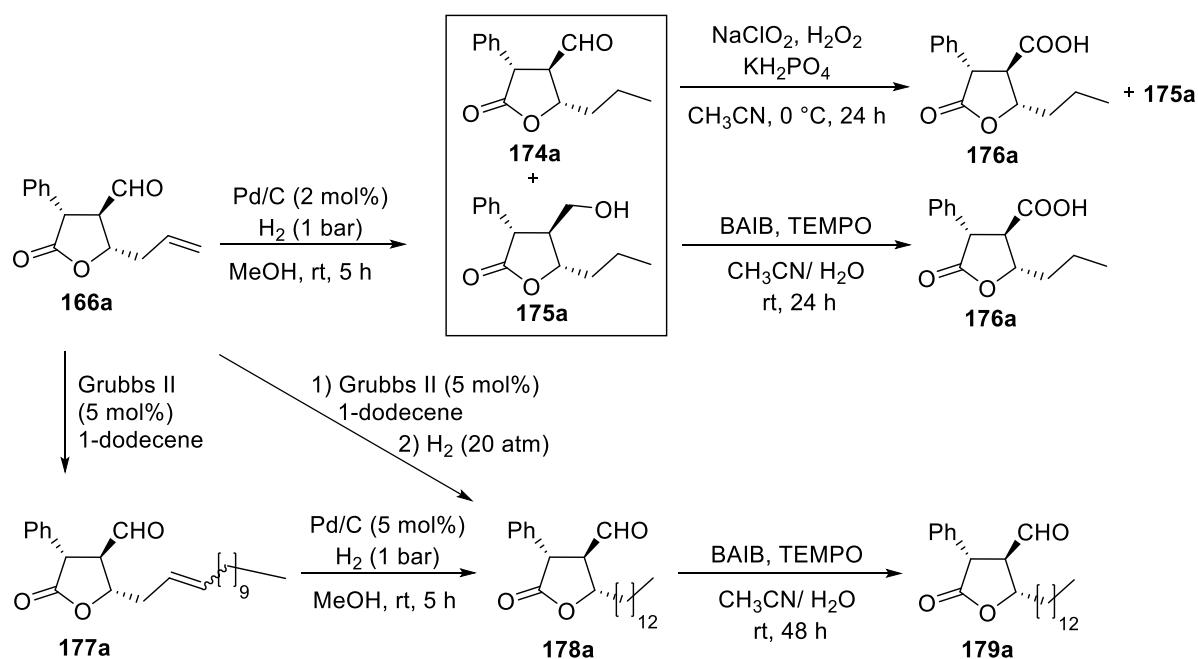
However, only traces of desired product **166a** were obtained when **169a** was treated with triethylamine in aprotic solvent systems. Instead, diene **173a** was formed *via* ring-opening, elimination of the alcohol moiety and base-induced isomerization<sup>129</sup> of the allyl double bond. Using *i*PrOH as solvent system, applying stoichiometric amounts of MeOH (5 equiv.) in THF, decreasing the reaction temperature to  $-78^{\circ}\text{C}$ , and employment of  $\text{Ba}(\text{OH})_2$  as base did not improve the situation. Attempts to isolate pure **166a** by column chromatography, kugelrohr distillation, preparative TLC, as well as recrystallization were unfruitful and led to a considerable loss of product. At this point, it was refrained from isolating the product at this stage as purification may be more convenient after oxidation of the aldehyde moiety in the last step of the planned route to paraconic acid derivatives **167**.



**Scheme 40.** Screening of different solvent systems.

<sup>†††</sup> The relative configuration of **166a** was established by X-ray analysis of downstream product **176a** (p. 62). The absolute configuration of **166a** was tentatively assigned by analogy to the stereochemical results observed for the synthesis of related disubstituted  $\gamma$ -butyrolactones.

The short-chain paraconic acid derivative **176a** was generated by hydrogenation of **166a** in the presence of Pd/C and a subsequent oxidation (scheme 41). Preliminary studies showed that simultaneous to hydrogenation of the double bond in **166a**, partial reduction of the aldehyde moiety occurred. Therefore, BAIB/TEMPO<sup>130</sup> was used for the oxidation to **176a** instead of the originally reported NaClO<sub>2</sub>/H<sub>2</sub>O<sub>2</sub>,<sup>17</sup> since this reagent is able to oxidize aldehydes as well as primary alcohol groups.



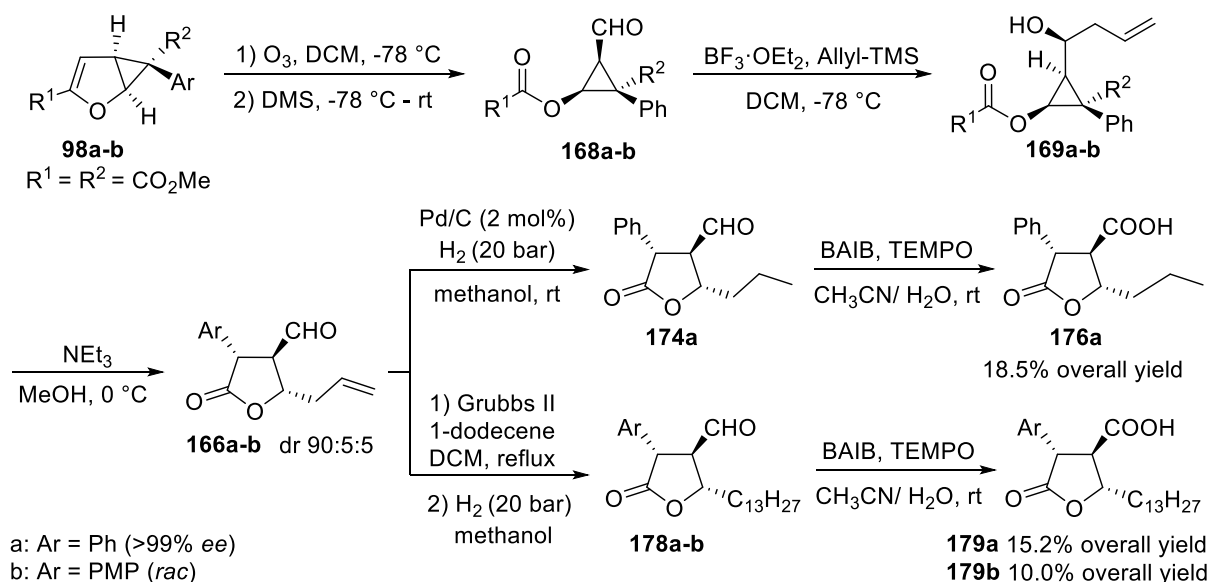
**Scheme 41.** Preliminary studies on the synthesis of paraconic acid derivatives **176a** and **179a**.

Utilizing the protocol of *Reiser* and co-workers,<sup>17</sup> installation of the long alkyl chain at the  $\gamma$ -carbon position of **177a** was achieved by cross metathesis with 1-dodecene applying Grubbs II as catalyst and hydrogenation in the presence of Pd/C gave access to intermediate **178a**. In order to increase the overall efficiency of this synthetic route and avoid the use of expensive palladium, performance of the elongation and hydrogenation step in a tandem sequence was investigated. Applying the metathesis/hydrogenation protocol reported by Grubbs and co-workers,<sup>131</sup>  $\gamma$ -butyrolactone **166a** was efficiently transformed to intermediate **178a** as judged by crude <sup>1</sup>H-NMR analysis. Subsequent oxidation using the modified conditions afforded paraconic acid derivative **179a**.

Gratifyingly, generation of the acid group in the last step enables the purification and finally the isolation of pure compounds **176a** and **176b**. Thus, it was refrained from purification of the intermediates in the following.

### 3.4 Synthesis of novel paraconic acid derivatives<sup>§§§</sup>

With the newly optimized reaction conditions at hand (see chapter B.3.3), the consecutive and straightforward transformation of cyclopropanes **98a** and **98b** to paraconic acid derivatives **176a** as well as **179a/b** was investigated (scheme 42).



**Scheme 42.** Consecutive synthesis of paraconic acid derivatives **176a** and **179a/b**.

The key allylation/retroaldol/lactonization cascade of ozonolysis products **168a/b** proceeded with high diastereoselectivity as judged by crude  $^1\text{H-NMR}$ , giving rise to intermediates **166a/b**. Short-chain derivative **176a** was readily generated in 18.5% overall yield *via* hydrogenation of the double bond in the presence of Pd/C and oxidation of the aldehyde moiety with BAIB/TEMPO.<sup>130</sup> Installation of the tridecyl-substituent in **179a/b**, the  $\alpha$ -aryl substituted analogues of (-)-roccellaric acid (**8**), was readily achieved by utilizing a metathesis/hydrogenation sequence.<sup>131</sup> Subsequent oxidation of the aldehyde moiety generated paraconic acid derivatives **179a/b** in 15.2/10.0% overall yields starting from cyclopropanes **98a/b**. It is notable that no chromatographic work-up of intermediates was required in the course of the sequence since the final carboxylic acids can be conveniently purified and isolated in pure form by column chromatography and subsequent recrystallization.

The relative configuration of paraconic acid derivatives **176a** and **179a/b** was established by X-ray analysis of (*rac*)-**176a** (figure 16). Since it was not feasible to get suitable crystals from

<sup>§§§</sup> This chapter is partially based on Lehner, V.; Davies, H. M. L.; Reiser, O. *Rh(II)-Catalyzed Cyclopropanation of Furans and Its Application to the Total Synthesis of Natural Product Derivatives*. *Org. Lett.* **2017** (accepted)

the enantiopure material (determined by chiral HPLC) the absolute configuration of **176a** and **179a** was tentatively assigned by analogy to the stereochemical results observed for the synthesis of related disubstituted  $\gamma$ -butyrolactones.<sup>17</sup>

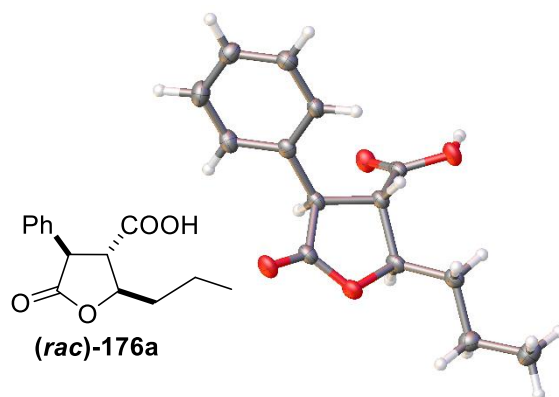
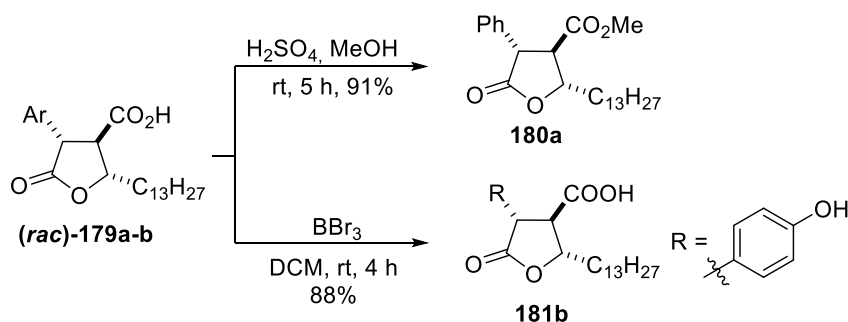


**Figure 16.** X-ray structure of paraconic acid derivative (*rac*)-**176a**.

To broaden the scope of paraconic acids and to analyze the influence of different substituents on the biological activities, modification of the different functional groups in **179a** and **179b** was investigated. On the one hand, (*rac*)-**179a** was transformed to ester **180a** by an acid-catalyzed esterification to examine the relevance of the acid group (scheme 43). On the other hand, demethylation of the aryl methyl ether in **179b** was investigated. Preliminary attempt using iodocyclohexane as HI source in DMF<sup>132</sup> or AlCl<sub>3</sub> in DCM,<sup>133</sup> which were shown to be suitable reagents to cleave aryl methyl ether without affecting  $\gamma$ -butyrolactone groups, resulted in low conversion of starting material. Increasing the temperature as well as prolonged reaction times led to the formation of byproducts as judged by crude <sup>1</sup>H-NMR analysis. However, the transformation of **179b** into paraconic acid derivative **181b**, bearing a free hydroxyl group, was achieved in 88% yield by BBr<sub>3</sub>-mediated<sup>134</sup> demethylation.



**Scheme 43.** Synthesis of paraconic acid derivatives **180a** and **181b**.

### 3.5 Biological evaluation

Naturally occurring paraconic acids are endowed with a host of biological activities (see chapter B.3.1). Thus, the biological profile of the newly synthesized derivatives was investigated in the following.

Cytotoxicity of the paraconic acid derivatives against HeLa cells was kindly measured by the Pharmaceutical Biology department (University of Regensburg) under the direction of Jörg Heilmann. A tetrazolium MTT reduction assay was used to evaluate the cell viability.<sup>135</sup> The IC<sub>50</sub> values are reported in table 9.

**Table 9.** Cytotoxicity of the investigated paraconic acid derivatives against HeLa cells (IC<sub>50</sub> in  $\mu\text{M}$ , means  $\pm$  SD,  $n = 8$ , 72 h)

Compd	HeLA (KB) cells
<b>(rac)-179a</b> (racemic)	74.4 $\pm$ 4.94
<b>179a</b> (99% <i>ee</i> )	67.0 $\pm$ 4.65
<b>(rac)-176a</b> (racemic)	> 600
<b>176a</b> (99% <i>ee</i> )	> 600
<b>179b</b> (racemic)	70.0 $\pm$ 4.87
<b>181b</b> (racemic)	95.3 $\pm$ 5.54
<b>180a</b> (racemic)	90.0 $\pm$ 8.73

Comparison of the IC<sub>50</sub> values of the different paraconic acid derivatives revealed that racemic and enantiopure compounds exhibit similar cytotoxicity. A significant increase of the toxic properties is observed as the length of alkyl chain at the  $\gamma$ -carbon position is increased. The ester derivative was slightly less active than the corresponding free acid compound. All of the tested compounds exhibited relatively low cytotoxic activities, which may be due to the absence of the *exo*-methylene group,<sup>114,136</sup> that is present in cytotoxic, naturally occurring paraconic acids.

Preliminary studies on the antibacterial activities of the derivatives were kindly conducted by the Analytical Chemistry department (University of Regensburg) under the direction of Antje Bäumner. A disk diffusion method (Müller-Hinton agar plates)<sup>137</sup> was utilized to assay the paraconic acid derivatives (60  $\mu\text{M}$ ) for bactericidal activity against *Staphylococcus aureus* (*Staphylococcus aureus* crude cell suspension, Sigma-Aldrich Chemie GmbH). After

incubation at 35 °C for 18 h, it was shown that compound (*rac*)-**179a**, **179a** and **181b** led to poor growth of the bacteria (figure 17). However, further test would be required to evaluate the MIC (minimal inhibitory concentration) and to produce comparable results.

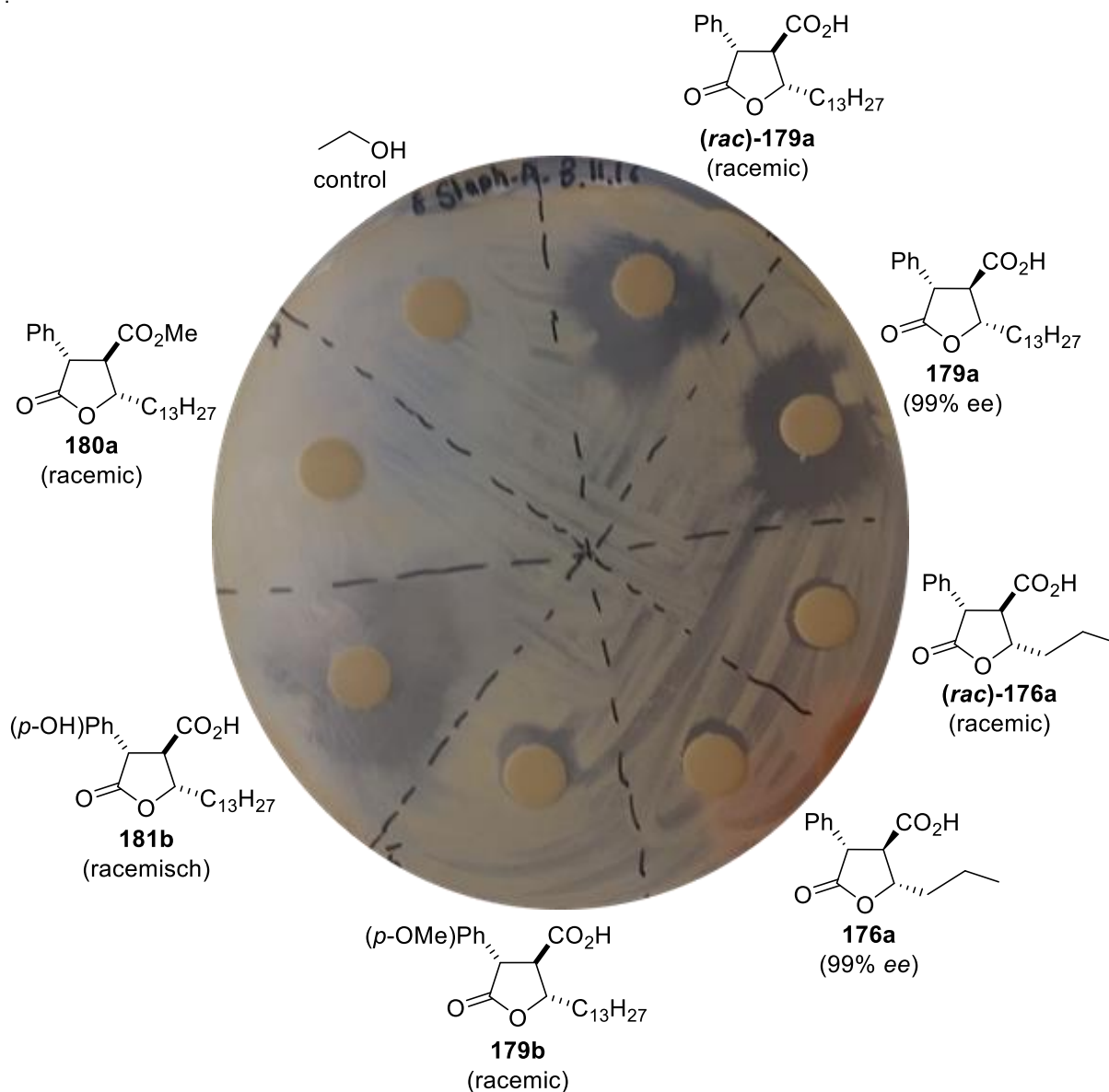
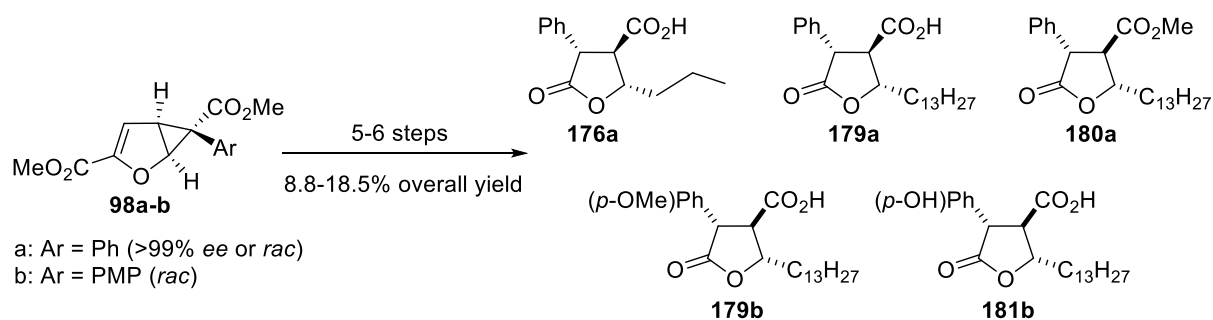


**Figure 17.** Disk diffusion test for bactericidal activity against *Staphylococcus aureus* (60  $\mu$ M).

### 3.6 Conclusion

In summary, the utility of monocyclopropanated furans was demonstrated with the synthesis of five novel paraconic acid derivatives bearing aryl substituents in  $\gamma$ -position (scheme 44). No chromatographic work-up of intermediates was required over the course of the sequence, since the final carboxylic acids can be conveniently purified and isolated in pure form by column chromatography and subsequent recrystallization. Key steps in this synthetic route were a diastereoselective allylation/retroaldol/lactonization cascade to establish the  $\gamma$ -butyrolactone framework and a tandem metathesis/ hydrogenation to introduce the C-13 alkyl chain at the  $\gamma$ -carbon atom. The applicability of the total sequence for the enantioselective construction of  $\gamma$ -butyrolactones was demonstrated with the synthesis of enantiopure **176a** and **179a**.



**Scheme 44.** Synthesized paraconic acid derivatives starting from cyclopropanes **98a-b**.



#### 4 References

- (1) a) Chen, D. Y.-K.; Pouwer, R. H.; Richard, J.-A. *Chem. Soc. Rev.* **2012**, *41*, 4631–4642; b) Donaldson, W. A. *Tetrahedron* **2001**, *57*, 8589–8627; c) Salaün, J. *Top. Curr. Chem.* **2000**, *207*, 1–67;
- (2) a) Kulinkovich, O. G. *Cyclopropanes in organic synthesis*, 2nd ed.; Wiley, Hoboken New Jersey, **2015**; b) Tang, P.; Qin, Y. *Synthesis* **2012**, *44*, 2969–2984;
- (3) a) Doyle, M. P.; Forbes, D. C. *Chem. Rev.* **1998**, *98*, 911–936; b) Lebel, H.; Marcoux, J.-F.; Molinaro, C.; Charette, A. B. *Chem. Rev.* **2003**, *103*, 977–1050; c) Maas, G. *Chem. Soc. Rev.* **2004**, *33*, 183–190; d) Pellissier, H. *Tetrahedron* **2008**, *64*, 7041–7095; e) Thumar, N. J.; Wei, Q. H.; Hu, W. H. *Adv. Organomet. Chem.* **2016**, *66*, 51–60;
- (4) Davies, H. M. L.; Walji, A. M. *Modern Rhodium-Catalyzed Organic Reactions*; Wiley-VHC, Weinheim, Germany, **2005**, 301–340.
- (5) Davies, H. M. L.; Beckwith, R. E. J. *Chem. Rev.* **2003**, *103*, 2861–2904.
- (6) Davies, H. M.; Panaro, S. A. *Tetrahedron* **2000**, *56*, 4871–4880.
- (7) a) Boruta, D. T.; Dmitrenko, O.; Yap, G. P. A.; Fox, J. M. *Chem. Sci.* **2012**, *3*, 1589–1593; b) Chen, Y.; Ruppel, J. V.; Zhang, X. P. *J. Chem. Soc.* **2007**, *129*, 12074–12075; c) Miller, J. A.; Jin, W.; Nguyen, S. T. *Angew. Chem. Int. Ed.* **2002**, *41*, 2953–2956; *Angew. Chem.* **2002**, *14*, 3077–3080; d) Wang, H.; Guptill, D. M.; Alvarez, A. V.; Musaev, D. G.; Davies, H. M. L. *Chem. Sci.* **2013**, *4*, 2844–2850; e) Zhu, S.; Perman, J. A.; Zhang, X. P. *Angew. Chem. Int. Ed.* **2008**, *47*, 8460–8463; *Angew. Chem.* **2008**, *120*, 8588–8591;
- (8) Qin, C.; Boyarskikh, V.; Hansen, J. H.; Hardcastle, K. I.; Musaev, D. G.; Davies, H. M. L. *J. Am. Chem. Soc.* **2011**, *133*, 19198–19204.
- (9) Davies, H. M. L.; Hedley, S. J. *Chem. Soc. Rev.* **2007**, *36*, 1109–1119.
- (10) a) Pirrung, M. C.; Zhang, J.; Lackey, K.; Sternbach, D. D.; Brown, F. *J. Org. Chem.* **1995**, *60*, 2112–2124; b) Gibe, R.; Kerr, M. A. *J. Org. Chem.* **2002**, *67*, 6247–6249;
- (11) Davies, H. M. L.; Antoulinakis, E. G. *Org. React.* **2001**, *57*, 1–326.
- (12) Pilsl, L. K. A.; Ertl, T.; Reiser, O. *Org. Lett.* **2017**, *19*, 2754–2757.
- (13) Glos, M. *Synthese von Oxazolinen als Bausteine für chirale Liganden*. **2000**, PhD Thesis, Universität Regensburg, Regensburg.
- (14) Özüdüru, G.; Schubach, T.; Boysen, M. M. K. *Org. Lett.* **2012**, *14*, 4990–4993.
- (15) Pilsl, L. K. A. *Enantioselective cyclopropanation of heterocycles and the use of high-pressure techniques for the conformational analysis of peptide foldamers*. **2006**, PhD Thesis, Universität Regensburg, Regensburg.

- (16) Harrar, K.; Reiser, O. *Chem. Commun.* **2012**, *48*, 3457–3459.
- (17) Chhor, R. B.; Nosse, B.; Soergel, S.; Boehm, C.; Seitz, M.; Reiser, O. *Chem. Eur. J.* **2003**, *9*, 260–270.
- (18) Reiser, O. *Isr. J. Chem.* **2016**, *56*, 531–539.
- (19) Salomon, R. G.; Kochi, J. K. *J. Am. Chem. Soc.* **1973**, *95*, 3300–3310.
- (20) Schinnerl, M.; Böhm, C.; Seitz, M.; Reiser, O. *Tetrahedron: Asymmetry* **2003**, *14*, 765–771.
- (21) Fritschi, H.; Lautenegger, U.; Pfaltz, A. *Helv. Chim. Acta* **1988**, *71*, 1553–1565.
- (22) Temme, O.; Taj, S.-A.; Andersson, P. G. *J. Org. Chem.* **1998**, *63*, 6007–6015.
- (23) Pelphrey, P.; Hansen, J.; Davies, H. M. L. *Chem. Sci.* **2010**, *1*, 254–257.
- (24) Davies, H. M. L.; Venkataramani, C. *Org. Lett.* **2003**, *5*, 1403–1406.
- (25) L. Davies, H. M. *Eur. J. Org. Chem.* **1999**, *1999*, 2459–2469.
- (26) Davies, H. M. L.; Bruzinski, P. R.; Lake, D. H.; Kong, N.; Fall, M. J. *J. Am. Chem. Soc.* **1996**, *118*, 6897–6907.
- (27) Hedley, S. J.; Ventura, D. L.; Dominiak, P. M.; Nygren, C. L.; Davies, H. M. L. *J. Org. Chem.* **2006**, *71*, 5349–5356.
- (28) Nowlan, D. T.; Gregg, T. M.; Davies, H. M. L.; Singleton, D. A. *J. Am. Chem. Soc.* **2003**, *125*, 15902–15911.
- (29) a) Reddy, R. P.; Davies, H. M. L. *J. Am. Chem. Soc.* **2007**, *129*, 10312–10313; b) Davies, H. M. L.; Matasi, J. J.; Hodges, L. M.; Huby, N. J. S.; Thornley, C.; Kong, N.; Houser, J. H. *J. Org. Chem.* **1997**, *62*, 1095–1105; c) Davies, H. M. L.; Huby, N. J. S. *Tetrahedron Lett.* **1992**, *33*, 6935–6938; d) Davies, H. M. L.; Young, W. B.; Smith, H. D. *Tetrahedron Lett.* **1989**, *30*, 4653–4656;
- (30) Davies, H. M. L.; Saikali, E.; Young, W. B. *J. Org. Chem.* **1991**, *56*, 5696–5700.
- (31) Davies, H. M. L.; Ahmed, G.; Churchill, M. R. *J. Am. Chem. Soc.* **1996**, *118*, 10774–10782.
- (32) Davies H. M. L.; Clark, D. M.; Alligood, D. B.; Eiband G. R. *Tetrahedron* **1987**, *43*, 4265–4270.
- (33) Davies, H. M. L.; Clarke, D. M., Smith, T. K. *Tetrahedron Lett.* **1985**, *26*, 5659–5662.
- (34) Davies, H. M. L. *Curr. Org. Chem.* **1998**, *2*, 463–488.
- (35) Goto, T.; Takeda, K.; Shimada, N.; Nambu, H.; Anada, M.; Shiro, M.; Ando, K.; Hashimoto, S. *Angew. Chem. Int. Ed.* **2011**, *50*, 6803–6808; *Angew. Chem.* **2011**, *123*, 6935–6940.

- (36) Yamawaki, M.; Tsutsui, H.; Kitagaki, S.; Anada M. Hashimoto, S. *Tetrahedron Lett.* **2002**, *43*, 9561–9564.
- (37) Tsutsui, H.; Yamaguchi, Y.; Kitagaki, S.; Nakamura, S.; Anada, M.; Hashimoto, S. *Tetrahedron: Asymmetry* **2003**, *14*, 817–821.
- (38) Watanabe, N.; Ogawa, T.; Ohtake, Y.; Ikegami, S.; Hashimoto, S. *Synlett* **1996**, 85–86.
- (39) Reddy, R. P.; Davies, H. M. L. *Org. Lett.* **2006**, *8*, 5013–5016.
- (40) Reddy, R. P.; Lee, G. H.; Davies, H. M. L. *Org. Lett.* **2006**, *8*, 3437–3440.
- (41) Müller, P.; Allenbach, Y.; Robert, E. *Tetrahedron: Asymmetry* **2003**, *14*, 779–785.
- (42) Pirrung, M. C.; Zhang, J. *Tetrahedron Lett.* **1992**, *33*, 5987–5990.
- (43) Hansen, J.; Autschbach, J.; Davies, H. M. L. *J. Org. Chem.* **2009**, *74*, 6555–6563.
- (44) Wong, F. M.; Wang, J.; Hengge, A. C.; Wu, W. *Org. Lett.* **2007**, *9*, 1663–1665.
- (45) Pirrung, M. C.; Liu, H.; Morehead, A. T. *J. Am. Chem. Soc.* **2002**, *124*, 1014–1023.
- (46) Callot, H. J.; Metz, F. *Tetrahedron* **1985**, *41*, 4495–4501.
- (47) Hoshino, Y.; Yamamoto, H. *J. Am. Chem. Soc.* **2000**, *122*, 10452–10453.
- (48) Chepiga, K. M.; Qin, C.; Alford, J. S.; Chennamadhavuni, S.; Gregg, T. M.; Olson, J. P.; Davies, H. M. L. *Tetrahedron* **2013**, *69*.
- (49) Davies, H. M. L.; Clark, T. J.; Kimmer, G. F. *J. Org. Chem.* **1991**, *56*, 6440–6447.
- (50) Ogawa, A.; Curran, D. P. *J. Org. Chem.* **1997**, *62*, 450–451.
- (51) Maas, G. *Angew. Chem. Int. Ed.* **2009**, *48*, 8186–8195; *Angew. Chem.* **2009**, *121*, 8332–8341.
- (52) Ford, A.; Miel, H.; Ring, A.; Slattery, C. N.; Maguire, A. R.; McKerverey, M. A. *Chem. Rev.* **2015**, *115*, 9981–10080.
- (53) a) Davies, H. M. L.; Hutchenson, D. K. *Tetrahedron Lett.* **1993**, *34*, 7243–7246; b) Davies, H. M. L.; Bruzinski, P. R.; Fall, M. J. *Tetrahedron Lett.* **1996**, *37*, 4133–4136;
- (54) a) Kaschel, J.; Schneider, T. F.; Schirmer, P.; Maa, C.; Stalke, D.; Werz, D. B. *Eur. J. Org. Chem.* **2013**, *2013*, 4539–4551; b) Waser, M.; Moher, E. D.; Borders, S. S. K.; Hansen, M. M.; Hoard, D. W.; Laurila, M. E.; LeTourneau, M. E.; Miller, R. D.; Phillips, M. L.; Sullivan, K. A.; Ward, J. A.; Xie, C.; Bye, C. A.; Leitner, T.; Herzog-Krimbacher, B.; Kordian, M.; Müllner, M. *Org. Process Res. Dev.* **2011**, *15*, 1266–1274;
- (55) Werlé, C.; Goddard, R.; Philipps, P.; Farès, C.; Fürstner, A. *Angew. Chem. Int. Ed.* **2016**, *55*, 10760–10765; *Angew. Chem.* **2016**, *128*, 10918–10923.
- (56) DeAngelis, A.; Boruta, D. T.; Lubin, J.-B.; Plampin, J. N., III; Yap, G. P. A.; Fox, J. M. *Chem. Commun.* **2010**, *46*, 4541–4543.
- (57) Lindsay, V. N. G.; Lin, W.; Charette, A. B. *J. Am. Chem. Soc.* **2009**, *131*, 16383–16385.

- (58) Maryanoff, B. E. *J. Org. Chem.* **1979**, *44*, 4410–4419.
- (59) a) Beumer, R.; Reiser, O. *Tetrahedron* **2001**, *57*, 6497–6503; b) Fowler, F. W. *J. Chem. Soc. D* **1969**, 1359–1360; c) Tanny, S. R.; Grossman, J.; Fowler, F. W. *J. Am. Chem. Soc.* **1972**, *94*, 6495–6501;
- (60) Jolicoeur, B.; Chapman, E. E.; Thompson, A.; Lubell, W. D. *Tetrahedron* **2006**, *62*, 11531–11563.
- (61) Grehn, L.; Ragnarsson, U. *Angew. Chem. Int. Ed.* **1984**, *23*, 296–297; *Angew. Chem.* **1984**, *96*, 291–292.
- (62) Boger, D. L.; Patel, M. *J. Org. Chem.* **52**, 2319–2323.
- (63) Zonta, C.; Fabris, F.; Lucchi, O. de. *Org. Lett.* **2005**, *7*, 1003–1006.
- (64) Krajewska, D.; Dabrowska, M.; Jakoniuk, P.; Róžańsk, A. *Acta Pol. Pharm.* **2002**, *59*, 127–132.
- (65) Egleton, J. E.; Thinnes, C. C.; Seden, P. T.; Laurieri, N.; Lee, S. P.; Hadavizadeh, K. S.; Measures, A. R.; Jones, A. M.; Thompson, S.; Varney, A.; Wynne, G. M.; Ryan, A.; Sim, E.; Russell, A. J. *Bioorg. Med. Chem.* **2014**, *22*, 3030–3054.
- (66) Goto, T.; Takeda, K.; Anada, M.; Ando, K.; Hashimoto, S. *Tetrahedron Lett.* **2011**, *52*, 4200–4203.
- (67) Bonge, H. T.; Hansen, T. *J. Org. Chem.* **2010**, *75*, 2309–2320.
- (68) Dalpozzo, R. *Chem. Soc. Rev.* **2015**, *44*, 742–778.
- (69) a) Chen, J.-B.; Jia, Y.-X. *Org. Biomol. Chem.* **2017**, *15*, 3550–3567; b) Bartoli, G.; Bencivenni, G.; Dalpozzo, R. *Chem. Soc. Rev.* **2010**, *39*, 4449–4465; c) Bandini, M.; Eichholzer, A. *Angew. Chem. Int. Ed.* **2009**, *48*, 9608–9644; *Angew. Chem.* **2009**, *121*, 9786–9824;
- (70) Berry, J. M.; Bradshaw, T. D.; Fichtner, I.; Ren, R.; Schwalbe, C. H.; Wells, G.; Chew, E.-H.; Stevens, M. F. G.; Westwell, A. D. *J. Med. Chem.* **2005**, *48*, 639–644.
- (71) a) Jui, N. T.; Garber, J. A. O.; Finelli, F. G.; MacMillan, D. W. C. *J. Am. Chem. Soc.* **2012**, *134*, 11400–11403; b) Galliford, C. V.; Scheidt, K. A. *Angew. Chem. Int. Ed.* **2007**, *46*, 8748–8758; *Angew. Chem.* **2007**, *119*, 8902–8912; c) Donohoe, T. J.; Bataille, C. J. R.; Churchill, G. H. *Annu. Rep. Prog. Chem., Sect. B* **2006**, *102*, 98–122; d) Felpin, F.-X.; Lebreton, J. *Eur. J. Org. Chem.* **2003**, 3693–3712;
- (72) a) Saraswat, P.; Jeyabalan, G.; Hassan, M. Z.; Rahman, M. U.; Nyola, N. K. *Synth. Commun.* **2016**, *46*, 1643–1664; b) Raghuraman, A.; Ko, E.; Perez, L. M.; Ioerger, T. R.; Burgess, K. *J. Am. Chem. Soc.* **2011**, *133*, 12350–12353; c) Lexa, K. W.; Carlson, H. A. *Proteins* **2011**, *79*, 2282–2290; d) Li, X.; Li, J. *Mini-Rev. Med. Chem.* **2010**, *10*, 794–805;

- e) Hensler, M. E.; Bernstein, G.; Nizet, V.; Nefzi, A. *Bioorg. Med. Chem. Lett.* **2006**, *16*, 5073–5079; f) Whitby, L. R.; Ando, Y.; Setola, V.; Vogt, P. K.; Roth, B. L.; Boger, D. L. *J. Am. Chem. Soc.* **2011**, *133*, 10184–10194;
- (73) a) Wyratt, M. A.; Patchett, A. A. M. *Med. Res. Rev.* **1985**, *5*, 483–531; b) Patchett, A. A.; Harris, E. W.; Tristram, E. W.; Wyratt, M. J.; Wu, M. T.; Taub, D.; Peterson, E. R.; Ikeler, T. J.; Broeke, J. L.; Payne, L. G.; Ondeyka, D. L.; Thorsett, E. D.; Greenlee, W. J.; Lohr, N. S.; Hoffsommer, R. D.; Joshua, H.; Ruyle, W. V.; Rothrock, J. W.; Aster, S. D.; Maycock, A. L.; Robinson, F. M.; Hirschmann, R.; Sweet, C. S.; Ulm, E. M.; Groos, D. M.; Vassil, T. C.; Stone, C. A. *Nature* **1980**, *288*, 280–283; c) Ondetti, M. A.; Rubin, B.; Cushman, D. W. *Science* **1977**, *196*, 441–444; d) Cushman, D. W.; Cheung, H. S.; Sabo, E. F.; Ondetti, M. A. *Biochemistry* **1977**, *16*, 5484–5491;
- (74) Parsons, A. F. *Tetrahedron* **1996**, *52*, 4149–4174.
- (75) a) Stathakis, C. I.; Yiotti, E. G.; Gallos, J. K. *Eur. J. Org. Chem.* **2012**, 4661–4673; b) Nitta, I.; Watase, H.; Tomile, Y. *Nature* **1958**, *181*, 761–762; c) Johnston, G. A. R.; Curtis, D. R.; Davies, J.; McCulloch, R. M. *Nature* **1974**, *249*, 804–805;
- (76) a) Clayden, J.; Read, B.; Hebditch, K. R. *Tetrahedron* **2005**, *61*, 5713–5724; b) Maeda, M.; Kodama, T.; Tanaka, T.; Ohfuné, Y.; Nomoto, K.; Nishimura, K.; Fujita, T. *J. Pesticide Sci.* **1984**, *9*, 27–32; c) Ohfuné, Y.; Tomita, M. *J. Am. Chem. Soc.* **1982**, *104*, 3511–3513;
- (77) Arévalo-García, E. B.; Colmenares, J. C. Q. *Tetrahedron Lett.* **2008**, *49*, 3995–3996.
- (78) Wagner, F. F.; Comins, D. L. *Tetrahedron* **2007**, *63*, 8065–8082.
- (79) Bhat, C.; Tilve, S. G. *RSC Adv.* **2014**, *4*, 5405–5452.
- (80) List, B. *Tetrahedron* **2002**, *58*, 5573–5590.
- (81) Zhang, S.; Wang, W., Eds. *Privileged chiral ligands and catalysts*; Wiley-VCH, Weinheim Germany, **2011**, 409–439.
- (82) Panday, S. K. *Tetrahedron: Asymmetry* **2011**, *22*, 1817–1847.
- (83) Mukherjee, S.; Yang, J. W.; Hoffmann, S.; List, B. *Chem. Rev.* **2007**, *107*, 5471–5569.
- (84) a) List, B.; Lerner, R. A.; Barbas, C. F. *J. Am. Chem. Soc.* **2000**, *122*, 2395–2396; b) Hajos, Z. G.; Parrish, D. R. *J. Org. Chem.* **1974**, *39*, 1615–1621;
- (85) a) Nagata, K.; Kuga, Y.; Higashi, A.; Kinoshita, A.; Kanemitsu, T.; Miyazaki, M.; Itoh, T. *J. Org. Chem.* **2013**, *78*, 7131–7136; b) Zhang, H.; Mifsud, M.; Tanaka, F.; Barbas, C. F. *J. Am. Chem. Soc.* **2006**, *128*, 9630–9631;
- (86) a) Wróblewska, A. *Synlett* **2012**, *23*, 953–954; b) Jensen, K. L.; Dickmeiss, G.; Jiang, H.; Albrecht, L.; Jørgensen, K. A. *Acc. Chem. Res.* **2012**, *45*, 248–264;

- (87) a) Fagg, G. E.; Foster, A. C. *Neuroscience* **1983**, *9*, 701–719; b) Curtis, D. R.; Johnston, G. A. R. *Ergebn. Physiol.* **1974**, *69*, 97–188;
- (88) Thorbek, P.; Hjeds, H.; Schaumburg, K. *Acta Chem. Scand.* **1981**, *B35*, 473–479.
- (89) Andersen, K. E.; Sørensen, J. L.; Lau, J.; Lundt, B. F.; Petersen, H.; Huusfeldt, P. O.; Suzdak, P. D.; Swedberg, M. D. B. *J. Med. Chem.* **2001**, *44*, 2152–2163.
- (90) Gálvez-Ruano, E.; Iriepa, I.; Morreale, A.; Boyd, D. B. *J. Mol. Graph. Model.* **2001**, *20*, 183–197.
- (91) Nielsen, L.; Brehm, L.; Krogsgaard-Larsen; P. *J. Med. Chem.* **1990**, *33*, 71–77.
- (92) Wein, T.; Petrera, M.; Allmendinger, L.; Höfner, G.; Pabel, J.; Wanner, K. T. *ChemMedChem* **2016**, *11*, 509–518.
- (93) a) Dalby, N. O. *Eur. J. Pharmacol.* **2003**, *479*, 127–137; b) Meldrum, B. S.; Chapman, A. G. *Epilepsia* **1999**, *40*, S2-S6;
- (94) a) Coldham, I.; Hufton, R. *Tetrahedron* **1996**, *52*, 12541–12552; b) Labouta, I. M.; Jacobsen, P.; Thorbek, P.; Krogsgaard-Larsen, P.; Hjeds, H. *Acta Chem. Scand.* **1982**, *B36*, 669–674;
- (95) a) Galeazzi, R.; Mobbili, G.; Orena, M. *Tetrahedron* **1996**, *52*, 1069–1084; b) Galeazzi, R.; Geremia, S.; Mobbili, G.; Orena, M. *Tetrahedron: Asymmetry* **1996**, *7*, 79–88; c) Cardillo, B.; Galeazzi, R.; Mobbili, G.; Orena, M. *Synlett* **1995**, 1159–1160;
- (96) a) Thomas, C.; Orecher, F.; Gmeiner, P. *Synthesis* **1998**, 1491–1496; b) Eustache, J.; Grob, A.; Lam, C.; Sellier, O.; Schulz, G. *Bioorg. Med. Chem. Lett.* **1998**, *8*, 2961–2966;
- (97) Ye, W.; Jiang, Z.; Zhao, Y.; Goh, S. L. M.; Leow, D.; Soh, Y.-T.; Tan, C.-H. *Adv. Synth. Catal.* **2007**, *349*, 2454–2458.
- (98) Felluga, F.; Gombac, V.; Pitacco, G.; Valentin, E. *Tetrahedron: Asymmetry* **2004**, *15*, 3323–3327.
- (99) a) Schneider, T. F.; Kaschel, J.; Werz, D. B. *Angew. Chem. Int. Ed.* **2014**, *53*, 5504–5523; *Angew. Chem.* **2014**, *126*, 5608–5628; b) Reissig, H.-U.; Zimmer, R. *Chem. Rev.* **2003**, *103*, 1151–1196;
- (100) a) Li, G.; Sharpless, K. B. *Acta. Chem. Scand.* **1996**, *50*, 649–651; b) Ohle, H.; Friedeberg, H.; Haeseler, G. *Ber. dtsh. Chem. Ges.* **1936**, *B69*, 2311–2324;
- (101) a) Davies, H. M. L.; Hopper, D. W.; Hansen, T.; Liu, Q.; Childers, S. R. *Bioorg. Med. Chem. Lett.* **2004**, *14*, 1799–1802; b) Meltzer, P. C.; Wang, P.; Blundell, P.; Madras, B. K. *J. Med. Chem.* **2003**, *46*, 1538–1545;
- (102) Myers, R. L. *The 100 Most Important Chemical Compounds: A Reference Guide*; Greenwood Publishing Group, Westport Connecticut, London, **2007**, 178-181.

- (103) Mao, B.; Geurts, K.; Fañanás-Mastral, M.; van Zijl, A. W.; Fletcher, S. P.; Minnaard, A. J.; Feringa, B. L. *Org. Lett.* **2011**, *13*, 948–951.
- (104) a) Hoffmann, H. M. R.; Rabe, J. *Angew. Chem. Int. Ed.* **1985**, *24*, 94–110; *Angew. Chem.* **1985**, *97*, 96–112.; b) Kitson, R. R. A.; Millemaggi, A.; Taylor, R. J. K. *Angew. Chem. Int. Ed.* **2009**, *48*, 9426–9451; *Angew. Chem.* **2009**, *121*, 9590–9615.;
- (105) a) Larik, F. A.; Saeed, A.; Shahzad, D.; Faisal, M.; El-Seedi, H.; Mehfooz, H.; Channar, P. A. *Steroids* **2017**, *118*, 76–92; b) Wuts, P. G. M.; Ritter, A. R. *J. Org. Chem.* **1989**, *54*, 5180–5182;
- (106) Allison, A. C.; Eugui, E. M. *Immunopharmacology* **2000**, *47*, 85–118.
- (107) a) Zhai, J.-D.; Li, D.; Long, J.; Zhang, H.-L.; Lin, J.-P.; Qiu, C.-J.; Zhang, Q.; Chen, Y. *J. Org. Chem.* **2012**, *77*, 7103–7107; b) Kalidindi, S.; Jeong, W. B.; Schall, A.; Bandichhor, R.; Nosse, B.; Reiser, O. *Angew. Chem. Int. Ed.* **2007**, *46*, 6361–6363; *Angew. Chem.* **2007**, *119*, 6478–6481.; c) Lone, S. H.; Bhat, K. A.; Khuroo, M. A. *Chem. Biol. Interact.* **2015**, *240*, 180–198;
- (108) Zhangabylov, N. S.; Dederer, L. Y.; Gorbacheva, L. B.; Vasil'eva, S. V.; Terekhov, A. S.; Adekenov, S. M. *Pharm. Chem. J.* **2004**, *38*, 651–653.
- (109) a) Adlercreutz, H. *Crit. Rev. Clin. Lab. Sci.* **2007**, *44*, 483–525; b) Wang, L.-Q. *J. Chromatogr. B* **2002**, *777*, 289–309;
- (110) a) Devalankar, D. A.; Karabal, P. U.; Sudalai, A. *Org. Biomol. Chem.* **2013**, *11*, 1280–1285; b) Kunesch, G.; Zagatti, P.; Lallemand, J. Y.; Dabal, A.; Vigneron, J. P. *Tetrahedron Lett.* **1981**, *22*, 5271–5274;
- (111) a) Ozeki, M.; Hashimoto, D.; Nishide, K.; Kajimoto, T.; Node, M. *Tetrahedron: Asymmetry* **2005**, *16*, 1663–1671; b) Tanaka, T.; Kouno, I. *J. Nat. Prod.* **1996**, *59*, 997–999;
- (112) Bandichhor, R.; Nosse, B.; Reiser, O. *Top. Curr. Chem.* **2005**, *243*, 43–72.
- (113) Kumar, K. C.; Müller, K. *J. Nat. Prod.* **1999**, *62*, 817–820.
- (114) Park, B. K.; Nakagawa, M.; Hirota, A.; Nakayama, M. *J. Antibiot.* **1988**, *41*, 751–758.
- (115) a) Mao, B.; Fañanás-Mastral, M.; Feringa, B. L. *Chem. Rev.* **2017**; b) Schall, A.; Reiser, O. *Eur. J. Org. Chem.* **2008**, 2353–2364; c) Seitz, M.; Reiser, O. *Curr. Opin. Chem. Biol.* **2005**, *9*, 285–292;
- (116) a) Bella, M.; Margarita, R.; Orlando, C.; Orsini, M.; Parlanti, L.; Piancatelli, G. *Tetrahedron* **2000**, *41*, 561–565; b) Mandal, P. K.; Roy, S. C. *Tetrahedron* **1999**, *55*, 11395–11398; c) Mandal, P. K.; Maiti, G.; Roy, S. C. *J. Org. Chem.* **1998**, *63*, 2829–2834; d) Ghatak, A.; Sarkar, S.; Ghosh, S. *Tetrahedron* **1997**, *53*, 17335–17342; e)

- Carlson, R. M.; Oyler, A. R. *J. Org. Chem.* **1976**, *41*, 4065–4069; f) Damon, R. E.; Schlessinger, R. H. *Tetrahedron Lett.* **1976**, *19*, 1561–1564; g) Martin, J.; Watts, P. C.; Johnson, F. *J. Org. Chem.* **1974**, *39*, 1676–1681; h) van Tamelen, E. E.; Bach, S. R. *J. Am. Chem. Soc.* **1958**, *80*, 3079–3086;
- (117) a) Ghosh, M.; Bose, S.; Maity, S.; Ghosh, S. *Tetrahedron Lett.* **2009**, *50*, 7102–7104; b) Schleth, F.; Vogler, T.; Harms, K.; Studer, A. *Chem. Eur. J.* **2004**, *10*, 4171–4185; c) Schleth, F.; Studer, A. *Angew. Chem. Int. Ed.* **2004**, *43*, 313–315; *Angew. Chem.* **2004**, *116*, 317–319.; d) Barros, M. T.; Maycock, C. D.; Ventura, M. R. *Org. Lett.* **2003**, *5*, 4097–4099; e) Masaki, Y.; Arasaki, H.; Itoh, A. *Tetrahedron Lett.* **1999**, *40*, 4829–4832;
- (118) a) Wang, H.; Tang, P.; Zhou, Q.; Zhang, D.; Chen, Z.; Huang, H.; Qin, Y. *J. Org. Chem.* **2015**, *80*, 2494–2502; b) Hajra, S.; Karmakar, A.; Giri, A. K.; Hazra, S. *Tetrahedron Lett.* **2008**, *49*, 3625–3627; c) Sibi, M. P.; Liu, P.; Ji, J.; Hajra, S.; Chen, J.-x. *J. Org. Chem.* **2002**, *67*, 1738–1745; d) Kongsaree, P.; Meepowpan, P.; Thebtaranonth, Y. *Tetrahedron: Asymmetry* **2001**, *12*, 1913–1922; e) Sibi, M. P.; Ji, J. *Angew. Chem. Int. Ed.* **1996**, *36*, 274–276; *Angew. Chem.* **1997**, *109*, 266–268.;
- (119) a) Amador, M.; Ariza, X.; Garcia, J.; Ortiz, J. *J. Org. Chem.* **2004**, *69*, 8172–8175; b) Martín, T.; Rodríguez, C. M.; Martín, V. S. *J. Org. Chem.* **1996**, *61*, 6450–6453; c) Takahata, H.; Uchida, Y.; Momose, T. *J. Org. Chem.* **1995**, *60*, 5628–5633;
- (120) Drioli, S.; Felluga, F.; Forzato, C.; Nitti, P.; Pitacco, G.; Valentin, E. *J. Org. Chem.* **1998**, *63*, 2385–2388.
- (121) a) Murta, M. M.; Azevedo, M. B. M. de; Greene, A. E. *J. Org. Chem.* **1993**, *58*, 7537–7541; b) Mariangela B. M. de; Murta, M. M.; Greene, A. E. *J. Org. Chem.* **1992**, *57*, 4567–4569;
- (122) a) Fernandes, R. A.; Halle, M. B.; Chowdhury, A. K.; Ingle, A. B. *Tetrahedron: Asymmetry* **2012**, *23*, 60–66; b) Fernandes, R. A.; Chowdhury, A. K. *Eur. J. Org. Chem.* **2011**, 1106–1112; c) Fernandes, R. A.; Chowdhury, A. K. *Tetrahedron: Asymmetry* **2011**, *22*, 1114–1119; d) Braukmüller, S.; Brückner, R. *Eur. J. Org. Chem.* **2006**, 2110–2118;
- (123) a) Perepogu, A. K.; Raman, D.; Murty, U. S. N.; Rao, V. J. *Synth. Commun.* **2010**, *40*, 686–696; b) Zhang, Z.; Xiyan, L. *Tetrahedron: Asymmetry* **1996**, *7*, 1923–1928; c) Mawson, S. D.; Weavers, R. T. *Tetrahedron* **1995**, *51*, 11257–11270;
- (124) a) Nallasivam, J. L.; Fernandes, R. A. *Org. Biomol. Chem.* **2017**, *15*, 708–716; b) Blanc, D.; Madec, J.; Popowyc, F.; Ayad, T.; Phansavath, P.; Ratovelomanana-Vidal, V.; Genêt, J.-P. *Adv. Synth. Catal.* **2007**, *349*, 943–950;



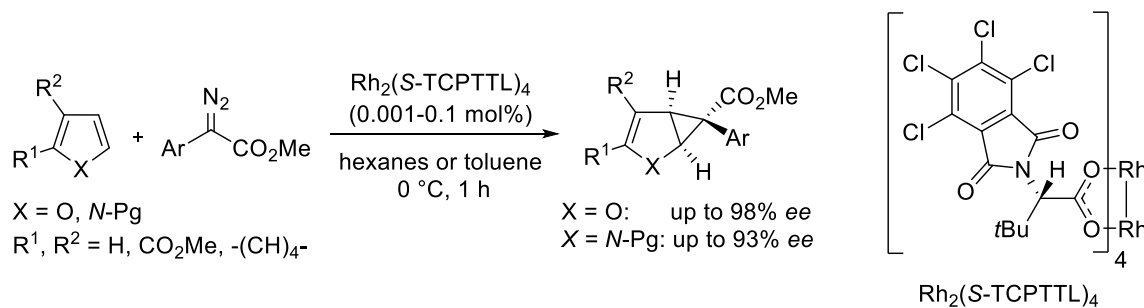
- (125) Howell, G. P.; Fletcher, S. P.; Geurts, K.; ter Horst, B.; Feringa, B. L. *J. Am. Chem. Soc.* **2006**, *128*, 14977–14985.
- (126) Fournier, J.; Lozano, O.; Menozzi, C.; Arseniyadis, S.; Cossy, J. *Angew. Chem. Int. Ed.* **2013**, *52*, 1257–1261; *Angew. Chem.* **2013**, *125*, 1295–1299.
- (127) Böhm, C.; Reiser, O. *Org. Lett.* **2001**, *3*, 1315–1318.
- (128) Mengel, A.; Reiser, O. *Chem. Rev.* **1999**, *99*, 1191–1224.
- (129) a) Hassam, M.; Taher, A.; Arnott, G. E.; Green, I. R.; van Otterlo, W. A. L. *Chem. Rev.* **2015**, *115*, 5462–5569; b) Cram, D. J.; Uyeda, R. T. *J. Am. Chem. Soc.* **1964**, *86*, 5466–5477;
- (130) Epp, J. B.; Widlanski, T. S. *J. Org. Chem.* **1999**, *64*, 293–295.
- (131) Louie, J.; Bielawski, C. W.; Grubbs, R. H. *J. Am. Chem. Soc.* **2001**, *123*, 11312–11313.
- (132) Zuo, L.; Yao, S.; Wang, W.; Duan, W. *Tetrahedron Letters* **2008**, *49*, 4054–4056.
- (133) Fernandes, R. A.; Chowdhury, A. K. *The Journal of organic chemistry* **2009**, *74*, 8826–8829.
- (134) Krabbe, S. W.; Johnson, J. S. *Org. Lett.* **2015**, *17*, 1188–1191.
- (135) Vlachy, N.; Touraud, D.; Heilmann, J.; Kunz, W. *Colloids Surf., B* **2009**, *70*, 278–280.
- (136) Park, B. K.; Nakagawa, M.; Hirota, A.; Nakayama, M. *Agric. BioL. Chem.*, **1987**, *51*, 3443–3444.
- (137) Shahverdi, A. R.; Fakhimi, A.; Shahverdi, H. R.; Minaian, S. *Nanomedicine* **2007**, *3*, 168–171.

## C Summary

Monocyclopropanated aromatic heterocycles have emerged as versatile building blocks in organic synthesis as a wide portfolio of natural products and bioactive compounds are accessible from these compounds. However, in most reported applications, simple acceptor diazo esters were used for the formation of the cyclopropanes (chapter A).

To expand the scope of these useful building blocks, the intermolecular monocyclopropanation of heteroarenes with donor-acceptor carbenoids was investigated in the first part of this thesis (chapter B.1). After screening ten Rh(II)-catalysts,  $\text{Rh}_2(\text{S-TCPTTL})_4$  was identified as a highly efficient and selective catalyst (up to 98% *ee*, TON 88000 and TOF  $24 \text{ s}^{-1}$ ) for the cyclopropanation of furans, with a variety of aryl diazoesters (scheme 45). In contrast, the developed protocol gave only poor results by using simple methyl diazoacetate.

In the case of pyrrole, it was demonstrated that the nature of the protecting group on the nitrogen has a great influence on the product formation (mono vs. doublecyclopropanation). The best results were obtained by using the *N*-tosyl derivative (61%, 93% *ee*). The interaction of  $\text{Rh}_2(\text{S-TCPTTL})_4$  and the *N*-tosyl protecting group was also shown to be beneficial for the reaction of indole. Thus, the first catalytic enantioselective reaction of indole with aryl diazoesters was achieved (75%, 80% *ee*), resulting in cyclopropanation of the heterocyclic ring.

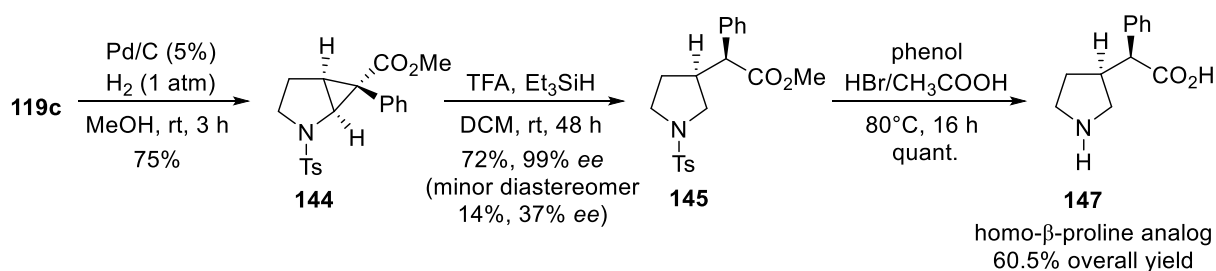


**Scheme 45.** Enantioselective cyclopropanation of aromatic heterocycles with aryl diazoesters.

In the second part of this thesis (chapter B.2 and B.3), the utility of these cyclopropanes as starting materials for the enantioselective construction of novel natural product derivatives bearing an additional aryl moiety was investigated.

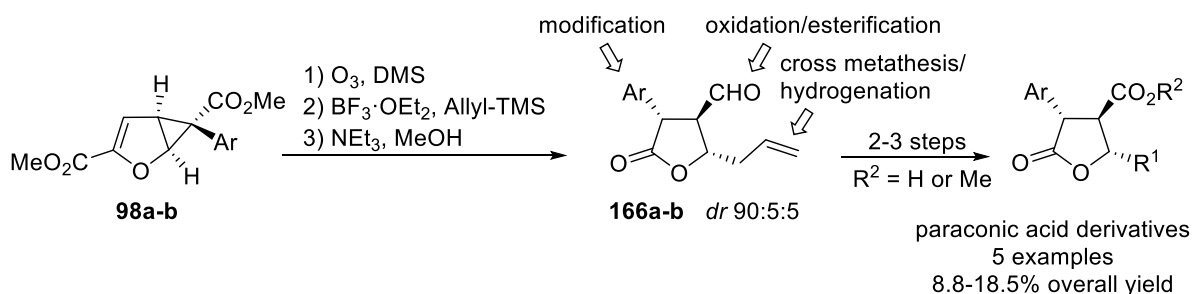
Starting from cyclopropane **119c**, homo- $\beta$ -proline analog **147** was synthesized in a three-step sequence (scheme 46). By utilizing the unique properties of donor-acceptor cyclopropanes in the key step, acid-catalyzed ring opening of **144** afforded pyrrolidine **145** as the major

diastereomer in 72% yield and 99% *ee*. Cleavage of the two protection groups in **145** was feasible in one step and thus, homo- $\beta$ -proline analog **147** was accessible in 60.5% overall yield.



**Scheme 46.** Enantioselective synthesis of homo- $\beta$ -proline analog **147** starting from cyclopropane **119c**.

Starting from cyclopropanes **98a-b**, five paraconic acid derivatives were synthesized in a 5-6 step sequence (scheme 47). The key transformation in this synthetic route was a diastereoselective allylation/retroaldol/lactonization cascade, which enabled the construction of highly functionalized  $\gamma$ -butyrolactones **166a-b**. Alkyl chains in the  $\gamma$ -position were introduced by simple hydrogenation of the allyl moiety in the presence of Pd/C ( $R = C_3H_7$ ) or by a tandem Grubbs II catalyzed metathesis/hydrogenation sequence ( $R = C_{13}H_{27}$ ). Subsequent oxidation of the aldehyde moiety with BAIB/TEMPO allowed for the synthesis of paraconic acid derivatives **176a** and **179a/b**. Two further derivatives were generated by either esterification of the carboxylic group or through modification of the aldehyde moiety. The applicability of this sequence for the enantioselective construction of  $\gamma$ -butyrolactones was demonstrated with the synthesis of enantiopure **176a** and **179a**



**Scheme 47.** Enantioselective and racemic synthesis of paraconic acid derivatives starting from cyclopropanes **98a-b**.

## D Zusammenfassung

Monocyclopropanierte aromatische Heterozyklen haben sich in der organischen Chemie als vielseitige Bausteine für die Synthese von Naturstoffen sowie biologisch aktiven Molekülen bewährt. Trotzdem ist das Potential dieser Verbindungen noch lange nicht ausgeschöpft, da im überwiegenden Teil der Literatur lediglich Akzeptor Diazoester im Cyclopropanierungsschritt verwendet werden (Kapitel A).

Im ersten Teil dieser Arbeit werden Forschungsergebnisse zur Synthese von monocyclopropanierten, aromatischen Heterozyklen unter Einsatz von Donor-Akzeptor Diazoestern vorgestellt (Kapitel B.1). In einem Screening von zehn Rh(II)-Katalysatoren zeigte sich, dass  $\text{Rh}_2(\text{S-TCPTTL})_4$  ein höchst effizienter und selektiver Katalysator (bis zu 98% *ee*, TON 88000 und TOF  $24 \text{ s}^{-1}$ ) für die Monocyclopropanierung von Furanen ist (Schema 45). Die entwickelte Methodik konnte für eine Vielzahl an Aryldiazoestern angewendet werden, wohingegen eine analoge Reaktion mit Methyl diazoacetat mäßige Ergebnissen erzielte.

Bei der Umsetzung von Pyrrolen wurde neben dem gewünschten monocyclopropanierten Produkten auch die entsprechenden doppelcyclopropanierten Produkte erhalten. In einer Studie konnte gezeigt werden, dass die Produktverteilung durch die Wahl der Schutzgruppe am Stickstoff steuerbar ist. Die besten Ergebnisse wurden hierbei mit dem *N*-Tosyl Derivat erzielt (61%, 93% *ee*). Die Anwendung dieser Methodik (*N*-Tosyl Schutzgruppe und  $\text{Rh}_2(\text{S-TCPTTL})_4$ ) ermöglichte schließlich die erste katalytische und enantioselektive Umsetzung von Indol mit Aryldiazoestern, in der selektiv die heteroaromatische Doppelbindung cyclopropaniert wurde (75%, 80% *ee*).

Im zweiten Teil dieser Arbeit (Kapitel B.2 und B.3) wurde die Anwendbarkeit dieser Cyclopropane als chirale Bausteine für die Synthese von neuen Naturstoffderivaten mit einer zusätzlich Arylgruppe untersucht.

Ausgehend von Cyclopropan **119c**, konnte Homo- $\beta$ -prolin Analogon **147** in 3 Stufen hergestellt werden (Schema 46). Den Schlüsselschritt dieser Sequenz stellte eine säurekatalysierte, diastereoselektive Ringöffnung von Donor-Akzeptor Cyclopropan **144** dar, wodurch Pyrrolidin **145** in 72% Ausbeute und 99% *ee* synthetisiert werden konnte. Die simultane Eliminierung der beiden Schutzgruppen von **145** ermöglichte letztendlich die Darstellung von Homo- $\beta$ -prolin Analog **147** in 60.5% Gesamtausbeute.

Ausgehend von Cyclopropanen **98a-b** konnten fünf Paraconsäurederivate in 5-6 Stufen hergestellt werden (Schema 47). Die Darstellung der hoch funktionalisierten  $\gamma$ -Butyrolactone **166a-b** wurde durch eine diastereoselektive Allylierung/Retroaldol/Laktonisierung Sequenz

erreicht. Die Einführung der Alkyl Seitenketten in  $\gamma$ -Position gelang durch Hydrierung der Allylgruppe mit Pd/C (R = C<sub>3</sub>H<sub>7</sub>) beziehungsweise einer Grubbs II katalysierten Metathese/Hydrierung Sequenz (R = C<sub>13</sub>H<sub>27</sub>). Durch die anschließende Oxidation der Aldehydgruppe mit BAIB/ TEMPO war die Darstellung von Paraconsäurederivate **176a** and **179a/b** möglich. Zusätzlich wurden noch zwei weitere Derivate durch Veresterung der Säuregruppe oder Modifizierung der Arylgruppe synthetisiert. Durch die Synthese der enantiomerenreinen Verbindungen **176a** und **179a** konnte abschließend gezeigt werden, dass diese Methode für die enantioselektive Darstellung von substituierten  $\gamma$ -Butyrolactonen geeignet ist.

## E Experimental part

### 1 General information

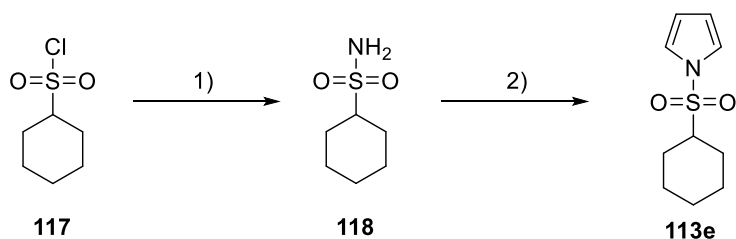
$^1\text{H}$ -NMR and  $^{13}\text{C}$ -NMR spectra were recorded on Bruker Avance 300 (300 MHz), Bruker Avance 400 (400 MHz) and Bruker Avance III 600 TCI Cryo (600 MHz). NMR spectra were recorded in  $\text{CDCl}_3$  or commercially available deuterated solvents at room temperature unless otherwise stated. Chemical shifts are reported as  $\delta$ , parts per million, relative to the signal of the solvent. The coupling constants ( $J$ ) are reported in Hertz (Hz). Abbreviations for signal coupling are as follows: s = singlet, bs = broad singlet, d = doublet, t = triplet, m = multiplet, dd = doublet of a doublet, ddd = doublet of a doublet of a doublet, dtd = doublet of a triplet of a doublet. Infrared spectroscopy (IR) was carried out on a Cary630 FT-IR spectrometer (Agilent Technologies) or a Biorad Excalibur FTS 3000 spectrometer (equipped with a Specac Golden Gate Diamond Single Reflection ATR-System). Mass spectrometry was performed in the Central Analytic Department on a ThermoQuest Finnigan TSQ 7000, Agilent Q-TOF 6540 UHD, Finnigan MAT 95 or a MAT SSQ 710 A at the Central Analytical Department (University of Regensburg). Melting points were recorded on an OptiMelt MPA 100 (uncorrected). Optical Rotation was measured in a Perkin Elmer Polarimeter or an ElmerAnton Paar MCP500 at 589 nm wavelength (sodium-d-line) in the specific solvent. Column chromatography was performed on silica gel 60 (0.063-0.200 mm, Merck) or flash silica gel 60 (0.040-0.063, Merck). Analytical thin layer chromatography was performed on Merck TLC aluminium sheets silica gel 60 F 254 (0.2 mm layer thickness). Eluated plates were visualized using a UV lamp ( $\lambda = 254$  nm or 366 nm) and/ or by staining with vanillin/ sulfuric acid solution or bromocresol green solution. X-ray measurements were performed by the crystallographic department of the University of Regensburg on Agilent Technologies SuperNova, Agilent Technologies Gemini R Ultra or Stoe IPDS I. Analytical HPLC was carried out on a Varian 920-LC with DAD. Chiralpak AS-H, Phenomenex Lux Cellulose-1 and 2 served as chiral stationary phase, and mixtures of *n*-heptane and *i*PrOH were used for elution. Reactions with moisture and oxygen sensitive reagents were performed in flame-dried, or oven-dried glassware under an atmosphere of pre-dried nitrogen or argon. Dry solvents were prepared according to standard procedures. Furan (**14**), furan-2-carboxylate (**19**) and methyl furan-3-carboxylate (**105**) were distilled prior to use. Unless otherwise stated, all other commercially available chemicals were used as received without further purification.

## 2 Synthesis of starting materials and catalysts

Following compounds were synthesized according to literature known procedures or were on stock in the laboratories of the *Reiser* or *Davies* group:

$\text{Rh}_2(\text{S-DOSP})_4$ ,<sup>1</sup>  $\text{Rh}_2(\text{S-BNP})_4$ ,<sup>2</sup>  $\text{Rh}_2(\text{S-BTPCP})_4$ ,<sup>3</sup>  $\text{Rh}_2(\text{S-NTTL})_4$ ,<sup>4</sup>  $\text{Rh}_2(\text{S-PTAD})_4$ ,<sup>5</sup>  $\text{Rh}_2(\text{S-TCPTAD})_4$ ,<sup>6</sup>  $\text{Rh}_2(\text{S-PTTL})_4$ ,<sup>7</sup>  $\text{Rh}_2(\text{S-TFPTTL})_4$ ,<sup>8</sup>  $\text{Rh}_2(\text{S-TCPTTL})_4$ ,<sup>9</sup>  $\text{Rh}_2(\text{S-TBPTTL})_4$ ,<sup>10</sup> Grubbs II,<sup>11</sup> methyl 2-diazoacetate (**79**),<sup>12</sup> *tert*-butyl 1H-pyrrole-1-carboxylate (**90**),<sup>13</sup> methyl 2-(4-bromophenyl)-2-diazoacetate (**91**),<sup>14</sup> methyl 2-diazo-2-phenylacetate (**97a**),<sup>14</sup> methyl 2-diazo-2-(4-methoxyphenyl)acetate (**97b**),<sup>14</sup> methyl 2-diazo-2-(*p*-tolyl)acetate (**97c**),<sup>14</sup> methyl 2-(4-chlorophenyl)-2-diazoacetate (**97d**),<sup>14</sup> methyl 2-diazo-2-(naphthalen-2-yl)acetate (**97f**),<sup>14</sup> methyl 2-diazo-2-(4-nitrophenyl)acetate (**97g**),<sup>14</sup> methyl 1H-pyrrole-1-carboxylate (**113a**),<sup>15</sup> *p*-tolyl 1H-pyrrole-1-carboxylate (**113b**),<sup>15</sup> 1-tosyl-1H-pyrrole (**113c**),<sup>16</sup> 1-(methylsulfonyl)-1H-pyrrole (**113d**),<sup>17</sup> 1-tosyl-1H-indole (**125**).<sup>18</sup>

1-(cyclohexylsulfonyl)-1H-pyrrole (**113e**)



Cyclohexanesulfonyl chloride (**117**) (1.50 g, 8.21 mmol, 1.0 equiv) was added to a 32% aqueous ammonia solution (30 mL) at rt within 10 minutes. The reaction mixture was allowed to stir for 90 min. The solution was acidified with 2 M HCl to pH = 7 and extracted with ethyl acetate (4 x 50 mL). The combined organic layers were dried over anhydrous  $\text{Na}_2\text{SO}_4$ , the solid was filtered off, and the filtrate was concentrated to give cyclohexanesulfonamide (**118**) which was directly used in the next step.<sup>20</sup>

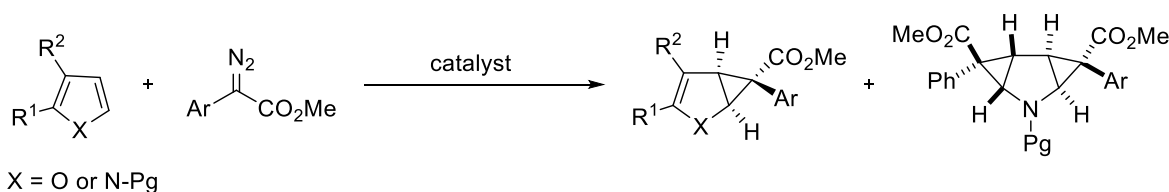
A solution of cyclohexanesulfonamide (**118**) (1.03 g, 6.29 mmol, 1.0 equiv) and 2,5-dimethoxytetrahydrofuran (0.98 mL, 7.22 mmol, 1.2 equiv) in acetic acid (8 mL) was refluxed for 4 h. The solvent was evaporated in vacuo and the crude product was purified by flash chromatography ( $\text{SiO}_2$ , hexanes/EtOAc, 9:1) to afford pyrrole **113e** as a white solid (1.24 mg, 71% yield over 2 steps).<sup>17</sup>

**m.p.** 63-64 °C; **R<sub>f</sub>** = 0.60 (hexanes: ethyl acetate = 5:1, Vanillin); **IR** (neat): 3167, 3122, 3120, 2945, 2863, 2102, 1610, 1573, 1536, 1454, 1370, 1342, 1271, 1219, 1182, 1156, 1059, 1037, 891, 850, 824, 749 cm<sup>-1</sup>; **<sup>1</sup>H NMR** (300 MHz, CDCl<sub>3</sub>) δ 7.08 – 7.05 (m, 2H), 6.36 – 6.30 (m, 2H), 3.08 (tt, *J* = 12.0, 3.5 Hz, 1H), 2.03 – 1.92 (m, 2H), 1.90 – 1.79 (m, 2H), 1.71 – 1.61 (m, 1H), 1.51 – 1.35 (m, 2H), 1.31 – 1.09 (m, 3H); **<sup>13</sup>C NMR** (75 MHz, CDCl<sub>3</sub>) δ 121.4, 112.6, 64.4, 26.2, 24.9, 24.8; **HRMS** (+APCI) calcd. for C<sub>10</sub>H<sub>16</sub>NO<sub>2</sub>S (M+H)<sup>+</sup> 214.0896 found 214.0901.



### 3 Synthesis of Cyclopropanes

#### 3.1 General procedures



#### General procedure (GP-1): Enantioselective cyclopropanation of furans with Rh<sub>2</sub>(S-TCPTTL)<sub>4</sub>

In a flame dried 25-mL round bottom flask equipped with a magnetic stir bar, furan (2.0 equiv) and Rh<sub>2</sub>(S-TCPTTL)<sub>4</sub> (0.1 mol%) were dissolved in dry hexanes (2 mL) and cooled to 0 °C. A solution of the diazo ester (1.0 mmol, 1.0 equiv) in dry hexanes (1.4-2 mL) and dry dichloromethane (0-0.6 mL) was added using a syringe pump for the duration of 1 h. Afterward, the reaction mixture was stirred for further 5 min and concentrated under reduced pressure. The residue was purified by column chromatography on silica gel using hexanes and ethyl acetate as eluents.

#### General procedure (GP-2): Enantioselective cyclopropanation of pyrroles and indole with Rh<sub>2</sub>(S-TCPTTL)<sub>4</sub>

In a flame dried 25-mL round bottom flask equipped with a magnetic stir bar, pyrrole/indole (2.0 equiv) and Rh<sub>2</sub>(S-TCPTTL)<sub>4</sub> (0.1 mol%) were dissolved in dry toluene (4 mL) and cooled to 0 °C. A solution of the diazo ester (1.0 mmol, 1.0 equiv) in dry toluene (2 mL) was added using a syringe pump for the duration of 1 h. Afterward, the reaction mixture was stirred for further 5 min and concentrated under reduced pressure. The residue was purified by column chromatography on silica gel using hexanes and ethyl acetate as eluents.

#### General procedure (GP-3): Racemic cyclopropanation of furans with Rh<sub>2</sub>(OPiv)<sub>4</sub>

In a flame dried 25-mL round bottom flask equipped with a magnetic stir bar, furan (2.0 equiv) and Rh<sub>2</sub>(OPiv)<sub>4</sub> (0.5 mol%) were dissolved in dry hexanes (2 mL). A solution of the diazo ester (0.5 mmol, 1.0 equiv) in dry hexanes (1.4-2 mL) and dry dichloromethane (0-0.6 mL) was added using a syringe pump for the duration of 1 h. Afterward, the reaction mixture was stirred for further 5 min and concentrated under reduced pressure. The residue was purified by column chromatography on silica gel using hexanes and ethyl acetate as eluents.

General procedure (GP-4): Racemic cyclopropanation of pyrroles with Cu(OTf)<sub>2</sub>

In a flame dried 25-mL round bottom flask equipped with a magnetic stir bar, pyrrole (2.0 equiv) and Cu(OTf)<sub>2</sub> (6.0 mol%) were dissolved in dry dichloromethane (0.6 mL). Phenylhydrazine (0.7 mol%) was added to the reaction mixture. A solution of the diazo ester (1.0 mmol, 1.0 equiv) in dry dichloromethane (0.6 mL) was added using a syringe pump for the duration of 3 h. The reaction mixture was stirred for further 5 min and afterward filtered through basic alumina and washed with DCM (100 mL). The solvent was evaporated in vacuo, and the residue was purified by column chromatography on silica gel using hexanes and ethyl acetate as eluents.

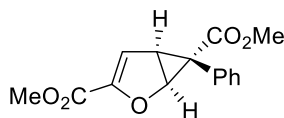
General procedure (GP-5): Racemic cyclopropanation of indole with Rh<sub>2</sub>(OAc)<sub>4</sub>

In a flame dried 25-mL round bottom flask equipped with a magnetic stir bar, indole (2.0 equiv) and Rh<sub>2</sub>(OAc)<sub>4</sub> (0.5 mol%) were dissolved in dry toluene (4 mL). A solution of the diazo ester (1.0 mmol, 1.0 equiv) in dry toluene (2 mL) was added using a syringe pump for the duration of 1 h. Afterward, the reaction mixture was stirred for further 5 min and then concentrated under reduced pressure. The residue was purified by column chromatography on silica gel using hexanes and ethyl acetate as eluents.

**3.2 Synthesis of cyclopropane 98a with 0.001 mol% Rh<sub>2</sub>(S-TCPTTL)<sub>4</sub>**

In a flame dried 250-mL round bottom flask equipped with a magnetic stir bar, methyl furan-2-carboxylate (**19**) (17.7 g, 140.4 mmol, 1.9 equiv) and Rh<sub>2</sub>(S-TCPTTL)<sub>4</sub> (1.3 mg, 0.72 μmol, 0.001 mol%) were dissolved in dry hexanes (45 mL) and cooled to 0 °C. A solution of the diazo ester **97a** (13.1 g, 74.2 mmol, 1.0 equiv) in dry hexanes (12 mL) was added using a syringe pump for the duration of 1 h. Afterward, the reaction mixture was stirred for further 5 min. The product, which precipitated from the reaction mixture, was filtered off and washed with cold hexanes. Thus, cyclopropane **98a** (17.5 g, 63.7 mmol, 86%, 96% *ee*) was obtained as a white solid, and a single recrystallization in refluxing methanol provided enantiomerically pure **98a** (14.5 g, 52.7 mmol, 71%, >99% *ee*).

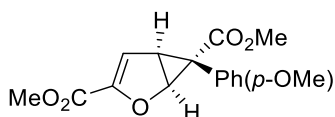
### 3.3 Characterization



dimethyl (1*S*,5*S*,6*R*)-6-phenyl-2-oxabicyclo[3.1.0]hex-3-ene-3,6-dicarboxylate (**98a**)

According to **GP-1** methyl furan-2-carboxylate (**19**) (251 mg, 2.0 mmol, 2.0 equiv) was cyclopropanated with diazo ester **97a** (178 mg, 1.0 mmol, 1.0 equiv) in 2 mL dry hexanes and Rh<sub>2</sub>(*S*-TCPTTL)<sub>4</sub> (1.8 mg, 1.0 μmol, 0.1 mol%). The crude product was purified by flash chromatography (SiO<sub>2</sub>, hexanes/EtOAc, 5:1) to afford cyclopropane **98a** as a white solid (245 mg, 88% yield).

**m.p.** 103-104 °C; **R<sub>f</sub>** = 0.25 (hexanes: ethyl acetate = 5: 1, Vanillin); **[α]<sub>D</sub><sup>20</sup>** -280.2° (c = 1.0, CHCl<sub>3</sub>); **IR** (neat): 3142, 3086, 3030, 2952, 2848, 1733, 1707, 1610, 1498, 1439, 1361, 1323, 1252, 1213, 1148, 1111, 1036, 958, 891, 842, 787 697cm<sup>-1</sup>; **<sup>1</sup>H-NMR** (300 MHz, CDCl<sub>3</sub>): δ 7.30 – 7.17 (m, 5H), 6.11 (d, *J* = 3.0 Hz, 1H), 5.23 (d, *J* = 5.4 Hz, 1H), 3.63 (s, 3H), 3.60 (s, 3H), 3.37 (dd, *J* = 5.4, 3.0 Hz, 1H); **<sup>13</sup>C-NMR** (75 MHz, CDCl<sub>3</sub>): δ 173.1, 158.8, 148.9, 132.3, 129.5, 128.1, 127.7, 114.1, 71.1, 52.9, 52.1, 39.5, 28.5; **HRMS** (+ESI) calcd. for C<sub>13</sub>H<sub>13</sub>O<sub>3</sub> (M+H)<sup>+</sup> 275.0914 found 275.0916; **HPLC** analysis: (Phenomenex Lux Cellulose-1, *n*-heptane: *i*-Propanol = 95:5, 1.0 mL/min, λ = 215 nm, 30 min, t<sub>R</sub> = 13.69 min, major; t<sub>R</sub> = 16.18 min, minor).

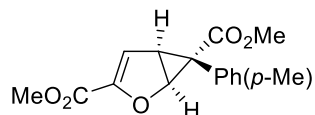


Dimethyl (1*S*,5*S*,6*R*)-6-(4-methoxyphenyl)-2-oxabicyclo[3.1.0]hex-3-ene-3,6-dicarboxylate (**98b**)

According to **GP-1** methyl furan-2-carboxylate (**19**) (251 mg, 2.0 mmol, 2.0 equiv) was cyclopropanated with diazo ester **97b** (208 mg, 1.0 mmol, 1.0 equiv) in 1.4 mL dry hexanes and 0.6 mL dry dichloromethane and Rh<sub>2</sub>(*S*-TCPTTL)<sub>4</sub> (1.8 mg, 1.0 μmol, 0.1 mol%). The crude product was purified by flash chromatography (SiO<sub>2</sub>, hexanes/EtOAc, 5:1) to afford cyclopropane **98b** as a yellowish solid (248 mg, 80% yield).

**m.p.** 115-116 °C; **R<sub>f</sub>** = 0.18 (hexanes: ethyl acetate = 5: 1, Vanillin); **[α]<sub>D</sub><sup>20</sup>** -229.0° (c = 1.0, CHCl<sub>3</sub>, 95% *ee*); **IR** (neat): 2955, 2839, 1708, 1612, 1516, 1436, 1338, 1245, 1213, 1176, 1147, 1113, 1034, 958, 913, 884, 848, 799, 731, 633, 538, 500 cm<sup>-1</sup>; **<sup>1</sup>H NMR** (300 MHz, CDCl<sub>3</sub>) δ

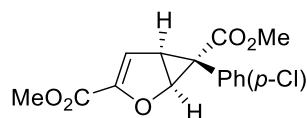
7.16 – 7.06 (m, 2H), 6.83 – 6.74 (m, 2H), 6.10 (d,  $J = 3.0$  Hz, 1H), 5.19 (d,  $J = 5.4$  Hz, 1H), 3.75 (s, 3H), 3.62 (s, 3H), 3.61 (s, 3H), 3.33 (dd,  $J = 5.4, 3.0$  Hz, 1H);  $^{13}\text{C}$  NMR (75 MHz,  $\text{CDCl}_3$ )  $\delta$  173.5, 158.9, 158.8, 149.0, 133.4, 121.4, 114.1, 113.6, 71.3, 55.1, 52.8, 52.1, 39.7, 27.8; **HRMS** (+ESI) calcd. for  $\text{C}_{16}\text{H}_{17}\text{O}_6$  ( $\text{M}+\text{H}$ ) $^+$  305.1020 found 305.1021; **HPLC** analysis: 95% *ee* (Phenomenex Lux Cellulose-1, *n*-heptane: *i*-Propanol = 95:5, 1.0 mL/min,  $\lambda = 215$  nm, 30 min,  $t_{\text{R}} = 17.23$  min, major;  $t_{\text{R}} = 23.71$  min, minor).



dimethyl (1*S*,5*S*,6*R*)-6-(*p*-tolyl)-2-oxabicyclo[3.1.0]hex-3-ene-3,6-dicarboxylate (**98c**)

According to **GP-1** methyl furan-2-carboxylate (**19**) (251 mg, 2.0 mmol, 2.0 equiv) was cyclopropanated with diazo ester **97c** (191 mg, 1.0 mmol, 1.0 equiv) in 1.8 mL dry hexanes and 0.2 mL dry dichloromethane and  $\text{Rh}_2(\text{S-TCPTTL})_4$  (1.8 mg, 1.0  $\mu\text{mol}$ , 0.1 mol%). The crude product was purified by flash chromatography ( $\text{SiO}_2$ , hexanes/EtOAc, 5:1) to afford cyclopropane **98c** as a white solid (247 mg, 85% yield).

**m.p.** 112-115  $^\circ\text{C}$ ; **R<sub>f</sub>** = 0.28 (hexanes: ethyl acetate = 5: 1, Vanillin); **[ $\alpha$ ]<sub>D</sub><sup>20</sup>** -266.1 $^\circ$  ( $c = 1.0$ ,  $\text{CHCl}_3$ , 95% *ee*); **IR** (neat): 3027, 2954, 2014, 1720, 1709, 1611, 1519, 1435, 1338, 1253, 1212, 1146, 1113, 1040, 1004, 958, 913, 884, 847, 820, 794, 758, 731, 623, 553, 528, 499, 455  $\text{cm}^{-1}$ ;  **$^1\text{H}$  NMR** (300 MHz,  $\text{CDCl}_3$ )  $\delta$  7.13 – 7.01 (m, 4H), 6.10 (d,  $J = 3.0$  Hz, 1H), 5.21 (d,  $J = 5.4$  Hz, 1H), 3.62 (s, 3H), 3.61 (s, 3H), 3.34 (dd,  $J = 5.4, 3.0$  Hz, 1H), 2.28 (s, 3H);  **$^{13}\text{C}$  NMR** (75 MHz,  $\text{CDCl}_3$ )  $\delta$  173.4, 158.9, 148.9, 137.3, 132.1, 128.9, 126.4, 114.2, 71.2, 52.9, 52.1, 39.6, 28.2, 21.3; **HRMS** (+ESI) calcd. for  $\text{C}_{16}\text{H}_{17}\text{O}_5$  ( $\text{M}+\text{H}$ ) $^+$  289.1071 found 289.1073; **HPLC** analysis: >99% *ee*, Phenomenex Lux Cellulose-1, *n*-heptane: *i*-Propanol = 95:5, 1.0 mL/min,  $\lambda = 215$  nm, 30 min,  $t_{\text{R}} = 11.95$  min (15.16 min)

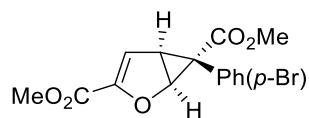


Dimethyl (1*S*,5*S*,6*R*)-6-(4-chlorophenyl)-2-oxabicyclo[3.1.0]hex-3-ene-3,6-dicarboxylate (**98d**)

According to **GP-1** methyl furan-2-carboxylate (**19**) (254 mg, 2.0 mmol, 2.0 equiv) was cyclopropanated with diazo ester **97d** (208 mg, 1.0 mmol, 1.0 equiv) in 2 mL dry hexanes and  $\text{Rh}_2(\text{S-TCPTTL})_4$  (1.8 mg, 1.0  $\mu\text{mol}$ , 0.1 mol%). The crude product was purified by flash

chromatography (SiO<sub>2</sub>, hexanes/EtOAc, 5:1) to afford cyclopropane **98d** as a white solid (249 mg, 82% yield).

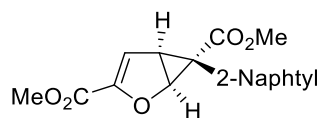
**m.p.** 86-87°C; **R<sub>f</sub>** = 0.23 (hexanes: ethyl acetate = 5: 1, Vanillin); **[α]<sub>D</sub><sup>20</sup>** -257.5° (c = 1.0, CHCl<sub>3</sub>, 98% *ee*); **IR** (neat): 2954, 1713, 1611, 1495, 1436, 1401, 1337, 1254, 1213, 1147, 1115, 1091, 1040, 1016, 958, 911, 885, 848, 796, 758, 739, 633, 591, 529, 493, 452, 419 cm<sup>-1</sup>; **<sup>1</sup>H NMR** (300 MHz, CDCl<sub>3</sub>) δ 7.26 – 7.20 (m, 2H), 7.19 – 7.09 (m, 2H), 6.11 (d, *J* = 2.9 Hz, 1H), 5.22 (d, *J* = 5.4 Hz, 1H), 3.63 (s, 6H), 3.37 (dd, *J* = 5.3, 3.0 Hz, 1H); **<sup>13</sup>C NMR** (75 MHz, CDCl<sub>3</sub>) δ 172.6, 158.7, 149.1, 133.7, 133.6, 128.5, 128.2, 113.8, 71.1, 52.9, 52.2, 39.6, 27.9; **HRMS** (+ESI) calcd. for C<sub>15</sub>H<sub>13</sub>ClO<sub>5</sub> (M+H)<sup>+</sup> 309.0524 found 309.0527; **HPLC** analysis: 98% *ee* (AD-H, *n*-hexane: *i*-Propanol = 99:1, 1.0 mL/min, λ = 230 nm, 60 min, t<sub>R</sub> = 27.86 min, minor; t<sub>R</sub> = 43.01 min, major).



Dimethyl (1*S*,5*S*,6*R*)-6-(4-bromophenyl)-2-oxabicyclo[3.1.0]hex-3-ene-3,6-dicarboxylate (**98e**)

According to **GP-1** methyl furan-2-carboxylate (**19**) (253 mg, 2.0 mmol, 2.0 equiv) was cyclopropanated with diazo ester **91** (253 mg, 1.0 mmol, 1.0 equiv) in 1.6 mL dry hexanes and 0.4 mL dry dichloromethane and Rh<sub>2</sub>(*S*-TCPTTL)<sub>4</sub> (1.8 mg, 1.0 μmol, 0.1 mol%). The crude product was purified by flash chromatography (SiO<sub>2</sub>, hexanes/EtOAc, 5:1) to afford cyclopropane **98e** as a white solid (275 mg, 78% yield).

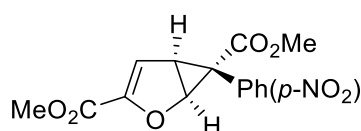
**m.p.** 89-90 °C; **R<sub>f</sub>** = 0.21 (hexanes: ethyl acetate = 5: 1, Vanillin); **[α]<sub>D</sub><sup>20</sup>** -° (c = 1.0, CHCl<sub>3</sub>, 98% *ee*); **IR** (neat): 2955, 1713, 1611, 1490, 1436, 1396, 1337, 1254, 1213, 1147, 1115, 1071, 1041, 1012, 958, 912, 847, 795, 758 733, 633, 583, 535, 499 cm<sup>-1</sup>; **<sup>1</sup>H NMR** (300 MHz, CDCl<sub>3</sub>) δ 7.44 – 7.35 (m, 2H), 7.14 – 7.00 (m, 2H), 6.10 (d, *J* = 2.9 Hz, 1H), 5.22 (d, *J* = 5.4 Hz, 1H), 3.64 (s, 3H), 3.63 (s, 3H), 3.37 (dd, *J* = 5.3, 3.0 Hz, 1H); **<sup>13</sup>C NMR** (75 MHz, CDCl<sub>3</sub>) δ 172.5, 158.7, 149.2, 133.9, 131.4, 128.7, 122.0, 113.8, 71.1, 53.0, 52.3, 39.6, 27.9; **HRMS** (+ESI) calcd. for C<sub>15</sub>H<sub>13</sub>BrO<sub>5</sub> (M+H)<sup>+</sup> 353.0019 found 353.0018; **HPLC** analysis: 98% *ee* (AD-H, *n*-hexane: *i*-Propanol = 99:1, 1.0 mL/min, λ = 230 nm, 60 min, t<sub>R</sub> = 29.22 min, minor; t<sub>R</sub> = 45.86 min, major).



Dimethyl (1*S*,5*S*,6*R*)-6-(naphthalen-2-yl)-2-oxabicyclo[3.1.0]hex-3-ene-3,6-dicarboxylate (**98f**)

According to **GP-1** methyl furan-2-carboxylate (**19**) (250 mg, 2.0 mmol, 2.0 equiv) was cyclopropanated with diazo ester **97f** (226 mg, 1.0 mmol, 1.0 equiv) in 1.4 mL dry hexanes and 0.6 mL dry dichloromethane and Rh<sub>2</sub>(*S*-TCPTTL)<sub>4</sub> (1.8 mg, 1.0 μmol, 0.1 mol%). The crude product was purified by flash chromatography (SiO<sub>2</sub>, hexanes/EtOAc, 5:1) to afford cyclopropane **98f** as a yellowish solid (211 mg, 65% yield).

**m.p.** 114-115 °C; **R<sub>f</sub>** = 0.18 (hexanes: ethyl acetate = 5: 1, Vanillin); **[α]<sub>D</sub><sup>20</sup>** -234.3° (c = 1.0, CHCl<sub>3</sub>, 94% *ee*); **IR** (neat): 3058, 2953, 2848, 1708, 1609, 1507, 1435, 1328, 1255, 1213, 1146, 1111, 1041, 976, 958, 911, 864, 827, 795, 732, 652, 634, 604, 534, 498 cm<sup>-1</sup>; **<sup>1</sup>H NMR** (300 MHz, CDCl<sub>3</sub>) δ 7.83 – 7.69 (m, 4H), 7.49 – 7.41 (m, 2H), 7.35 – 7.26 (m, 1H), 6.16 (d, *J* = 3.0 Hz, 1H), 5.33 (d, *J* = 5.4 Hz, 1H), 3.63 (s, 3H), 3.51 (s, 3H), 3.45 (dd, *J* = 5.4, 3.0 Hz, 1H); **<sup>13</sup>C NMR** (75 MHz, CDCl<sub>3</sub>) δ 173.2, 158.8, 149.2, 133.0, 132.8, 131.7, 129.5, 128.0, 127.9, 127.6, 127.0, 126.1, 125.9, 113.9, 71.5, 52.9, 52.1, 39.8, 28.6; **HRMS** (+ESI) calcd. for C<sub>19</sub>H<sub>17</sub>O<sub>5</sub> (M+H)<sup>+</sup> 325.1071 found 325.1075; **HPLC** analysis: 94% *ee* (Phenomenex Lux Cellulose-1, *n*-heptane: *i*-Propanol = 95:5, 1.0 mL/min, λ = 215 nm, 30 min, t<sub>R</sub> = 16.11 min, major; t<sub>R</sub> = 22.78 min, minor)

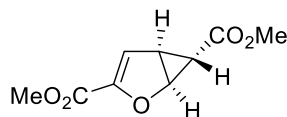


dimethyl (1*S*,5*S*,6*R*)-6-(4-nitrophenyl)-2-oxabicyclo[3.1.0]hex-3-ene-3,6-dicarboxylate (**98g**)

According to **GP-1** methyl furan-2-carboxylate (**19**) (250 mg, 2.0 mmol, 2.0 equiv) in dry toluene (2 mL) was cyclopropanated with diazo ester **97g** (215 mg, 1.0 mmol, 1.0 equiv) in dry toluene (6 mL) and Rh<sub>2</sub>(*S*-TCPTTL)<sub>4</sub> (1.8 mg, 1.0 μmol, 0.1 mol%). The crude product was purified by flash chromatography (SiO<sub>2</sub>, hexanes/EtOAc, 3:1) to afford cyclopropane **98g** as a yellowish solid (172 mg, 57% yield).

**m.p.** 106-107 °C; **R<sub>f</sub>** = 0.28 (hexanes: ethyl acetate = 3: 1, Vanillin); **[α]<sub>D</sub><sup>20</sup>** -211.8° (c = 1.0, CHCl<sub>3</sub>, 87% *ee*); **IR** (neat): 3105, 3070, 3004, 2956, 1700, 1592, 1495, 1435, 1308, 1246, 1148, 1061, 1018, 977, 954, 885, 738, 701 cm<sup>-1</sup>; **<sup>1</sup>H NMR** (300 MHz, CDCl<sub>3</sub>) δ 8.22 – 8.10 (m, 2H),

7.48 – 7.35 (m, 2H), 6.13 (d,  $J = 3.0$  Hz, 1H), 5.30 (d,  $J = 5.4$  Hz, 1H), 3.65 (s, 3H), 3.62 (s, 3H), 3.46 (dd,  $J = 5.4, 3.0$  Hz, 1H);  $^{13}\text{C}$  NMR (101 MHz,  $\text{CDCl}_3$ )  $\delta$  171.6, 158.5, 149.3, 147.4, 137.4, 133.3, 123.4, 113.4, 71.1, 53.1, 52.3, 39.7, 28.0; **HRMS** (+ESI) calcd. for  $\text{C}_{15}\text{H}_{14}\text{NO}_7$  ( $\text{M}+\text{H}$ ) $^+$  320.0765 found 320.0767; **HPLC** analysis: 87% *ee* (Phenomenex Lux Cellulose-2, *n*-heptane: *i*-Propanol = 70:30, 0.5 mL/min,  $\lambda = 254$  nm, 60 min,  $t_{\text{R}} = 24.96$  min, major;  $t_{\text{R}} = 36.80$  min, minor).

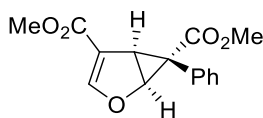


dimethyl (1*S*,5*S*,6*S*)-2-oxabicyclo[3.1.0]hex-3-ene-3,6-dicarboxylate (**83**)

According to GP-1 methyl furan-2-carboxylate (**19**) (251 mg, 2.0 mmol, 2.0 equiv) was cyclopropanated with diazo ester **79** (290 mg, 35 wt % in pentane, 1.0 mmol, 1.0 equiv) in 1.8 mL dry hexanes and  $\text{Rh}_2(\text{S-TCPTTL})_4$  (1.8 mg, 1.0  $\mu\text{mol}$ , 0.1 mol%). The crude product was purified by flash chromatography ( $\text{SiO}_2$ , hexanes/EtOAc, 14:1  $\rightarrow$  5:1) to afford cyclopropane **83** as a white solid (73 mg, 36% yield).

Spectroscopic data matched well with those reported in literature.<sup>21</sup>

$^1\text{H}$  NMR (300 MHz,  $\text{CDCl}_3$ )  $\delta$  6.38 (d,  $J = 2.9$  Hz, 1H), 4.97 (dd,  $J = 5.3, 1.0$  Hz, 1H), 3.80 (s, 3H), 3.70 (s, 3H), 2.86 (ddd,  $J = 5.5, 2.8, 2.8$  Hz, 1H), 1.17 (dd,  $J = 2.7, 1.0$  Hz, 1H). **HPLC** analysis: 8% *ee* (Phenomenex Lux Cellulose-2, *n*-heptane: *i*-Propanol = 99:1, 1.0 mL/min,  $\lambda = 254$  nm, 70 min,  $t_{\text{R}} = 41.29$  min, major;  $t_{\text{R}} = 48.23$  min, minor).

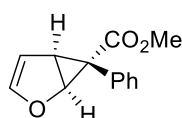


dimethyl (1*S*,5*S*,6*R*)-6-phenyl-2-oxabicyclo[3.1.0]hex-3-ene-4,6-dicarboxylate (**108**)

According to GP-1 methyl furan-3-carboxylate (**105**) (254 mg, 2.0 mmol, 2.0 equiv) was cyclopropanated with diazo ester **97a** (177 mg, 1.0 mmol, 1.0 equiv) in 2 mL dry hexanes and  $\text{Rh}_2(\text{S-TCPTTL})_4$  (1.8 mg, 1.0  $\mu\text{mol}$ , 0.1 mol%). The crude product was purified by flash chromatography ( $\text{SiO}_2$ , hexanes/EtOAc, 19:1  $\rightarrow$  5:1) to afford cyclopropane **108** as a white solid (201 mg, 73% yield). The enantioselectivity was enriched to 99% *ee* by recrystallization in refluxing methanol.

**m.p.** 100-101  $^\circ\text{C}$ ; **R<sub>f</sub>** = 0.20 (hexanes: ethyl acetate = 95: 5, Vanillin); **[ $\alpha$ ]<sub>D</sub><sup>20</sup>** -138.5 $^\circ$  ( $c = 1.0$ ,  $\text{CHCl}_3$ , 99% *ee*); **IR** (neat): 3109, 3030, 2956, 2848, 2363, 1711, 1607, 1498, 1439, 1375, 1331,

1286, 1252, 1141 1100, 1006, 969, 910, 850, 794, 753, 701  $\text{cm}^{-1}$ ;  **$^1\text{H-NMR}$**  (300 MHz,  $\text{CDCl}_3$ ):  $\delta$  7.29 – 7.22 (m, 3H), 7.18 – 7.12 (m, 2H), 6.68 (d,  $J = 0.6$  Hz, 1H), 5.29 (dd,  $J = 5.7, 0.8$  Hz, 1H), 3.69 (s, 3H), 3.60 (s, 3H), 3.54 (d,  $J = 5.7$  Hz, 1H);  **$^{13}\text{C-NMR}$**  (75 MHz,  $\text{CDCl}_3$ ):  $\delta$  172.9, 164.1, 156.3, 132.2, 129.6, 128.2, 127.8, 113.8, 72.5, 52.8, 51.5, 36.9, 28.2; **HRMS** (+ESI) calcd. for  $\text{C}_{15}\text{H}_{15}\text{O}_5$  ( $\text{M}+\text{H}$ ) $^+$  275.0914 found 275.0921; **HPLC** analysis: 99% *ee* (Phenomenex Lux Cellulose-1, *n*-heptane: *i*-Propanol = 95:5, 1.0 mL/min,  $\lambda = 215$  nm, 30 min,  $t_{\text{R}} = 8.46$  min, major;  $t_{\text{R}} = 10.03$  min, minor).



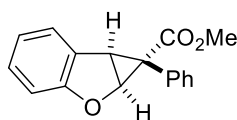
methyl (1*S*,5*S*,6*R*)-6-phenyl-2-oxabicyclo[3.1.0]hex-3-ene-6-carboxylate (**109**)

According to **GP-1** furan (**14**) (136 mg, 2.0 mmol, 2.0 equiv) was cyclopropanated with diazo ester **97a** (176 mg, 1.0 mmol, 1.0 equiv) in 2 mL dry hexanes and  $\text{Rh}_2(\text{S-TCPTTL})_4$  (1.8 mg, 1.0  $\mu\text{mol}$ , 0.1 mol%). The crude product was purified by flash chromatography ( $\text{SiO}_2$ , hexanes/EtOAc, 5:1) to afford cyclopropane **109** as a white solid (155 mg, 72% yield). The enantioselectivity was enriched to 99% *ee* by recrystallization in refluxing methanol.

Spectroscopic data matches well with those reported in the literature for (*rac*)-**109**.<sup>22</sup>

**m.p.** 72-73  $^\circ\text{C}$ ;  **$R_f$**  = 0.35 (hexanes: ethyl acetate = 5: 1, Vanillin);  **$[\alpha]_{\text{D}}^{20}$**  -105.1 $^\circ$  ( $c = 0.10$ ,  $\text{CHCl}_3$ , 74% *ee*); **IR** (neat): 3105, 3004, 2956, 2844, 2102, 1990, 1700, 1592, 1495, 1435, 1308, 1255, 1148, 1051, 1018, 977, 954, 835, 738, 701  $\text{cm}^{-1}$ ;  **$^1\text{H-NMR}$**  (300 MHz,  $\text{CDCl}_3$ ):  $\delta$  7.33 – 7.24 (m, 3H), 7.22 – 7.16 (m, 2H), 5.91 (dd,  $J = 2.6, 0.6$  Hz, 1H), 5.23 (dd,  $J = 2.6, 2.6$  Hz, 1H), 5.14 (dd,  $J = 5.6, 0.7$  Hz, 1H), 3.62 (s, 3H), 3.31 (dd,  $J = 5.6, 2.7$  Hz, 1H);  **$^{13}\text{C-NMR}$**  (75 MHz,  $\text{CDCl}_3$ ):  $\delta$  173.9, 147.4, 132.7, 130.7, 127.8, 127.3, 104.0, 70.8, 52.6, 39.3, 27.8; **HRMS** (+APCI) calcd. for  $\text{C}_{13}\text{H}_{13}\text{O}_3$  ( $\text{M}+\text{H}$ ) $^+$  217.0859 found 217.0861; **HPLC analysis**: 74% *ee* (Phenomenex Lux Cellulose-1, *n*-heptane: *i*-Propanol = 99:1, 1.0 mL/min,  $\lambda = 215$  nm, 60 min,  $t_{\text{R}} = 8.22$  min, major;  $t_{\text{R}} = 9.29$  min, minor).

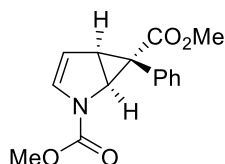




Methyl (1*R*,1*aS*,6*bS*)-1-phenyl-1*a*,6*b*-dihydro-1*H*-cyclopropa[*b*]benzofuran-1-carboxylate (**110**)

According to **GP-1** benzofuran (**106**) (236 mg, 2.0 mmol, 2.0 equiv) was cyclopropanated with diazo ester **97a** (176 mg, 1.0 mmol, 1.0 equiv) in 2 mL dry hexanes and Rh<sub>2</sub>(*S*-TCPTTL)<sub>4</sub> (1.8 mg, 1.0 μmol, 0.1 mol%). The crude product was purified by flash chromatography (SiO<sub>2</sub>, hexanes/EtOAc, 9:1) to afford cyclopropane **110** as a white solid (243 mg, 91% yield).

**m.p.** 122 °C; **R<sub>f</sub>** = 0.46 (hexanes: ethyl acetate = 5:1, Vanillin); **[α]<sub>D</sub><sup>20</sup>** -119.2° (c = 0.5, CHCl<sub>3</sub>, 27% *ee*); **IR** (neat): 3053, 2952, 2848, 1703, 1619, 1595, 1465, 1439, 1323, 1260, 1252, 1156, 1088, 1029, 965, 894, 854, 813, 753, 697 cm<sup>-1</sup>; **<sup>1</sup>H-NMR** (300 MHz, CDCl<sub>3</sub>): δ 7.38 (dd, *J* = 7.3, 1.4 Hz, 1H), 7.14 – 7.05 (m, 5H), 6.95 – 6.88 (m, 1H), 6.82 (td, *J* = 7.4, 1.1 Hz, 1H), 6.50 – 6.46 (m, 1H), 5.40 (d, *J* = 5.5 Hz, 1H), 3.82 (d, *J* = 5.5 Hz, 1H), 3.67 (s, 3H); **<sup>13</sup>C-NMR** (75 MHz, CDCl<sub>3</sub>): δ 173.4, 159.5, 132.6, 129.6, 128.1, 127.6, 127.2, 126.5, 125.1, 121.2, 109.7, 70.5, 52.8, 37.4, 30.9; **HRMS** (+APCI) calcd. for C<sub>17</sub>H<sub>15</sub>O<sub>3</sub> (M+H)<sup>+</sup> 267.1016 found 267.1017; **HPLC** analysis: 27% *ee* (Phenomenex Lux Cellulose-1, *n*-heptane: *i*-Propanol = 90:10, 1.0 mL/min, λ = 215 nm, 20 min, t<sub>R</sub> = 5.86 min, major; t<sub>R</sub> = 7.23 min, minor)

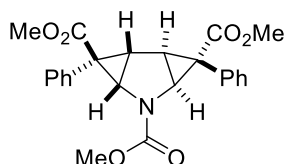


dimethyl (1*S*,5*S*,6*R*)-6-phenyl-2-azabicyclo[3.1.0]hex-3-ene-2,6-dicarboxylate (**119a**)

According to **GP-2** pyrrole (**113a**) (250 mg, 2.0 mmol, 2.0 equiv) was cyclopropanated with diazo ester **97a** (176 mg, 1.0 mmol, 1.0 equiv) and Rh<sub>2</sub>(*S*-TCPTTL)<sub>4</sub> (1.8 mg, 1.0 μmol, 0.1 mol%). The crude product was purified by flash chromatography (SiO<sub>2</sub>, hexanes/EtOAc, 5:1) to afford cyclopropane **119a** as a white solid (26 mg, 8% yield).

**m.p.** 113-115°C; **R<sub>f</sub>** = 0.27 (hexanes : ethyl acetate = 5:1, Vanillin); **[α]<sub>D</sub><sup>20</sup>** -47.6° (c = 0.3, CHCl<sub>3</sub>, 7% *ee*); **IR** (neat): 3116, 3060, 3030, 2956, 1707, 1592, 1498, 1446, 1398, 1334, 1245, 1193, 1144, 1059, 1006, 973, 891, 854, 805, 755, 705 cm<sup>-1</sup>; **<sup>1</sup>H NMR** (400 MHz, CDCl<sub>3</sub>) δ 7.29 – 7.22 (m, 3H), 7.14 – 7.02 (m, 2H), 6.19 – 5.97 (m, 1H), 5.27 – 5.15 (m, 1H), 4.78 – 4.61 (m, 1H), 3.92 – 3.72 (m, 3H), 3.65 – 3.60 (m, 3H), 3.37 – 3.30 (m, 1H); **<sup>13</sup>C NMR** (101 MHz, CDCl<sub>3</sub>) δ 173.9, 173.7, 152.9, 132.6, 132.3, 131.0, 130.9, 130.8, 129.9, 128.1, 127.9, 127.5,

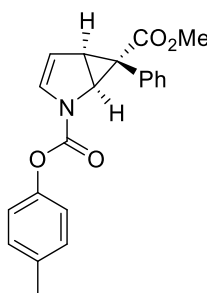
127.4, 108.5, 108.4, 53.3, 53.3, 52.7, 52.6, 49.5, 49.3, 39.2, 38.1, 29.9, 29.6; **HRMS** (+ESI) calcd. for  $C_{15}H_{15}NO_4$  (M+H)<sup>+</sup> 274.1074 found 274.1076; **HPLC** analysis: 7% *ee* (Phenomenex Lux Cellulose-2, *n*-heptane: *i*-Propanol = 70:30, 0.5 mL/min,  $\lambda$  = 254 nm, 60 min,  $t_R$  = 18.05 min, major;  $t_R$  = 30.14 min, minor).



Trimethyl-*rel*-(1*S*,2*S*,3*R*,4*S*,6*S*,7*R*)-3,7-diphenyl-5-azatricyclo[4.1.0.02,4]heptane-3,5,7-tricarboxylate (**120a**)

Double cyclopropanated pyrrole **120a** (111 mg, 26% yield) was obtained as a side product of **119a** following **GP-2**. The crude mixture was purified by flash chromatography (SiO<sub>2</sub>, hexanes/EtOAc, 5:1) to obtain **120a** as a white solid.

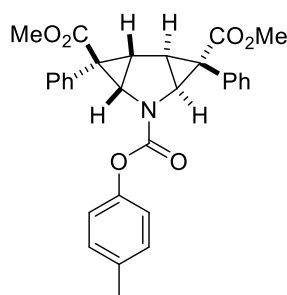
**m.p.** 203-205 °C; **R<sub>f</sub>** = 0.13 (hexanes : ethyl acetate = 5:1, Vanillin); **IR** (neat): 3064, 3030, 2956, 2363, 2255, 1703, 1498, 1454, 1409, 1331, 1323, 1238, 1129, 1077, 1029, 989, 910, 865, 790, 727, 699 cm<sup>-1</sup>; **<sup>1</sup>H NMR** (300 MHz, CDCl<sub>3</sub>)  $\delta$  7.44 – 7.32 (m, 6H), 7.29 – 7.17 (m, 4H), 3.84 – 3.77 (m, 3H), 3.57 – 3.47 (m, 6H), 3.12 – 2.96 (m, 2H), 2.66 – 2.58 (m, 2H); **<sup>13</sup>C NMR** (75 MHz, CDCl<sub>3</sub>)  $\delta$  171.7, 171.5, 155.9, 131.6, 131.6, 131.5, 131.3, 128.8, 128.6, 127.9, 127.8, 53.1, 52.7, 52.7, 48.1, 47.8, 37.7, 37.4, 33.2, 32.1; **HRMS** (+ESI) calcd. for  $C_{24}H_{24}NO_6$  (M+H)<sup>+</sup> 422.1598 found 422.1608.



6-methyl 2-(*p*-tolyl) (1*S*,5*S*,6*R*)-6-phenyl-2-azabicyclo[3.1.0]hex-3-ene-2,6-dicarboxylate (**119b**)

According to **GP-2** pyrrole **113b** (402 mg, 2.0 mmol, 2.0 equiv) was cyclopropanated with diazo ester **97a** (176 mg, 1.0 mmol, 1.0 equiv) and Rh<sub>2</sub>(*S*-TCPTTL)<sub>4</sub> (1.8 mg, 1.0  $\mu$ mol, 0.1 mol%). The crude product was purified by flash chromatography (SiO<sub>2</sub>, hexanes/EtOAc, 5:1) to afford cyclopropane **119b** as a sticky colorless oil (141 mg, 40% yield).

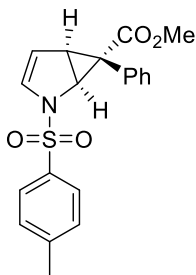
**R<sub>f</sub>** = 0.33 (hexanes : ethyl acetate = 5:1, Vanillin); [**α**]<sub>D</sub><sup>20</sup> -236.4 (c = 1.0, CHCl<sub>3</sub>, 57% *ee*); **IR** (neat): 3034, 2952, 2363, 2255, 1707, 1595, 1510, 1402, 1334, 1245, 1200, 1167, 1118, 1003, 965, 906, 861, 723 cm<sup>-1</sup>; **<sup>1</sup>H NMR** (400 MHz, CDCl<sub>3</sub>) δ 7.37 – 7.27 (m, 3H), 7.25 – 7.11 (m, 5H), 6.98 – 6.93 (m, 1H), 6.27 – 6.19 (m, 1H), 5.38 – 5.29 (m, 1H), 4.91 – 4.79 (m, 1H), 3.67 – 3.63 (m, 3H), 3.45 – 3.37 (m, 1H), 2.41 – 2.34 (m, 3H); **<sup>13</sup>C NMR** (101 MHz, CDCl<sub>3</sub>) δ 173.7, 173.5, 151.0, 150.9, 148.4, 148.4, 135.7, 135.6, 132.7, 132.4, 130.9, 130.9, 130.8, 130.1, 130.1, 130.0, 128.2, 128.1, 127.7, 127.6, 121.2, 109.4, 109.3, 52.8, 52.7, 49.5, 49.4, 39.1, 38.1, 30.6, 30.2, 20.9, 20.9; **HRMS** (+APCI) calcd. for C<sub>21</sub>H<sub>20</sub>NO<sub>4</sub> (M+H)<sup>+</sup> 350.1387 found 350.1392; **HPLC** analysis: 57% *ee* (Phenomenex Lux Cellulose-2, *n*-heptane: *i*-Propanol = 70:30, 0.5 mL/min, λ = 254 nm, 40 min, t<sub>R</sub> = 16.74 min, major; t<sub>R</sub> = 23.26 min, minor).



3,7-dimethyl 5-(*p*-tolyl)-*rel*-(1*S*,2*S*,3*R*,4*S*,6*S*,7*R*)-3,7-diphenyl-5-azatricyclo[4.1.0.0.2,4]heptane-3,5,7-tricarboxylate (**120b**)

Double cyclopropanated pyrrole **120b** (136 mg, 27% yield) was obtained as a side product of **119b** following **GP-2**. The crude mixture was purified by flash chromatography (SiO<sub>2</sub>, hexanes/EtOAc, 5:1→2:1) to obtain **120b** as a white solid.

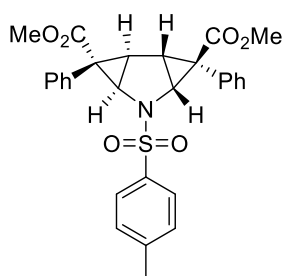
**m.p.** 223-225 °C; **R<sub>f</sub>** = 0.15 (hexanes : ethyl acetate = 5:1, Vanillin); **IR** (neat): 3407, 3060, 3034, 2956, 1715, 1603, 1510, 1416, 1323, 1238, 1200, 1167, 1118, 1081, 969, 738, 705 cm<sup>-1</sup>; **<sup>1</sup>H NMR** (300 MHz, CDCl<sub>3</sub>) δ 7.50 – 7.32 (m, 10H), 7.25 – 7.18 (m, 2H), 7.05 – 6.98 (m, 2H), 3.58 – 3.50 (m, 6H), 3.28 – 3.13 (m, 2H), 2.77 – 2.68 (m, 2H), 2.37 (s, 3H); **<sup>13</sup>C NMR** (75 MHz, CDCl<sub>3</sub>) δ 171.6, 171.4, 153.9, 148.54, 135.5, 131.7, 131.6, 131.5, 131.4, 130.0, 128.9, 128.7, 128.1, 128.0, 121.2, 52.8, 52.7, 48.1, 37.9, 37.7, 33.2, 32.3, 20.9; **HRMS** (+ESI) calcd. for C<sub>30</sub>H<sub>28</sub>NO<sub>6</sub> (M+H)<sup>+</sup> 498.1911 found 498.1917.



methyl (1*S*,5*S*,6*R*)-6-phenyl-2-tosyl-2-azabicyclo[3.1.0]hex-3-ene-6-carboxylate (**119c**)

According to **GP-2** pyrrole **113c** (442 mg, 2.0 mmol, 2.0 equiv) was cyclopropanated with diazo ester **97a** (176 mg, 1.0 mmol, 1.0 equiv) and Rh<sub>2</sub>(*S*-TCPTTL)<sub>4</sub> (1.8 mg, 1.0 μmol, 0.1 mol%). The crude product was purified by flash chromatography (SiO<sub>2</sub>, hexanes/EtOAc, 5:1) to afford cyclopropane **119c** as a white solid (226 mg, 61% yield).

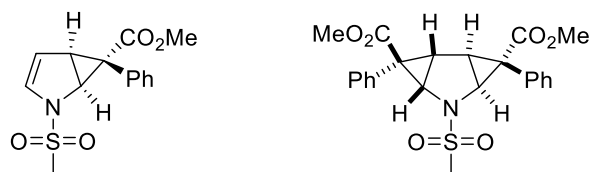
**m.p.** 120-122 °C; **R<sub>f</sub>** = 0.21 (hexanes : ethyl acetate = 5:1, Vanillin); **[α]<sub>D</sub><sup>20</sup>** -670.2° (c = 0.10, CHCl<sub>3</sub>); **IR** (neat): 3109, 3064, 3030, 2952, 2259, 1707, 1584, 1495, 1435, 1357, 1252, 1167, 1137, 1077, 1051, 989, 910, 813, 727 cm<sup>-1</sup>; **<sup>1</sup>H-NMR** (300 MHz, CDCl<sub>3</sub>): δ 7.73 – 7.68 (m, 2H), 7.37 – 7.31 (m, 2H), 7.29 – 7.16 (m, 5H), 5.95 (dd, *J* = 3.9, 1.4 Hz, 1H), 5.28 (dd, *J* = 3.9, 2.5 Hz, 1H), 4.53 (dd, *J* = 6.5, 1.4 Hz, 1H), 3.60 (s, 3H), 3.14 (dd, *J* = 6.5, 2.5 Hz, 1H), 2.45 (s, 3H); **<sup>13</sup>C-NMR** (75 MHz, CDCl<sub>3</sub>): δ 173.7, 144.4, 134.8, 132.5, 130.9, 130.4, 130.0, 127.8, 127.5, 127.2, 111.4, 52.9, 52.2, 38.7, 28.0, 21.7; **HRMS** (+ESI) calcd. for C<sub>20</sub>H<sub>20</sub>NO<sub>4</sub>S (M+H)<sup>+</sup> 370.1108 found 370.1112; **HPLC** analysis: >99% *ee* (Phenomenex Lux Cellulose-1, *n*-heptane: *i*-Propanol = 95:5, 0.5 mL/min, λ = 215 nm, 60 min, t<sub>R</sub> = 35.04 min (t<sub>R</sub> = 41.66 min)).



Dimethyl-*rel*-(1*R*,2*R*,3*S*,4*R*,6*R*,7*S*)-3,7-diphenyl-5-tosyl-5-azatricyclo[4.1.0.0<sub>2,4</sub>]heptane-3,7-dicarboxylate (**120c**)

Double cyclopropanated pyrrole **120c** (80 mg, 15% yield) was obtained as a side product of **119c** following **GP-2**. The crude mixture was purified by flash chromatography (SiO<sub>2</sub>, hexanes/EtOAc, 5:1 → 2:1) to obtain **120c** as a white solid. Analytical data were identical to those of its enantiomer and can be found in chapter E.3.4

**HPLC analysis:** 37 % ee (Phenomenex Lux Cellulose-1, *n*-heptane: *i*-Propanol = 70:30, 0.5 mL/min,  $\lambda$  = 215 nm, 40 min,  $t_R$  = 14.45 min, minor;  $t_R$  = 19.35 min, major).



methyl (1*S*,5*S*,6*R*)-2-(methylsulfonyl)-6-phenyl-2-azabicyclo[3.1.0]hex-3-ene-6-carboxylate (**119d**)

dimethyl-*rel*-(1*S*,2*S*,3*R*,4*S*,6*S*,7*R*)-5-(methylsulfonyl)-3,7-diphenyl-5-azatricyclo[4.1.0.0.2,4]heptane-3,7-dicarboxylate (**120d**)

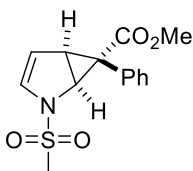
According to **GP-2** pyrrole **113d** (290 mg, 2.0 mmol, 2.0 equiv) was cyclopropanated with diazo ester **97a** (176 mg, 1.0 mmol, 1.0 equiv) and Rh<sub>2</sub>(*S*-TCPTTL)<sub>4</sub> (1.8 mg, 1.0  $\mu$ mol, 0.1 mol%). The crude product was purified by flash chromatography (SiO<sub>2</sub>, hexanes/EtOAc, 5:1) to afford a mixture of cyclopropane **119d** and side product **120d** (87 mg, ratio **119d**/**120d** = 1/0.85).

**R<sub>f</sub>** = 0.21 (hexanes : ethyl acetate = 3:1, Vanillin) (**119d** and **120d**)

**HPLC analysis:** 87% *ee* (Chiralpak AS-H, *n*-heptane: *i*-Propanol = 70:30, 0.5 mL/min,  $\lambda$  = 215 nm, 60 min,  $t_R$  = 24.47 min, minor;  $t_R$  = 33.12 min, major) (**119d**)

**HPLC analysis:** n.d. (Chiralpak AS-H, *n*-heptane: *i*-Propanol = 70:30, 0.5 mL/min,  $\lambda$  = 215 nm, 60 min,  $t_R$  = min, minor;  $t_R$  = min, major) (**120d**)

The analytical data of **119d** and **120d** are in accordance with those described below for (*rac*)-**119d** and (*rac*)-**120d**. Because it was not feasible to separate **119d** and **120d**, determination of the enantiomeric excess was performed with a mixture of **119d** and **120d**.

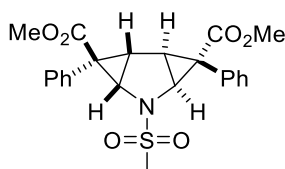


methyl-*rel*-(1*S*,5*S*,6*R*)-2-(methylsulfonyl)-6-phenyl-2-azabicyclo[3.1.0]hex-3-ene-6-carboxylate ((*rac*)-**119d**)

According to **GP-4** pyrrole **113d** (290 mg, 2.0 mmol, 2.0 equiv) was cyclopropanated with diazo ester **97a** (178 mg, 1.0 mmol, 1.0 equiv), Cu(OTf)<sub>2</sub> (21 mg, 58  $\mu$ mol, 6 mol%) and

phenylhydrazine (7  $\mu\text{L}$ , 71,  $\mu\text{mol}$ , 7 mol%). The crude product was purified by flash chromatography ( $\text{SiO}_2$ , hexanes/EtOAc, 3:1) to afford cyclopropane (*rac*)-**119d** as a white solid (14 mg, 5% yield).

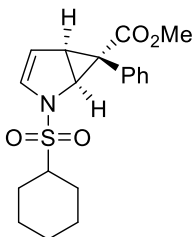
**m.p.** 119-120  $^\circ\text{C}$ ; **R<sub>f</sub>** = 0.16 (hexanes : ethyl acetate = 3:1, Vanillin); **IR** (neat): 3474, 3064, 3027, 2956, 2128, 1707, 1584, 1498, 1435, 1342, 1258, 1163, 1081, 1003, 958, 891, 760, 734, 701  $\text{cm}^{-1}$ ; **<sup>1</sup>H NMR** (300 MHz,  $\text{CDCl}_3$ )  $\delta$  7.38 – 7.14 (m, 5H), 5.87 (dd,  $J$  = 3.9, 1.4 Hz, 1H), 5.43 (dd,  $J$  = 3.8, 2.6 Hz, 1H), 4.69 (dd,  $J$  = 6.4, 1.3 Hz, 1H), 3.63 (s, 3H), 3.37 (dd,  $J$  = 6.4, 2.5 Hz, 1H), 2.97 (s, 3H); **<sup>13</sup>C NMR** (101 MHz,  $\text{CDCl}_3$ )  $\delta$  173.5, 132.5, 130.6, 130.2, 127.9, 127.6, 111.9, 52.9, 52.3, 38.8, 38.6, 28.2; **HRMS** (+CI) calcd. for  $\text{C}_{14}\text{H}_{16}\text{NO}_4\text{S}$  ( $\text{M}+\text{H}$ )<sup>+</sup> 294.07946 found 294.07941.



dimethyl-*rel*-(1*S*,2*S*,3*R*,4*S*,6*S*,7*R*)-5-(methylsulfonyl)-3,7-diphenyl-5-azatricyclo[4.1.0.0.2,4]heptane-3,7-dicarboxylate (*rac*)-**120d**)

According to **GP-5** pyrrole **113d** (290 mg, 2.0 mmol, 2.0 equiv) was cyclopropanated with diazo ester **97a** (176 mg, 1.0 mmol, 1.0 equiv) and  $\text{Rh}_2(\text{OAc})_4$  (2.2 mg, 5.0  $\mu\text{mol}$ , 0.5 mol%). The crude product was purified by flash chromatography ( $\text{SiO}_2$ , hexanes/EtOAc, 3:1) to afford double cyclopropane (*rac*)-**120d** as a white solid (137 mg, 31% yield).

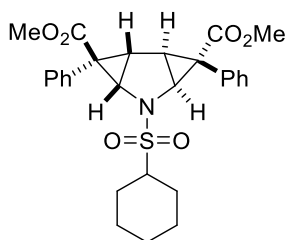
**m.p.** 216-217  $^\circ\text{C}$ ; **R<sub>f</sub>** = 0.21 (hexanes : ethyl acetate = 3:1, Vanillin); **IR** (neat): 3034, 2956, 2363, 2259, 1707, 1603, 1498, 1435, 1342, 1252, 1219, 1148, 1103, 1006, 962, 910, 857, 760, 731  $\text{cm}^{-1}$ ; **<sup>1</sup>H NMR** (300 MHz,  $\text{CDCl}_3$ )  $\delta$  7.55 – 7.48 (m, 4H), 7.47 – 7.37 (m, 6H), 3.53 (s, 6H), 3.22 (d,  $J$  = 7.0 Hz, 2H), 2.83 (s, 3H), 2.80 (d,  $J$  = 7.0 Hz, 2H); **<sup>13</sup>C NMR** (75 MHz,  $\text{CDCl}_3$ )  $\delta$  171.5, 132.1, 131.0, 128.6, 128.3, 52.9, 51.0, 42.6, 38.0, 32.7; **HRMS** (+ESI) calcd. for  $\text{C}_{23}\text{H}_{24}\text{NO}_6\text{S}$  ( $\text{M}+\text{H}$ )<sup>+</sup> 442.1319 found 442.1329.



Methyl (1*S*,5*S*,6*R*)-2-(cyclohexylsulfonyl)-6-phenyl-2-azabicyclo[3.1.0]hex-3-ene-6-carboxylate (**119e**)

According to **GP-2** pyrrole **113e** (426 mg, 2.0 mmol, 2.0 equiv) was cyclopropanated with diazo ester **97a** (176 mg, 1.0 mmol, 1.0 equiv) and Rh<sub>2</sub>(*S*-TCPTTL)<sub>4</sub> (1.8 mg, 1.0 μmol, 0.1 mol%). The crude product was purified by flash chromatography (SiO<sub>2</sub>, hexanes/EtOAc, 5:1) to afford cyclopropane **119e** as a sticky oil (147 mg, 41% yield).

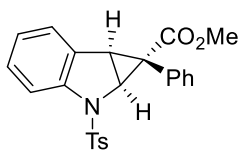
**R<sub>f</sub>** = 0.33 (hexanes : ethyl acetate = 5:1, Vanillin); [**α**]<sub>D</sub><sup>20</sup> -388.2° (c = 0.50, CHCl<sub>3</sub>, 94% *ee*); **IR** (neat): 3054, 3033, 2937, 2859, 2262, 1707, 1584, 1498, 1455, 1435, 1334, 1252, 1156, 1081, 999, 910, 783, 727 cm<sup>-1</sup>; **<sup>1</sup>H NMR** (300 MHz, CDCl<sub>3</sub>) δ 7.34 – 7.20 (m, 5H), 5.84 (dd, *J* = 3.9, 1.3 Hz, 1H), 5.28 (dd, *J* = 3.9, 2.6 Hz, 1H), 4.71 (dd, *J* = 6.7, 1.3 Hz, 1H), 3.61 (s, 3H), 3.38 (dd, *J* = 6.7, 2.5 Hz, 1H), 3.09 (tt, *J* = 12.1, 3.4 Hz, 1H), 2.22 – 2.09 (m, 1H), 2.00 – 1.82 (m, 3H), 1.76 – 1.66 (m, 1H), 1.61 – 1.45 (m, 2H), 1.36 – 1.17 (m, 3H); **<sup>13</sup>C NMR** (75 MHz, CDCl<sub>3</sub>) δ 173.8, 132.6, 131.7, 130.5, 127.8, 127.5, 109.0, 63.0, 53.0, 52.8, 38.8, 27.7, 26.2, 25.1, 25.0; **HRMS** (+ESI) calcd. for C<sub>19</sub>H<sub>24</sub>NO<sub>4</sub>S (M+H)<sup>+</sup> 362.1421 found 362.1426; **HPLC** analysis: 94% *ee* (Phenomenex Lux Cellulose-2, *n*-heptane: *i*-Propanol = 70:30, 0.5 mL/min, λ = 215 nm, 40 min, t<sub>R</sub> = 14.63 min, minor; t<sub>R</sub> = 17.70 min, major )



Dimethyl-*rel*-(1*S*,2*S*,3*R*,4*S*,6*S*,7*R*)-5-(cyclohexylsulfonyl)-3,7-diphenyl-5-azatricyclo[4.1.0.0.2,4]heptane-3,7-dicarboxylate (**120e**)

Double cyclopropanated pyrrole **120e** (106 mg, 21% yield) was obtained as a side product of **119e** following **GP-2**. The crude mixture was purified by flash chromatography (SiO<sub>2</sub>, hexanes/EtOAc, 5:1) to obtain **120e** as a white solid.

**m.p.** 215-216 °C; **R<sub>f</sub>** = 0.15(hexanes : ethyl acetate = 5:1, Vanillin); **IR** (neat): 3038, 3008, 2941, 2855, 1703, 1498, 1435, 1334, 1249, 1211, 1144, 1081, 1010, 962, 895, 857, 764, 731, 705 cm<sup>-1</sup>; **<sup>1</sup>H NMR** (300 MHz, CDCl<sub>3</sub>) δ 7.57 – 7.49 (m, 4H), 7.48 – 7.35 (m, 10H), 3.52 (s, 6H), 3.25 (d, *J* = 7.0 Hz, 2H), 2.99 – 2.85 (m, 1H), 2.81 (d, *J* = 6.9 Hz, 2H), 2.29 – 2.15 (m, 1H), 1.97 – 1.84 (m, 1H), 1.73 – 1.47 (m, 3H), 1.36 – 1.09 (m, 5H); **<sup>13</sup>C NMR** (75 MHz, CDCl<sub>3</sub>) δ 171.6, 132.0, 131.1, 128.5, 128.1, 64.0, 52.8, 52.4, 38.1, 32.7, 26.1, 26.1, 25.2, 25.0, 24.9; **HRMS** (+ESI) calcd. for C<sub>28</sub>H<sub>32</sub>NO<sub>6</sub>S (M+H)<sup>+</sup> 510.1945 found 510.1960



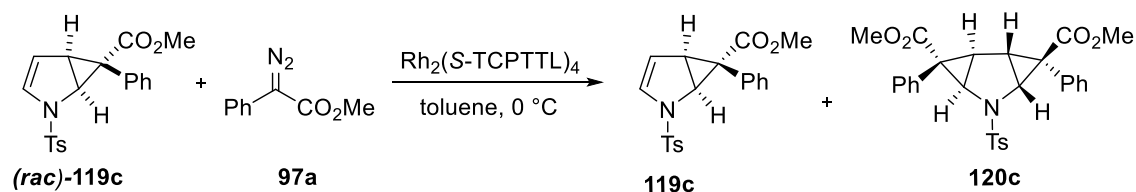
methyl (1*R*,1*aS*,6*bS*)-1-phenyl-2-tosyl-1,1*a*,2,6*b*-tetrahydrocyclopropa[*b*]indole-1-carboxylate (**126**)

According to **GP-2** indole **125** (542 mg, 2.0 mmol, 2.0 equiv) was cyclopropanated with diazo ester **97a** (176 mg, 1.0 mmol, 1.0 equiv) and Rh<sub>2</sub>(*S*-TCPTTL)<sub>4</sub> (1.8 mg, 1.0 μmol, 0.1 mol%). The crude product was purified by flash chromatography (SiO<sub>2</sub>, hexanes/EtOAc, 5:1) to afford cyclopropane **126** as a white solid (316 mg, 75% yield).

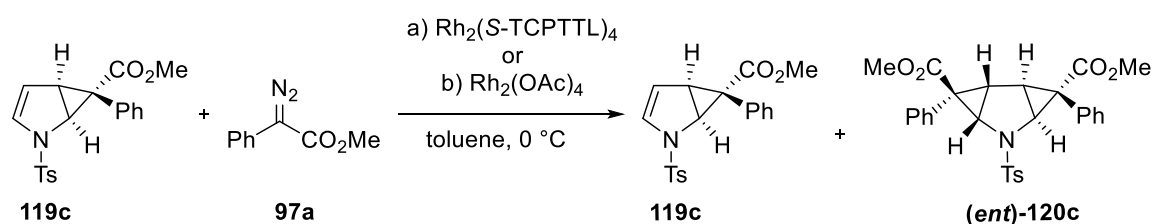
**m.p.** 53-55 °C; **R<sub>f</sub>** = 0.23 (hexanes: ethyl acetate = 5: 1, Vanillin); [**α**]<sub>D</sub><sup>20</sup> -82.2° (c = 0.10, CHCl<sub>3</sub>, 80% *ee*); **IR** (neat): 3060, 3030, 2952, 2113, 1711, 1599, 1461, 1435, 1361, 1252, 1167, 1118, 992, 939, 883, 854, 813, 753, 701, 664 cm<sup>-1</sup>; **<sup>1</sup>H-NMR** (300 MHz, CDCl<sub>3</sub>): δ 7.68 (d, *J* = 8.3 Hz, 2H), 7.32 (dd, *J* = 7.3, 1.2 Hz, 1H), 7.25 – 7.17 (m, 3H), 7.14 – 7.04 (m, *J* = 7.1 Hz, 5H), 7.01 – 6.87 (m, 2H), 4.94 (d, *J* = 6.6 Hz, 1H), 3.66 (s, 3H), 3.61 (d, *J* = 6.6 Hz, 1H), 2.36 (s, 3H); **<sup>13</sup>C-NMR** (75 MHz, CDCl<sub>3</sub>): δ 173.3, 144.5, 141.3, 135.3, 132.4, 129.9, 129.5, 129.5, 127.8, 127.6, 127.3, 126.9, 125.7, 123.6, 114.3, 53.1, 53.0, 35.2, 30.7, 21.6; **HRMS** (CI<sup>+</sup>) calcd. for C<sub>24</sub>H<sub>22</sub>NO<sub>4</sub>S (M+H)<sup>+</sup> 420.1264 found 420.1268; **HPLC** analysis: 80% *ee* (Phenomenex Lux Cellulose-1, *n*-heptane: *i*-Propanol = 95:5, 0.5 mL/min, λ = 215 nm, 60 min, t<sub>R</sub> = 24.13 min, major; t<sub>R</sub> = 46.16 min, minor).



### 3.4 Kinetic resolution experiments



In a flame dried Schlenk flask, **(rac)-119c** (237 mg, 640  $\mu\text{mol}$ , 1.0 equiv) and  $\text{Rh}_2(\text{S-TCPTTL})_4$  (1.2 mg, 0.67  $\mu\text{mol}$ , 0.1 mol%) were dissolved in dry toluene (2 mL) and cooled to 0  $^\circ\text{C}$ . A solution of the diazo ester **97a** (56 mg, 320  $\mu\text{mol}$ , 0.5 equiv) in dry toluene (1 mL) was added using a syringe pump for the duration of 1 h. Afterward, the reaction mixture was stirred for further 5 min and concentrated under reduced pressure. The crude product was purified by flash chromatography ( $\text{SiO}_2$ , hexanes/EtOAc, 4:1) to afford cyclopropane **119c** (170 mg, 72% yield, 29% *ee*) and double cyclopropane **120c** (81 mg, 24%, 88% *ee*).



a) In a flame dried Schlenk flask, **119c** (75 mg, 203  $\mu\text{mol}$ , 1.0 equiv, >99% *ee*) and  $\text{Rh}_2(\text{S-TCPTTL})_4$  (7.3 mg, 4.1  $\mu\text{mol}$ , 2.0 mol%) were dissolved in dry toluene (1.5 mL) and cooled to 0  $^\circ\text{C}$ . A solution of the diazo ester **97a** (36 mg, 203  $\mu\text{mol}$ , 1.0 equiv) in dry toluene (1 mL) was added using a syringe pump for the duration of 1 h. Afterward, the reaction mixture was stirred for further 5 min and concentrated under reduced pressure. The crude product was purified by flash chromatography ( $\text{SiO}_2$ , hexanes/EtOAc, 4:1) to afford cyclopropane **119c** (22 mg, 29% yield, >99% *ee*) and double cyclopropane **(ent)-120c** (67 mg, 64%, >99% *ee*).

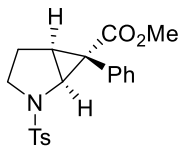
b) a) In a flame dried Schlenk flask, **119c** (75 mg, 203  $\mu\text{mol}$ , 1.0 equiv, >99% *ee*) and  $\text{Rh}_2(\text{OAc})_4$  (1.8 mg, 4.1  $\mu\text{mol}$ , 2.0 mol%) were dissolved in dry toluene (1.5 mL) and cooled to 0  $^\circ\text{C}$ . A solution of the diazo ester **97a** (36 mg, 203  $\mu\text{mol}$ , 1.0 equiv) in dry toluene (1 mL) was added using a syringe pump for the duration of 1 h. Afterward, the reaction mixture was stirred for further 5 min and concentrated under reduced pressure. The crude product was purified by

flash chromatography (SiO<sub>2</sub>, hexanes/EtOAc, 4:1) to afford exclusively double cyclopropane (*ent*)-**120c** (96 mg, 91%, >99% *ee*).

Analytical data of compound (*ent*)-**120c**:

**m.p.** 173 °C decomposition; **R<sub>f</sub>** = 0.09 (hexanes: ethyl acetate = 5:1, Vanillin); **[α]<sub>D</sub><sup>20</sup>** -131.6° (c = 0.5, CHCl<sub>3</sub>); **IR** (neat): 3064, 2997, 2952, 2359, 2113, 1976, 1707, 1599, 1498, 1435, 1349, 1252, 1215, 1163, 1111, 1077, 1018, 965, 857, 734, 705 cm<sup>-1</sup>; **<sup>1</sup>H NMR** (300 MHz, CDCl<sub>3</sub>) δ 7.72 – 7.62 (m, 2H), 7.40 – 7.34 (m, 2H), 7.32 – 7.25 (m, 2H), 7.23 – 7.15 (m, 4H), 7.12 – 7.05 (m, 4H), 3.51 (s, 6H), 3.31 (d, *J* = 7.1 Hz, 2H), 2.69 (d, *J* = 7.0 Hz, 2H), 2.53 (s, 3H); **<sup>13</sup>C NMR** (75 MHz, CDCl<sub>3</sub>) δ 171.6, 143.8, 138.6, 131.9, 130.7, 130.0, 128.4, 127.8, 127.2, 52.8, 51.3, 38.0, 32.5, 21.7; **HRMS** (+ESI) calcd. for C<sub>29</sub>H<sub>28</sub>NO<sub>6</sub>S (M+H)<sup>+</sup> 518.1632 found 518.1636; **HPLC** analysis: >99% *ee* (Phenomenex Lux Cellulose-1, *n*-heptane: *i*-Propanol = 70:30, 0.5 mL/min, λ = 215 nm, 60 min, t<sub>R</sub> = 14.75 min)

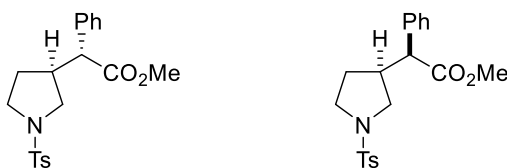
Analytical data of compound **119c** can be found in chapter E.3.3

4 Synthesis of homo- $\beta$ -proline derivative **147**

methyl (1*S*,5*S*,6*R*)-6-phenyl-2-tosyl-2-azabicyclo[3.1.0]hexane-6-carboxylate (**144**)

A Schlenk flask was charged with **119c** (211 mg, 571  $\mu$ mol, 1.0 equiv), methanol (8 mL) and Pd/C (10 wt%, 30 mg Pd/C, 29  $\mu$ mol Pd, 5 mol% Pd). The resulting solution was flushed with hydrogen gas for ten times (balloon, 1 atm) and stirred under hydrogen atmosphere at room temperature for 2.5 h. After completion the crude mixture was filtered through two consecutive folded filter and washed with methanol. The solvent was removed under vacuo and **144** (177 mg, 84%) was obtained as a white solid.

**m.p.** 140 °C; **R<sub>f</sub>** = 0.28 (hexanes: ethyl acetate = 4: 1, Vanillin); **[ $\alpha$ ]<sub>D</sub><sup>20</sup>** -58.8° (c = 0.54, CHCl<sub>3</sub>); **IR** (neat): 3060, 3030, 2952, 2363, 2121, 1715, 1599, 1495, 1435, 1346, 1252, 1159, 1103, 1014, 982, 872, 813, 731, 701, 664 cm<sup>-1</sup>; **<sup>1</sup>H-NMR** (300 MHz, CDCl<sub>3</sub>):  $\delta$  7.75 – 7.70 (m, 2H), 7.36 – 7.28 (m, 7H), 4.25 (d, *J* = 6.7 Hz, 1H), 3.57 (s, 3H), 3.24 – 3.13 (m, 1H), 2.49 – 2.45 (m, 1H), 2.44 (s, 3H), 1.96 – 1.73 (m, 3H); **<sup>13</sup>C-NMR** (75 MHz, CDCl<sub>3</sub>):  $\delta$  171.8, 143.6, 136.4, 131.5, 131.2, 129.9, 128.6, 127.8, 127.0, 52.7, 51.8, 48.0, 37.1, 30.6, 25.0, 21.6; **HRMS** (+ESI) calcd. for C<sub>20</sub>H<sub>22</sub>NO<sub>4</sub>S (M+H)<sup>+</sup> 372.1264 found 372.1266.



methyl (*R*)-2-phenyl-2-((*S*)-1-tosylpyrrolidin-3-yl)acetate (**145**)

methyl-*rel*-(*S*)-2-phenyl-2-(*rel*-(*S*)-1-tosylpyrrolidin-3-yl)acetate (**146**)

In a round-bottom flask, cyclopropane **144** (131 mg, 351  $\mu$ mol, 1.0 equiv) was dissolved in DCM (7 mL). Triethylsilane (168  $\mu$ L, 1.1 mmol, 3.0 equiv) and trifluoroacetic acid (54  $\mu$ L, 703  $\mu$ mol, 2.0 equiv) were added, and the solution was stirred at room temperature for 2 d. The solvent was evaporated under reduced pressure and the crude product (*dr* (**145/146**) = 83/17, crude <sup>1</sup>H-NMR) was purified by flash chromatography (SiO<sub>2</sub>, hexanes/EtOAc, 4:1) to give main

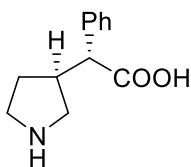
diastereomer **145** (95 mg, 72%) as a white solid and minor diastereomer **146** (19 mg, 14%) as an off-white solid.

Analytical data of compound **145**

**m.p.** 140 °C; **R<sub>f</sub>** = 0.30 (hexanes: ethyl acetate = 4: 1, Vanillin); **[α]<sub>D</sub><sup>20</sup>** 46.3 (c = 1.01, CHCl<sub>3</sub>, 99% *ee*); **IR** (neat): 3064, 3030, 2952, 2878, 2363, 1733, 1599, 1495, 1454, 1342, 1215, 1122, 1092, 1033, 824, 745, 709 cm<sup>-1</sup>; **<sup>1</sup>H-NMR** (400 MHz, CDCl<sub>3</sub>): δ 7.62 (d, *J* = 8.2 Hz, 2H), 7.35 – 7.27 (m, 5H), 7.21 – 7.16 (m, 2H), 3.61 (s, 3H), 3.42 (ddd, *J* = 9.8, 8.4, 3.9 Hz, 1H), 3.29 (d, *J* = 10.8 Hz, 1H), 3.22 (ddd, *J* = 9.8, 8.4, 7.5 Hz, 1H), 3.04 (dd, *J* = 9.7, 6.9 Hz, 1H), 2.84 – 2.68 (m, 2H), 2.44 (s, 3H), 2.10 (dtd, *J* = 10.9, 6.9, 3.9 Hz, 1H), 1.59 – 1.48 (m, 1H); **<sup>13</sup>C-NMR** (75 MHz, CDCl<sub>3</sub>): δ 173.1, 143.5, 136.9, 133.5, 129.7, 129.0, 128.0, 127.9, 127.5, 54.9, 52.2, 51.1, 47.6, 41.7, 30.5, 21.6; **HRMS** (+ESI) calcd. for C<sub>20</sub>H<sub>24</sub>NO<sub>4</sub>S (M+H)<sup>+</sup> 374.1421 found 374.1422; **HPLC** analysis: >99% *ee* (Phenomenex Lux Cellulose-2, *n*-heptane: *i*-Propanol = 50:50, 0.5 mL/min, λ = 215 nm, 60 min, t<sub>R</sub> = 33.14 min, major).

Analytical data of compound **146**

**m.p.** 122-123°C; **R<sub>f</sub>** = 0.41 (hexanes: ethyl acetate = 4: 1, Vanillin); **[α]<sub>D</sub><sup>20</sup>** -17.9 (c = 0.54, CHCl<sub>3</sub>, 37% *ee*); **IR** (neat): 3064, 3030, 2952, 2878, 2356, 1730, 1599, 1495, 1454, 1342, 1223, 1159, 1122, 1092, 1036, 819, 786, 735, 697, 673 cm<sup>-1</sup>; **<sup>1</sup>H NMR** (400 MHz, CDCl<sub>3</sub>) δ 7.72 (d, *J* = 8.1 Hz, 2H), 7.34 (d, *J* = 8.0 Hz, 2H), 7.30 – 7.25 (m, 3H), 7.20 -7.15 (m, 2H), 3.63 (s, 3H), 3.54 (dd, *J* = 10.0, 7.5 Hz, 1H), 3.34 (m, 1H), 3.27 (d, *J* = 11.1 Hz, 1H), 3.03 (m, 2H), 2.82 – 2.72 (m, 1H), 2.45 (s, 3H), 1.59 – 1.49 (m, 1H + H<sub>2</sub>O-Peak), 1.38 – 1.28 (m, 1H); **<sup>13</sup>C NMR** (101 MHz, CDCl<sub>3</sub>) δ 173.2, 143.5, 137.1, 133.6, 129.7, 128.9, 128.0, 127.8, 127.6, 55.0, 52.3 (2 C), 47.3, 41.6, 29.3, 21.6; **HRMS** (+ESI) calcd. for C<sub>20</sub>H<sub>24</sub>NO<sub>4</sub>S (M+H)<sup>+</sup> 374.1421 found 374.1426; **HPLC** analysis: 37% *ee* (Chiralpak AS-H, *n*-heptane: *i*-Propanol = 70:30, 0.5 mL/min, λ = 215 nm, 60 min, t<sub>R</sub> = 41.96 min, minor; t<sub>R</sub> = 49.49 min, major).



(*R*)-2-phenyl-2-((*S*)-pyrrolidin-3-yl)acetic acid (**147**)

Under nitrogen atmosphere a flame dried heavy-wall Schlenk tube was charged with **145** (50 mg, 134 μmol, 1.0 equiv), phenol (39 mg) and HBr in acetic acid (0.75 mL). The resulting

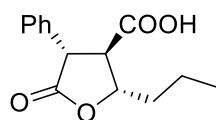
solution was stirred at 80 °C for 16 h. Afterwards, distilled water (0.75 mL) was added and the reaction mixture was stirred at 50 °C for 20 min. The solvent was evaporated under reduced pressure to yield **147** as TFA salt. To purify the crude product and remove the trifluoroacetate, the residue was loaded onto a column with Dowex 50WX8-400 (preactivated with 0.1 M HCl). The resin washed with water (300 mL) and subsequently eluted with aqueous ammonia solution (15%) to afford **147** (27 mg, quant.) as an off-white solid.

**m.p.** >250 °C (limit of detection); **R<sub>f</sub>** = 0.72 (methanol, ninhydrin); **[ $\alpha$ ]<sub>D</sub><sup>20</sup>** 40.0° (c = 1.02, H<sub>2</sub>O); **IR** (neat): 2952, 2714, 2617, 2363, 2113, 1644, 1566, 1491, 1457, 1375, 1245, 1171, 1111, 1074, 1006, 980, 910, 731, 700 cm<sup>-1</sup>; **<sup>1</sup>H NMR** (400 MHz, D<sub>2</sub>O)  $\delta$  7.30 – 7.16 (m, 5H), 3.35 – 3.13 (m, 3H), 3.01 – 2.81 (m, 2H), 2.62 (dd, *J* = 11.3, 8.7 Hz, 1H), 2.25 – 2.13 (m, 1H), 1.71 – 1.57 (m, 1H); **<sup>13</sup>C NMR** (101 MHz, D<sub>2</sub>O)  $\delta$  180.1, 139.5, 129.0, 127.8, 127.5, 58.5, 48.3, 45.4, 40.8, 29.3; **HRMS** (-ESI) calcd. for C<sub>12</sub>H<sub>14</sub>NO<sub>2</sub> (M-H)<sup>-</sup> 204.1030 found 204.1033.

## 5 Synthesis of paraconic acid derivatives

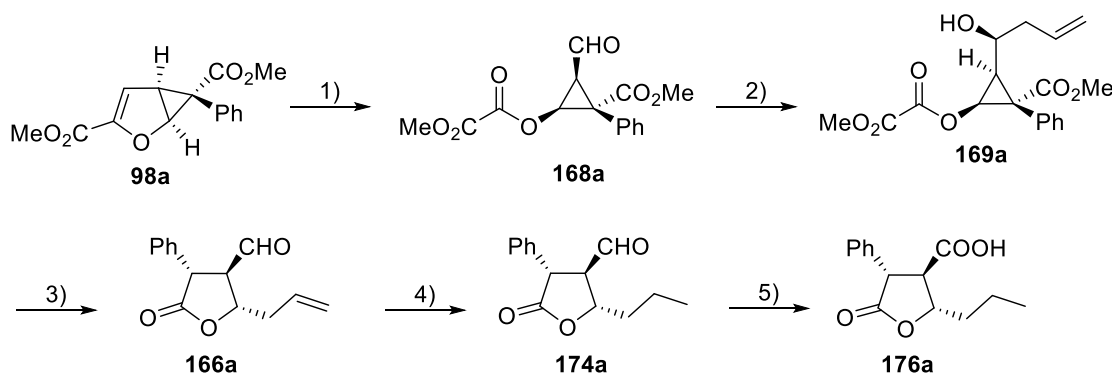
Trisubstituted  $\gamma$ -butyrolactones **166a/b** were synthesized according to a protocol that was recently developed by the Reiser group for the synthesis of disubstituted  $\gamma$ -butyrolactones.<sup>19</sup> Starting from cyclopropanes **98a/b**, paraconic acid derivatives **176a** and **179a/b** were synthesized in 5 consecutive steps without purification of the intermediates.

### 5.1 Enantioselective synthesis of paraconic acid derivatives **176a** and **179a**



(2*S*,3*R*,4*S*)-5-oxo-4-phenyl-2-propyltetrahydrofuran-3-carboxylic acid (**176a**)

a) Overview of consecutive steps



b) Procedure

1) A flame dried Schlenk tube was charged with cyclopropane **98a** (1.5 g, 5.47 mmol, 1.0 equiv) and anhydrous DCM (18 ml). The reaction was cooled to  $-78\text{ }^{\circ}\text{C}$  and ozone was passed through the reaction mixture until a blue color appeared. Excess of ozone was expelled by passing a constant stream of oxygen through the solution until it turned colorless. The stream of oxygen continued for further 5 min and DMS (2.0 ml, 27.4 mmol, 5.0 equiv) was added. The reaction mixture was allowed to warm up to room temperature overnight in an unfreezing cooling bath. The solution was washed with sat.  $\text{NaHCO}_3$  (8 ml) and water (8 ml). After drying over  $\text{Na}_2\text{SO}_4$

and filtration, the solvent was removed under reduced pressure to afford crude **168a** (1.46 g, 87% crude yield) as a sticky yellow oil.

2) In a flame dried Schlenk flask crude aldehyde **168a** (theoretical: 1.46 g, 4.77 mmol, 1.0 equiv) was dissolved in dry DCM (30 mL) and the solution was cooled to -78 °C. Boron trifluoride diethyl etherate (0.68 mL, 5.48 mmol, 1.15 equiv) was added, and the reaction mixture was stirred for 30 min. Subsequently, allyltrimethylsilane (0.98 mL, 6.2 mmol, 1.3 equiv) was added, and the resulting solution was stirred for 18 h. The reaction was stopped with sat. NaHCO<sub>3</sub> (10 mL) and allowed to warm up to rt. The phases were separated, and the aqueous phase was extracted with DCM (3 x 20 mL). After drying over MgSO<sub>4</sub> and filtration, the solvent was removed under reduced pressure to afford crude **169a** (1.55 g, 93% crude yield) as a sticky yellow oil.

3) A solution of crude allyl **169a** (theoretical: 0.29 g, 0.84 mmol, 1.0 equiv) in methanol (5 mL) was cooled to 0 °C. Subsequently, triethylamine (0.29 mL, 2.09 mmol, 2.5 equiv) in methanol (1.5 mL) was added using a syringe pump for the duration of 2 h, and the solution was stirred for 14 h in the unfreezing cooling bath. After removal of the solvent in vacuo, the residue was treated with water (5 mL) and DCM (5 mL). The phases were separated, and the aqueous layer was extracted with DCM (6x5 mL). After drying over Na<sub>2</sub>SO<sub>4</sub> and filtration, the volatiles were removed under reduced pressure (crude yield (**166a**) > 100%).

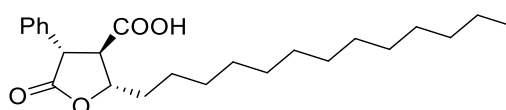
4) A Schlenk flask was charged with crude **166a** (theoretical: 192 mg, 0.83 mmol, 1.0 equiv), methanol (10 mL) and Pd/C (10 wt %, 18 mg Pd/C, 17 μmol Pd, 2 mol% Pd). The resulting solution was flushed with hydrogen gas for ten times (balloon, 1 atm) and stirred under hydrogen atmosphere at room temperature for 5 h. After completion, the crude mixture was filtered through two consecutive folded filter and washed with methanol, and the solvent was removed under reduced pressure.

5) A round-bottom flask was charged with crude **174a** (theoretical: 193 mg, 0.83 mmol, 1.0 equiv), BAIB (0.59 g, 1.83 mmol, 2.2 equiv), TEMPO (26 mg, 0.17 mmol, 0.2 equiv) and a mixture of acetonitrile and water (1:1, 4 mL). The reaction mixture was stirred at rt for 20 h. Subsequently, a solution of Na<sub>2</sub>SO<sub>3</sub> (0.13 g) in water (1 mL) was added, and stirring was continued for additional 30 min before the reaction mixture was acidified to pH 2 by the addition of aqueous HCl (1 M). The mixture was extracted with ethyl acetate (5x10 ml), and the combined organic layers were consecutively washed with brine (10 mL) and water (10 mL), dried over Na<sub>2</sub>SO<sub>4</sub> and filtered. The solvent was evaporated under reduced pressure, and the crude product was purified by flash chromatography (SiO<sub>2</sub>, hexanes/EtOAc, 2:1 + 1% formic

acid) to afford **176a** (47 mg, 18.5% yield over 5 steps starting from cyclopropane **98a**) as a white solid.

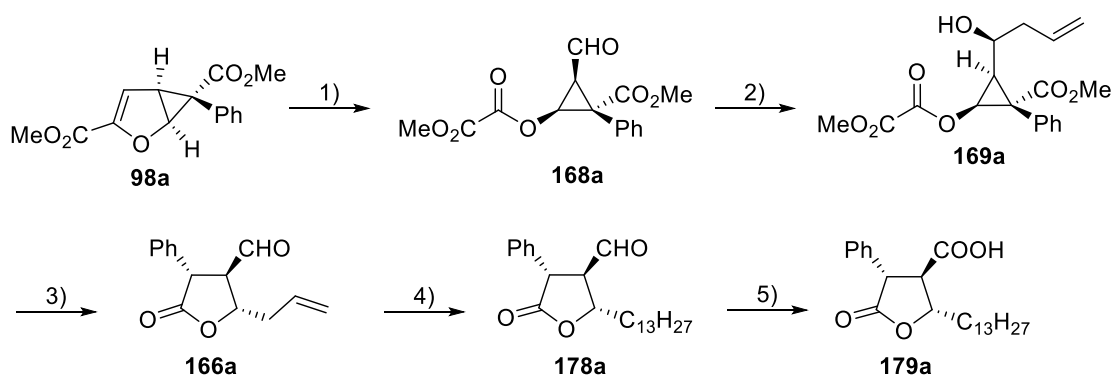
c) Characterization of **176a**

**m.p.** 130-131 °C; **R<sub>f</sub>** = 0.35 (hexanes : ethyl acetate = 2:1 + 1% acetic acid, bromocresol green); **[α]<sub>D</sub><sup>20</sup>** 33.9(c = 1.0, CHCl<sub>3</sub>); **IR** (neat): 3034, 2960, 2878, 1748, 1722, 1502, 1454, 1394, 1349, 1312, 1223, 1170, 1122, 1096, 1018, 977, 924, 861, 805, 746, 693 cm<sup>-1</sup>; **<sup>1</sup>H NMR** (400 MHz, CDCl<sub>3</sub>) δ 10.36 (bs, 1H), 7.41 – 7.30 (m, 3H), 7.28 – 7.21 (m, 2H), 4.57 (td, *J* = 8.6, 3.9 Hz, 1H), 4.25 (d, *J* = 11.4 Hz, 1H), 3.22 (dd, *J* = 11.4, 9.3 Hz, 1H), 1.96 – 1.75 (m, 2H), 1.69 – 1.44 (m, 2H), 1.00 (t, *J* = 7.4 Hz, 3H); **<sup>13</sup>C NMR** (101 MHz, CDCl<sub>3</sub>) δ 175.8, 174.6, 134.9, 129.1, 128.3, 128.3, 79.4, 55.0, 50.6, 37.0, 18.7, 13.7; **HRMS** (-ESI) calcd. for C<sub>14</sub>H<sub>15</sub>O<sub>4</sub> (M-H)<sup>-</sup> 247.0976 found 247.0982; **HPLC** analysis: >99% *ee* (Chiralpak AS-H, *n*-heptane: *i*-Propanol = 90:10, 1.0 mL/min, λ = 215 nm, 60 min, t<sub>R</sub> = 26.94 min)



(2*S*,3*R*,4*S*)-5-oxo-4-phenyl-2-tridecyltetrahydrofuran-3-carboxylic acid (**179a**)

a) Overview of consecutive steps:



b) Procedure:

1) A flame dried Schlenk tube was charged with cyclopropane **98a** (2.0 g, 7.29 mmol, 1.0 equiv) and anhydrous DCM (18 ml). The reaction was cooled to -78 °C and ozone was passed through the reaction mixture until a blue color appeared. Excess of ozone was expelled by passing a



constant stream of oxygen through the solution until it turned colorless. The stream of oxygen continued for further 5 min and DMS (2.7 ml, 36.5 mmol, 5.0 equiv) was added. The reaction mixture was allowed to warm up to room temperature overnight in an unfreezing cooling bath. The solution was washed with sat. NaHCO<sub>3</sub> (10 ml) and water (10 ml). After drying over Na<sub>2</sub>SO<sub>4</sub> and filtration, the solvent was removed under reduced pressure to afford crude **168a** (1.85 g, 83% crude yield) as a sticky yellow oil.

2) In a flame dried Schlenk flask crude aldehyde **168a** (theoretical: 1.85 g, 6.04 mmol, 1.0 equiv) was dissolved in dry DCM (35 mL) and the solution was cooled to -78 °C. Boron trifluoride diethyl etherate (0.86 mL, 6.95 mmol, 1.15 equiv) was added, and the reaction mixture was stirred for 30 min. Subsequently, allyltrimethylsilane (1.25 mL, 7.85 mmol, 1.3 equiv) was added, and the resulting solution was stirred for 18 h. The reaction was stopped with sat. NaHCO<sub>3</sub> (10 mL) and allowed to warm up to rt. The phases were separated, and the aqueous phase was extracted with DCM (3 x 20 mL). After drying over MgSO<sub>4</sub> and filtration, the solvent was removed under reduced pressure to afford crude **169a** (2.03 g, 97% crude yield) as a sticky yellow oil.

3) A solution of crude allyl **169a** (theoretical: 2.03 g, 5.82 mmol, 1.0 equiv) in methanol (30 mL) was cooled to 0 °C. Subsequently, triethylamine (2.03 mL, 14.54 mmol, 2.5 equiv) was added using a syringe pump for the duration of 2 h, and the solution was stirred for 14 h in the unfreezing cooling bath. After removal of the solvent in vacuo, the residue was treated with water (20 mL) and DCM (20 mL). The phases were separated, and the aqueous layer was extracted with DCM (6x10 mL). After drying over Na<sub>2</sub>SO<sub>4</sub> and filtration, the volatiles were removed under reduced pressure (crude yield (**166a**) > 100%).

4) A flame dried Schlenk flask was charged with crude lactone **166a** (theoretical: 1.35 g, 5.86 mmol, 1.0 equiv) and anhydrous DCM (50 mL, bubbling nitrogen through the solvent for 10 min before use). Afterward, Grubbs II (0.25 g, 0.29 mmol, 5 mol%) and 1-dodecene (7.8 mL, 35.18 mmol, 6.0 equiv) were added and the solution was refluxed for 16 h. After removal of the solvent under reduced pressure the crude mixture was dissolved in methanol (40 mL). The reaction mixture was vigorously stirred in an autoclave at rt for 24 h under 20 atm of hydrogen gas. The crude mixture was filtered (removal of tetracosane), washed with methanol the solvent was removed under reduced pressure. (crude yield (**178a**) > 100%)

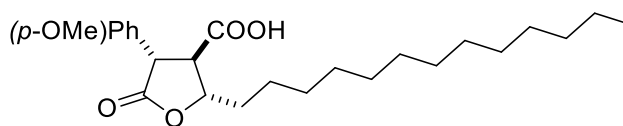
5) A round-bottom flask was charged with crude **178a** (theoretical: 2.18 g, 5.86 mmol, 1.0 equiv), BAIB (4.15 g, 12.87 mmol, 2.2 equiv), TEMPO (183 mg, 1.17 mmol, 0.2 equiv) and a mixture of acetonitrile and water (1:1, 30 mL). The reaction mixture was stirred at rt for 48 h. Subsequently, a solution of Na<sub>2</sub>SO<sub>3</sub> (1.5 g) in water (10 mL) was added, and stirring was

continued for additional 30 min before the reaction mixture was acidified to pH 2 by the addition of aqueous HCl (1 M). The mixture was extracted with ethyl acetate (3×30 ml), and the combined organic layers were consecutively washed with brine (15 mL) and water (15 mL), dried over Na<sub>2</sub>SO<sub>4</sub> and filtered. The solvent was evaporated under reduced pressure, and the crude product was purified by flash chromatography (SiO<sub>2</sub>, hexanes/EtOAc, 5:1 + 1% formic acid) and recrystallized in refluxing methanol to afford **179a** (432 mg, 1.11 mmol, 15.2% yield over 5 steps starting from cyclopropane **98a**) as a white solid.

c) Characterization of **179a**:

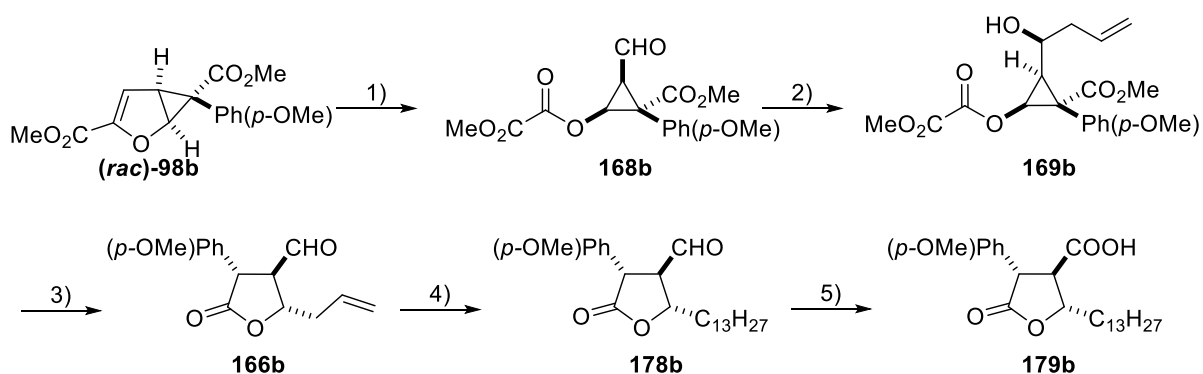
**m.p.** 75-76 °C; **R<sub>f</sub>** = 0.51 (hexanes : ethyl acetate = 5:1 + 1% formic acid, bromocresol green); **[α]<sub>D</sub><sup>20</sup>** 10.4° (c = 1.0, CHCl<sub>3</sub>, 99% *ee*); **IR** (neat): 3034, 2919, 2851, 2363, 2110, 1744, 1729, 1498, 1454, 1424, 1364, 1323, 1234, 1170, 1003, 921, 874, 753, 727, 693 cm<sup>-1</sup>; **<sup>1</sup>H-NMR** (300 MHz, CDCl<sub>3</sub>): δ 7.42 – 7.31 (m, 3H), 7.29 – 7.22 (m, 2H), 4.56 (td, *J* = 8.6, 3.8 Hz, 1H), 4.25 (d, *J* = 11.4 Hz, 1H), 3.21 (dd, *J* = 11.4, 9.3 Hz, 1H), 1.99 – 1.73 (m, 2H), 1.67 – 1.42 (m, *J* = 9.5 Hz, 2H), 1.41 – 1.18 (m, 20H), 0.89 (t, *J* = 6.6 Hz, 3H); **<sup>13</sup>C-NMR** (75 MHz, CDCl<sub>3</sub>): δ 175.8, 174.6, 134.8, 129.1, 128.3, 128.3, 79.6, 55.0, 50.6, 35.0, 31.9, 29.7, 29.7 (2C) 29.6, 29.5, 29.4, 29.4, 29.3, 25.3, 22.7, 14.2; **HRMS** (-ESI) calcd. for C<sub>24</sub>H<sub>35</sub>O<sub>4</sub> (M-H) 387.2541 found 387.2555

## 5.2 Racemic synthesis of paraconic acid derivatives **179b**, **180a** and **181b**



*rel*-(2*S*,3*R*,4*S*)-4-(4-methoxyphenyl)-5-oxo-2-tridecyltetrahydrofuran-3-carboxylic acid (**179b**)

a) Overview of consecutive steps:



b) Procedure

1) A flame dried Schlenk tube was charged with **(rac)-98b** (2.42 g, 7.95 mmol, 1.0 equiv) and anhydrous DCM (20 ml). The reaction was cooled to  $-78\text{ }^{\circ}\text{C}$  and ozone was passed through the reaction mixture until a blue color appeared. Excess of ozone was expelled by passing a constant stream of oxygen through the solution until it turned colorless. The stream of oxygen continued for further 5 min and DMS (2.9 ml, 39.76 mmol, 5.0 equiv) was added. The reaction mixture was allowed to warm up to room temperature overnight in an unfreezing cooling bath. The solution was washed with sat.  $\text{NaHCO}_3$  (8 ml) and water (8 ml). After drying over  $\text{MgSO}_4$  and filtration, the solvent was removed under reduced pressure to afford crude **168b** (2.36 g, 88% crude yield) as a sticky yellow oil

2) In a flame dried Schlenk flask crude aldehyde **168b** (theoretical: 2.36 g, 7.0 mmol, 1.0 equiv) was dissolved in dry DCM (50 mL) and the solution was cooled to  $-78\text{ }^{\circ}\text{C}$ . Boron trifluoride diethyl etherate (0.99 mL, 8.0 mmol, 1.15 equiv) was added, and the reaction mixture was stirred for 30 min. Subsequently, allyltrimethylsilane (1.4 mL, 9.1 mmol, 1.3 equiv) was added, and the resulting solution was stirred for 18 h. The reaction was stopped with sat.  $\text{NaHCO}_3$  (15 mL) and allowed to warm up to rt. The phases were separated, and the aqueous phase was

extracted with DCM (3 x 20 mL). After drying over Na<sub>2</sub>SO<sub>4</sub> and filtration, the solvent was removed under reduced pressure to afford crude **169b** (2.48 g, 94% crude yield) as a sticky yellow oil.

3) A solution of crude allyl **169b** (theoretical: 2.48 g, 6.6 mmol, 1.0 equiv) in methanol (23 mL) was cooled to 0 °C. Subsequently, triethylamine (2.3 mL, 16.4 mmol, 2.5 equiv) was added using a syringe pump for the duration of 2 h, and the solution was stirred for 18 h in the unfreezing cooling bath. After removal of the solvent in vacuo, the residue was treated with water (15 mL) and DCM (15 mL). The phases were separated, and the aqueous layer was extracted with DCM (7x12 mL). After drying over MgSO<sub>4</sub> and filtration, the volatiles were removed under reduced pressure. Attempts were made to purify the residue by flash chromatography (SiO<sub>2</sub>, hexanes/EtOAc, 2:1) and afforded crude **166b** (551 mg, 32% crude yield) as yellow oil.

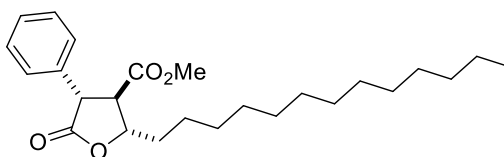
4) A flame dried Schlenk flask was charged with crude lactone **166b** (theoretical: 226 mg, 0.87 mmol, 1.0 equiv), anhydrous DCM (35 mL, bubbling nitrogen through the solvent for 10 min before use), Grubbs II (41 mg, 48 μmol, 6 mol%) and 1-dodecene (1.30 mL, 5.76 mmol, 6.6 equiv). The resulting solution was refluxed for 16 h. After removal of the solvent under reduced pressure the crude mixture was dissolved in methanol (8 mL). The reaction mixture was vigorously stirred in an autoclave at rt for 24 h under 20 atm of hydrogen gas. The crude mixture was filtered (removal of tetracosane) and washed with methanol (crude yield (**178b**) > 100%).

5) A round-bottom flask was charged with crude **178b** (theoretical: 350 mg, 0.87 mmol, 1.0 equiv), BAIB (616 mg, 1.91 mmol, 2.2 equiv), TEMPO (27 mg, 0.17 mmol, 0.2 equiv) and a mixture of acetonitrile and water (1:1, 30 mL). The reaction mixture was stirred at rt for 48 h. Subsequently, a solution of Na<sub>2</sub>SO<sub>3</sub> (1.6 g) in water (2 mL) was added, and stirring was continued for additional 30 min before the reaction mixture was acidified to pH 2 by the addition of aqueous HCl (1 M). The mixture was extracted with ethyl acetate (3x30 mL), and the combined organic layers were consecutively washed with brine (2 mL) and water (2 mL), dried over Na<sub>2</sub>SO<sub>4</sub> and filtered. The solvent was evaporated under reduced pressure, and the crude product was purified by flash chromatography (SiO<sub>2</sub>, hexanes/EtOAc, 2:1 + 1% formic acid) and recrystallization in refluxing methanol to afford **179b** (138 mg, 0.33 mmol, 10.0% yield over 5 steps starting from cyclopropane **98b**) as a white solid

#### c) Characterization

**m.p.** 107-109 °C; **R<sub>f</sub>** = 0.43 (hexanes : ethyl acetate = 2:1 + 1% formic acid, bromocresol green); **IR** (neat): 3004, 2919, 2851, 1737, 1618, 1521, 1469, 1349, 1290, 1264, 1167, 1029, 977, 865,

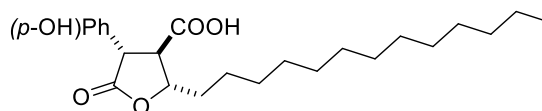
824, 723, 682  $\text{cm}^{-1}$ ;  **$^1\text{H NMR}$**  (400 MHz,  $\text{CDCl}_3$ )  $\delta$  7.19 – 7.13 (m, 2H), 6.93 – 6.87 (m, 2H), 4.54 (td,  $J = 8.7, 3.6$  Hz, 1H), 4.19 (d,  $J = 11.4$  Hz, 1H), 3.79 (s, 3H), 3.16 (dd,  $J = 11.1, 9.6$  Hz, 1H), 1.95 – 1.74 (m, 2H), 1.62 – 1.43 (m, 2H), 1.37 – 1.19 (m, 20H), 0.89 (t,  $J = 6.6$  Hz, 3H);  **$^{13}\text{C NMR}$**  (101 MHz,  $\text{CDCl}_3$ )  $\delta$  175.7, 174.9, 159.5, 129.5, 126.9, 114.5, 79.5, 55.3, 55.1, 50.1, 35.0, 32.0, 29.7, 29.7 (2C), 29.6, 29.5, 29.4, 29.4, 29.3, 25.3, 22.7, 14.1; **HRMS** (-ESI) calcd. for  $\text{C}_{25}\text{H}_{37}\text{O}_5$  (M-H) $^-$  417.2646 found 417.2656.



Methyl- *rel*-(2*S*,3*R*,4*S*)-5-oxo-4-phenyl-2-tridecyltetrahydrofuran-3-carboxylate (**180a**)

A solution of acid (*rac*)-**179** (51 mg, 0.13 mmol, 1.0 equiv) in methanol (3 mL) was treated with sulfuric acid (3 drops) and the reaction mixture was stirred for 5 h at room temperature. After removal of the solvent under vacuo, the residue was treated with water (6 mL) and diethyl ether (10 mL). The phases were separated and the aqueous layer was extracted with diethyl ether (3x10 mL). The combined organic layers were washed with aqueous  $\text{NaHCO}_3$ , dried over  $\text{MgSO}_4$ , filtered and the solvent was removed under reduced. The crude product was purified by flash chromatography ( $\text{SiO}_2$ , hexanes/EtOAc, 95:5) to afford ester **180a** as a white solid (48 mg, 91% yield).

**m.p.** 53-54°C; **R<sub>f</sub>** = 0.28 (hexanes : ethyl acetate = 9:1, UV); **IR** (neat): 3064, 3034, 2915, 2851, 2363, 2106, 1774, 1733, 1603, 1498, 1457, 1372, 1334, 1279, 1167, 1126, 1003, 969, 861, 749, 701, 667  $\text{cm}^{-1}$ ;  **$^1\text{H NMR}$**  (300 MHz,  $\text{CDCl}_3$ )  $\delta$  7.41 – 7.29 (m, 3H), 7.26 – 7.18 (m, 2H), 4.52 (ddd,  $J = 9.3, 7.9, 4.4$  Hz, 1H), 4.25 (d,  $J = 11.6$  Hz, 1H), 3.71 (s, 3H), 3.16 (dd,  $J = 11.5, 9.4$  Hz, 1H), 1.92 – 1.69 (m, 2H), 1.63 – 1.41 (m, 2H), 1.38 – 1.19 (m, 20H), 0.87 (t,  $J = 6.7$  Hz, 3H);  **$^{13}\text{C NMR}$**  (75 MHz,  $\text{CDCl}_3$ )  $\delta$  174.7, 170.9, 135.1, 129.1, 128.3, 128.1, 79.8, 55.4, 52.8, 51.0, 34.9, 31.9, 29.7, 29.7 (2C), 29.6, 29.5, 29.4, 29.4, 29.3, 25.2, 22.7, 14.2; **HRMS** (+ESI) calcd. for  $\text{C}_{25}\text{H}_{39}\text{O}_4$  (M+H) $^+$  403.2843 found 403.2837



*rel*-(2*S*,3*R*,4*S*)-4-(4-hydroxyphenyl)-5-oxo-2-tridecyltetrahydrofuran-3-carboxylic acid (**181b**)

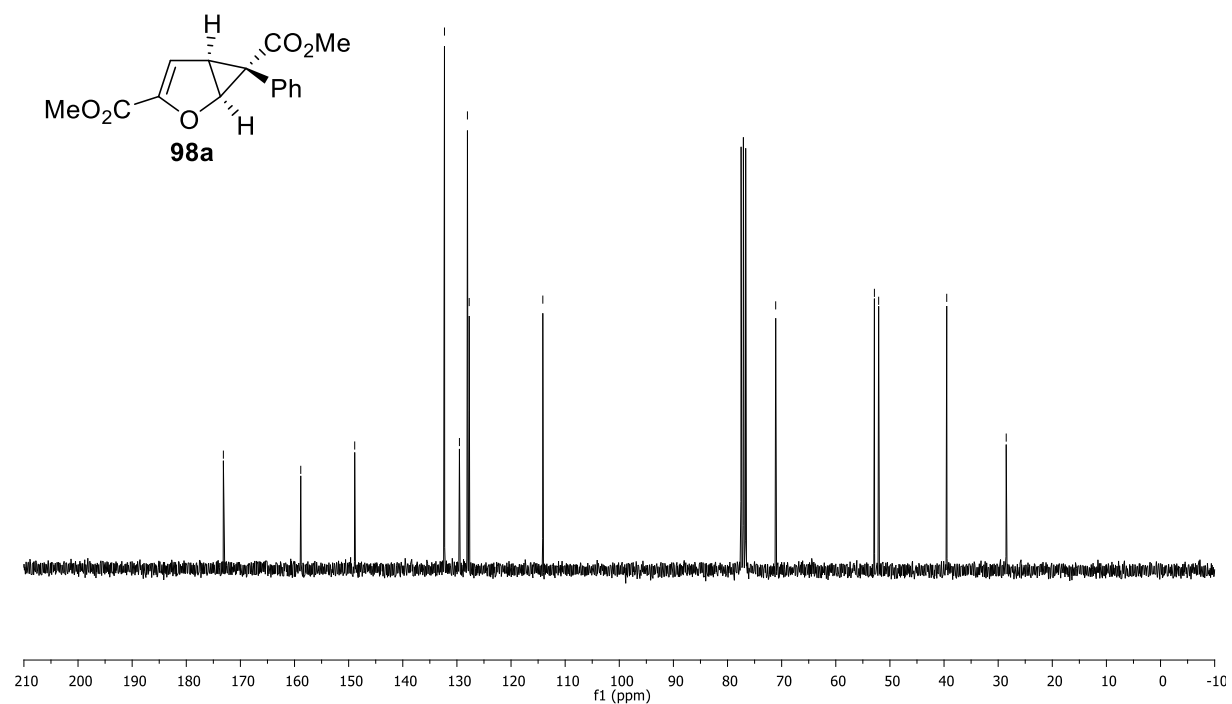
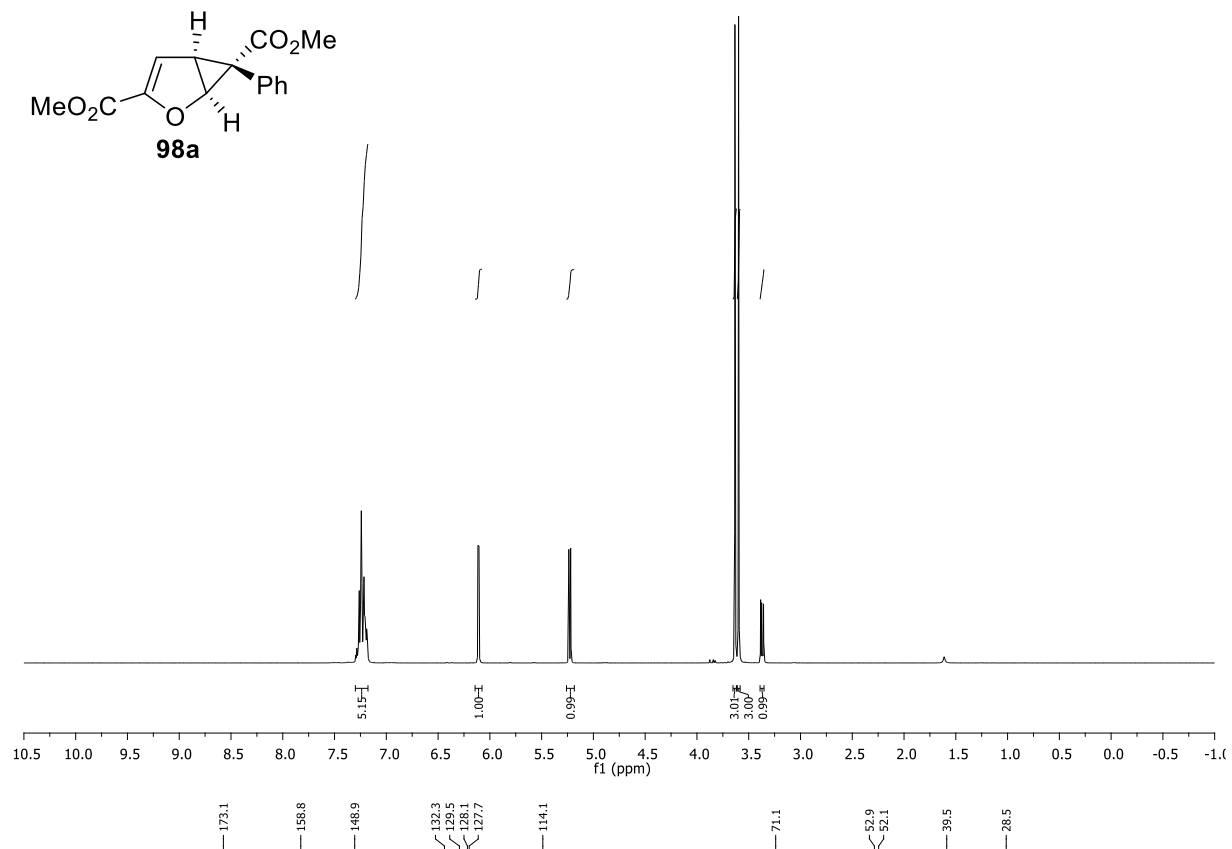
A flame dried 2-neck-Schlenk flask equipped with a reflux condenser was charged with acid **179b** (40 mg, 96  $\mu$ mol, 1.0 equiv) and anhydrous DCM (8 mL). The solution was cooled to 0  $^{\circ}$ C and  $\text{BBr}_3$  (92  $\mu$ L, 0.96 mmol, 10 equiv) in anhydrous DCM (2 mL) was added within 5 min. The reaction mixture was stirred for 4 h in the unfreezing ice bath and subsequently aqueous NaOH (0.1 M, 4 mL) was added. The phases were separated and the aqueous phase was extracted with ethyl acetate (2x3 mL). After drying over  $\text{Na}_2\text{SO}_4$  and filtration, the solvent was removed under reduced pressure. The crude product was purified by flash chromatography ( $\text{SiO}_2$ , hexanes/EtOAc, 2:1 + 1% formic acid) to afford alcohol **181b** as a white solid (33.5 mg, 87% yield).

**m.p.** 119-123  $^{\circ}$ C; **R<sub>f</sub>** = 0.43(hexanes : ethyl acetate = 2:1 + 1% formic acid, bromocresol green); **IR** (neat): 3269, 2922, 2855, 2363, 1737, 1707, 1618, 1607, 1521, 1489, 1446, 1364, 1174, 1129, 1006, 977, 876, 828, 723, 690  $\text{cm}^{-1}$ ; **<sup>1</sup>H NMR** (400 MHz, acetone)  $\delta$  7.19 – 7.13 (m, 2H), 6.86 – 6.81 (m, 2H), 4.57 (ddd,  $J$  = 9.1, 8.3, 4.3 Hz, 1H), 4.21 (d,  $J$  = 11.7 Hz, 1H), 3.25 (dd,  $J$  = 11.7, 9.4 Hz, 1H), 1.99 – 1.82 (m, 2H), 1.63 – 1.46 (m, 2H), 1.39 – 1.24 (m, 20H), 0.89 (t,  $J$  = 6.8 Hz, 3H); **<sup>13</sup>C NMR** (101 MHz, acetone)  $\delta$  174.4, 171.2, 156.9, 129.7, 127.1, 115.4, 79.3, 55.0, 50.2, 34.5, 31.7, 29.5 (hidden under acetone peak), 29.5, 29.5 (2C), 29.4, 29.3, 29.2, 29.2 (hidden under acetone peak), 25.3, 22.4, 13.5; **HRMS** (-ESI) calcd. for  $\text{C}_{24}\text{H}_{35}\text{O}_5$  (M-H)<sup>-</sup> 403.2490 found 403.2482

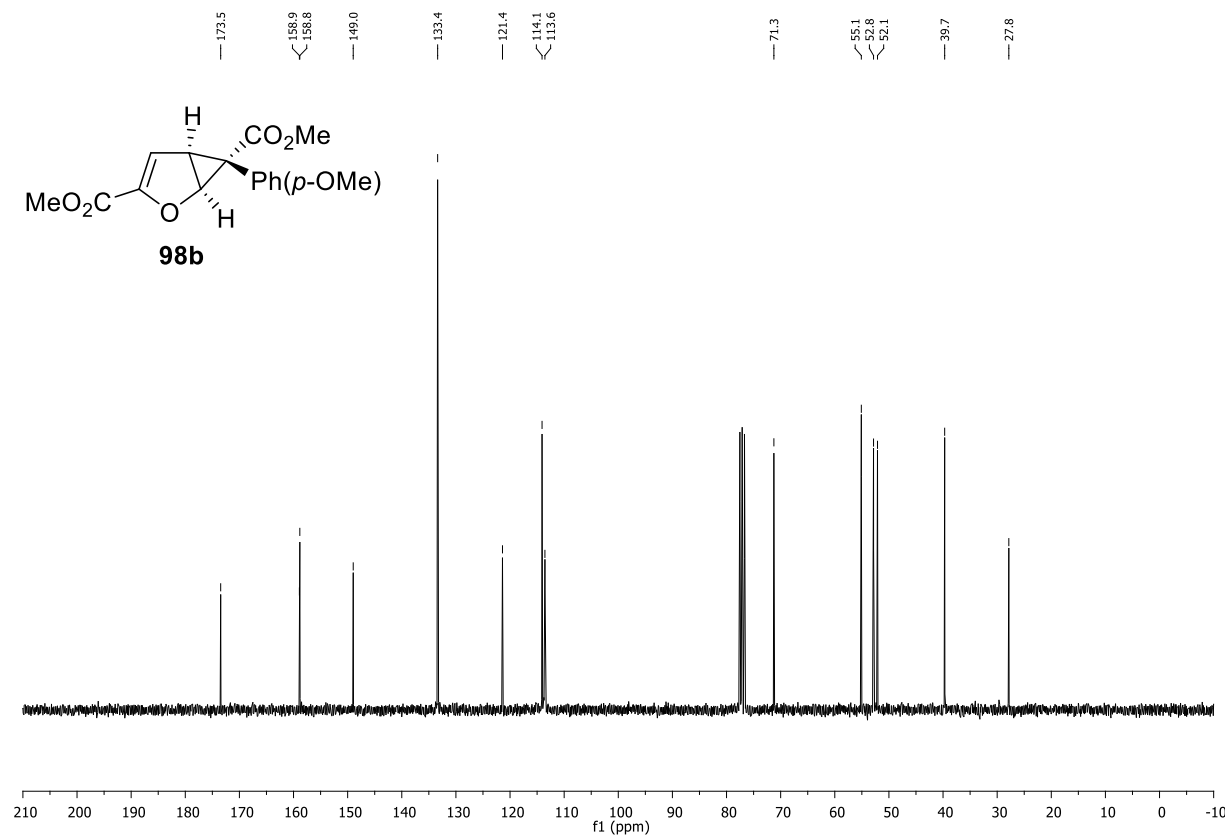
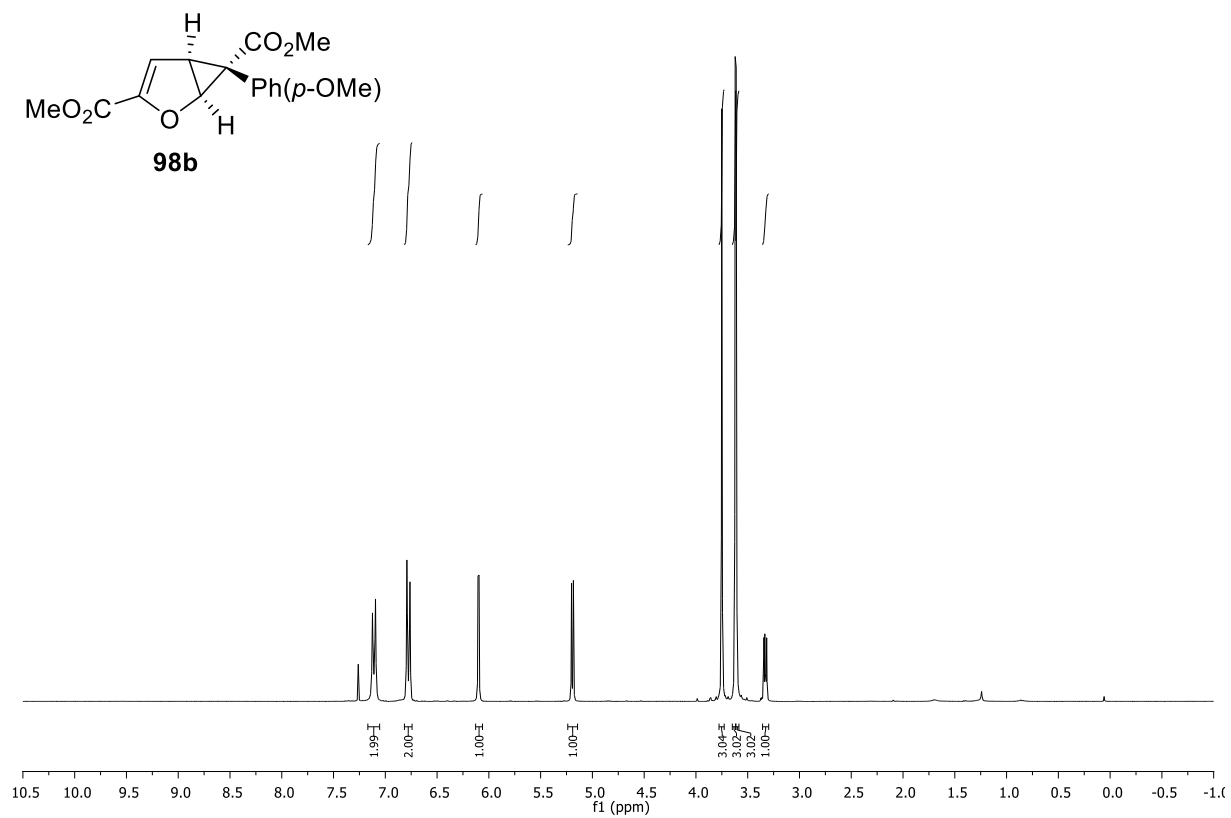
## 6 References

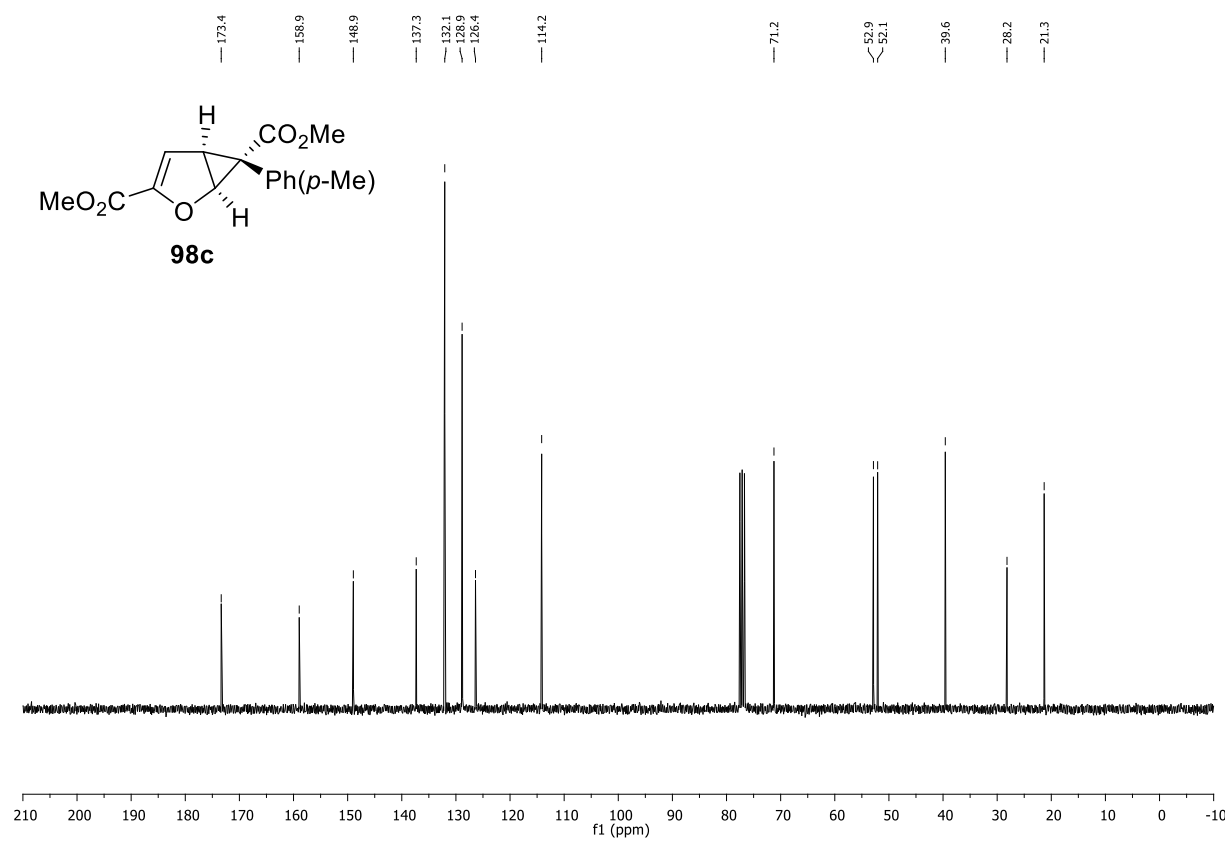
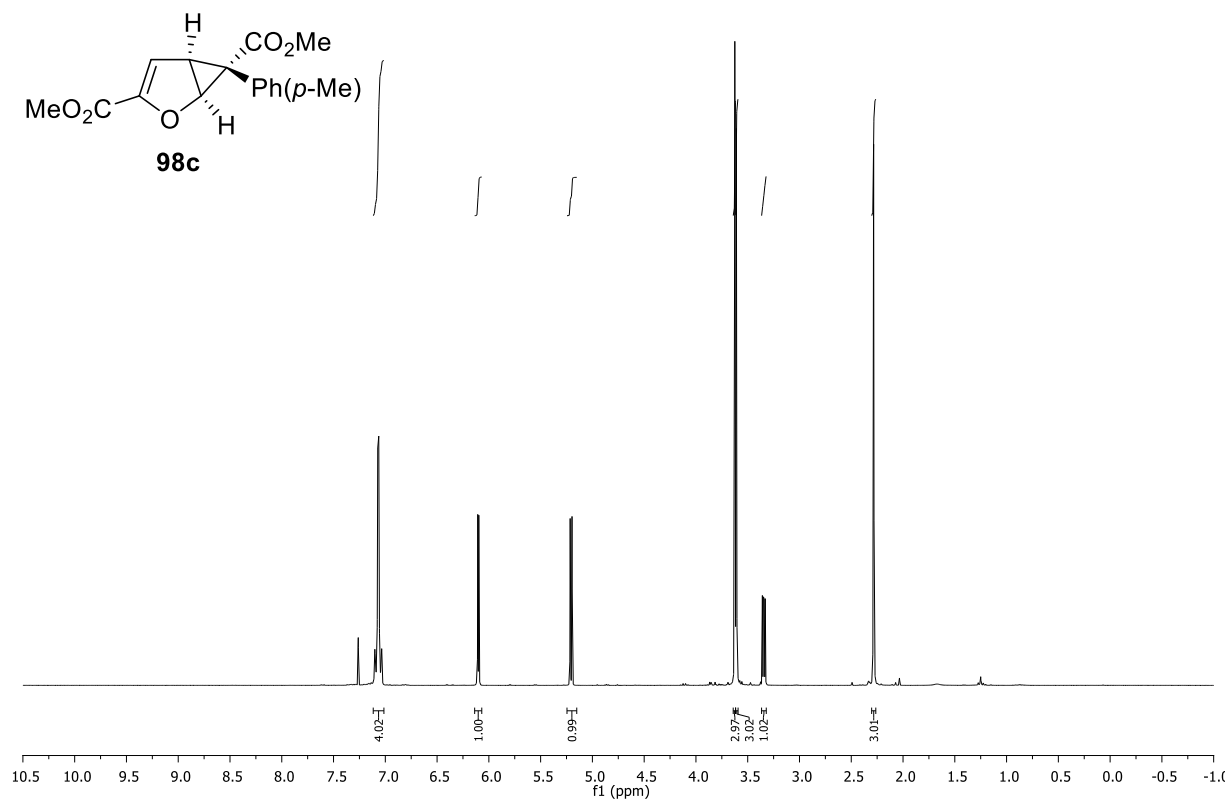
- (1) Davies, H. M. L.; Bruzinski, P. R.; Lake, D. H.; Kong, N.; Fall, M. J. *J. Am. Chem. Soc.* **1996**, *118*, 6897–6907.
- (2) Pirrung, M. C.; Zhang, J. *Tetrahedron Lett.* **1992**, *33*, 5987–5990.
- (3) Qin, C.; Boyarskikh, V.; Hansen, J. H.; Hardcastle, K. I.; Musaev, D. G.; Davies, H. M. L. *J. Am. Chem. Soc.* **2011**, *133*, 19198–19204.
- (4) Müller, P.; Allenbach, Y.; Robert, E. *Tetrahedron: Asymmetry* **2003**, *14*, 779–785.
- (5) Reddy, R. P.; Lee, G. H.; Davies, H. M. L. *Org. Lett.* **2006**, *8*, 3437–3440.
- (6) Reddy, R. P.; Davies, H. M. L. *Org. Lett.* **2006**, *8*, 5013–5016.
- (7) a) Hashimoto, S.; Watanabe, N.; Ikegami, S. *Tetrahedron Lett.* **1990**, *31*, 5173–5174; b) Watanabe, N.; Ogawa, T.; Ohtake, Y.; Ikegami, S.; Hashimoto, S. *Synlett* **1996**, 85–86;
- (8) Tsutsui, H.; Yamaguchi, Y.; Kitagaki, S.; Nakamura, S.; Anada, M.; Hashimoto, S. *Tetrahedron: Asymmetry* **2003**, *14*, 817–821.
- (9) Yamawaki, M.; Tsutsui, H.; Kitagaki, S.; Anada, M.; Hashimoto, S. *Tetrahedron Lett.* **2002**, *43*, 9561–9564.
- (10) Goto, T.; Takeda, K.; Shimada, N.; Nambu, H.; Anada, M.; Shiro, M.; Ando, K.; Hashimoto, S. *Angew. Chem. Int. Ed.* **2011**, *50*, 6803–6808; *Angew. Chem.* **2011**, *123*, 6935–6940.
- (11) a) Scholl, M.; Ding, S.; Lee, C. W.; Grubbs, R. H. *Org. Lett.* **1999**, *1*, 953–956; b) Garber, S. B.; Kingsbury, J. S.; Gray, B. L.; Hoveyda, A. H. *J. Am. Chem. Soc.* **2000**, *122*, 8168–8179;
- (12) Sanda, F.; Komiya, T.; Endo, T. *Macromol. Chem. Phys.* **1998**, *199*, 2165–2172.
- (13) Grehn, L.; Ragnarsson, U. *Angew. Chem. Int. Ed.* **1984**, *23*, 296–297; *Angew. Chem.* **1984**, *96*, 291–292.
- (14) Davies, H. M. L.; Hansen, T.; Churchill, M. R. *J. Am. Chem. Soc.* **2000**, *122*, 3063–3070.
- (15) Boger, D. L.; Patel, M. J. *Org. Chem.* **52**, 2319–2323.
- (16) Zonta, C.; Fabris, F.; Lucchi, O. de. *Org. Lett.* **2005**, *7*, 1003–1006.
- (17) Krajewska, D.; Dabrowska, M.; Jakoniuk, P.; Róžańsk, A. *Acta Pol. Pharm.* **2002**, *59*, 127–132.
- (18) Berry, J. M.; Bradshaw, T. D.; Fichtner, I.; Ren, R.; Schwalbe, C. H.; Wells, G.; Chew, E.-H.; Stevens, M. F. G.; Westwell, A. D. *J. Med. Chem.* **2005**, *48*, 639–644.
- (19) Chhor, R. B.; Nosse, B.; Soergel, S.; Boehm, C.; Seitz, M.; Reiser, O. *Chem. Eur. J.* **2003**, *9*, 260–270.
- (20) Egleton, J. E.; Thinnes, C. C.; Seden, P. T.; Laurieri, N.; Lee, S. P.; Hadavizadeh, K. S.; Measures, A. R.; Jones, A. M.; Thompson, S.; Varney, A.; Wynne, G. M.; Ryan, A.; Sim, E.; Russell, A. J. *Bioorg. Med. Chem.* **2014**, *22*, 3030–3054.
- (21) Böhm, C.; Schinnerl, M.; Bubert, C.; Zabel, M.; Labahn, T.; Parisini, E.; Reiser, O. *Eur. J. Org. Chem.* **2000**, 2955–2965.
- (22) Hansen, J.; Li, B.; Dikarev, E.; Autschbach, J.; Davies, H. M. L. *J. Org. Chem.* **2009**, *74*, 6564–6571.

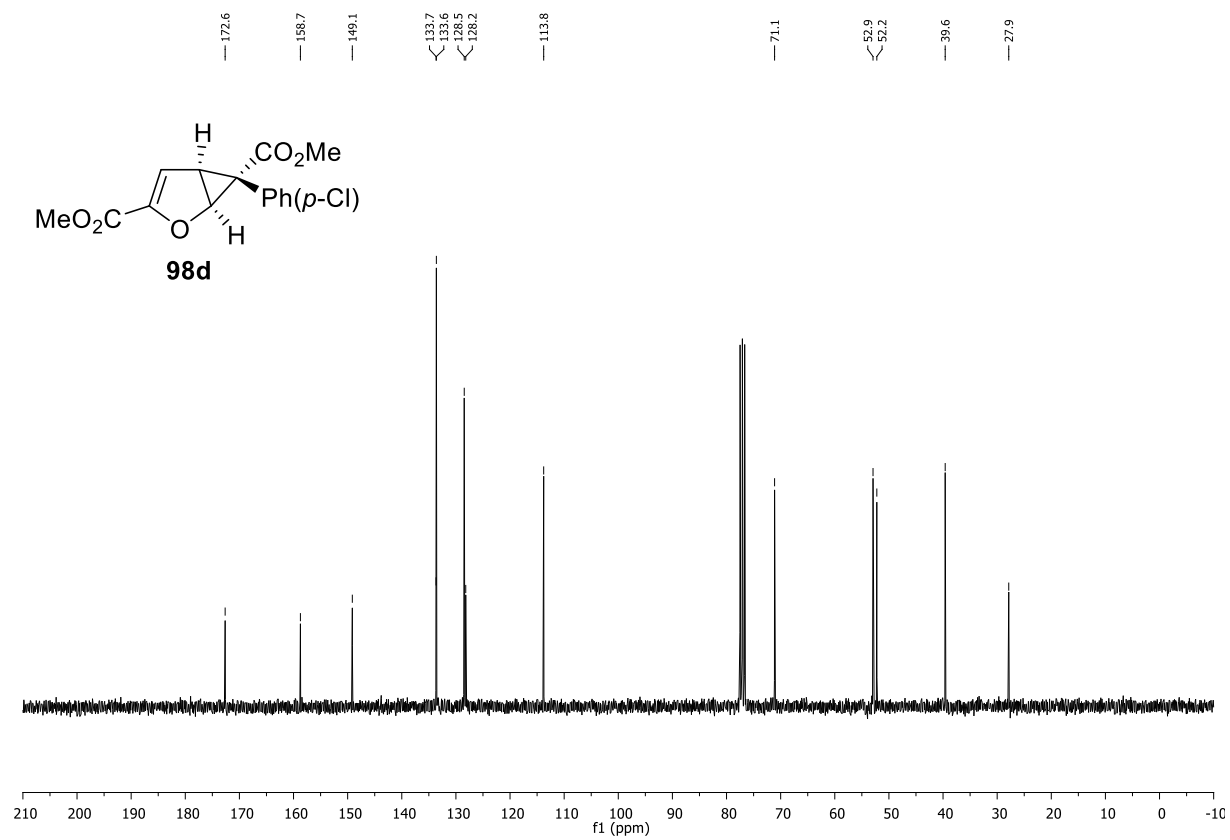
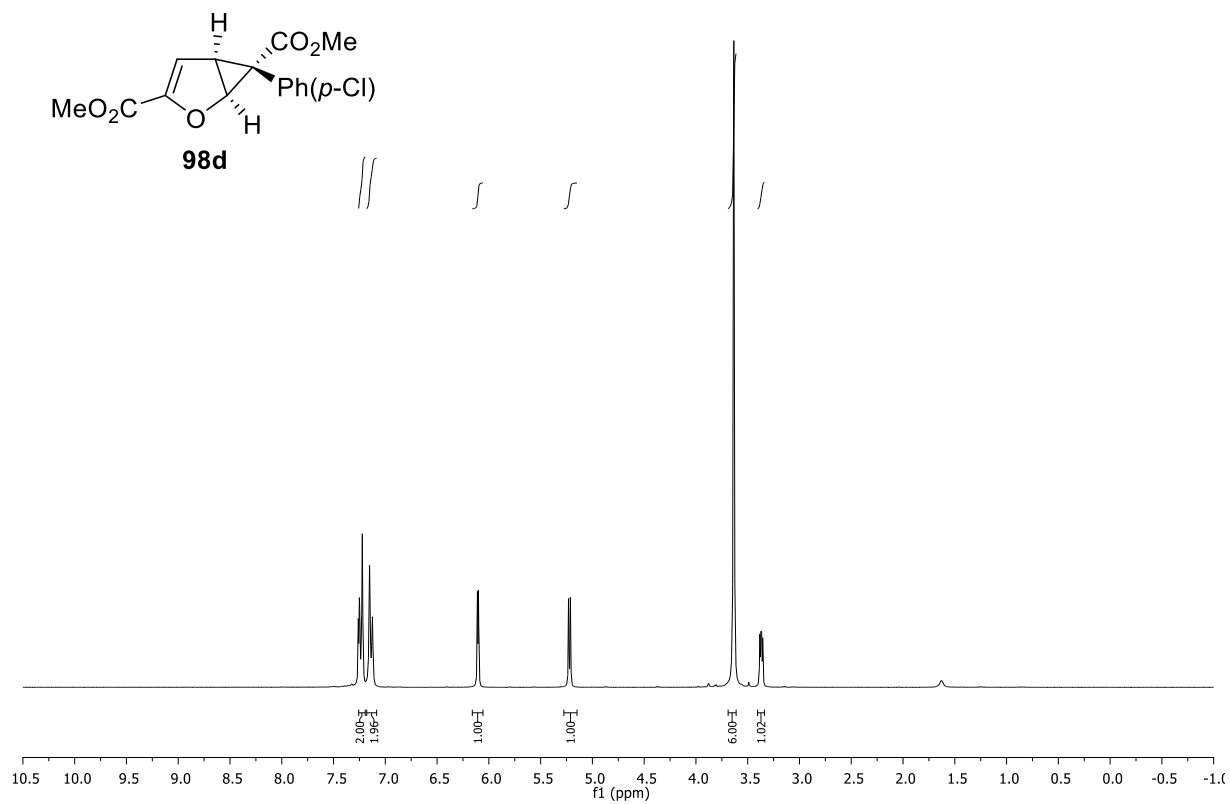
## F Appendix

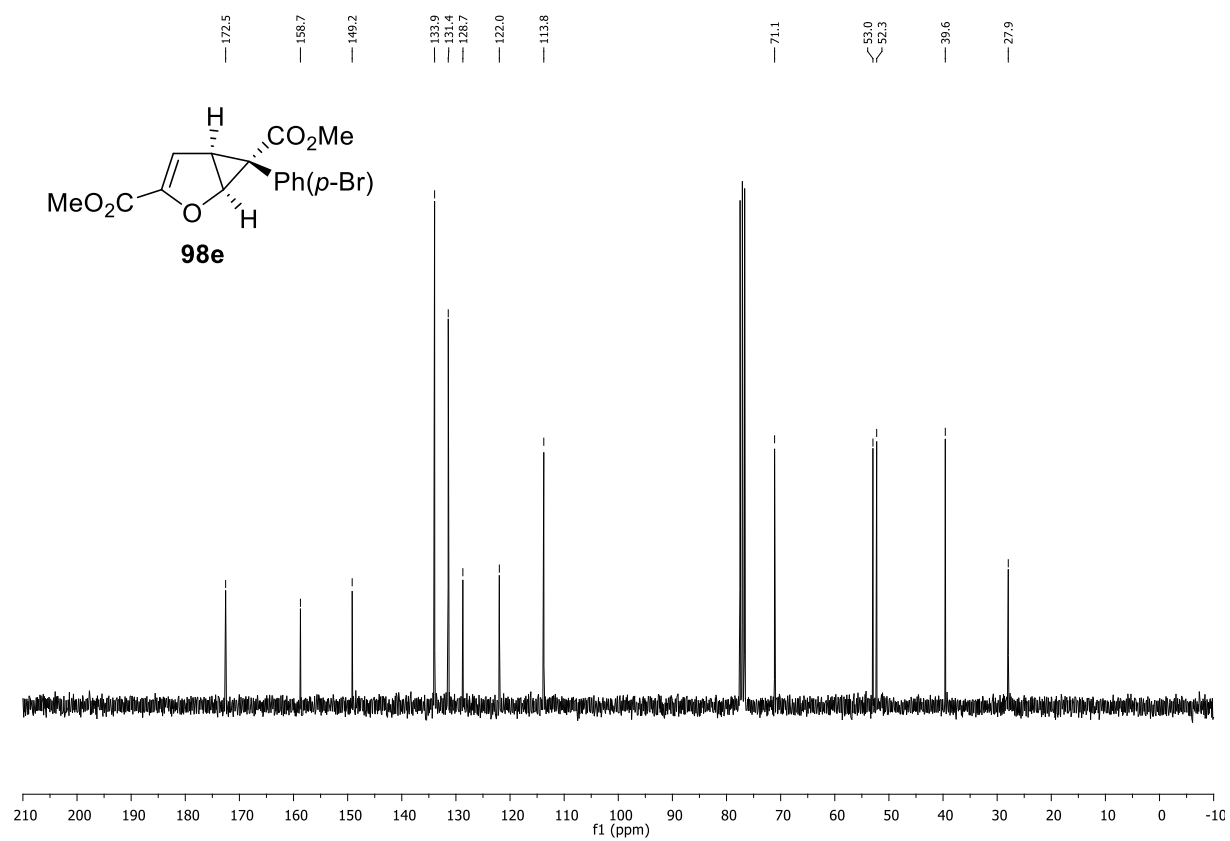
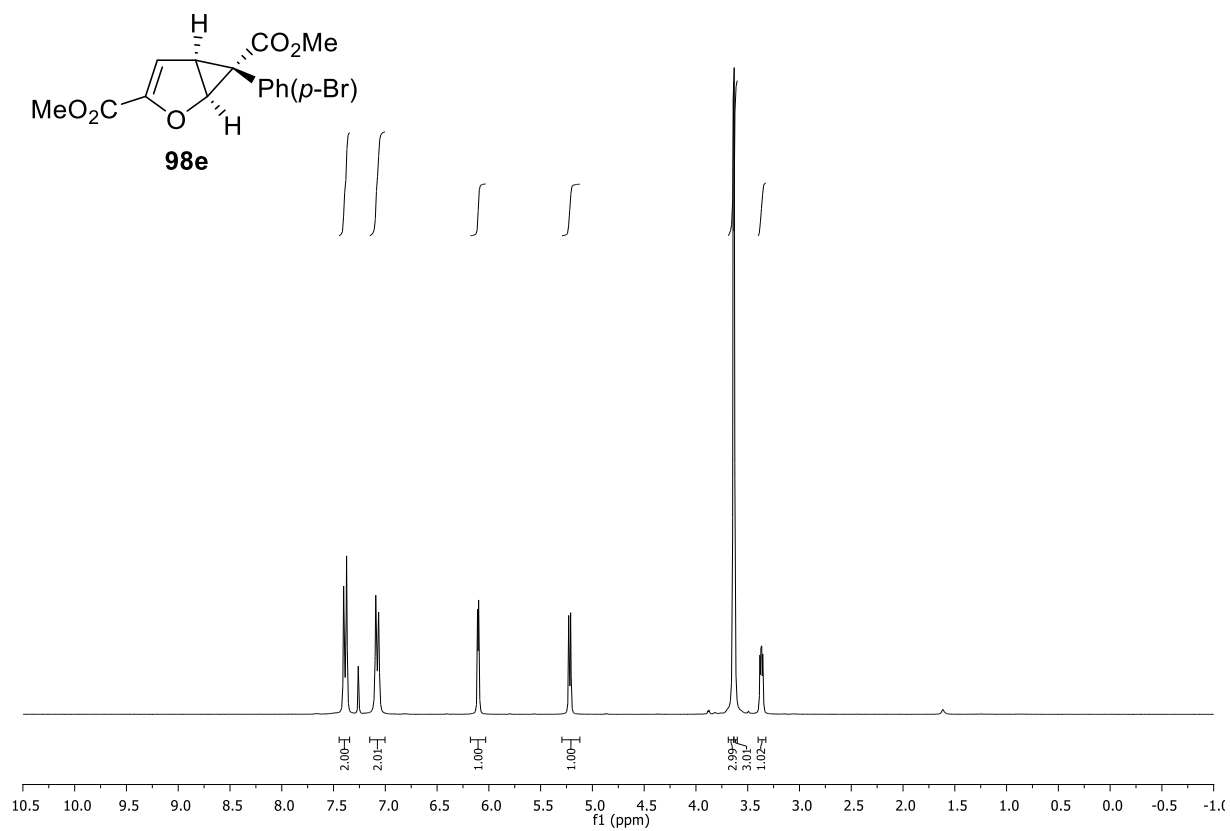
1 <sup>1</sup>H and <sup>13</sup>C NMR spectra

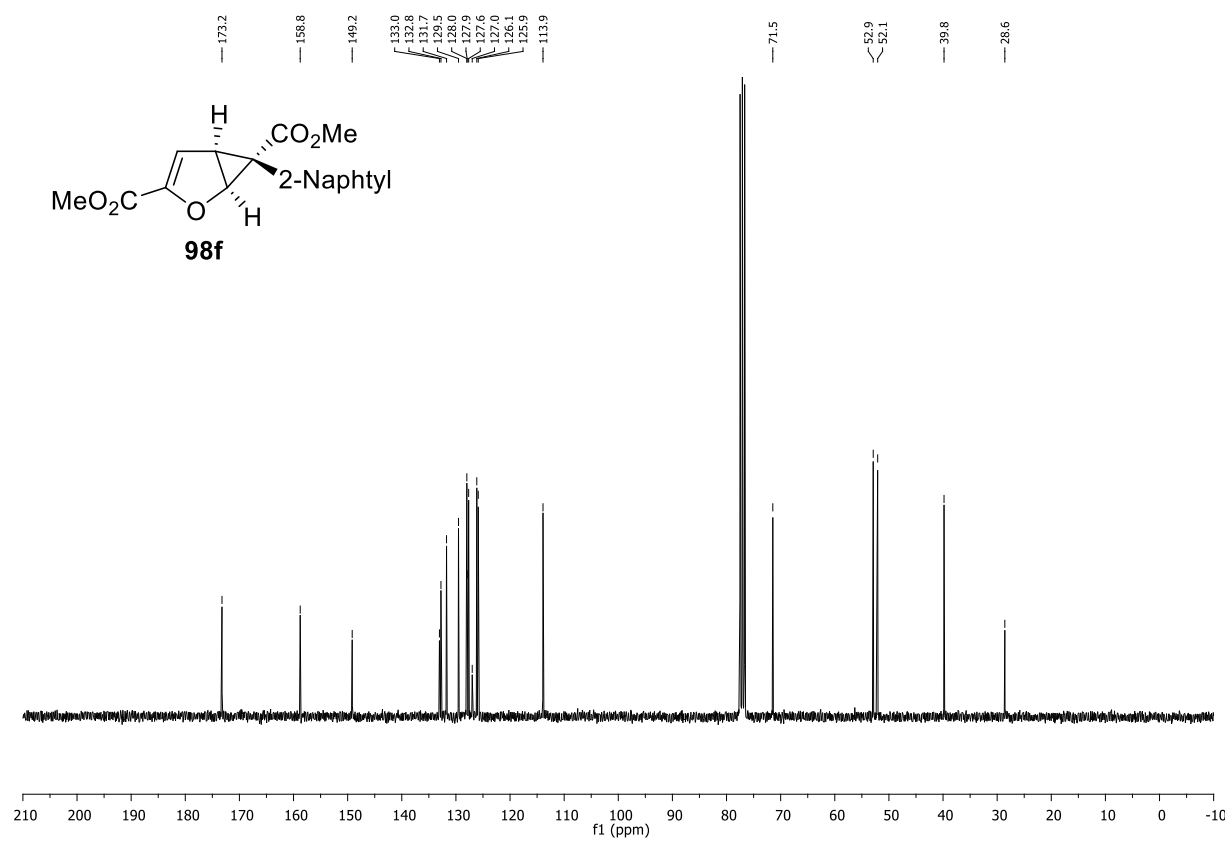
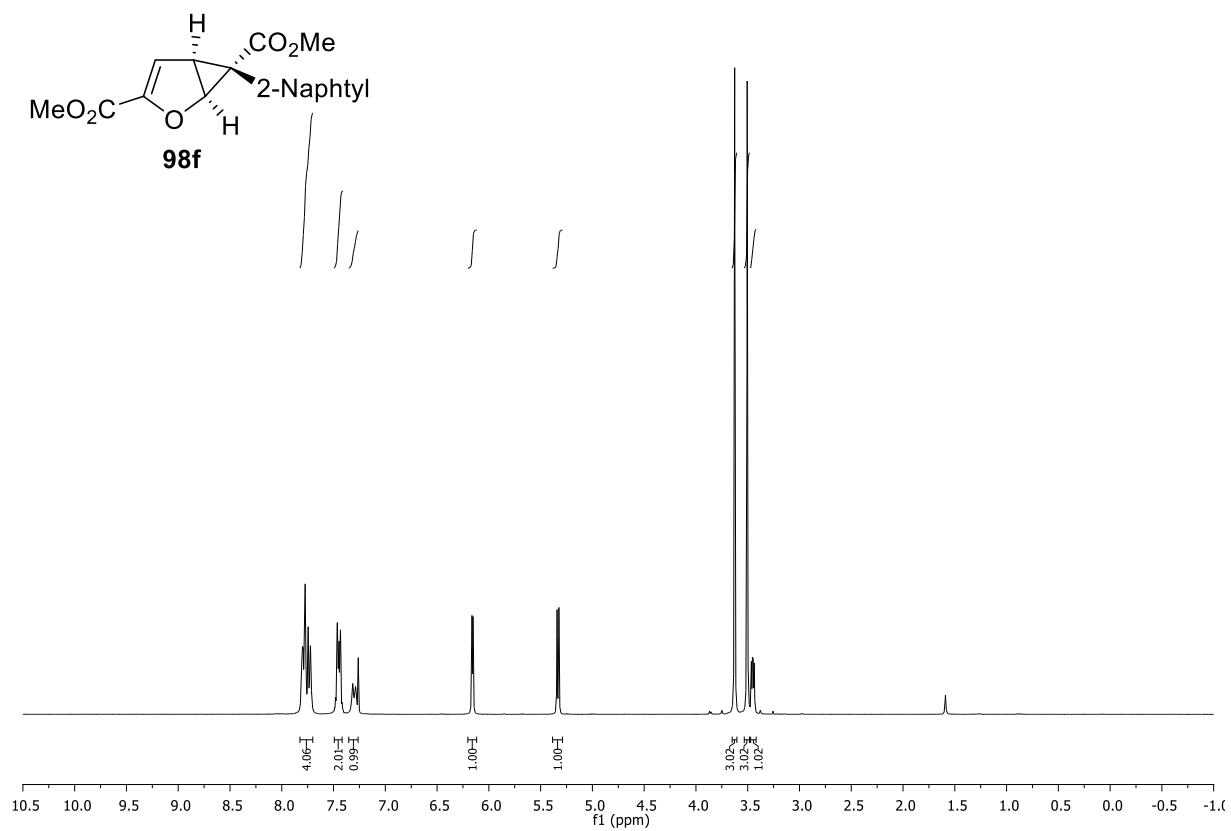


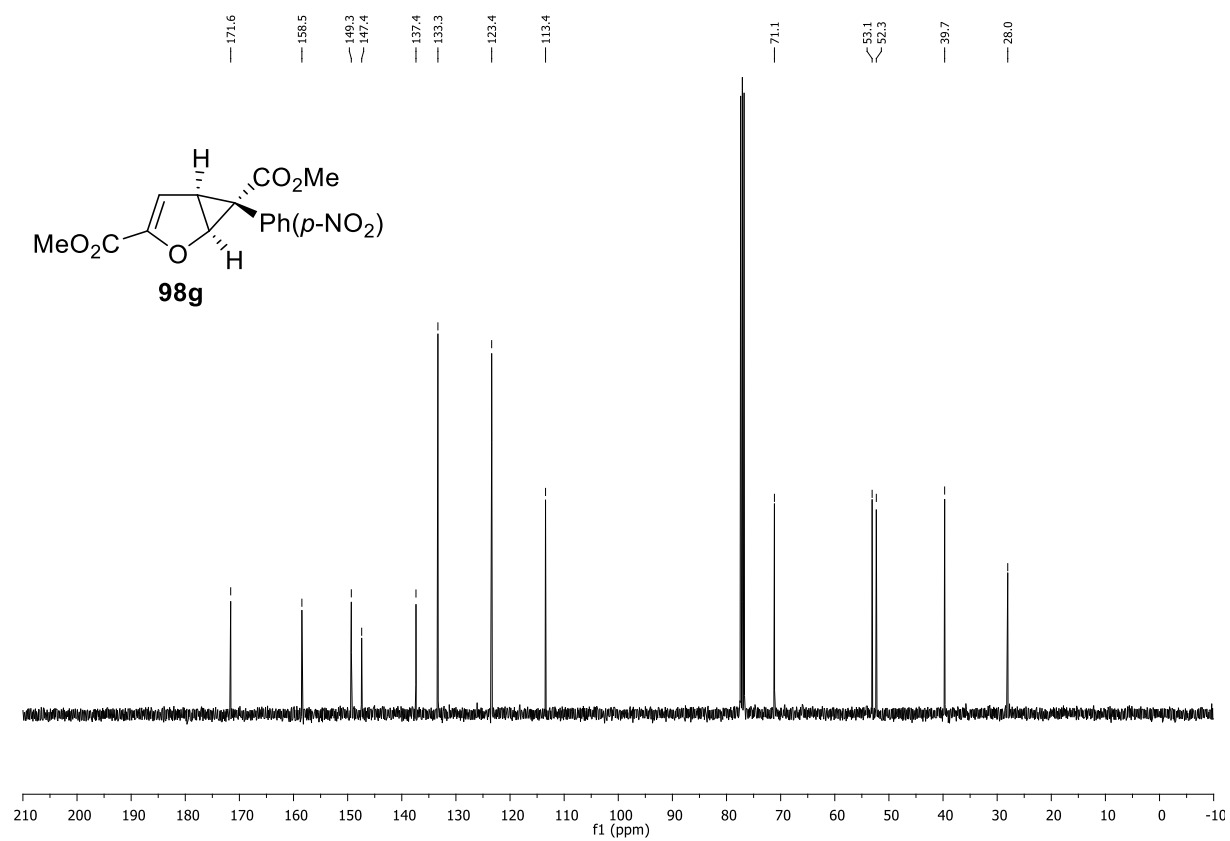
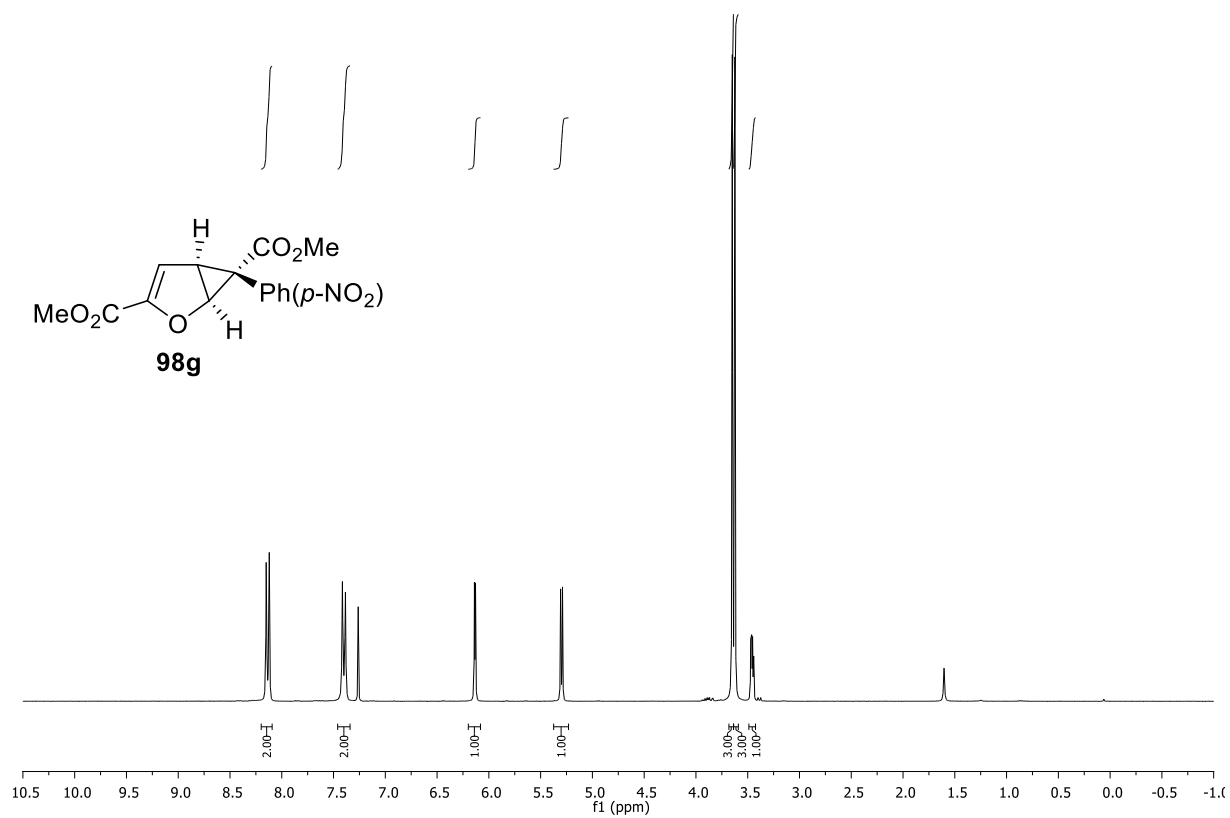


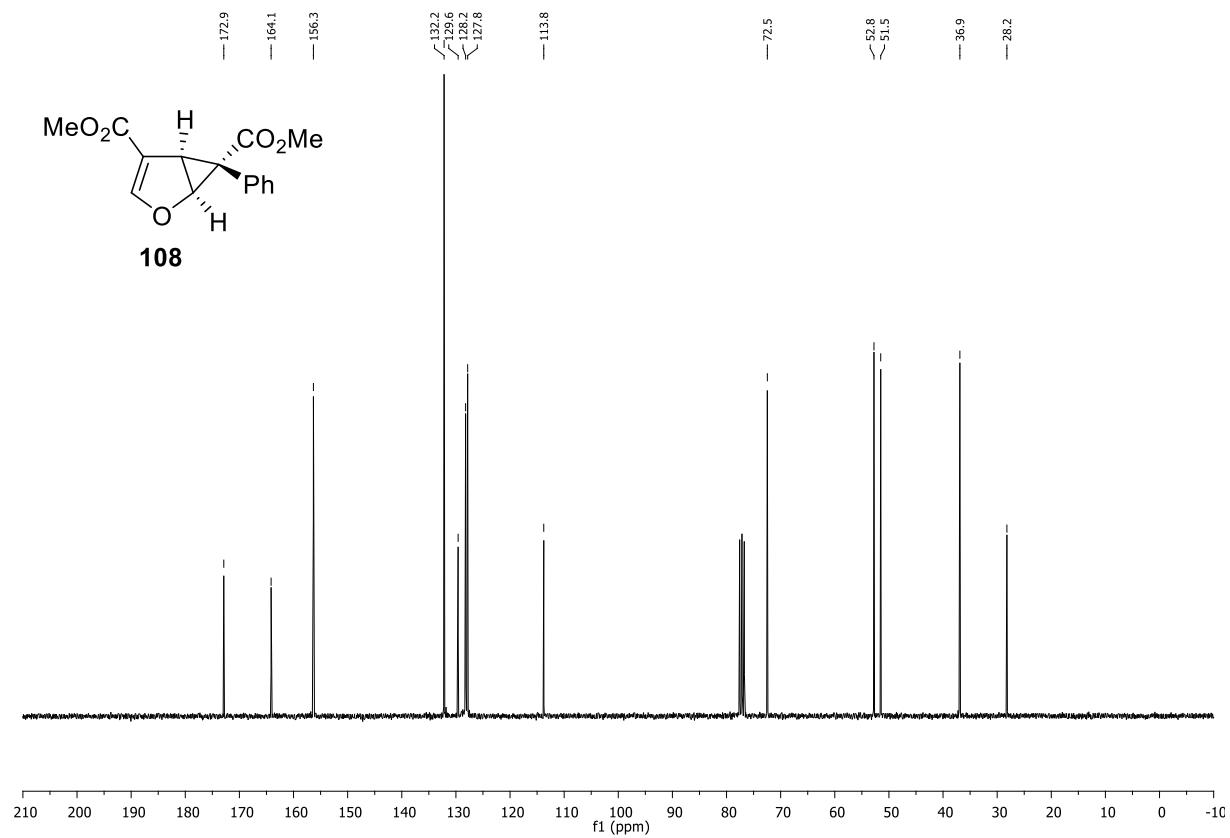
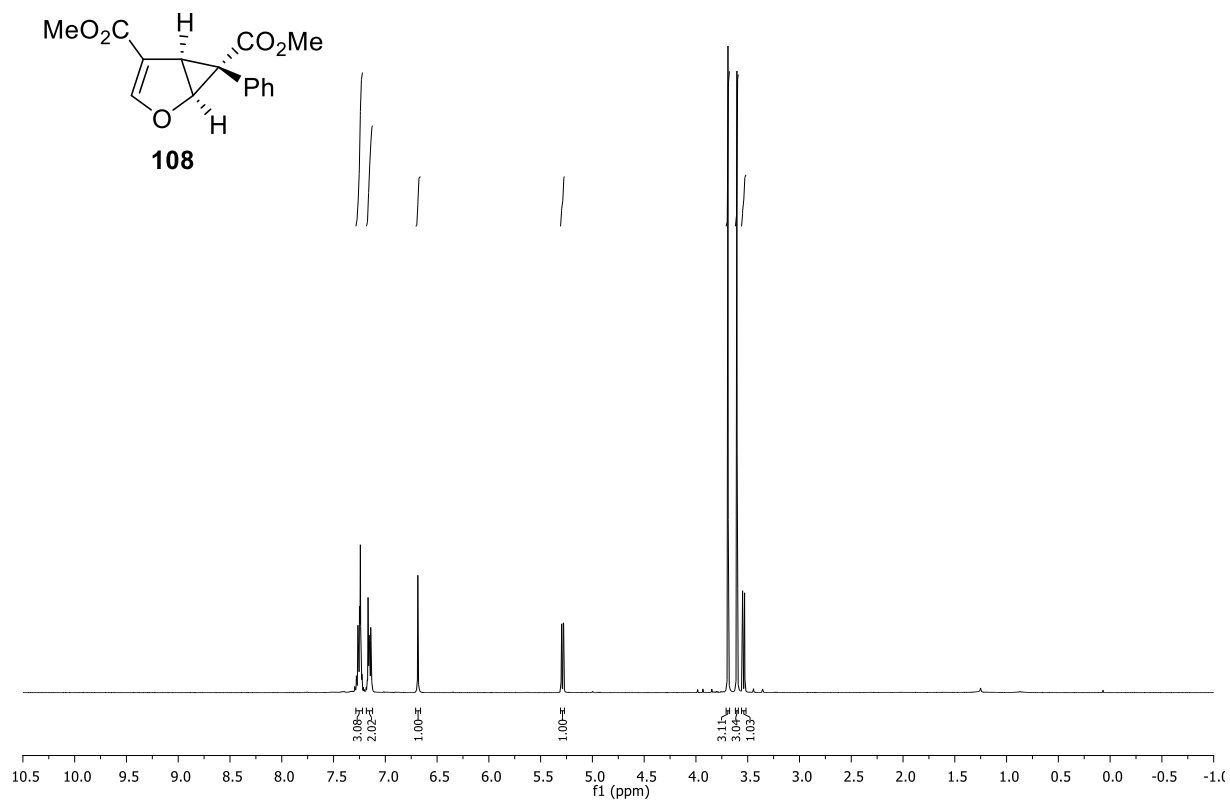


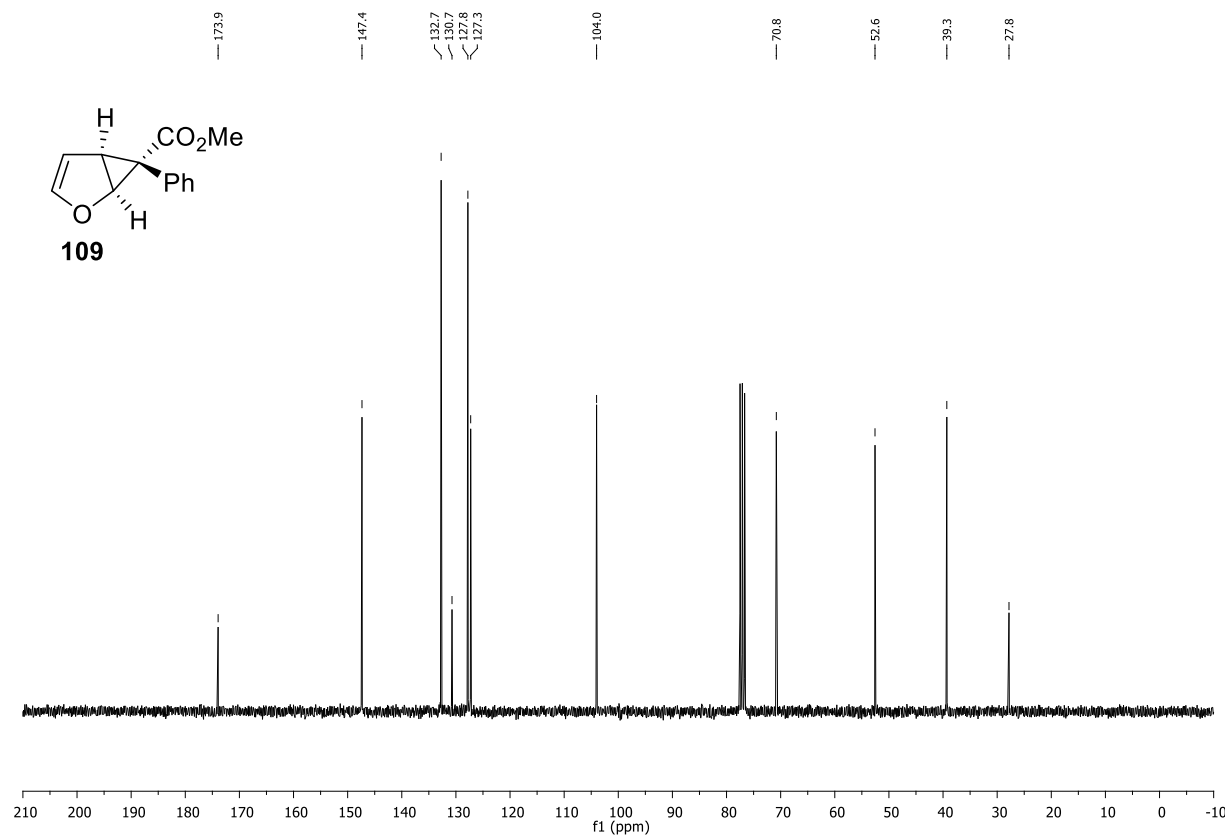
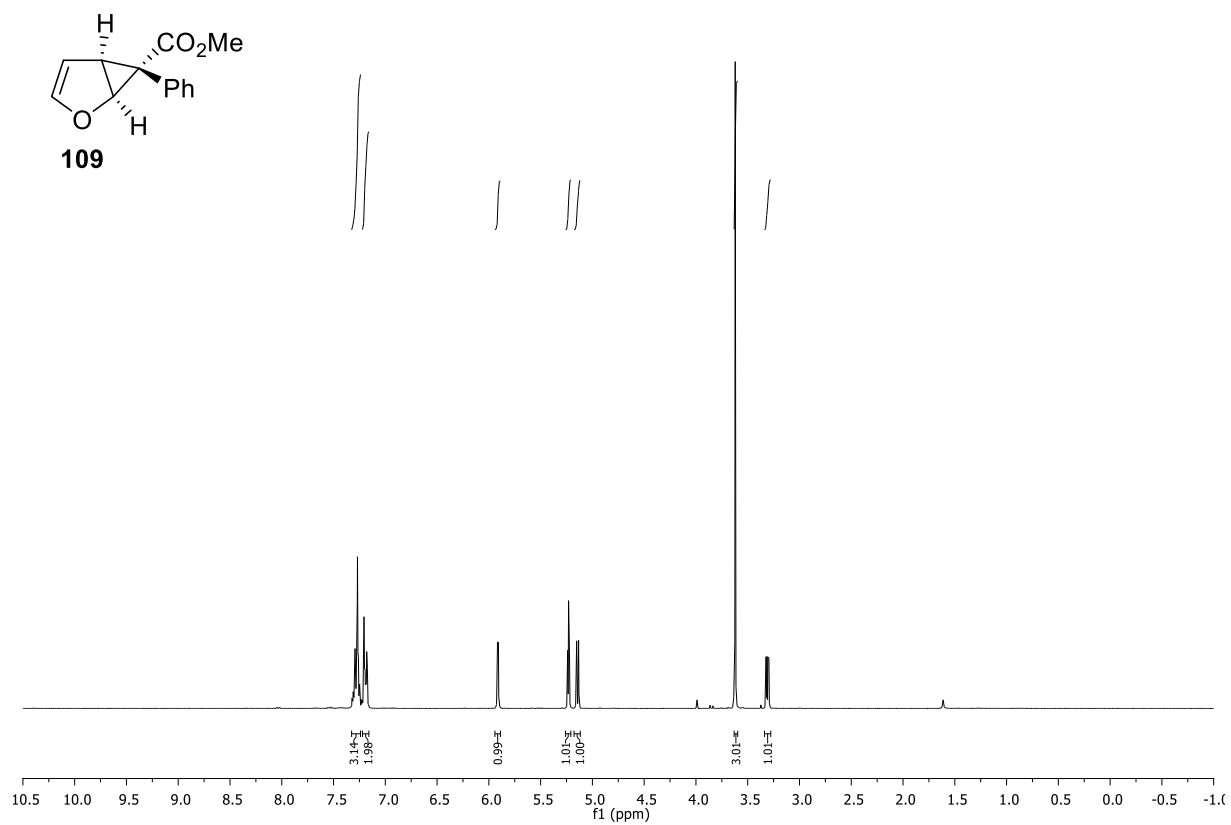




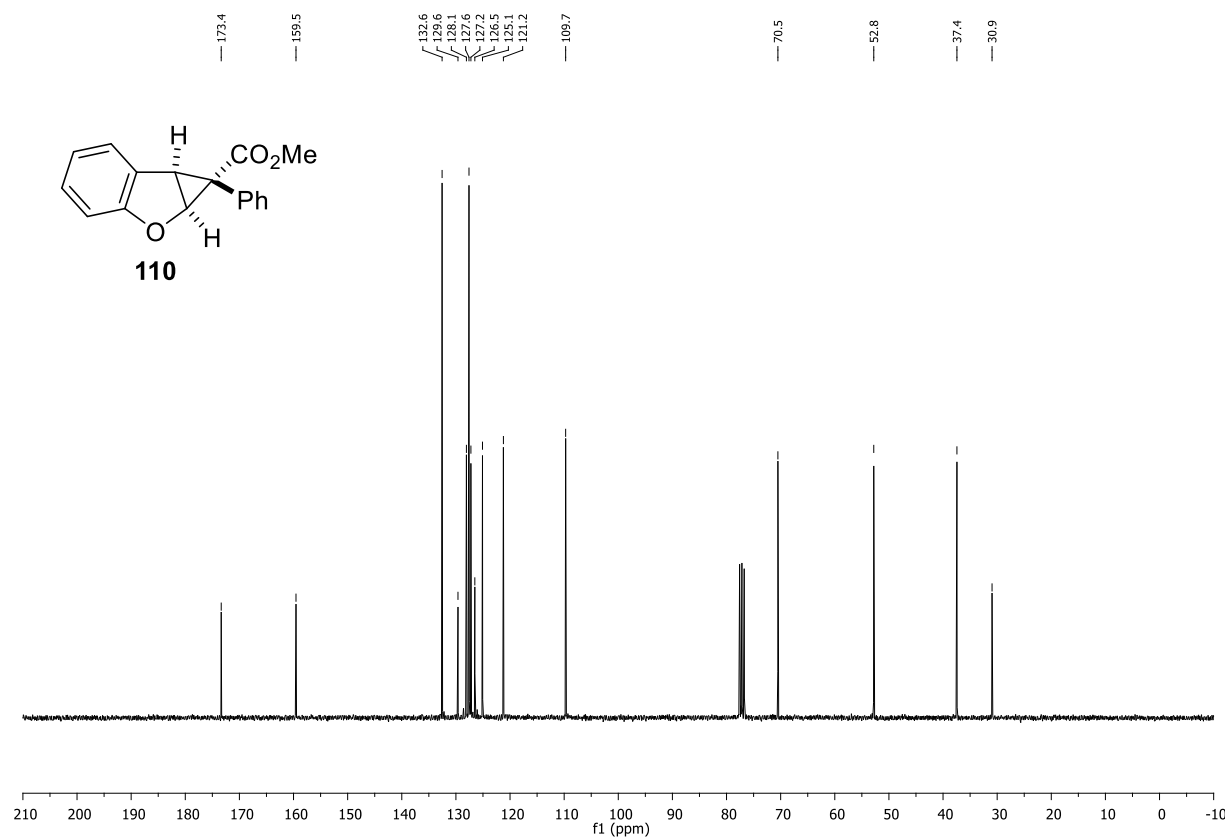
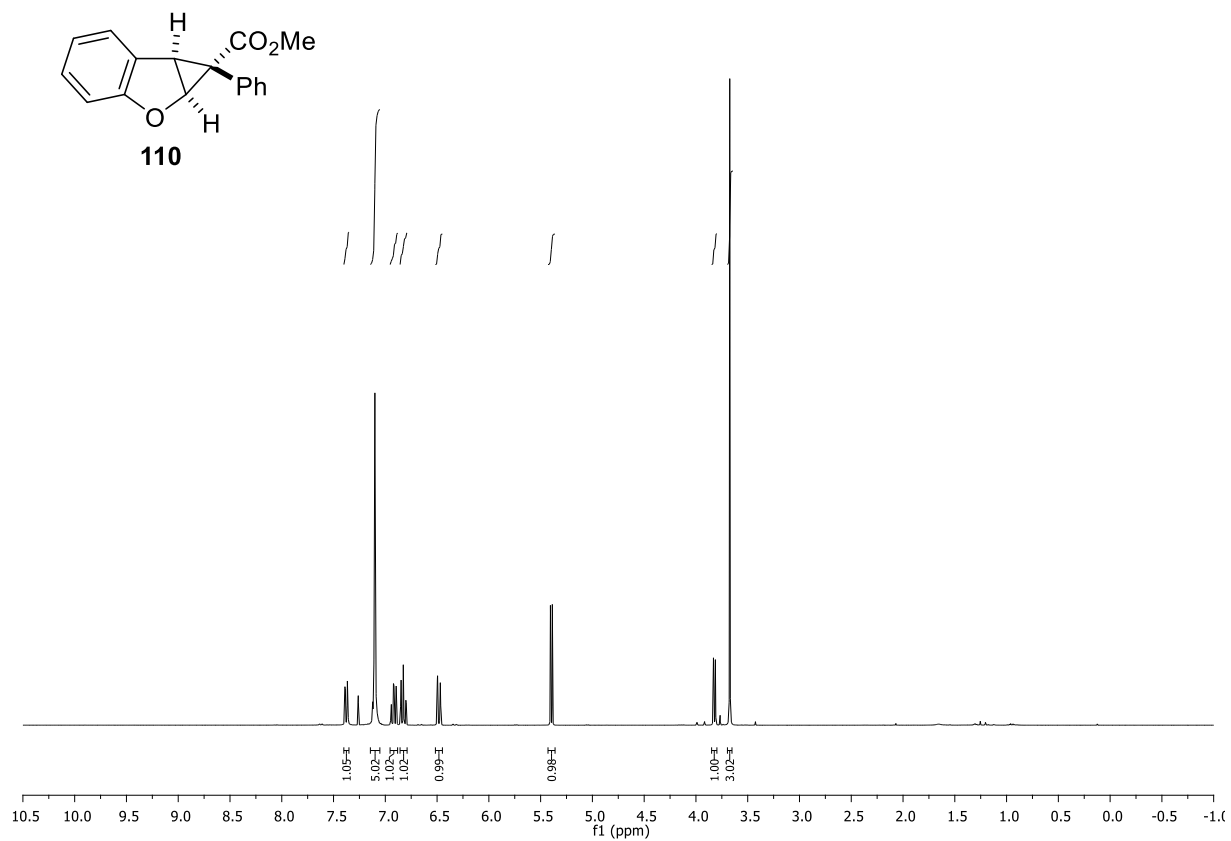


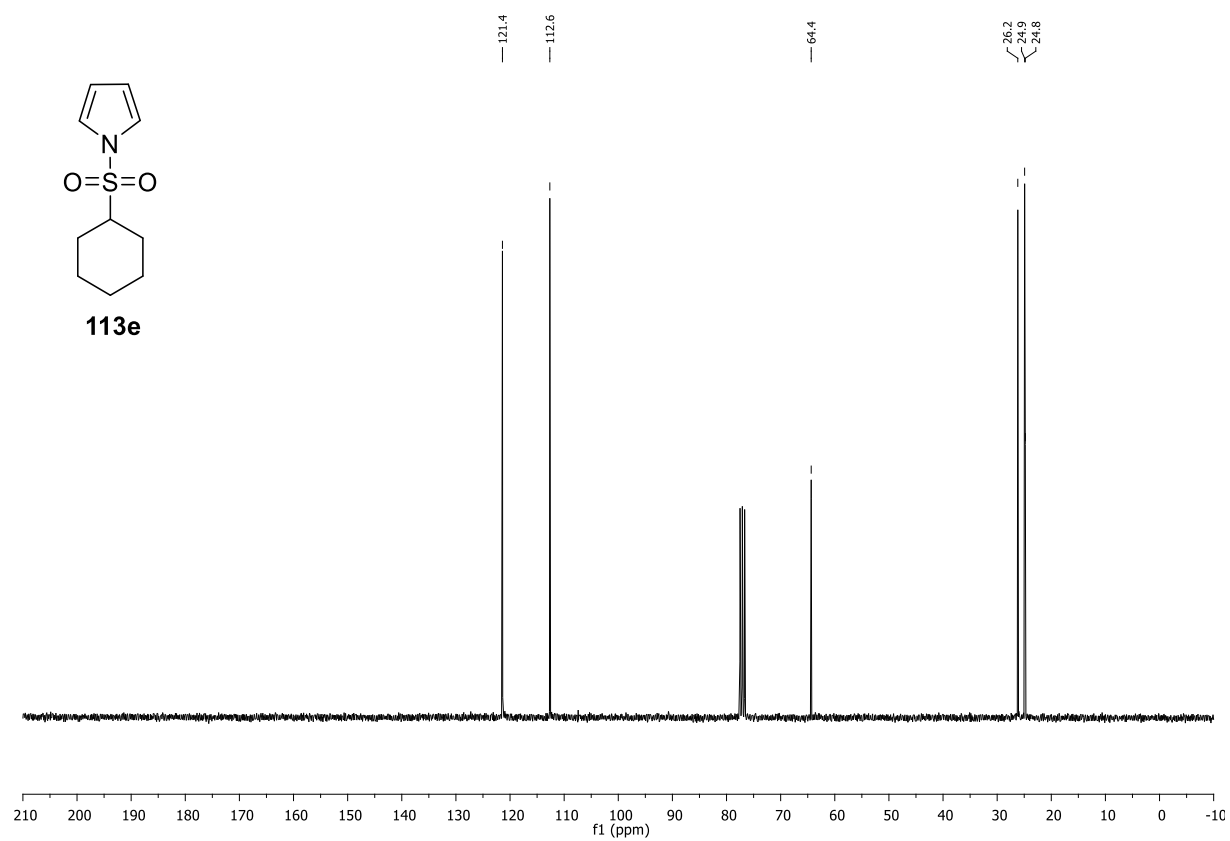
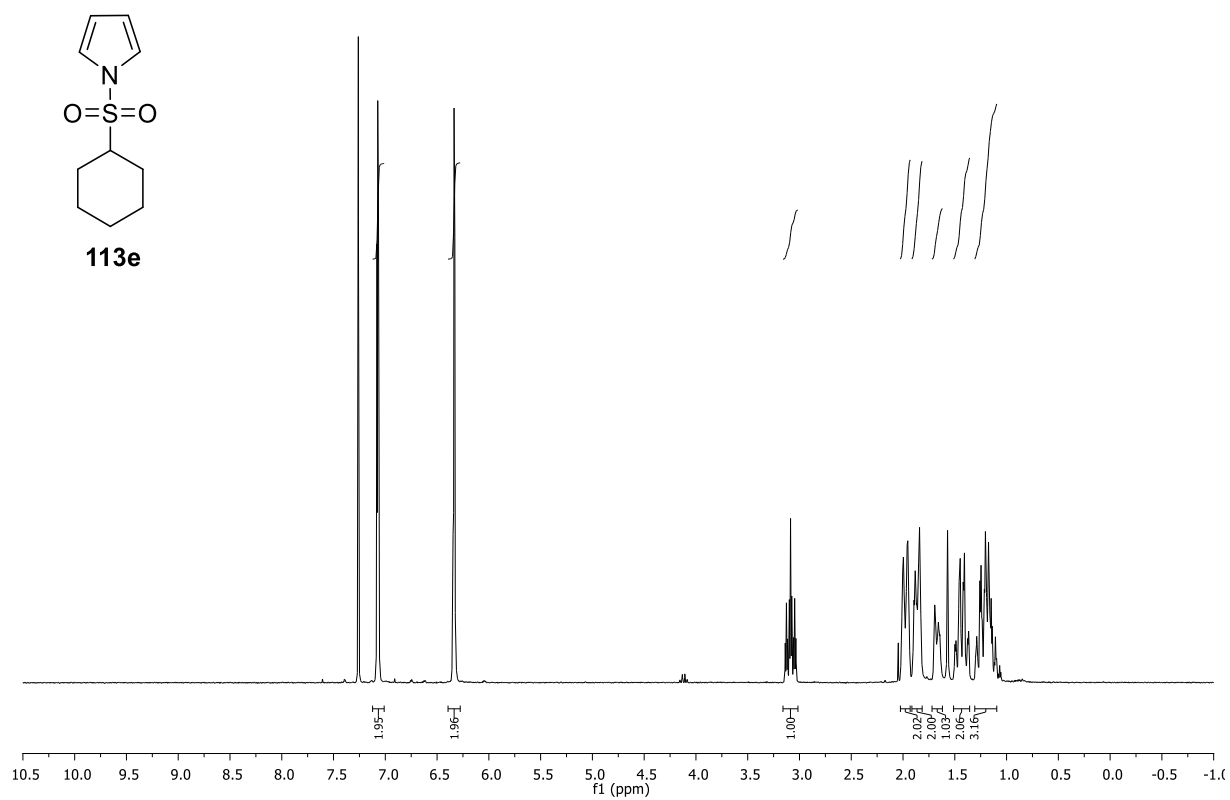


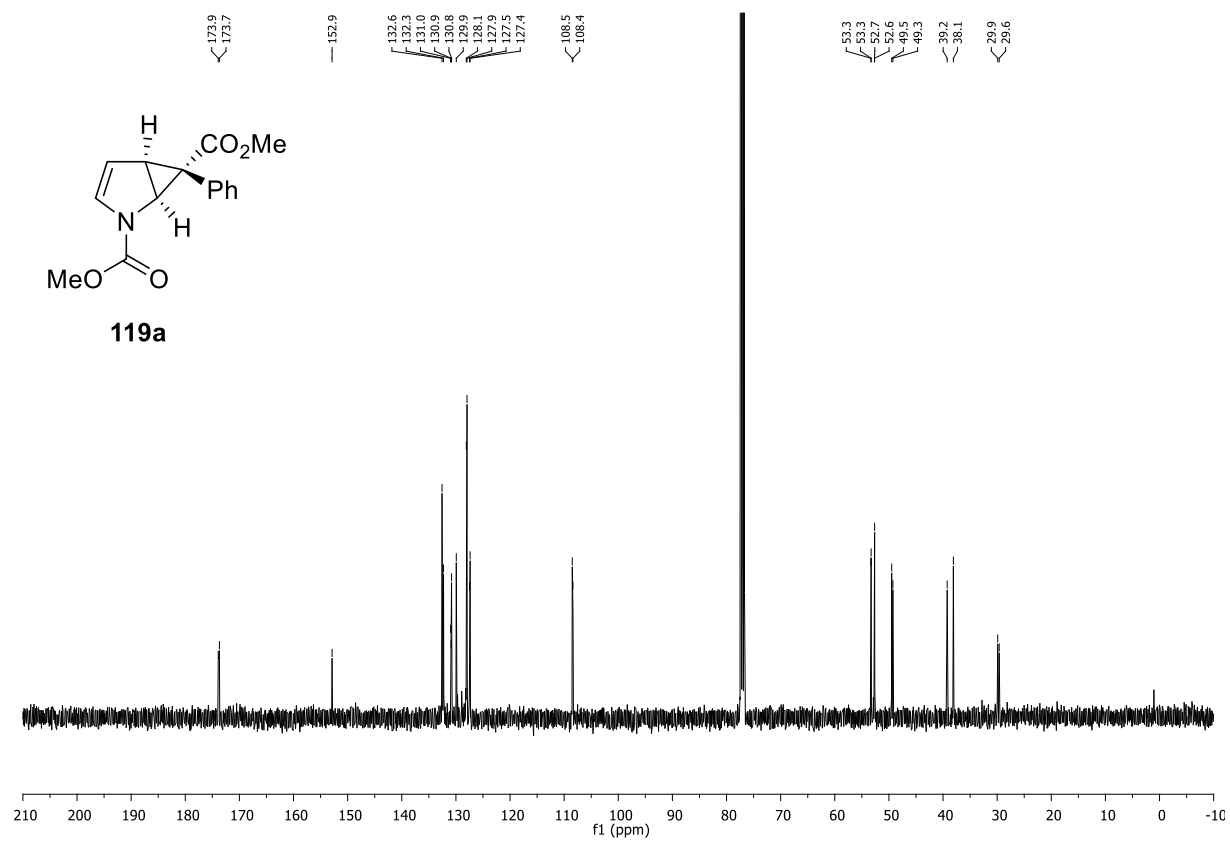
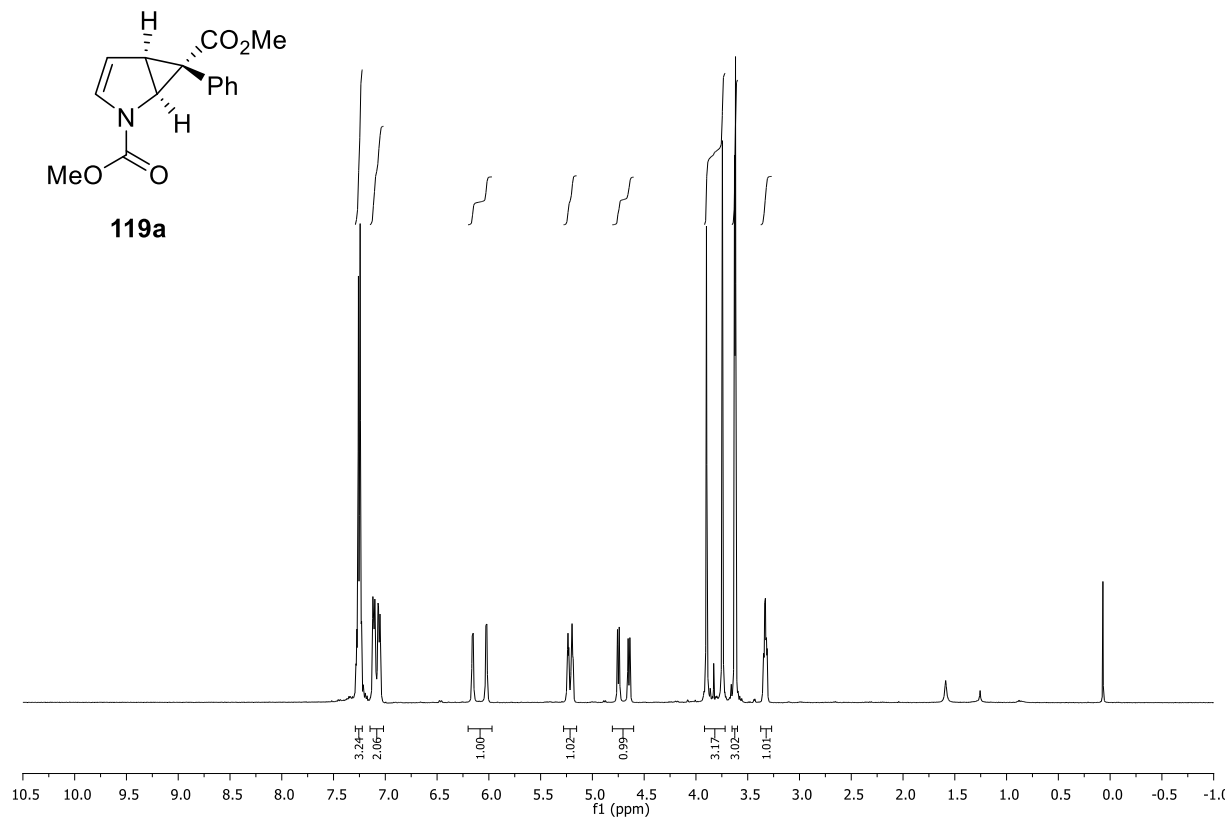


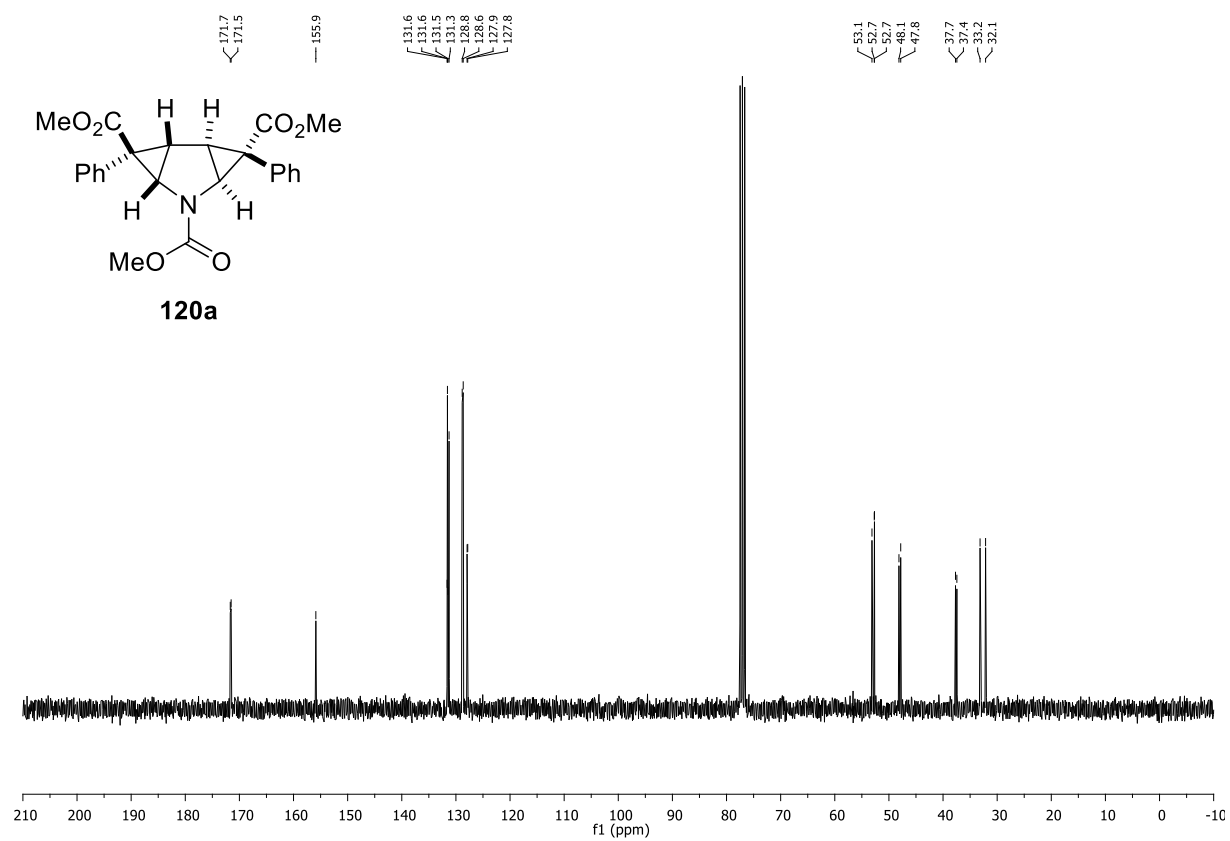
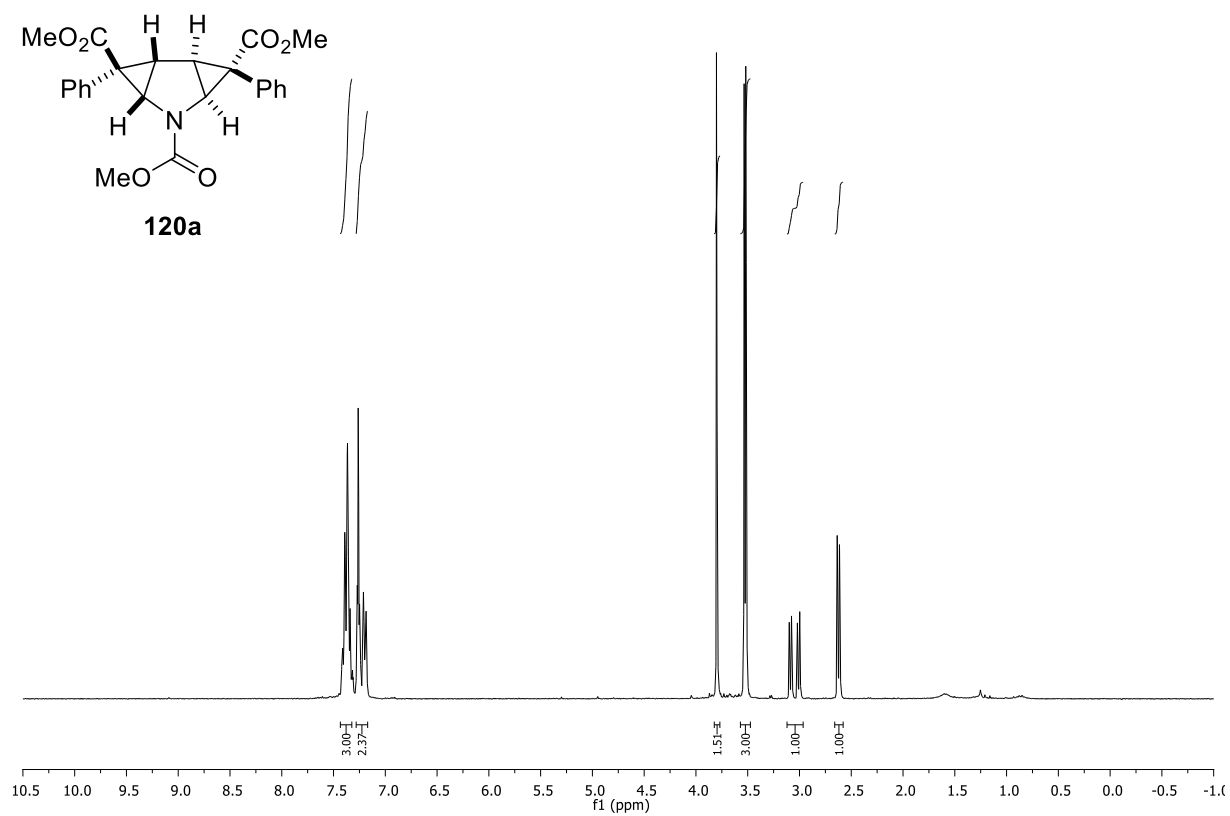


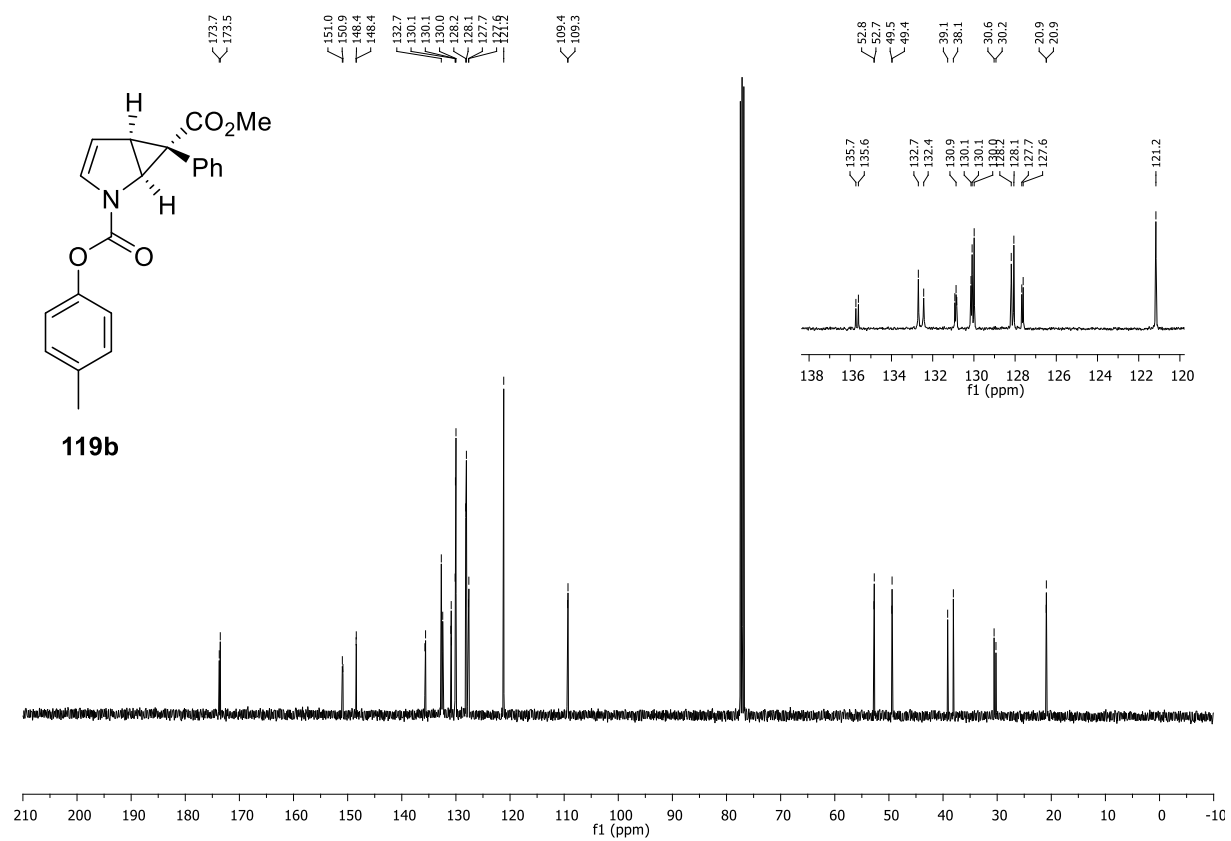
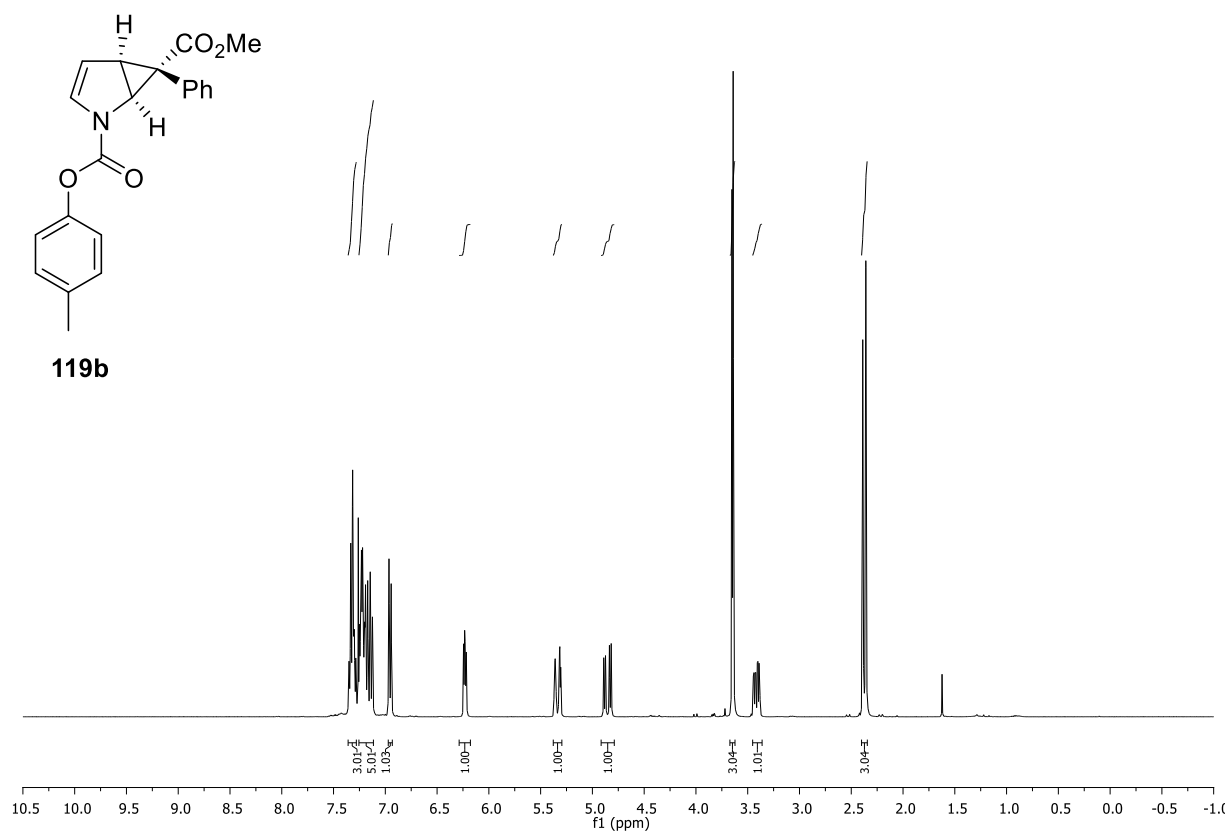


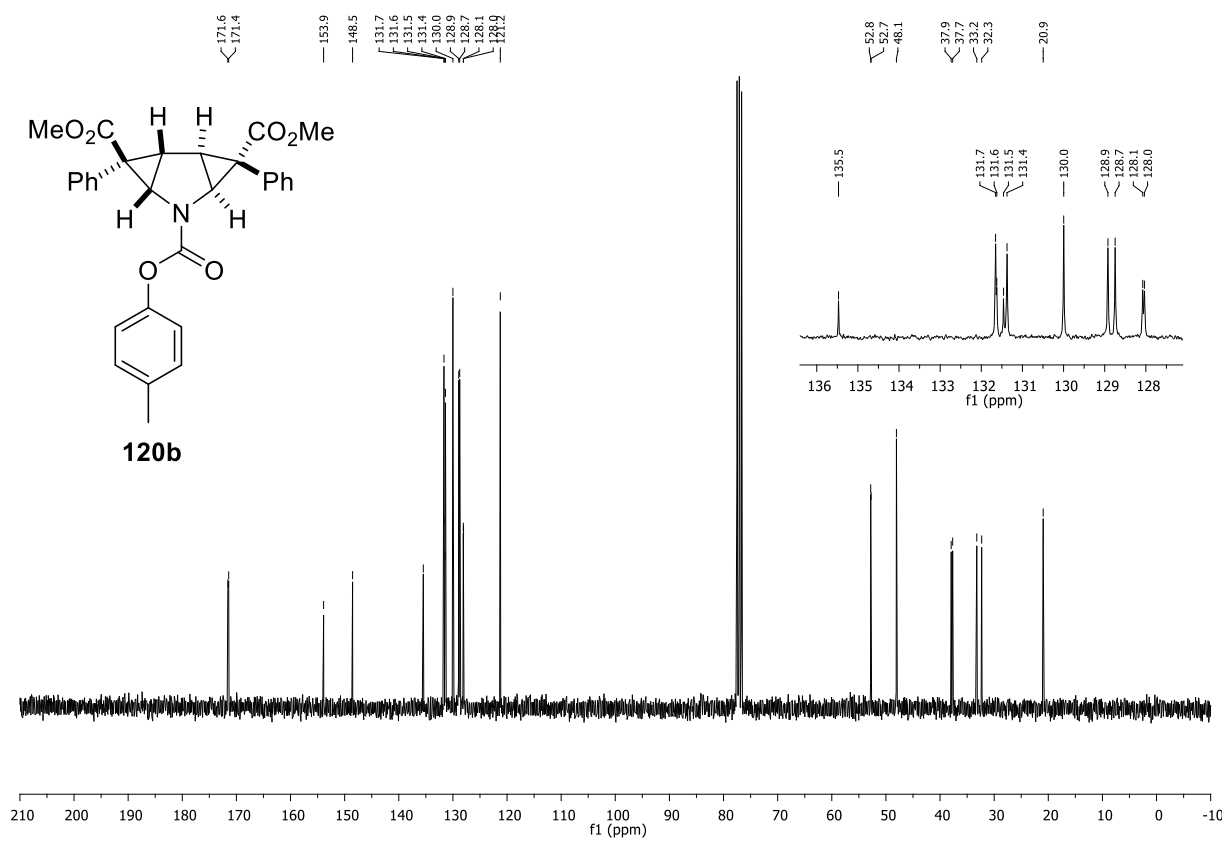
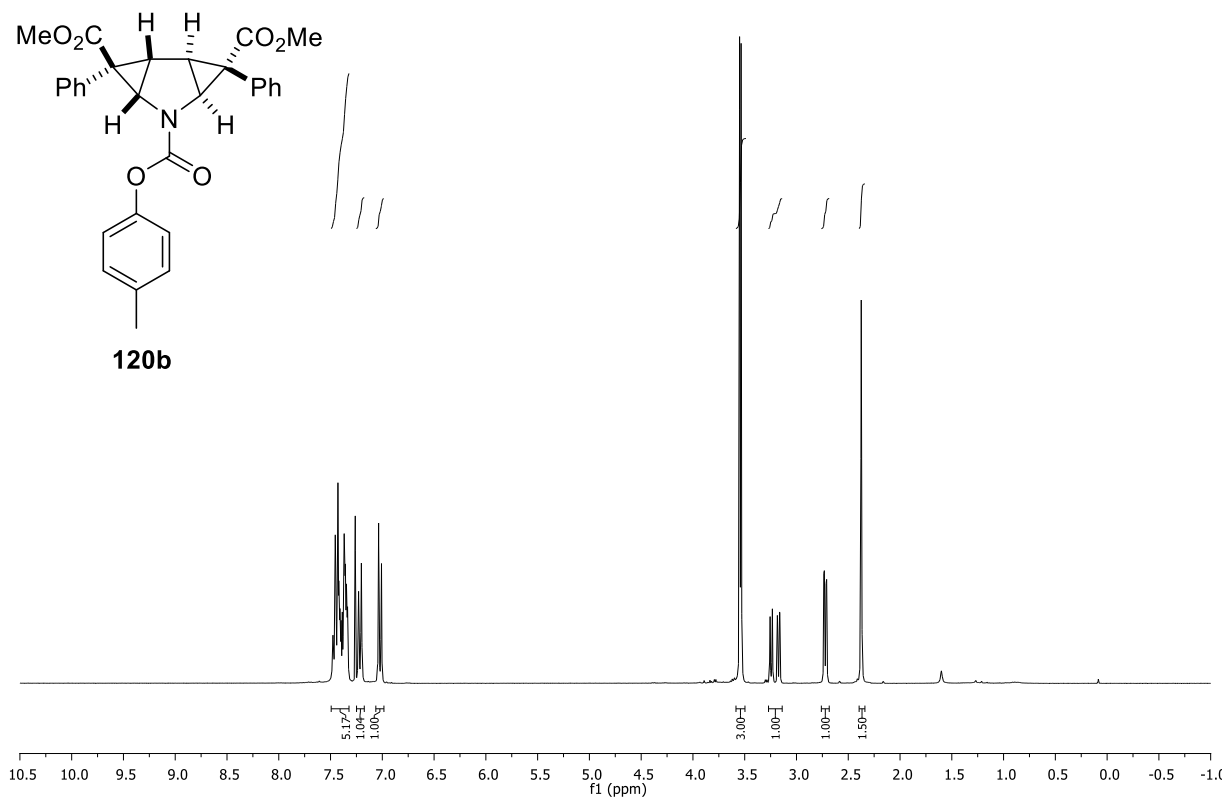


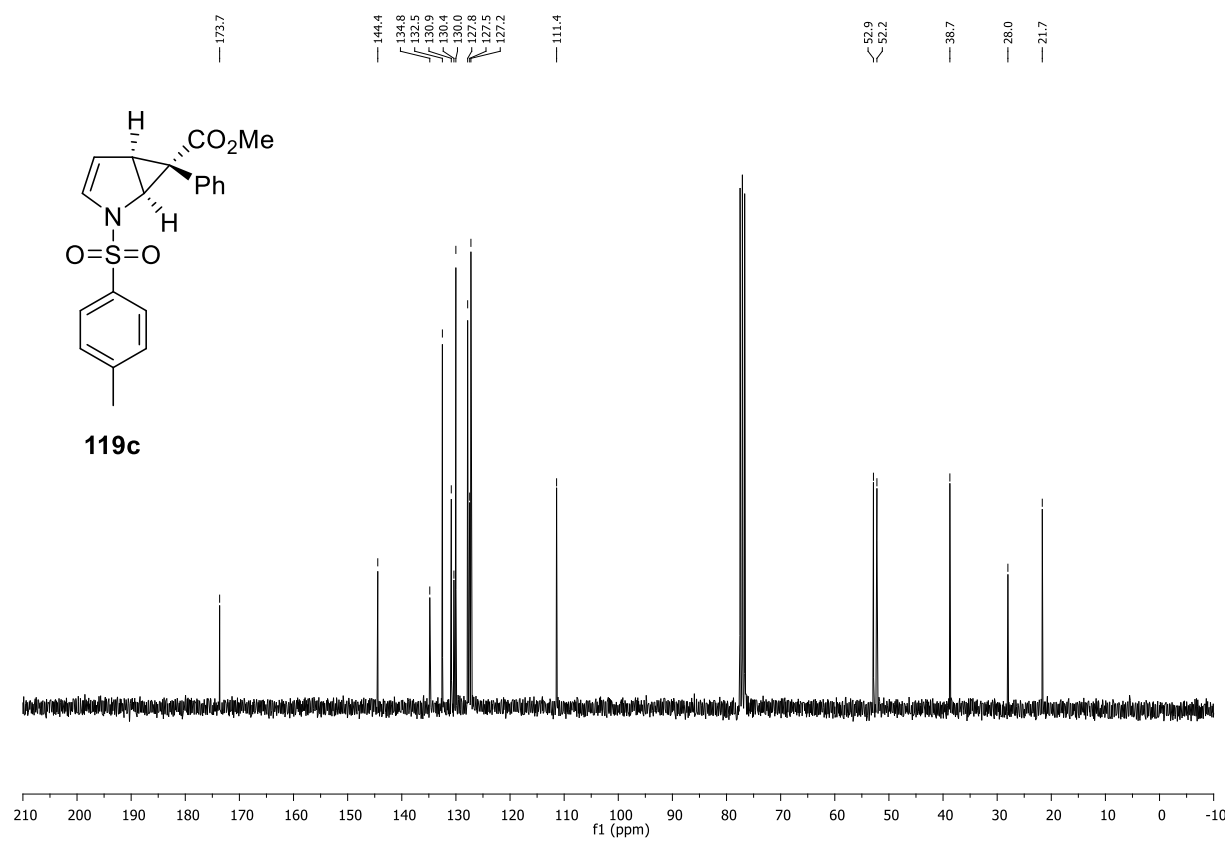
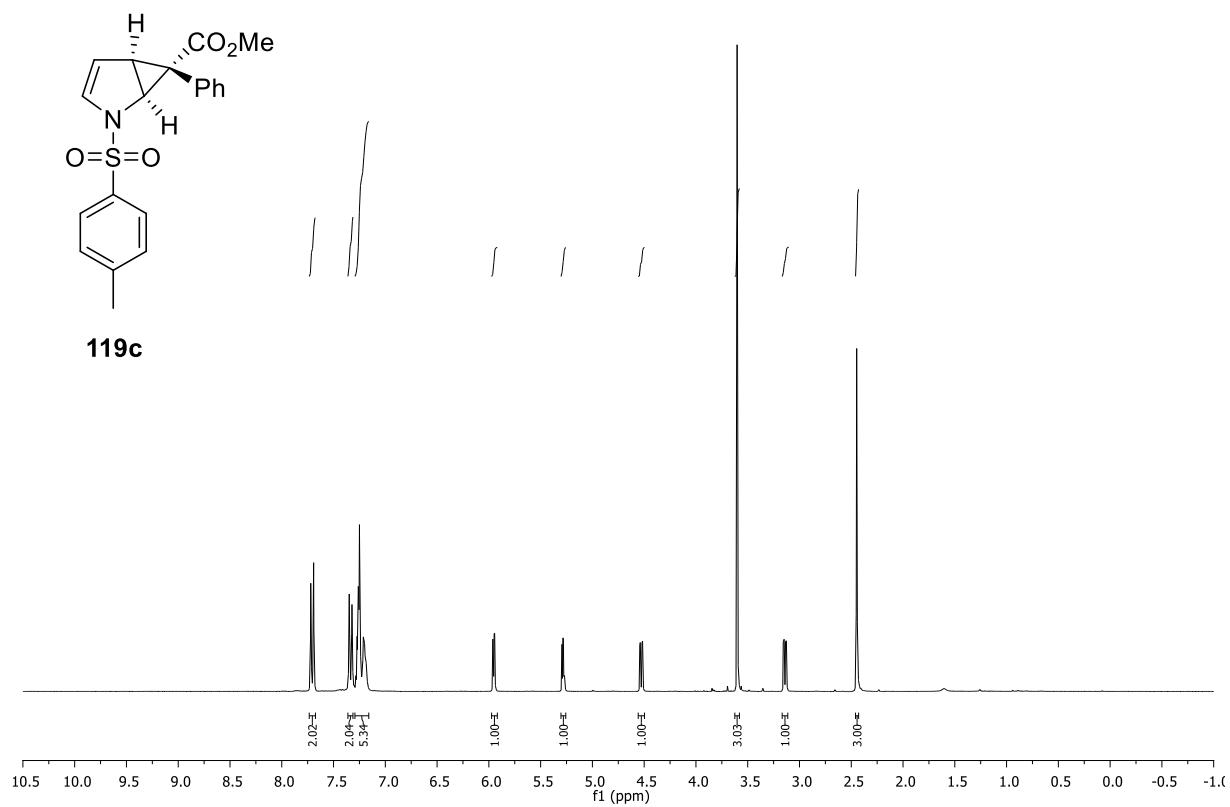


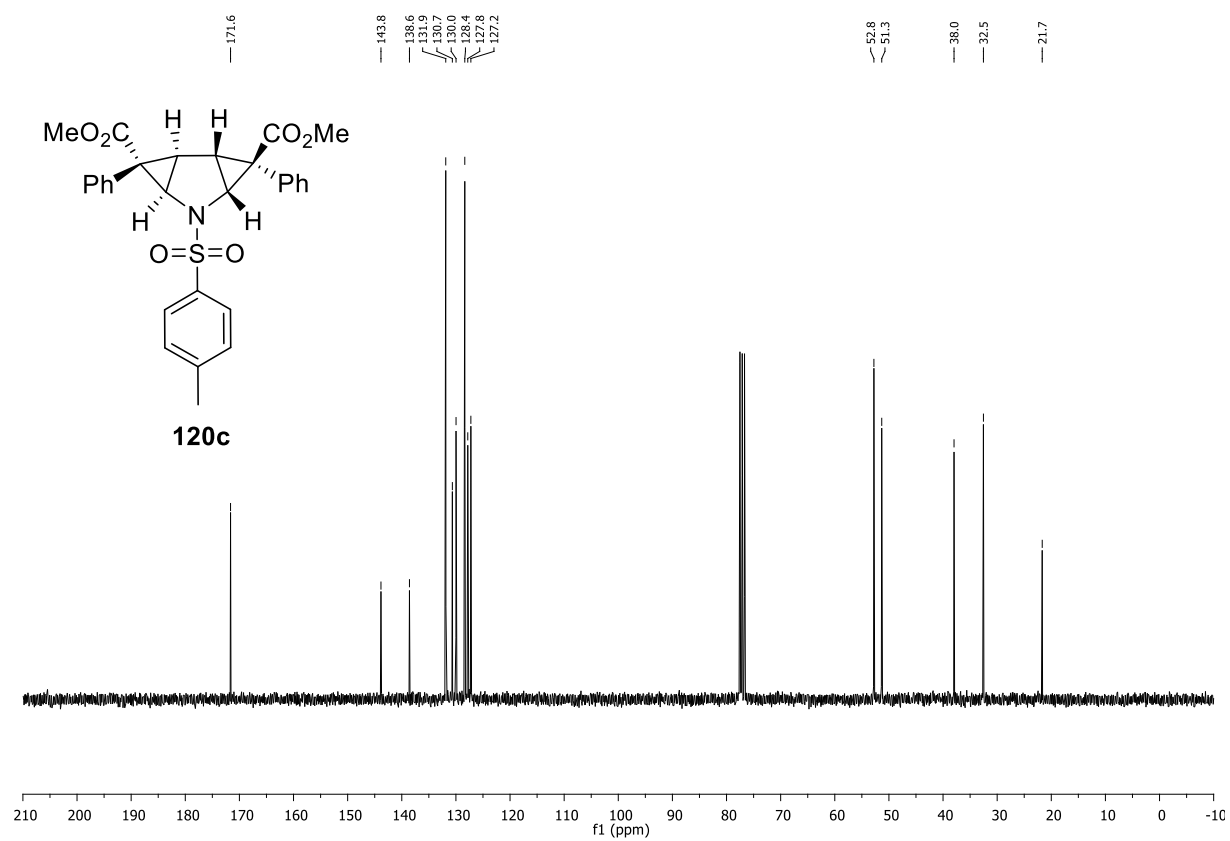
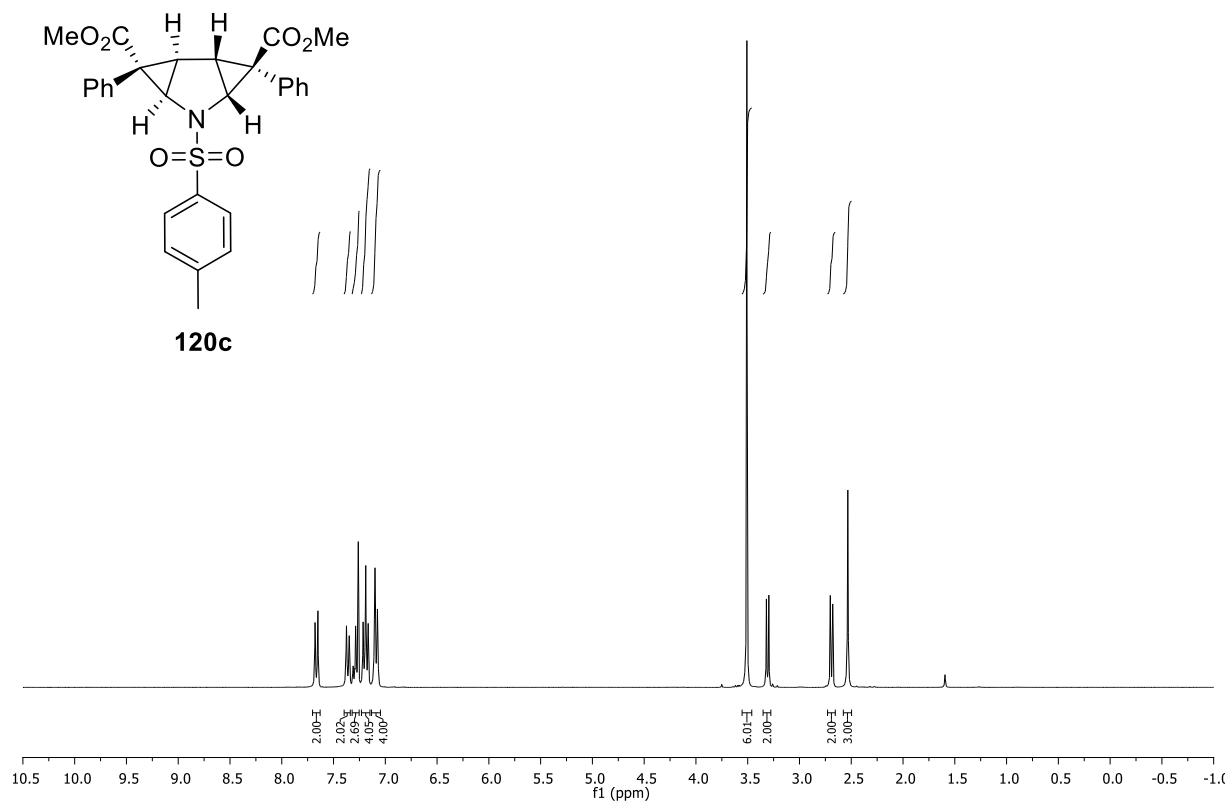




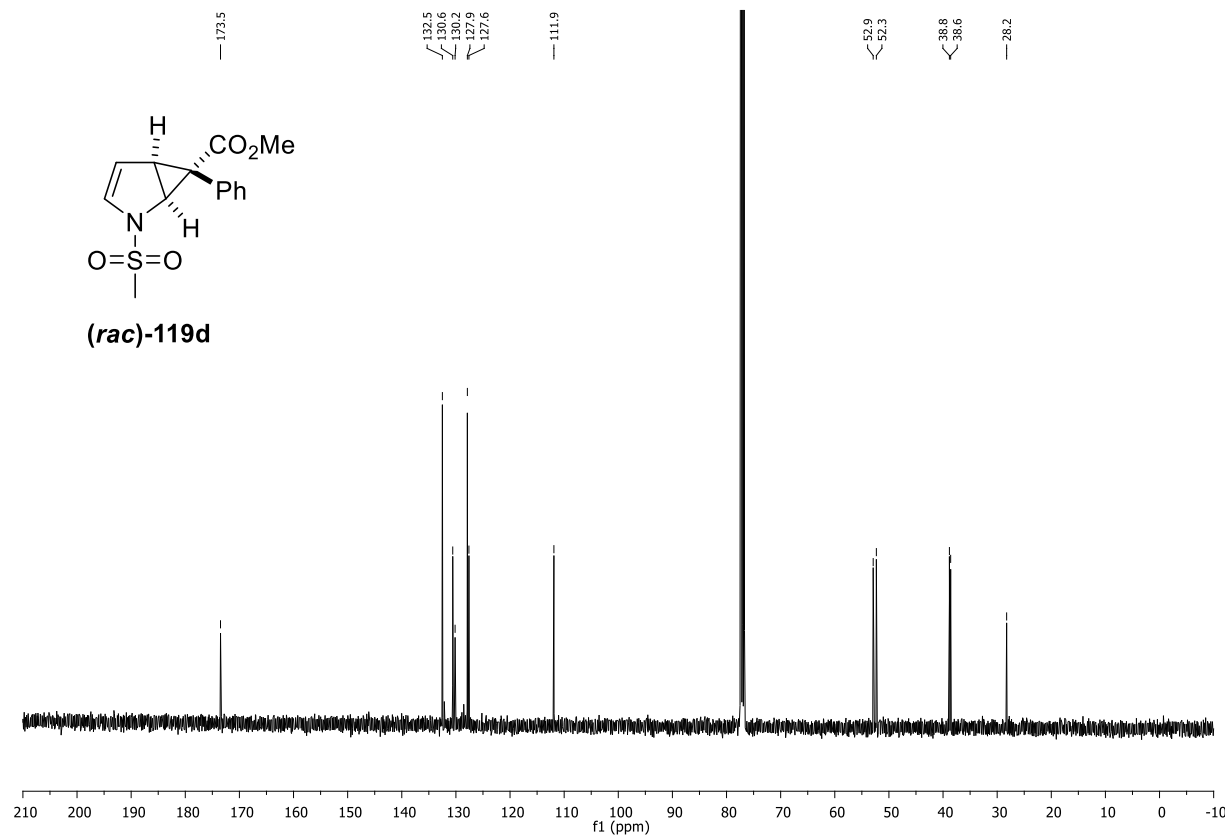
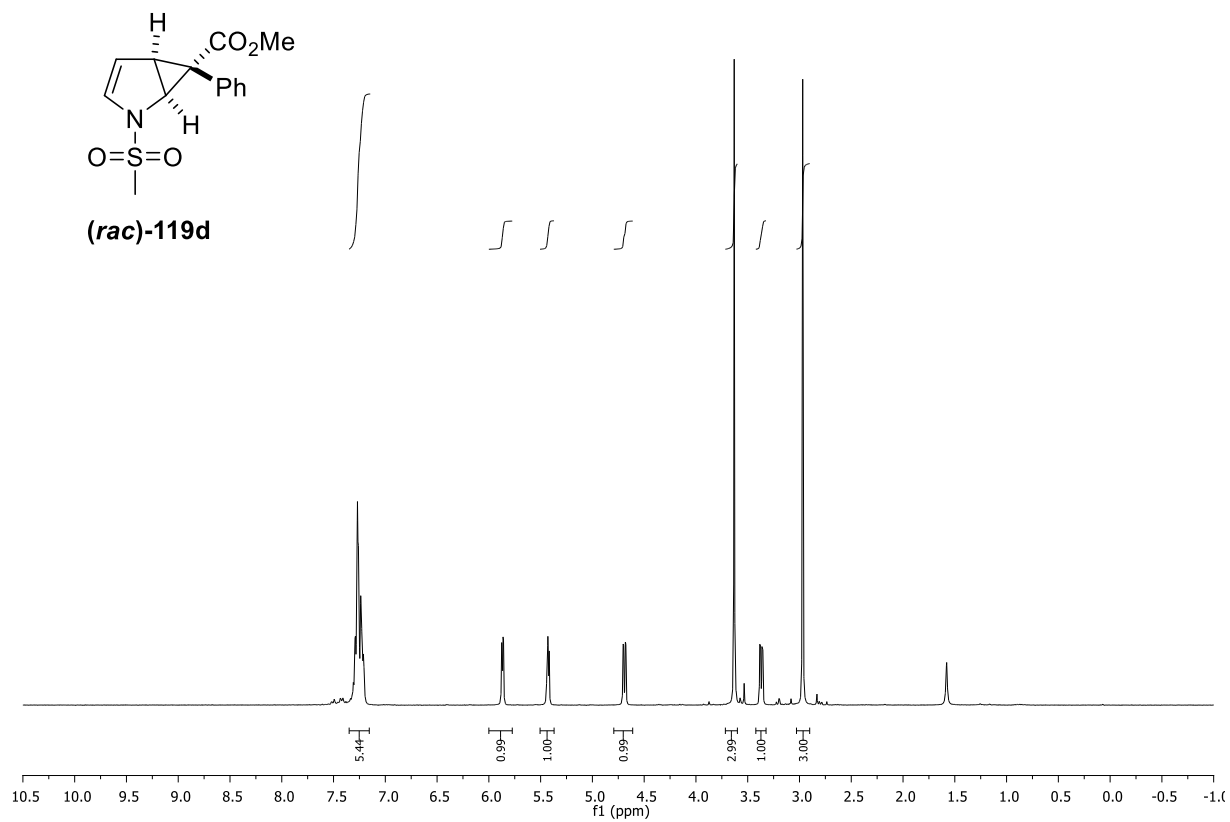


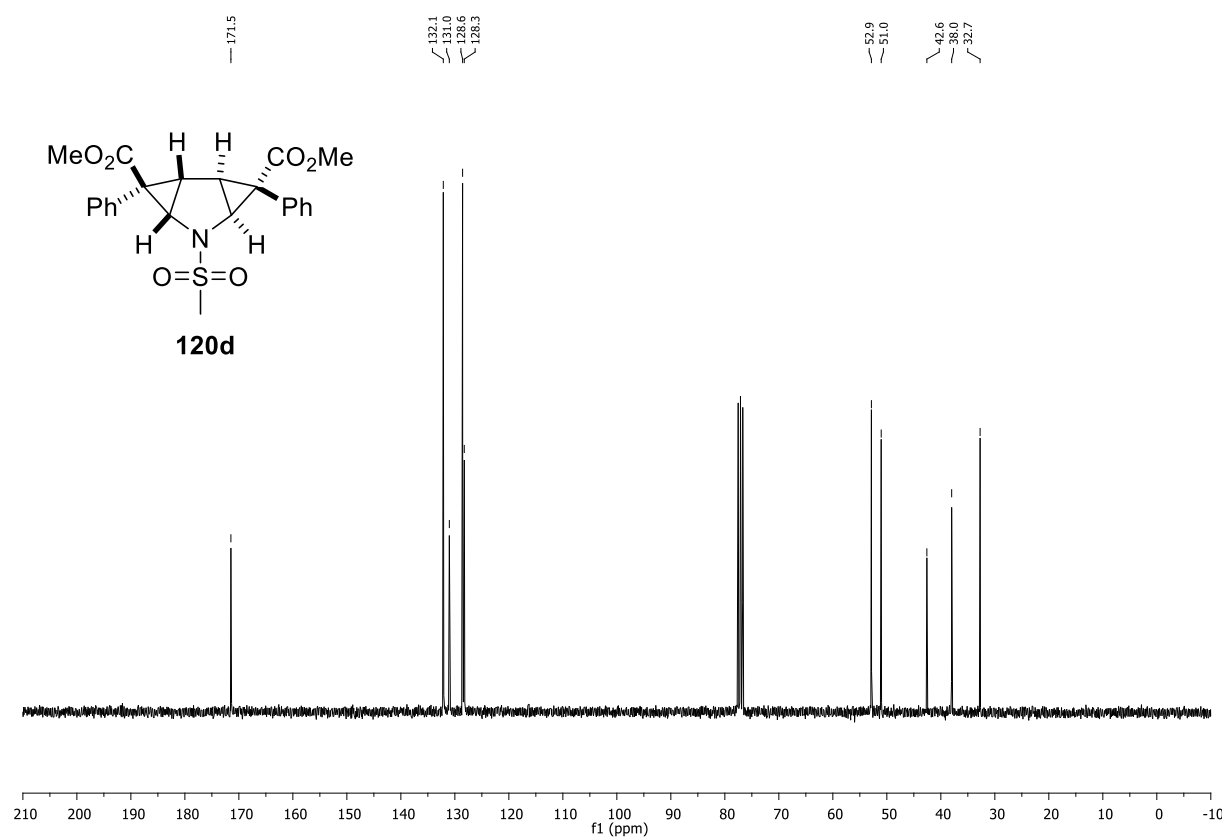
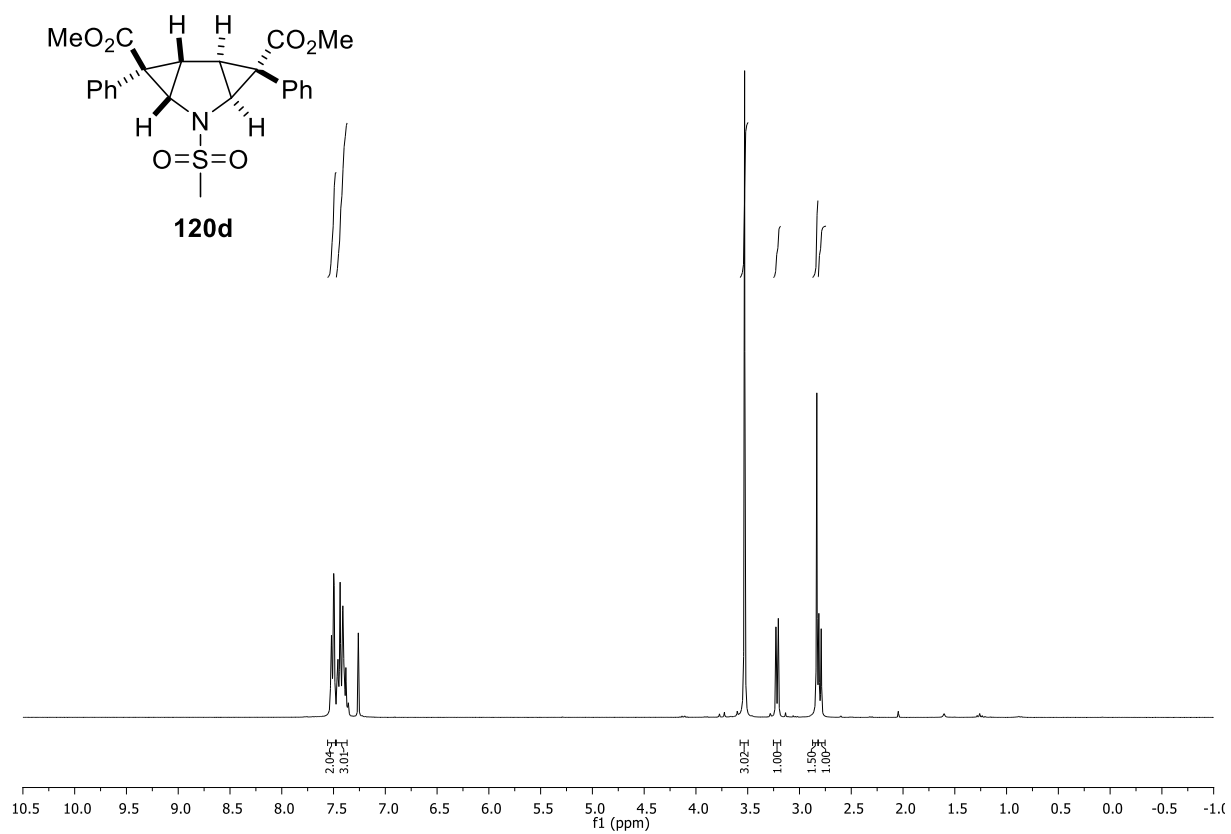


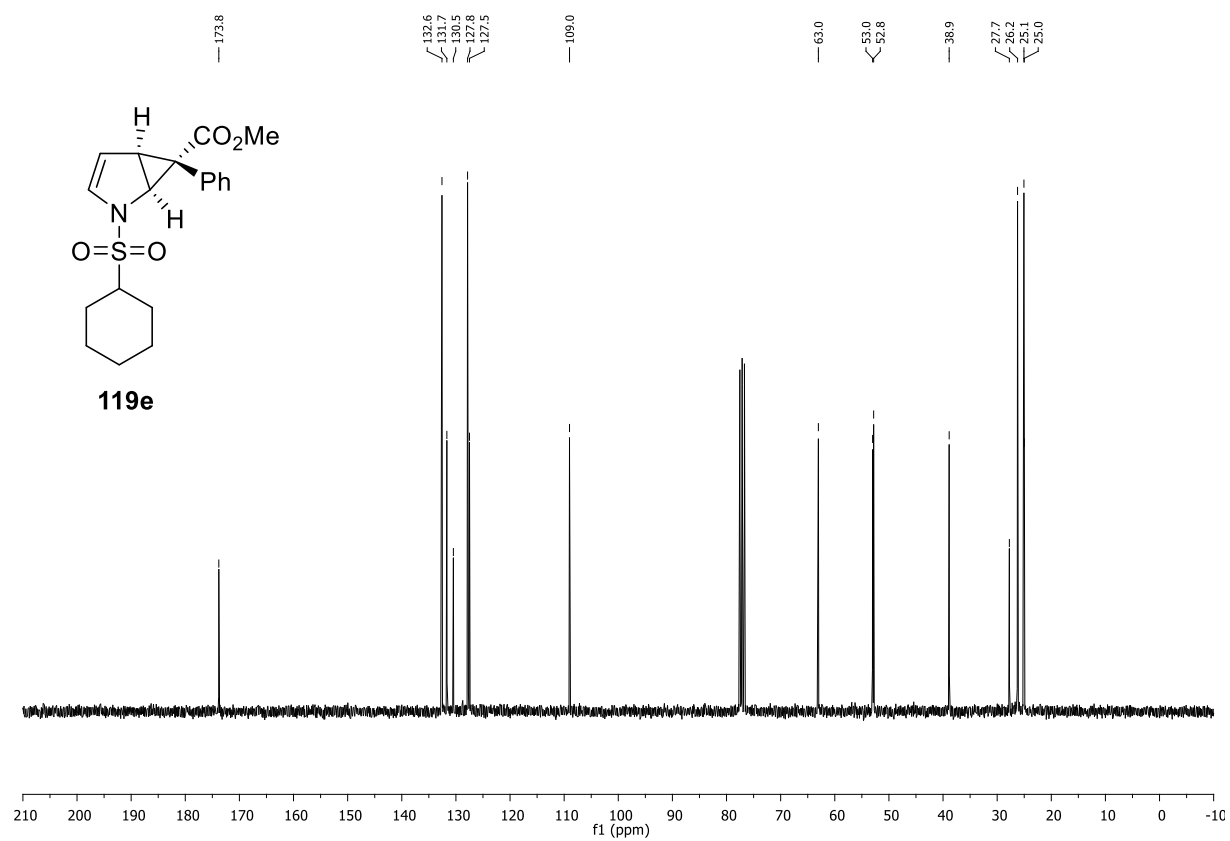
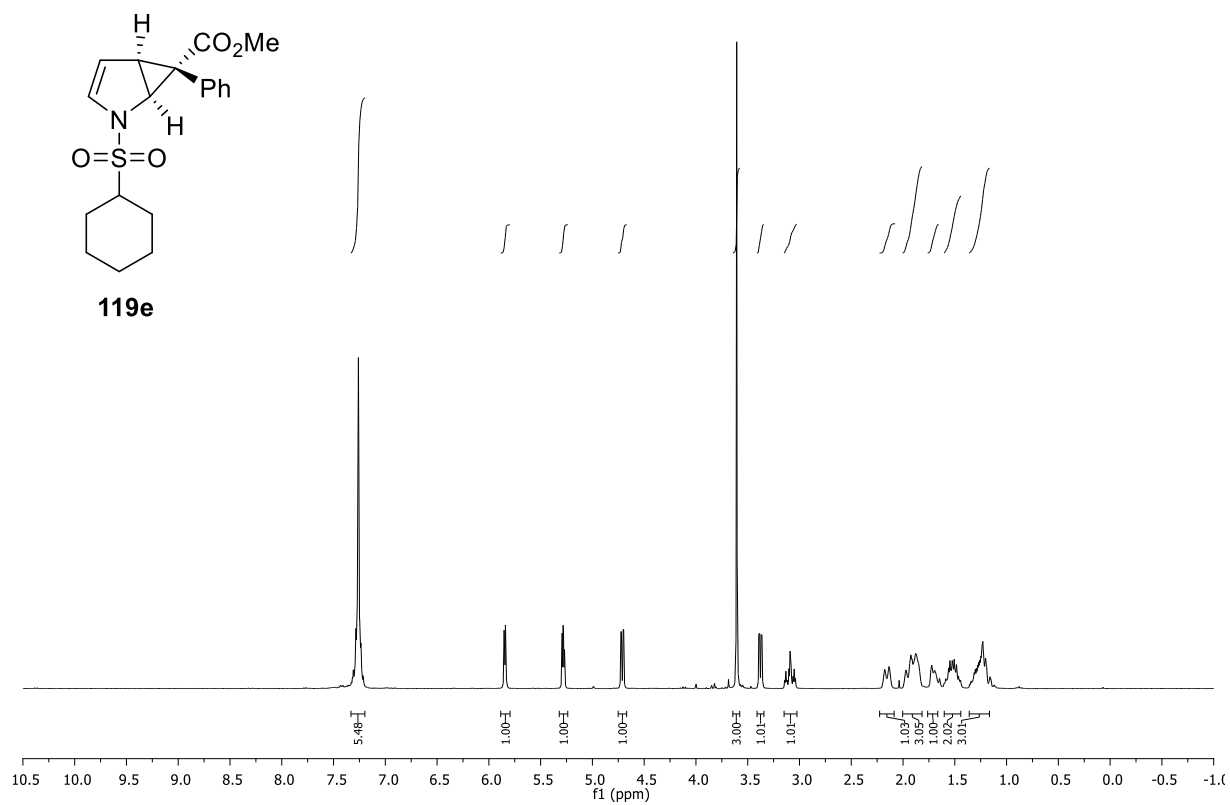


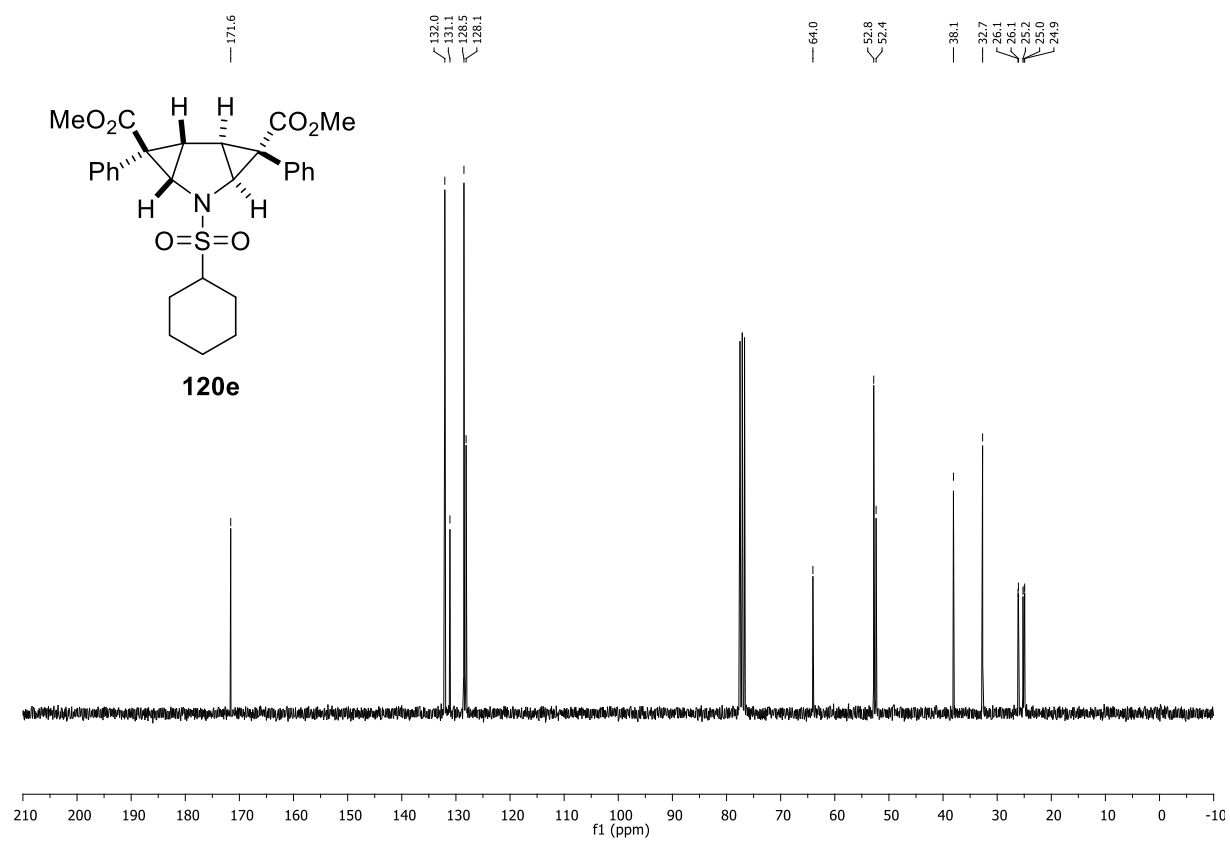
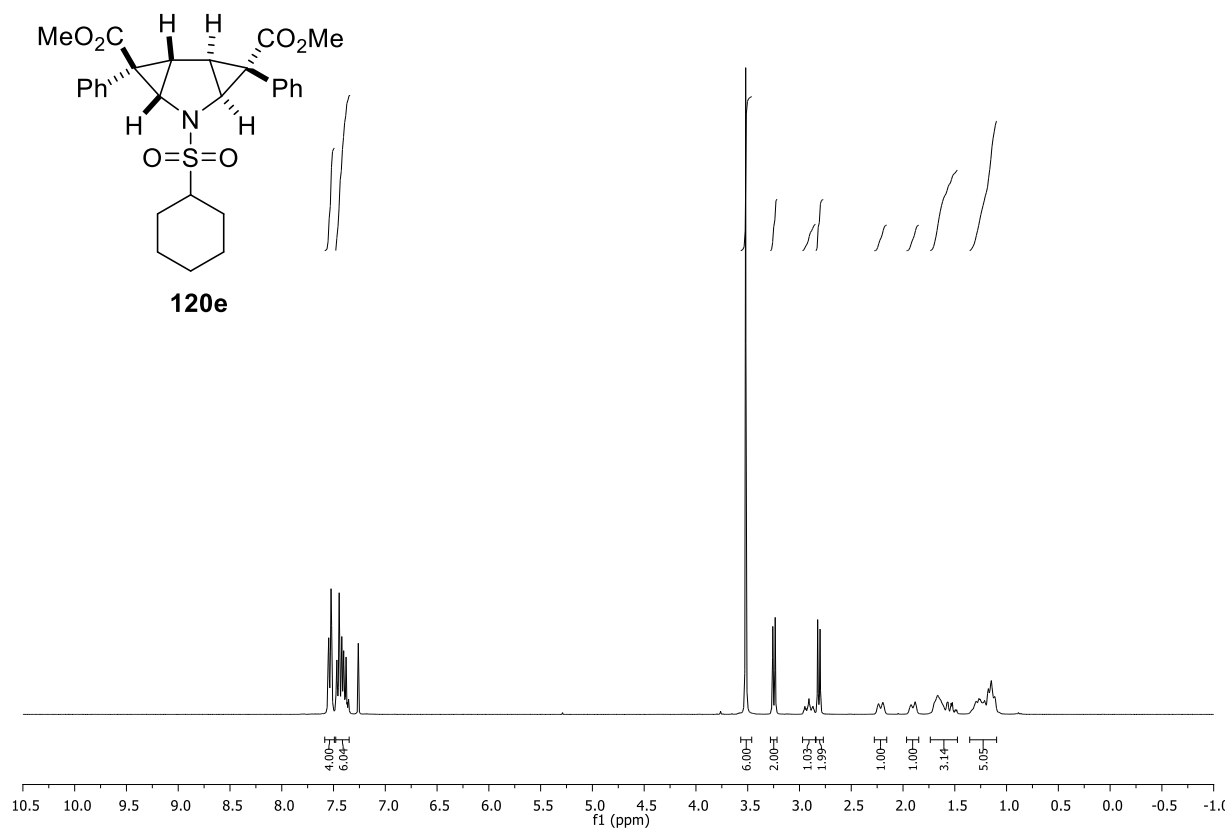


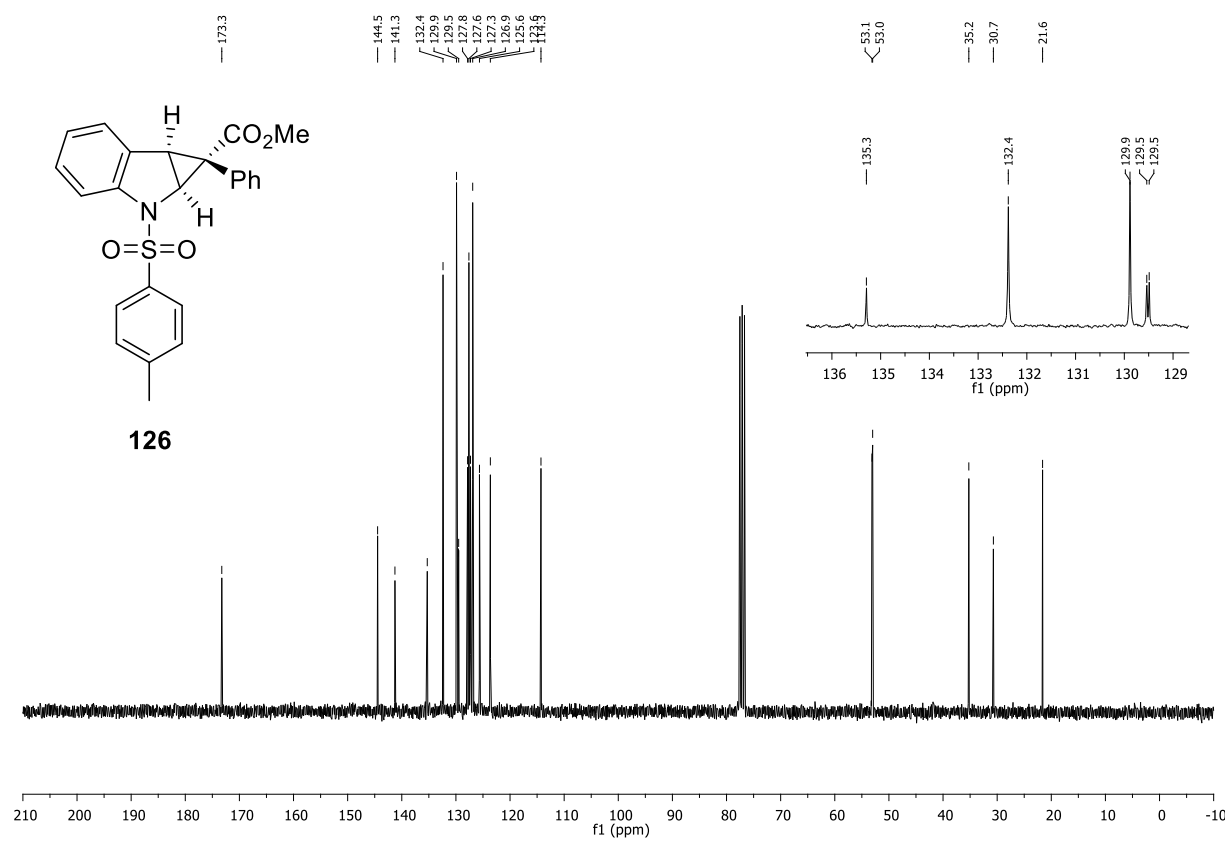
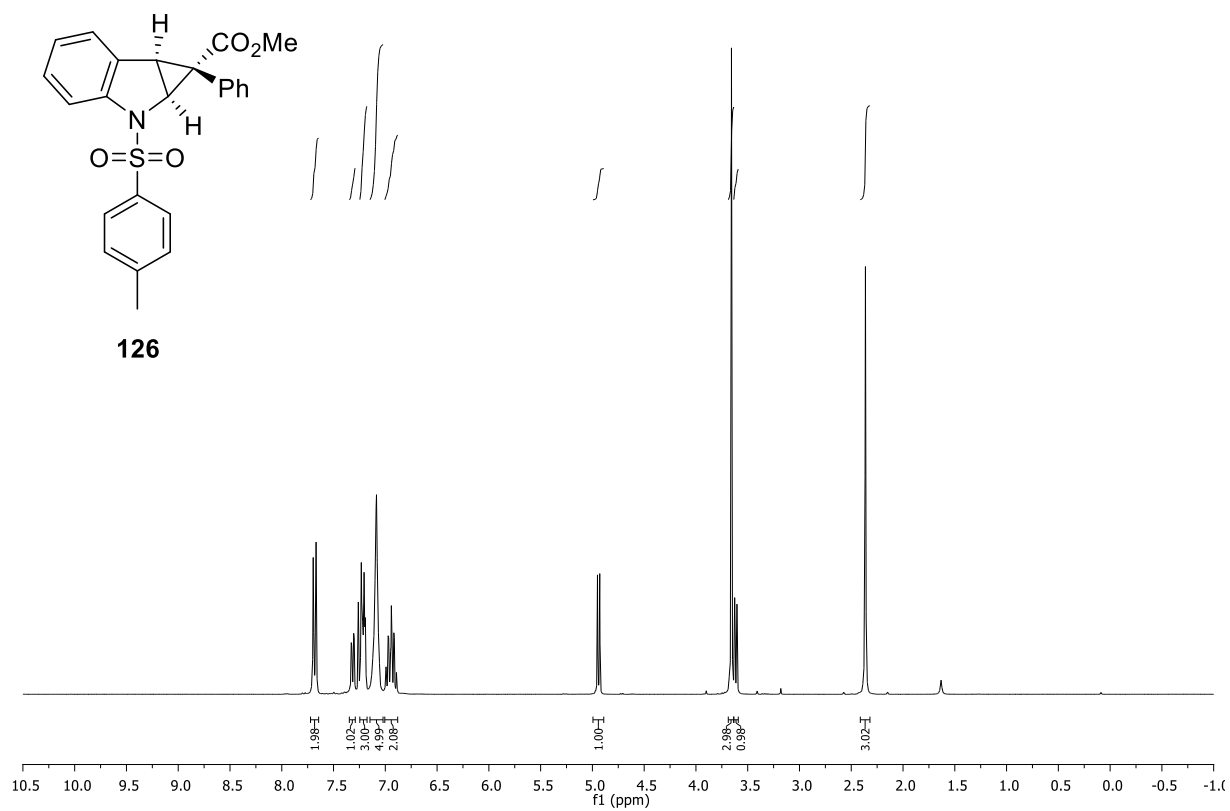


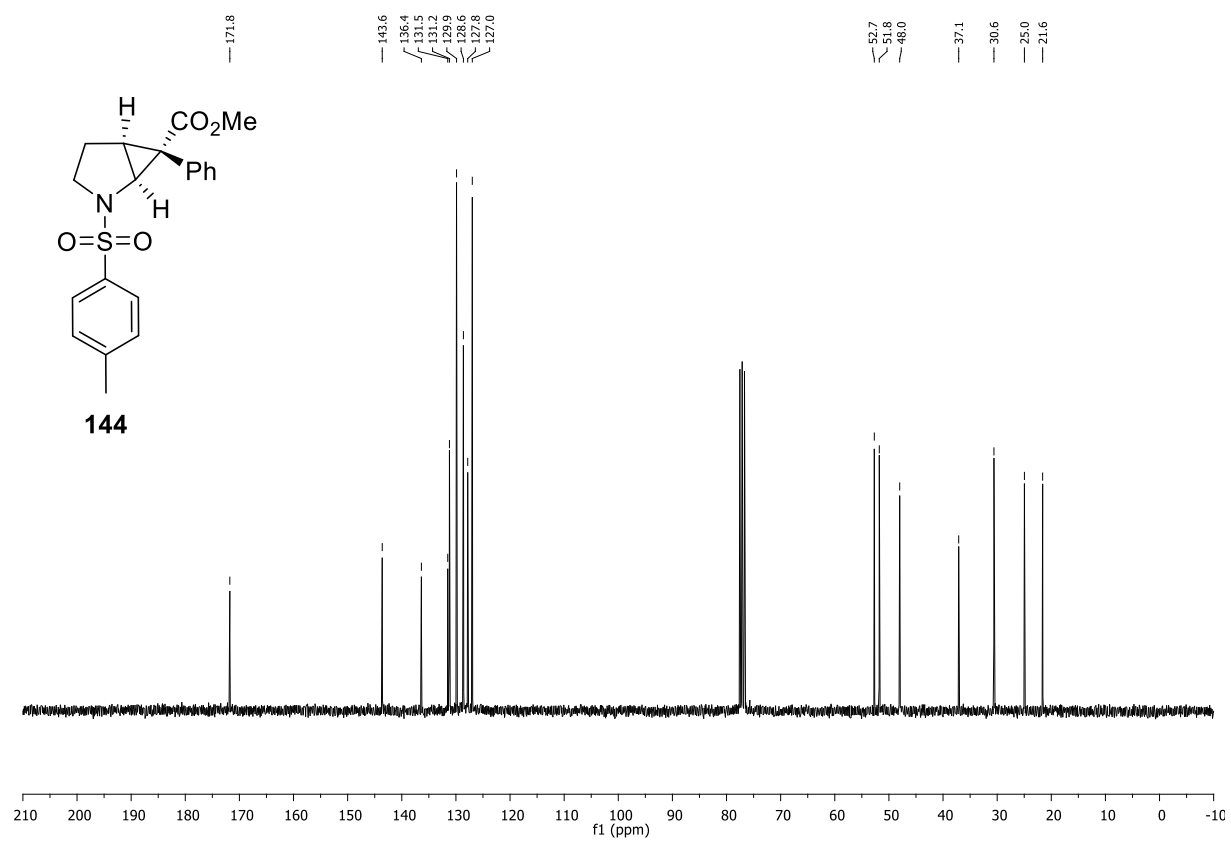
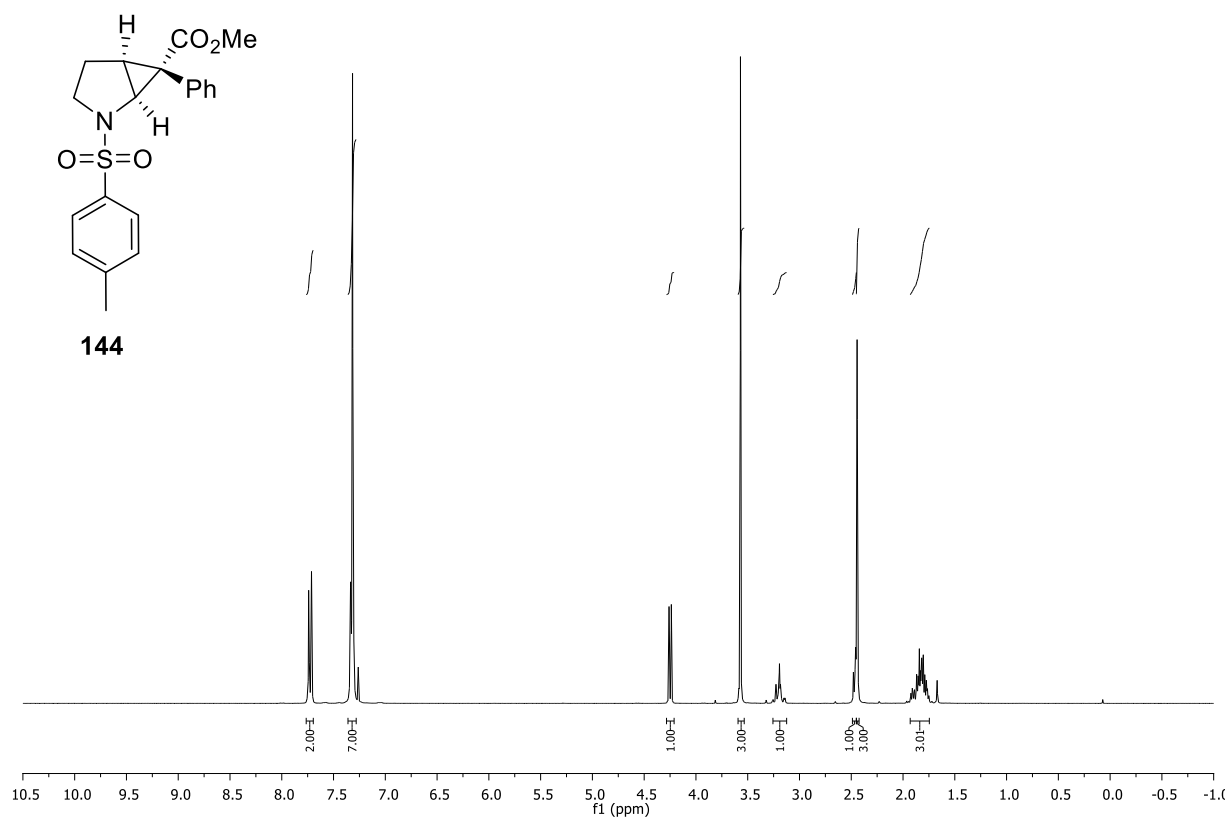


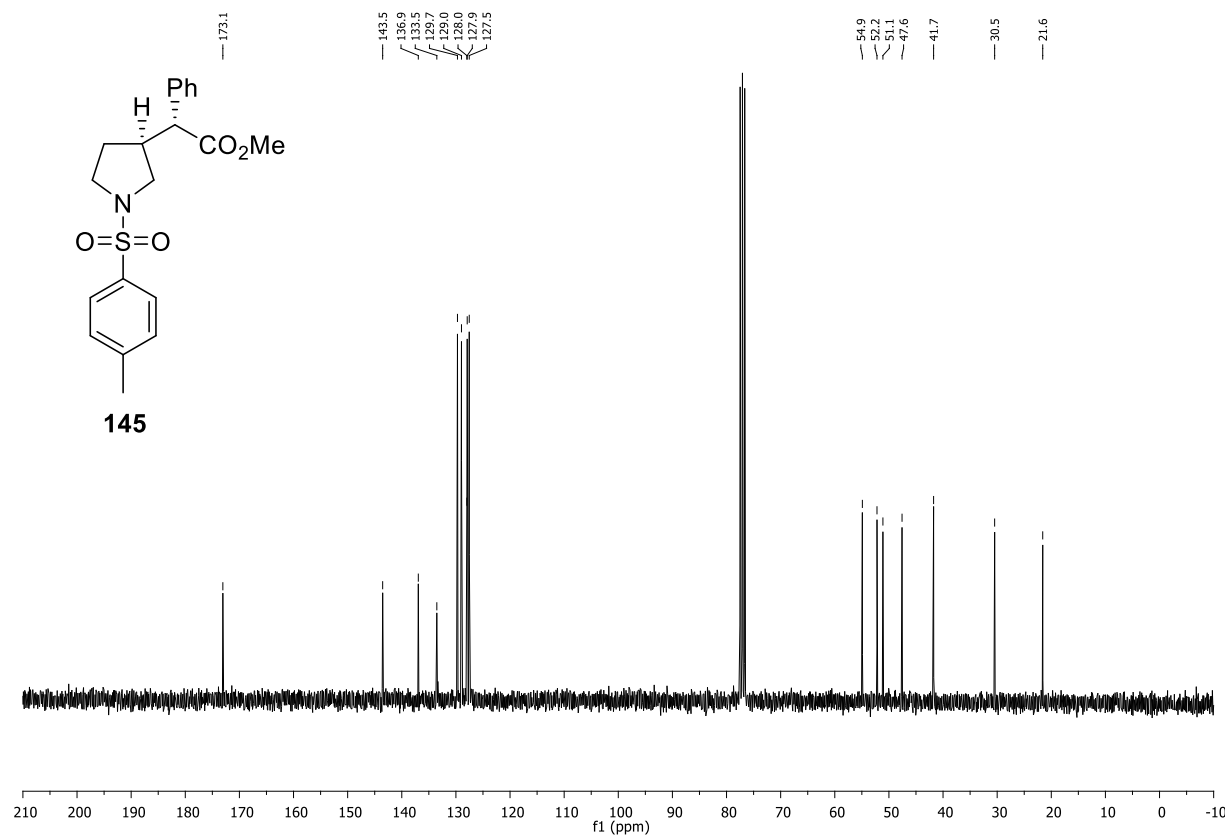
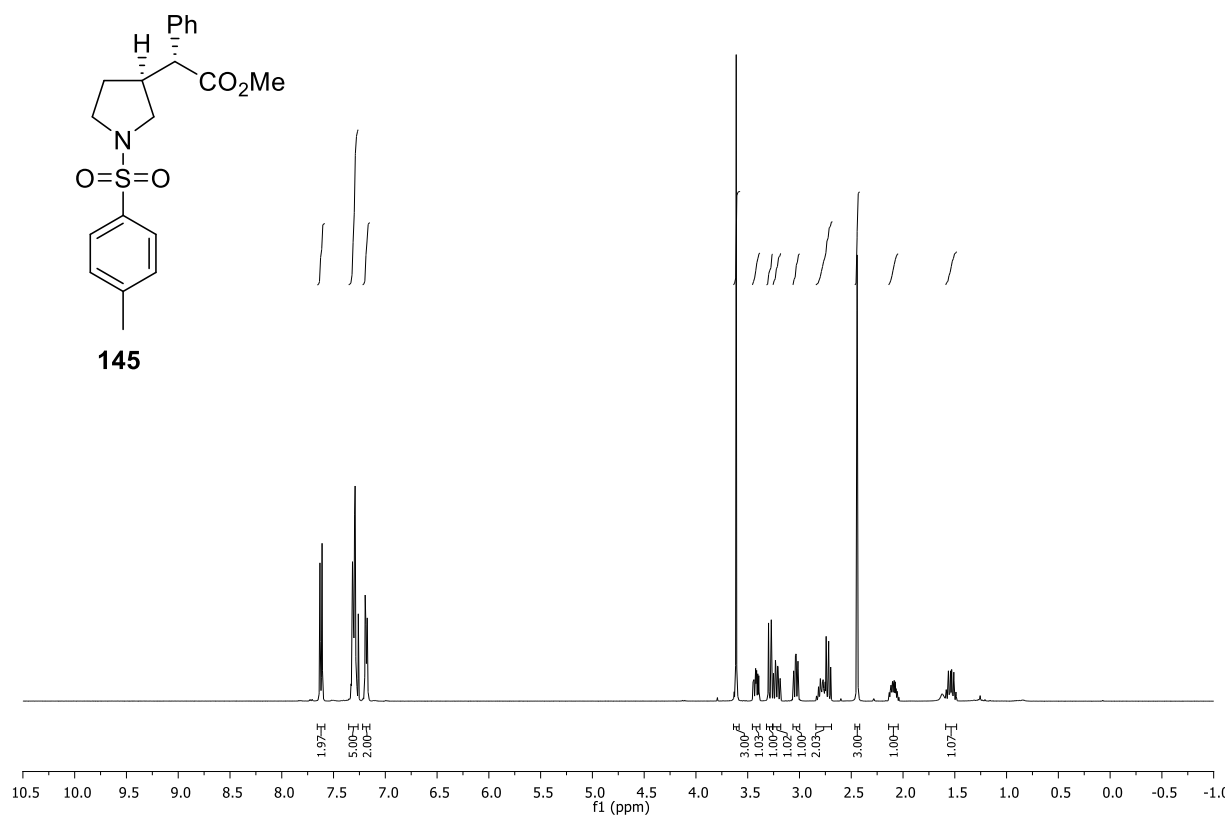


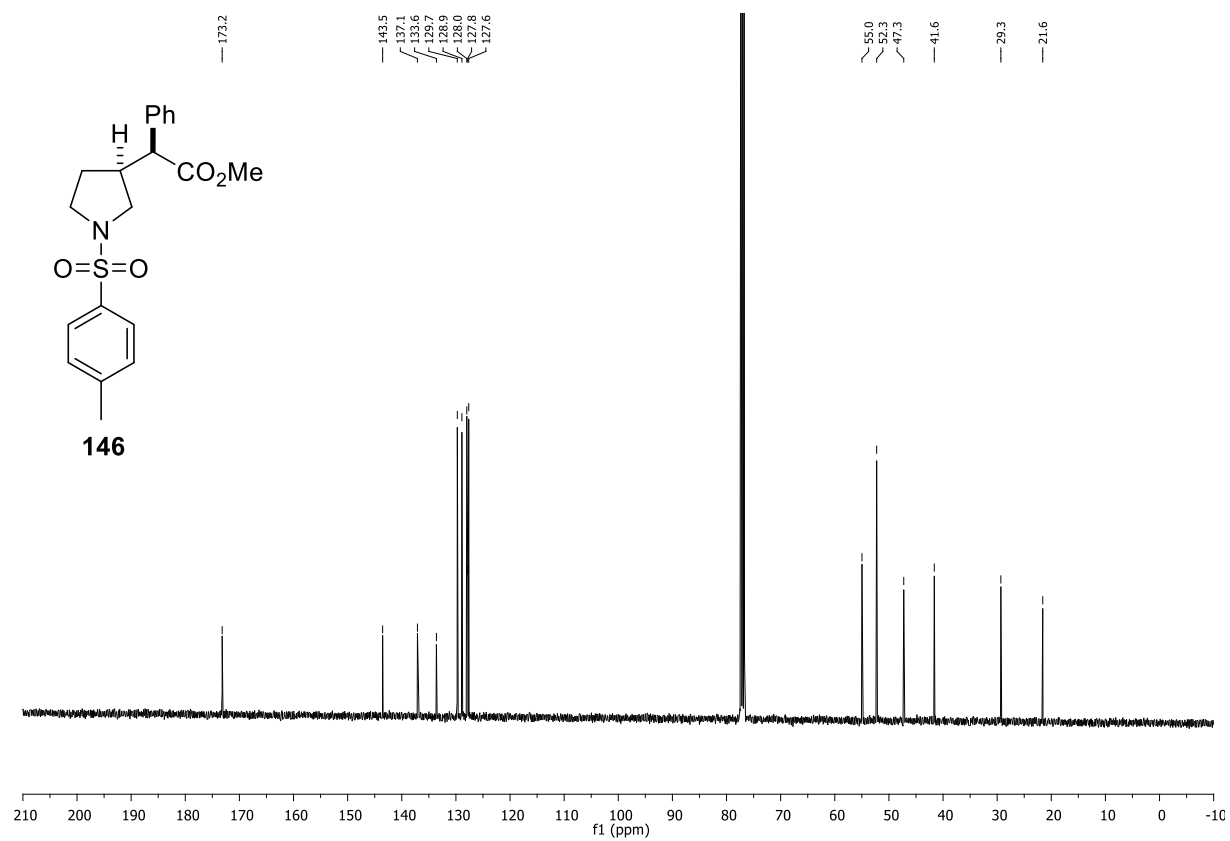
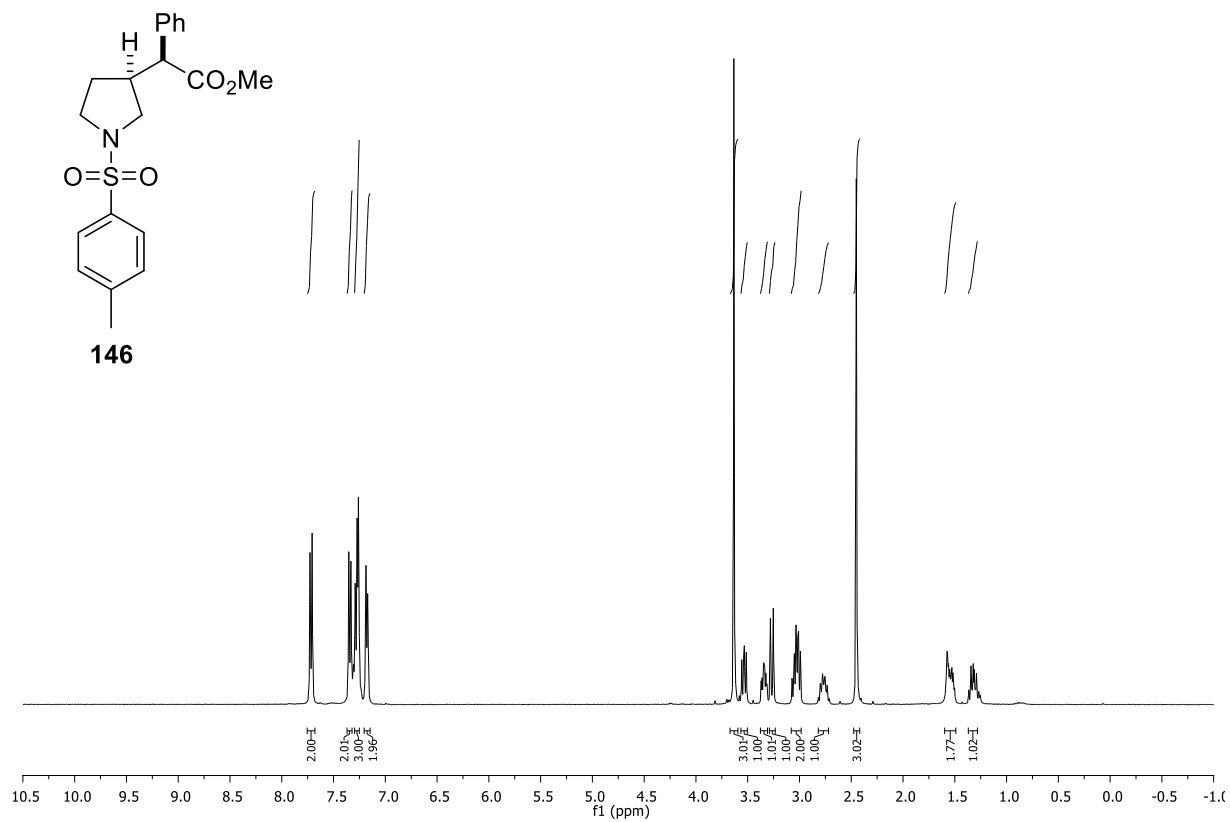




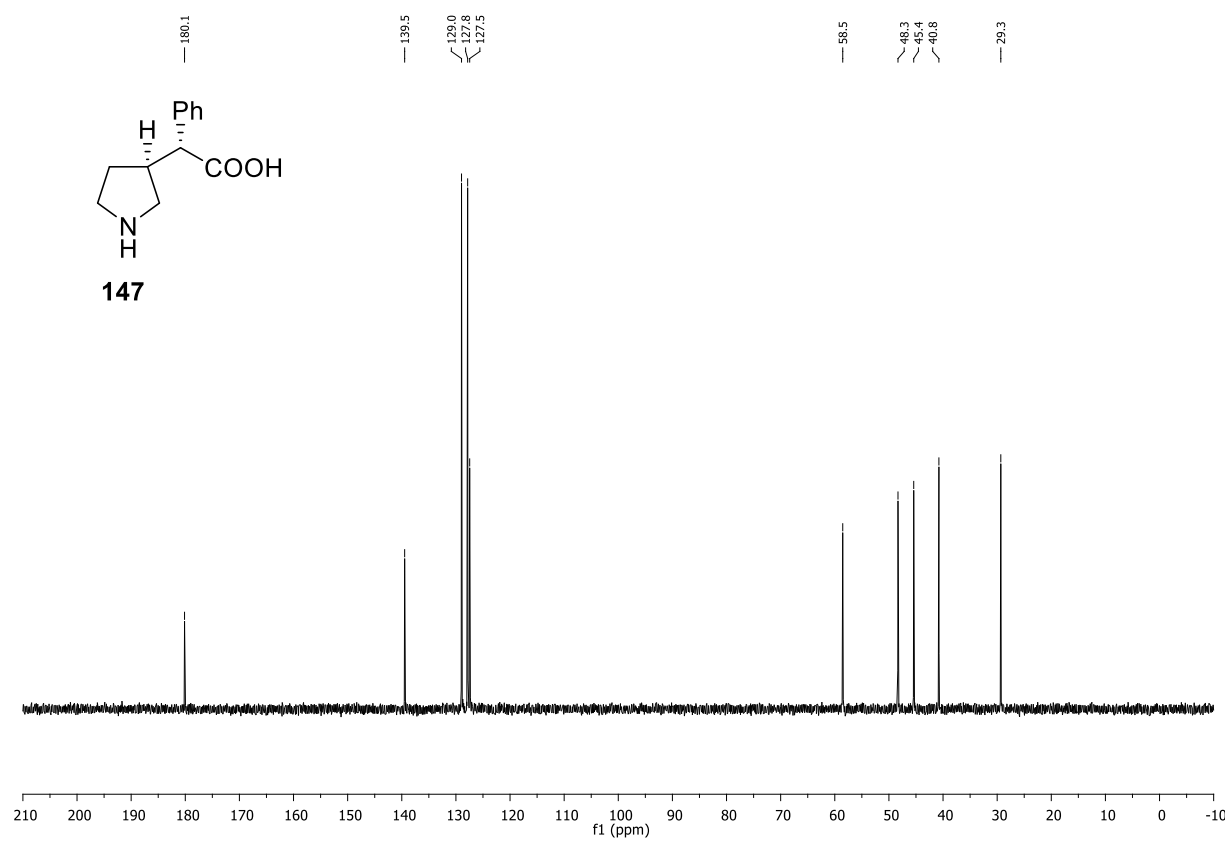
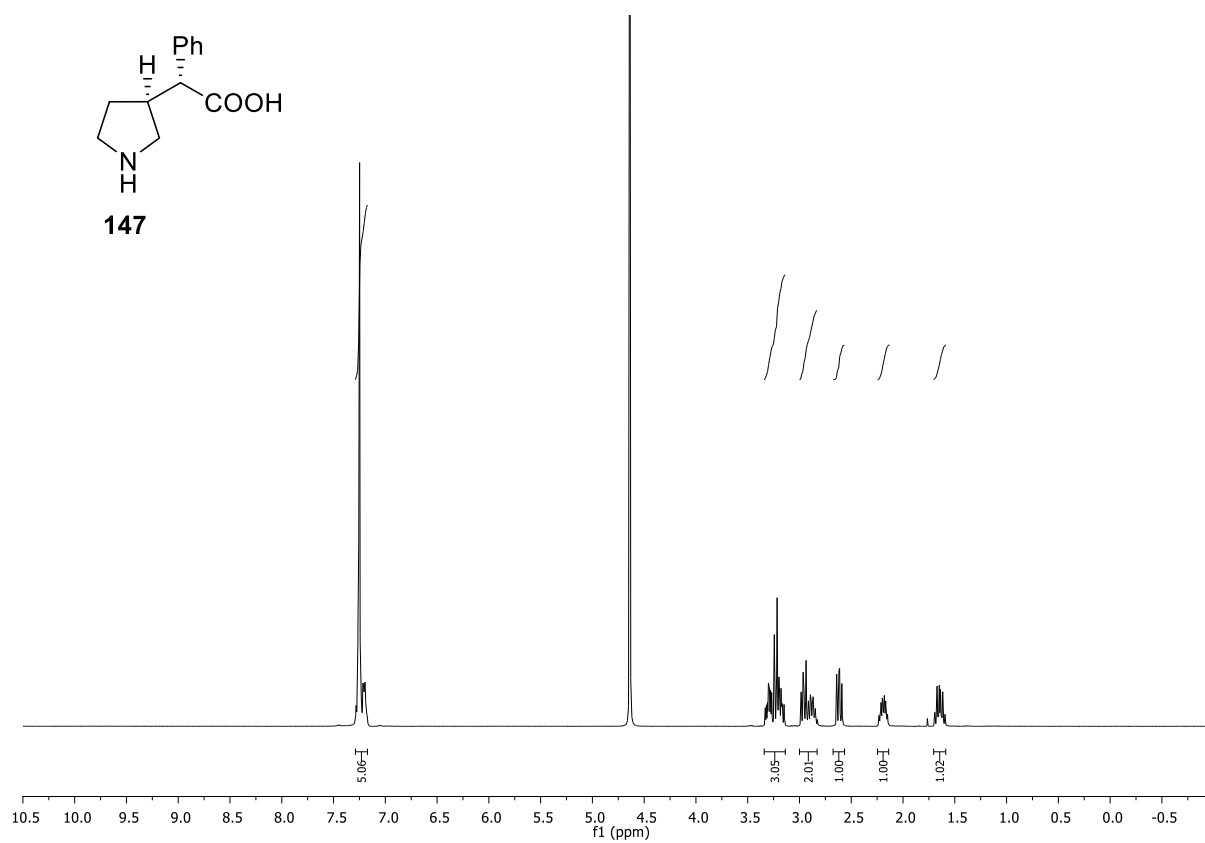


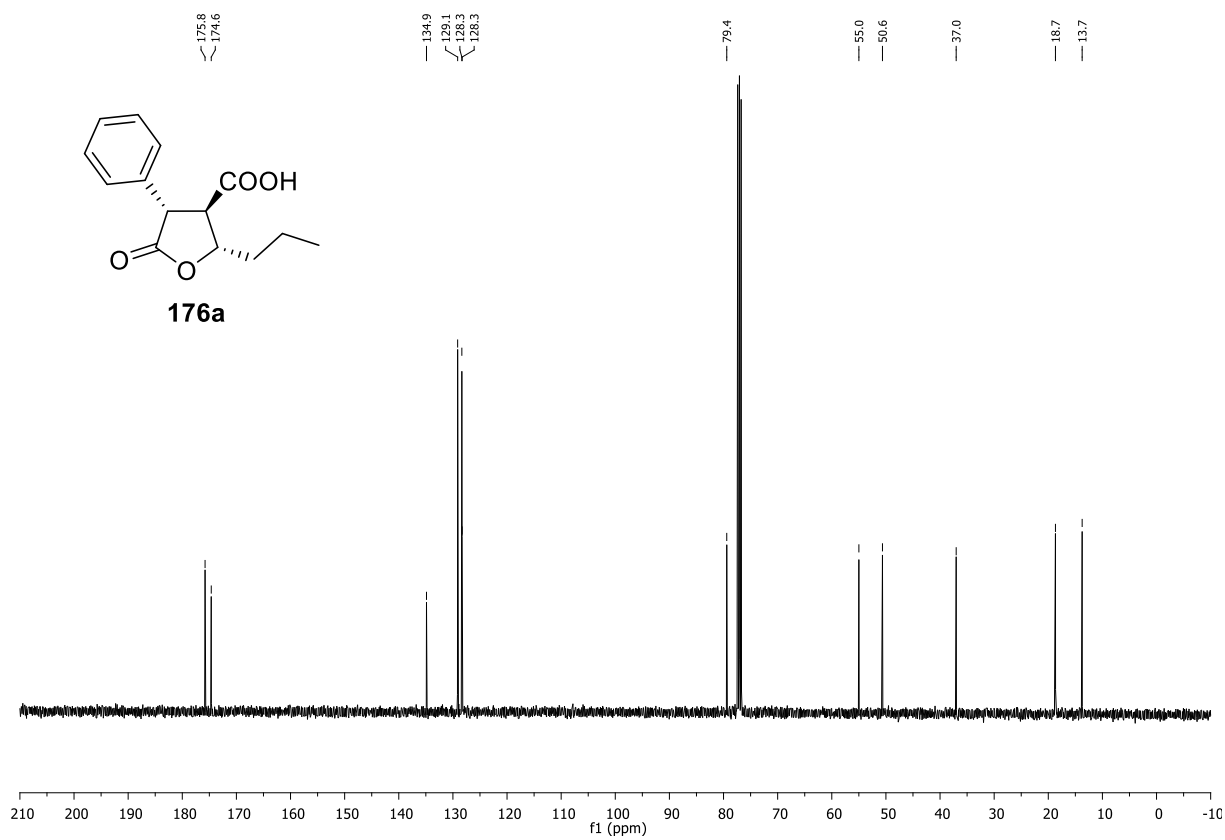
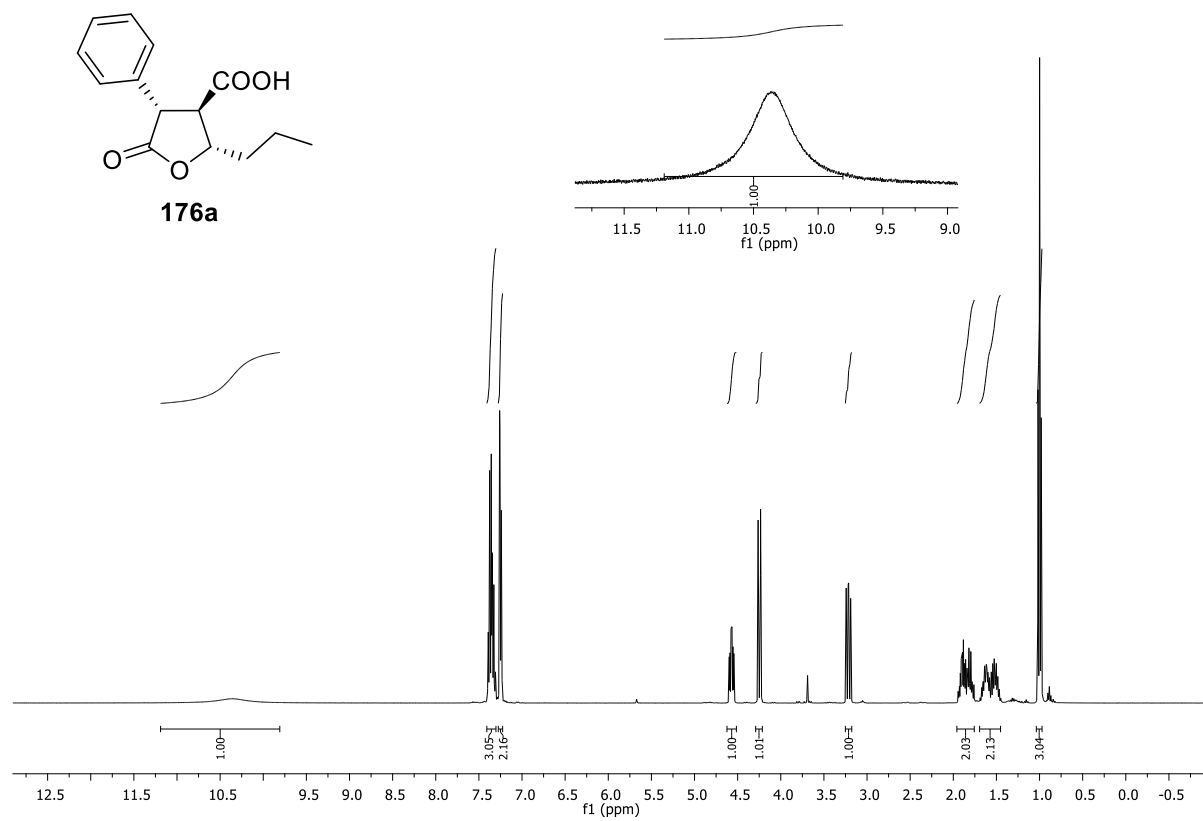


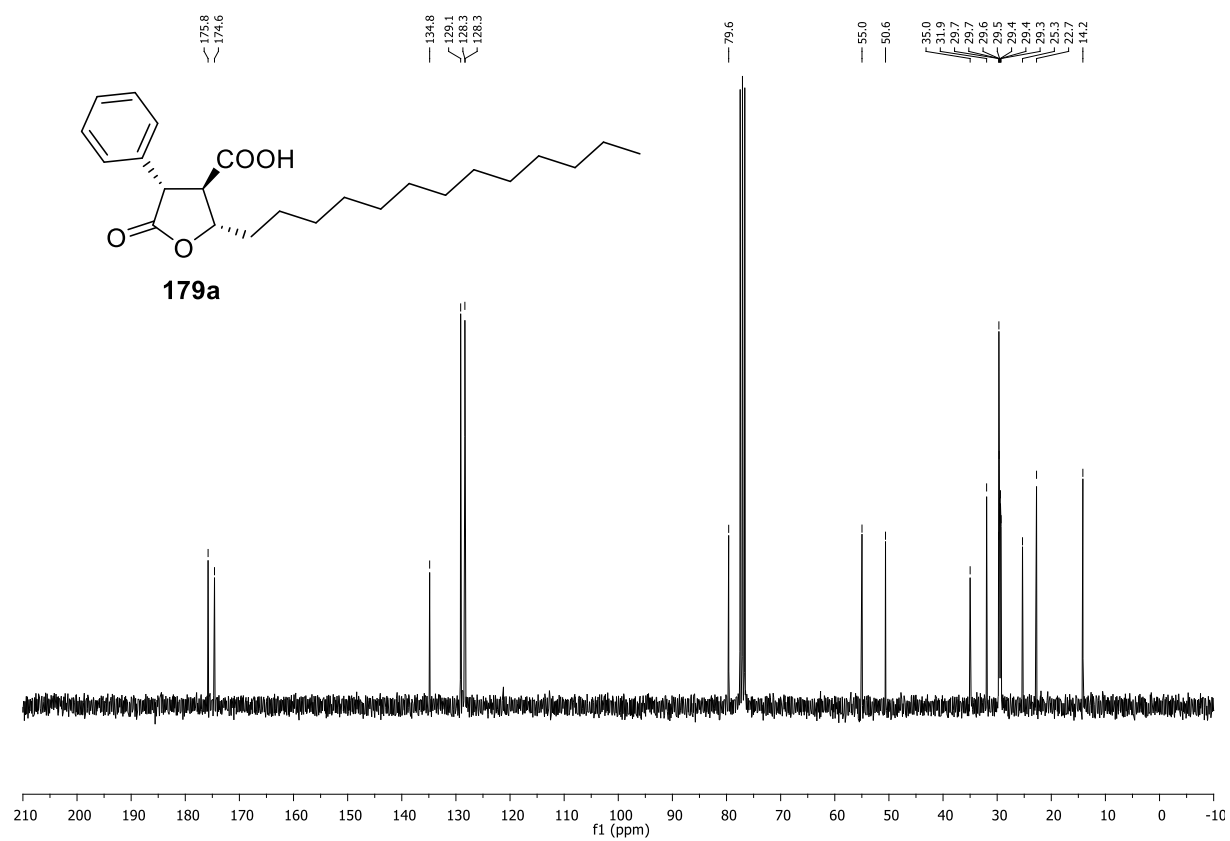
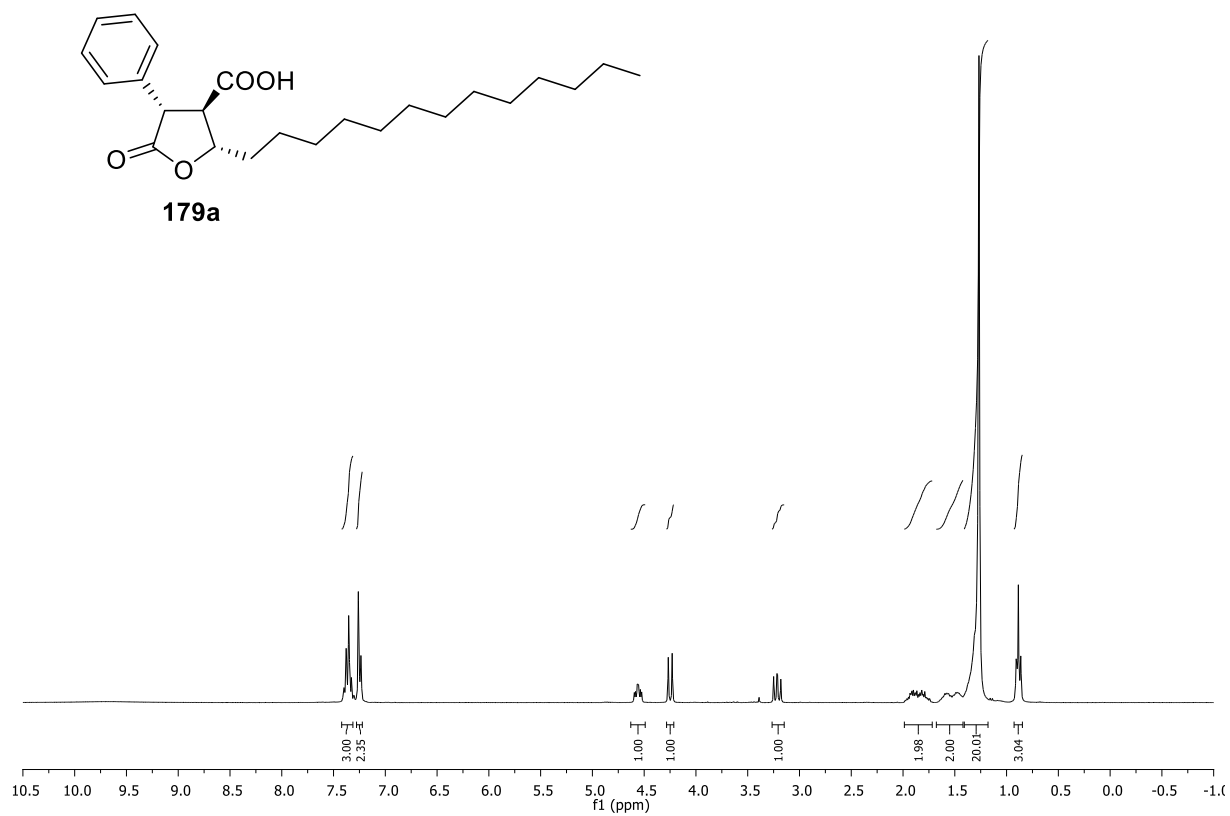


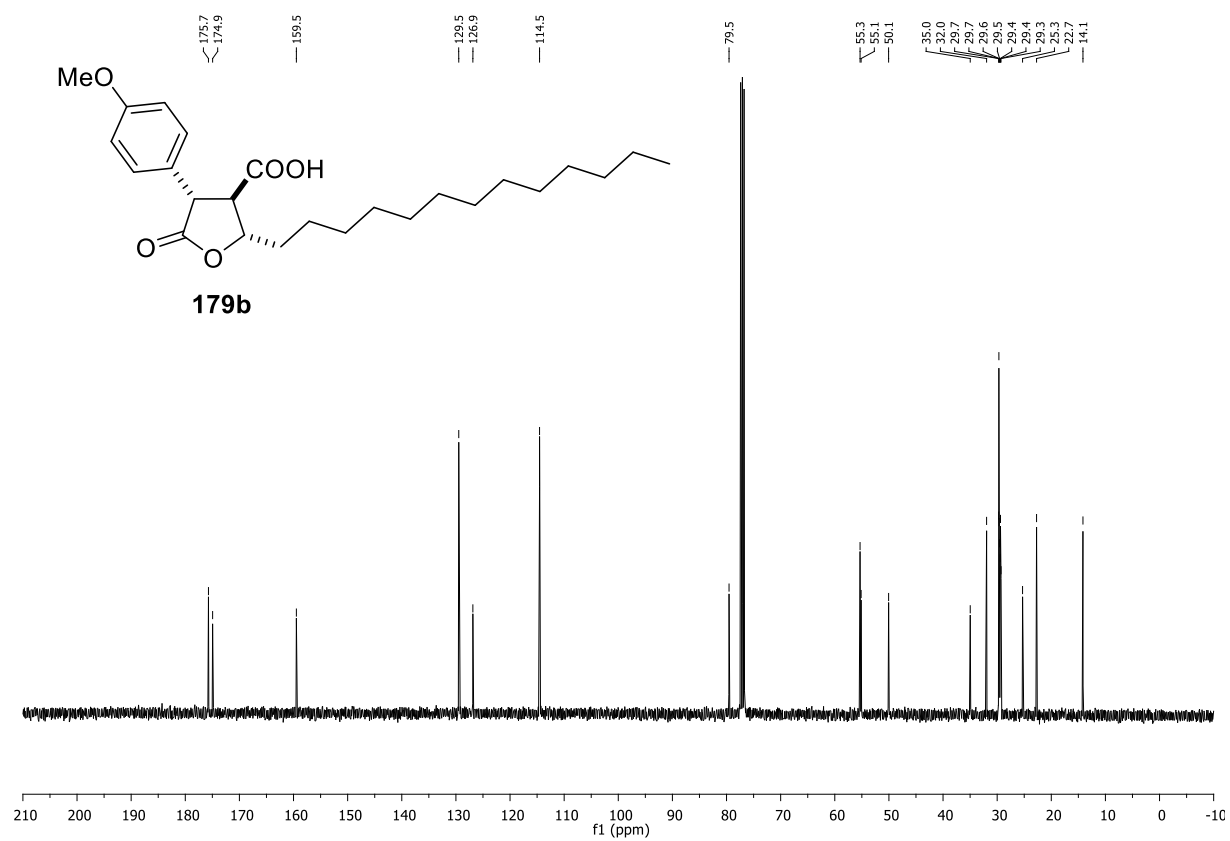
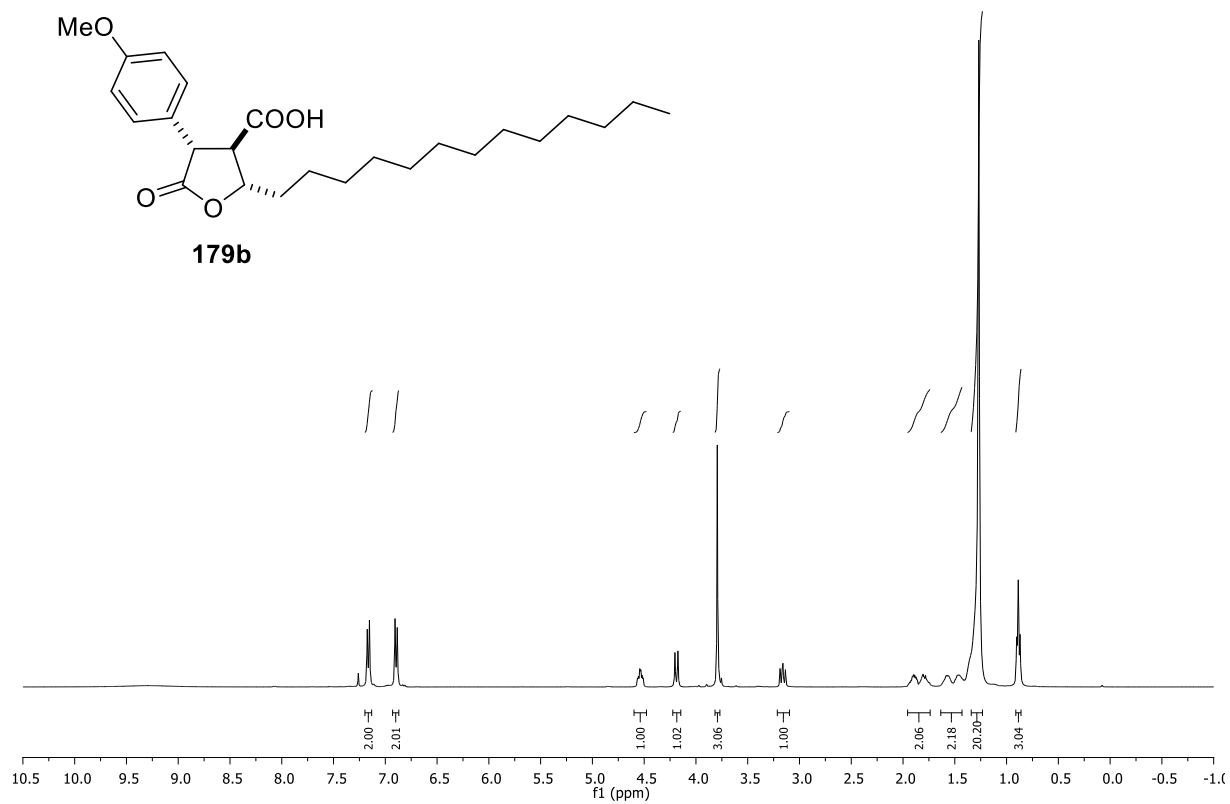


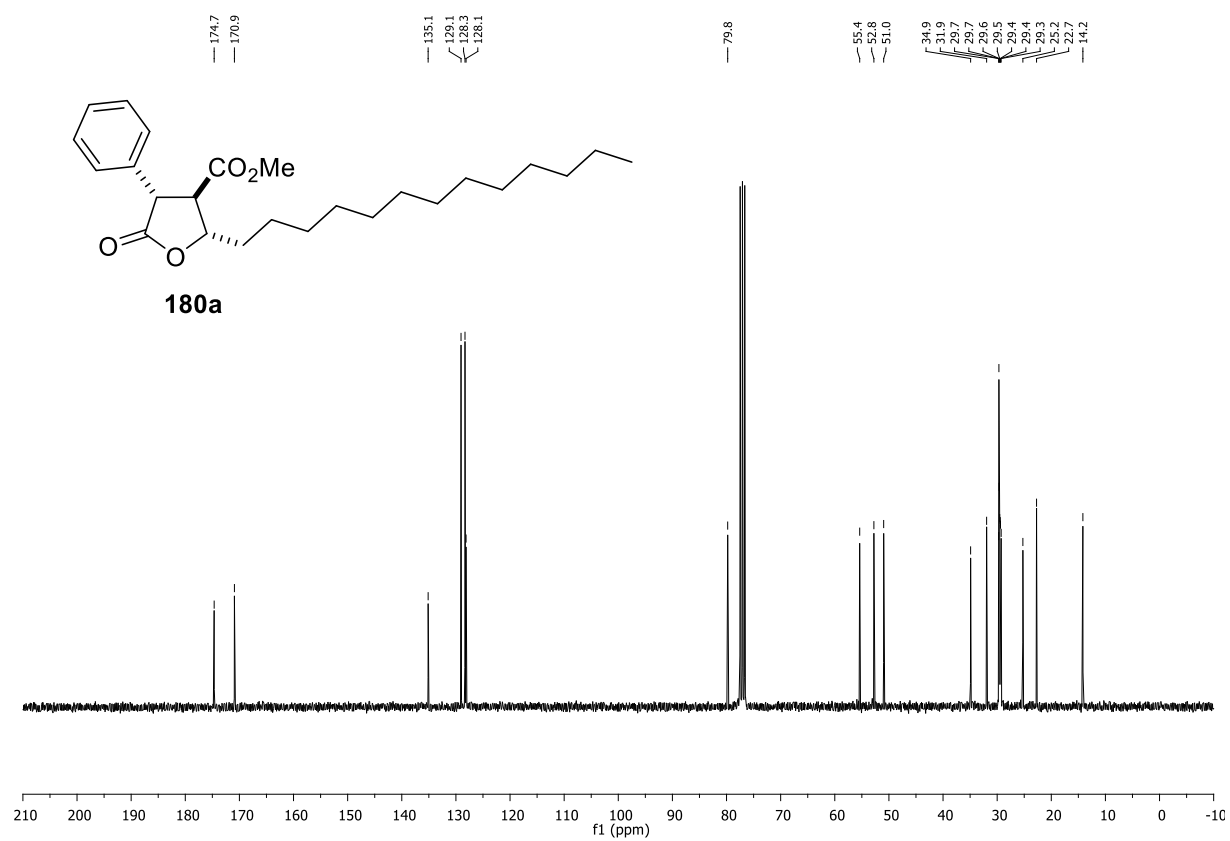
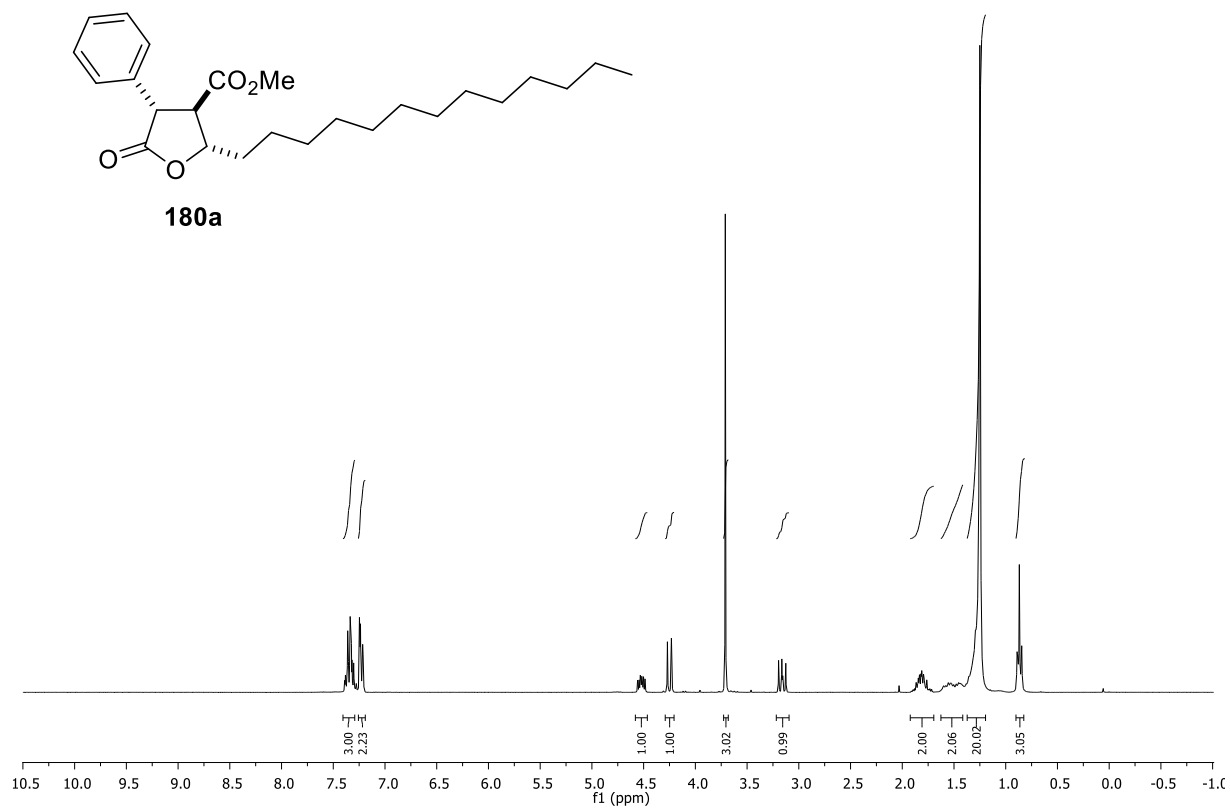


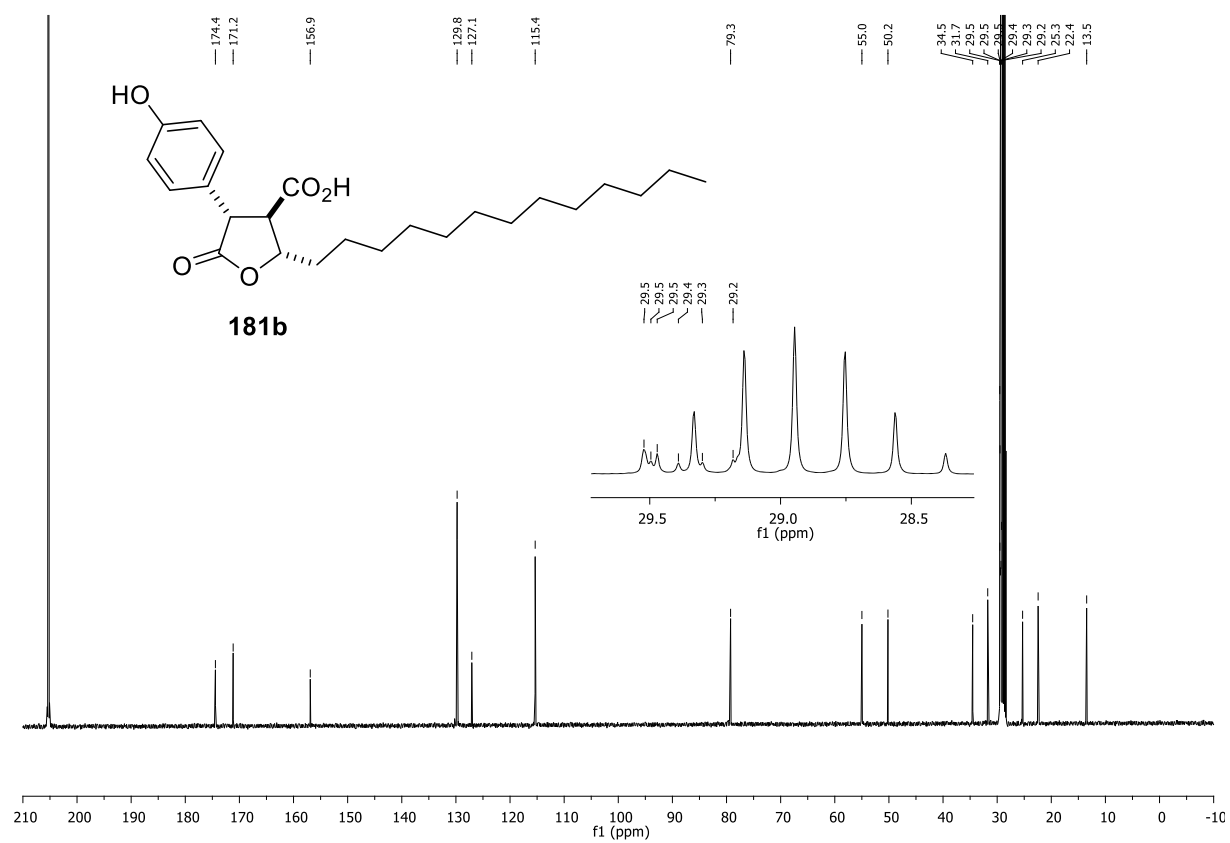
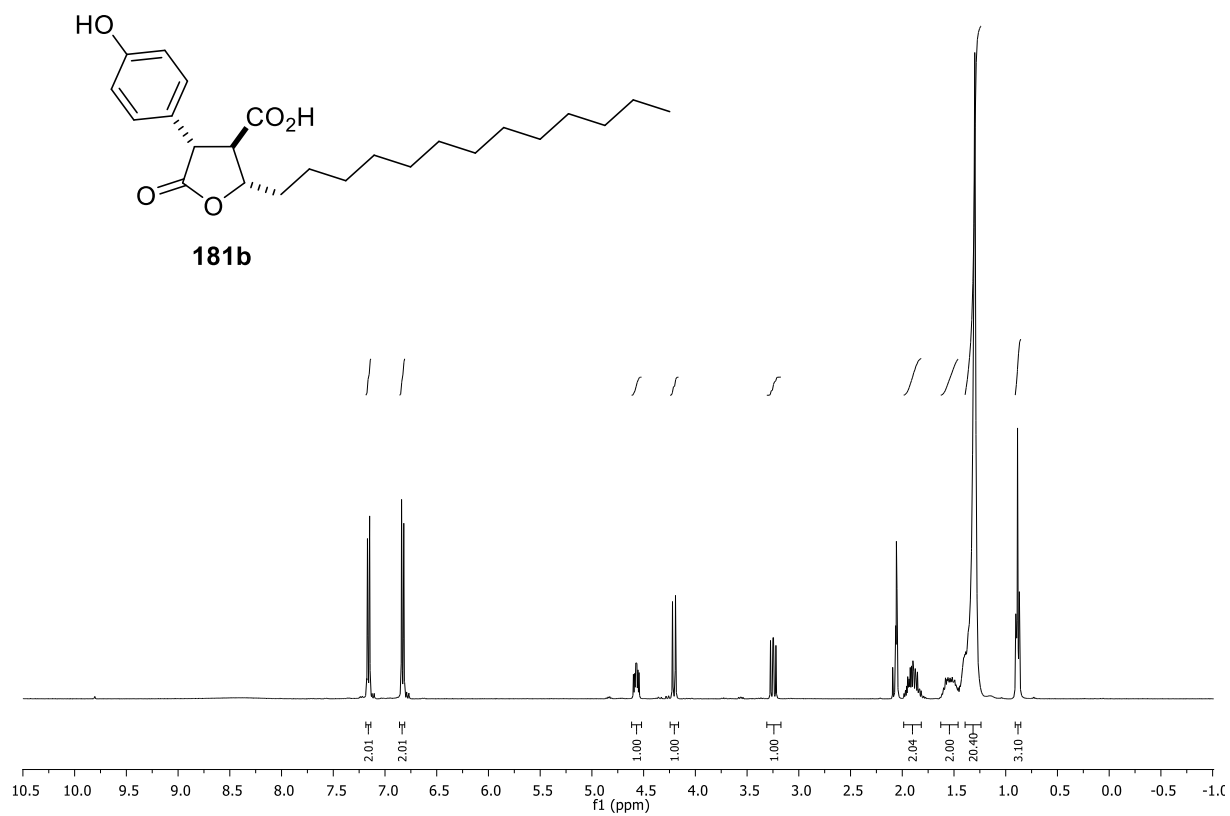




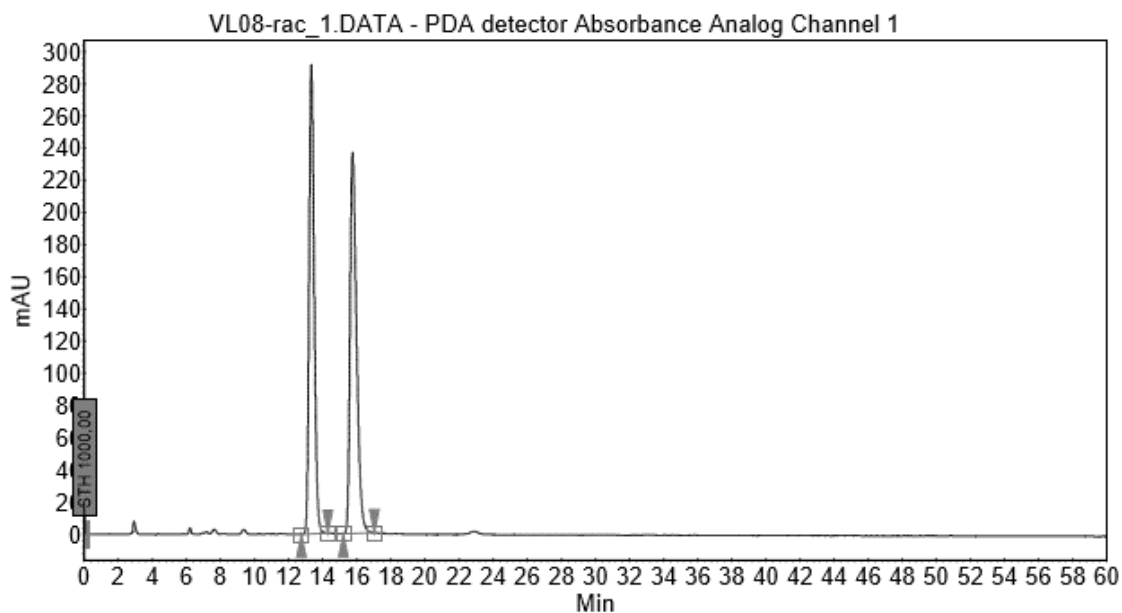






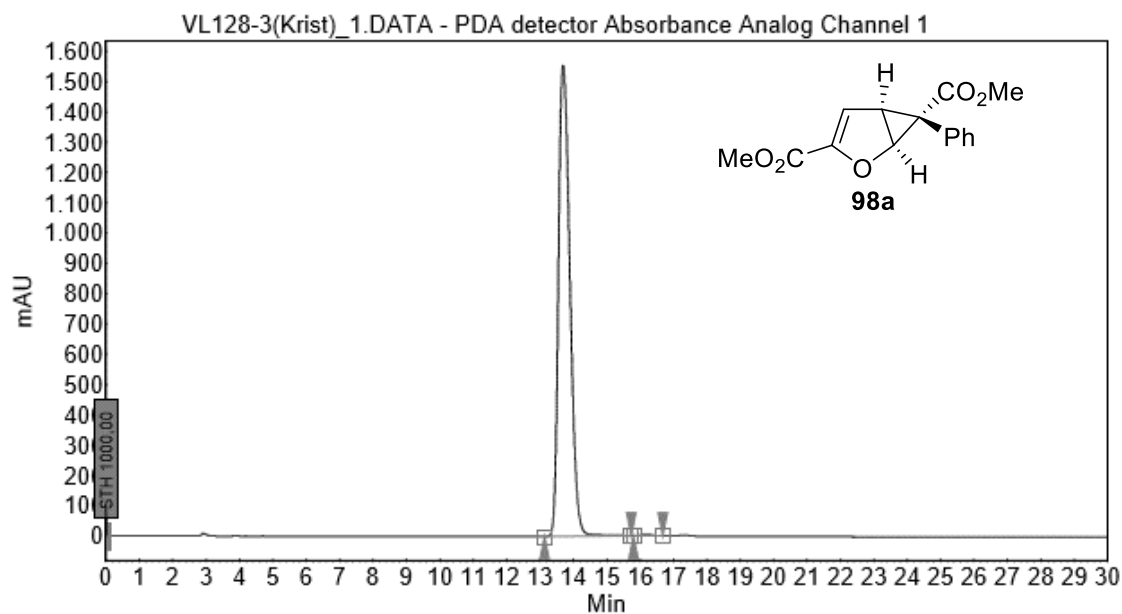


## 2 Chiral HPLC data



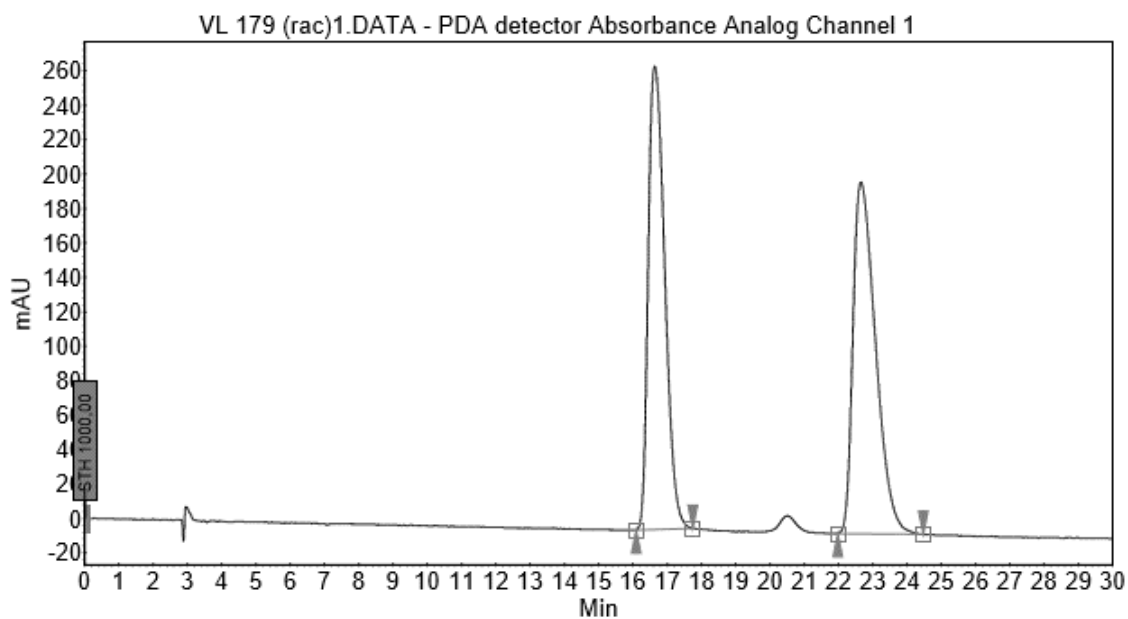
## Peak Results :

Index	Name	Time [Min]	Quantity [% Area]	Height [mAU]	Area [mAU.Min]	Area % [%]
1	UNKNOWN	13.33	48.75	291.9	99.7	48.754
2	UNKNOWN	15.75	51.25	237.2	104.8	51.246
Total			100.00	529.0	204.4	100.000



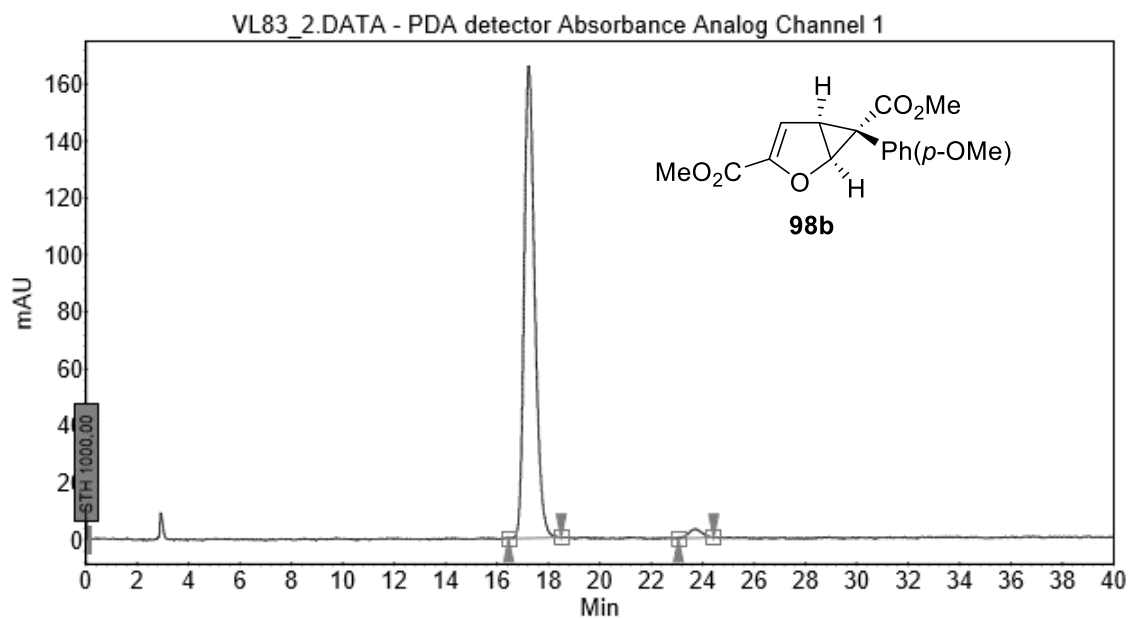
## Peak Results :

Index	Name	Time [Min]	Quantity [% Area]	Height [mAU]	Area [mAU.Min]	Area % [%]
1	UNKNOWN	13.69	99.75	1554.9	618.2	99.748
2	UNKNOWN	16.18	0.25	4.1	1.6	0.252
Total			100.00	1559.0	619.8	100.000



### Peak Results :

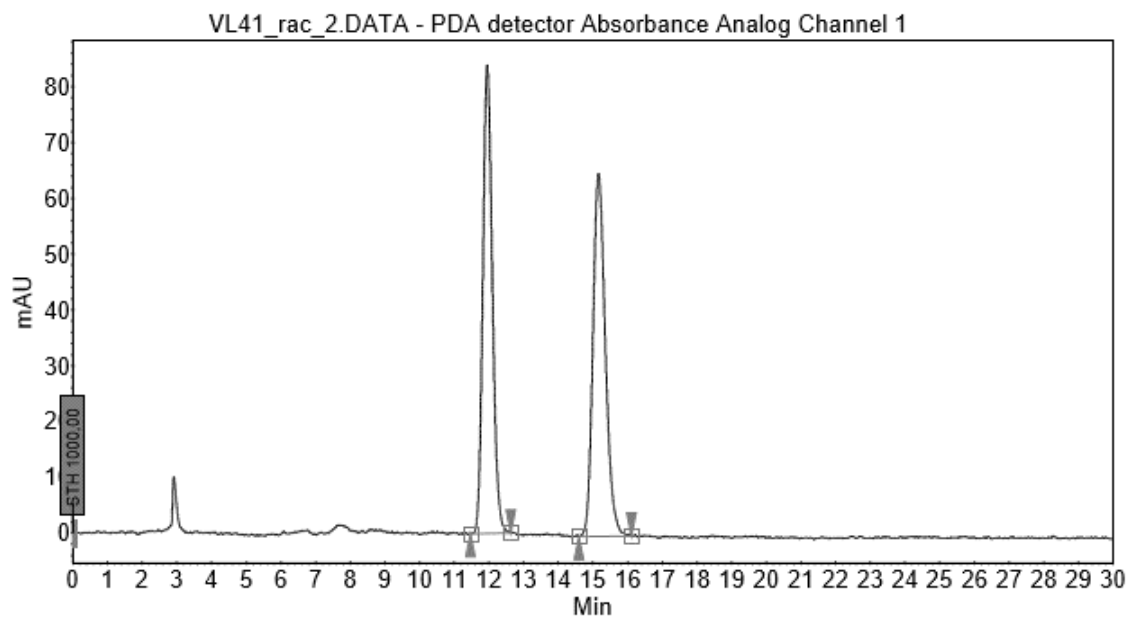
Index	Name	Time [Min]	Quantity [% Area]	Height [mAU]	Area [mAU.Min]	Area % [%]
1	UNKNOWN	16.64	49.13	269.0	150.1	49.129
2	UNKNOWN	22.65	50.87	204.1	155.5	50.871
Total			100.00	473.1	305.6	100.000



### Peak Results :

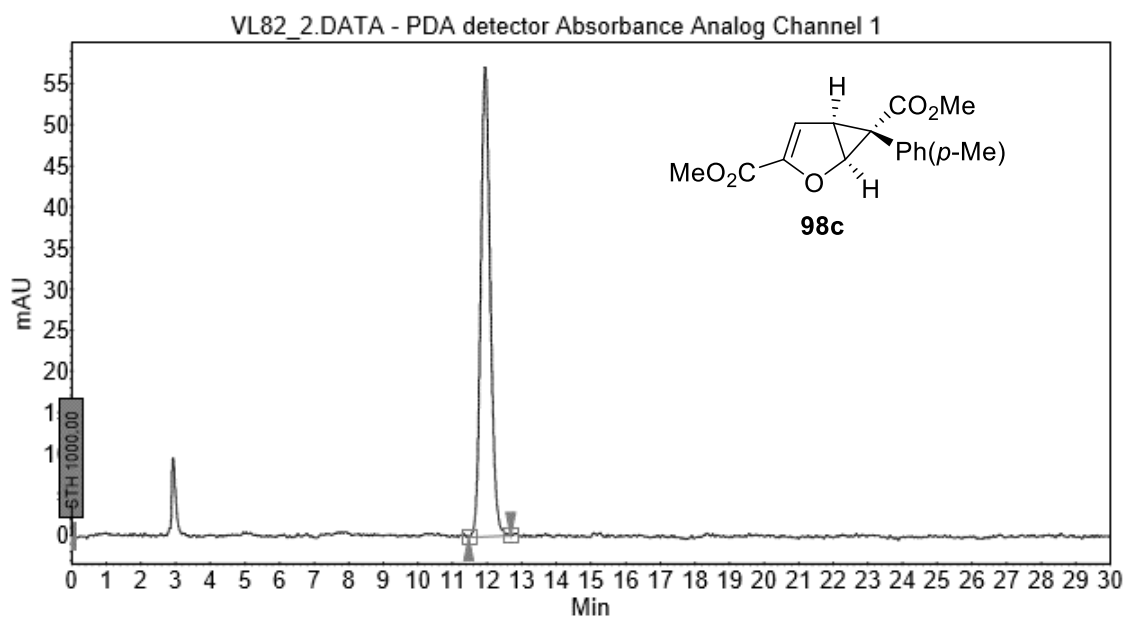
Index	Name	Time [Min]	Quantity [% Area]	Height [mAU]	Area [mAU.Min]	Area % [%]
1	UNKNOWN	17.23	97.67	166.0	79.4	97.666
2	UNKNOWN	23.71	2.33	3.1	1.9	2.334
Total			100.00	169.1	81.3	100.000





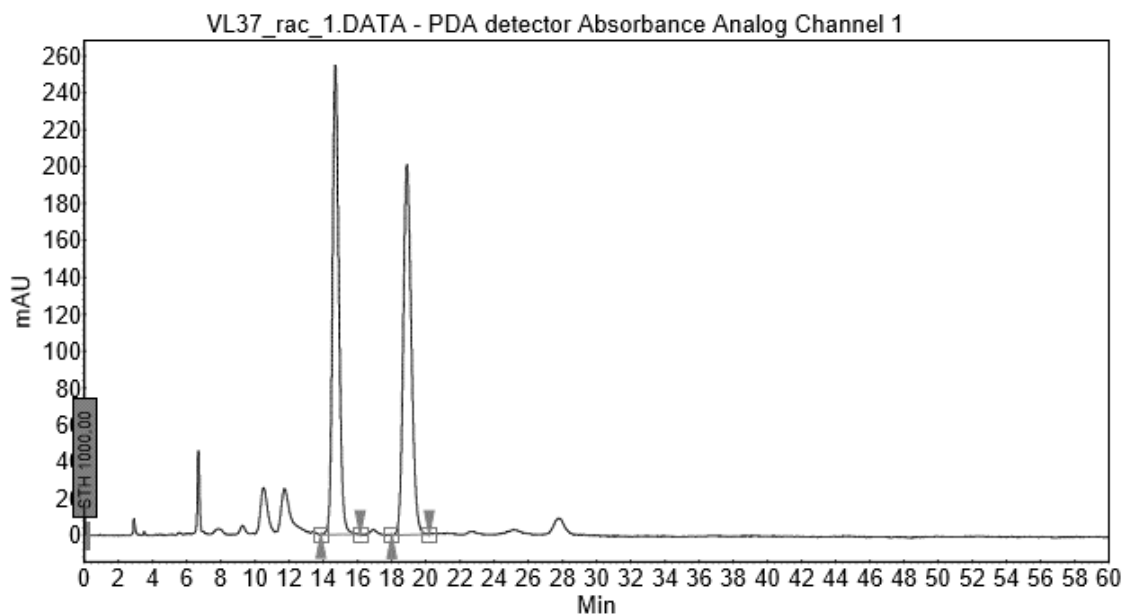
### Peak Results :

Index	Name	Time [Min]	Quantity [% Area]	Height [mAU]	Area [mAU.Min]	Area % [%]
1	UNKNOWN	11.95	49.75	84.1	26.7	49.745
2	UNKNOWN	15.16	50.25	65.0	27.0	50.255
Total			100.00	149.1	53.6	100.000



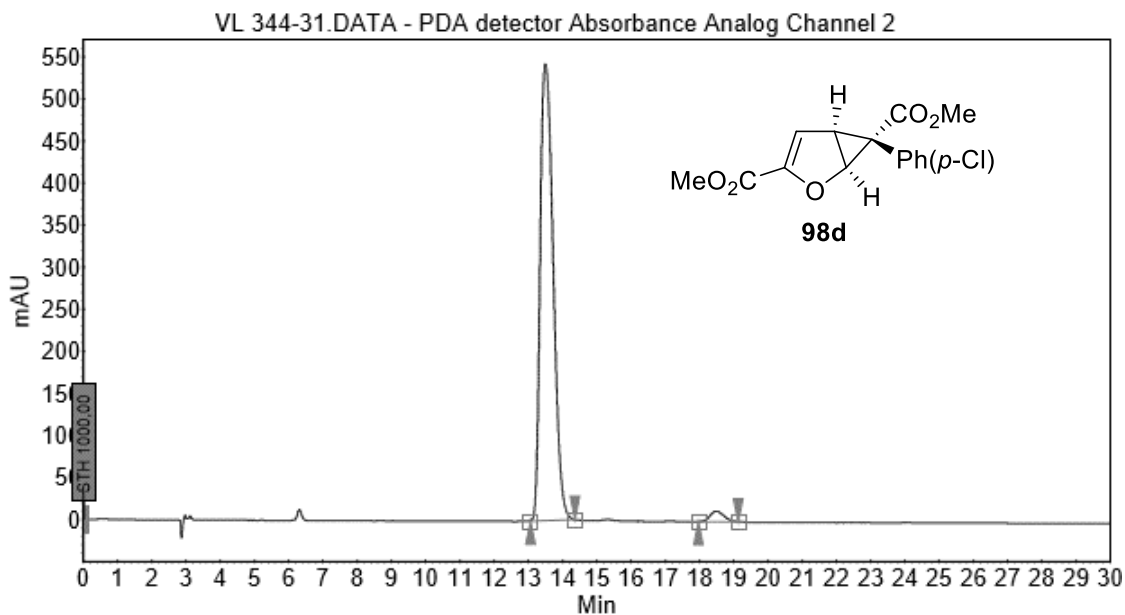
### Peak Results :

Index	Name	Time [Min]	Quantity [% Area]	Height [mAU]	Area [mAU.Min]	Area % [%]
1	UNKNOWN	11.95	100.00	57.2	18.3	100.000
Total			100.00	57.2	18.3	100.000



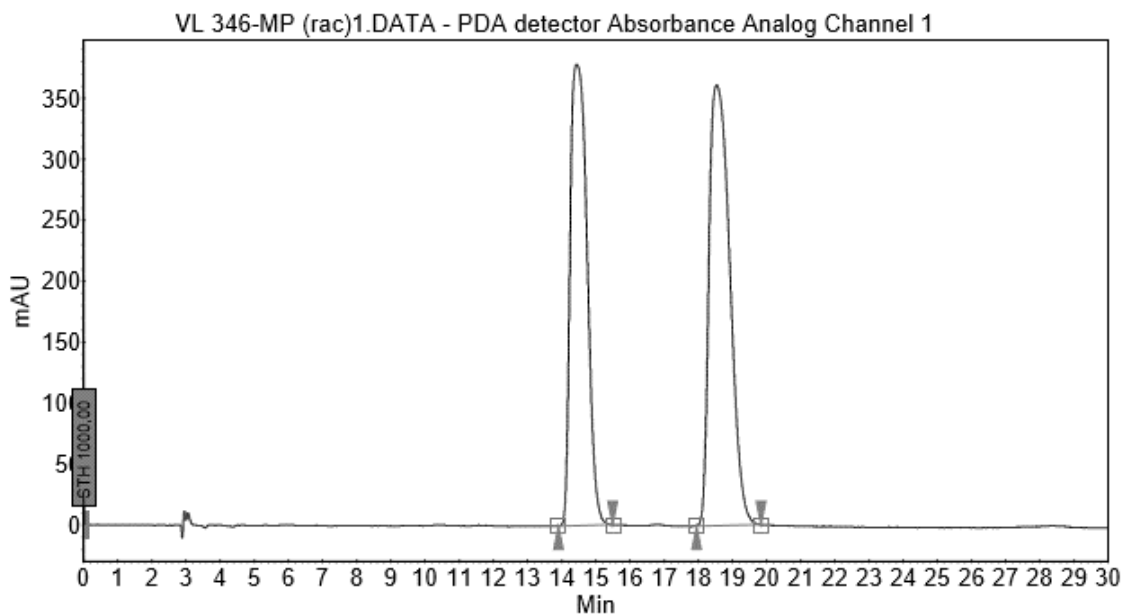
### Peak Results :

Index	Name	Time [Min]	Quantity [% Area]	Height [mAU]	Area [mAU.Min]	Area % [%]
1	UNKNOWN	14.70	49.86	254.9	109.8	49.864
2	UNKNOWN	18.89	50.14	201.0	110.4	50.136
Total			100.00	455.9	220.3	100.000



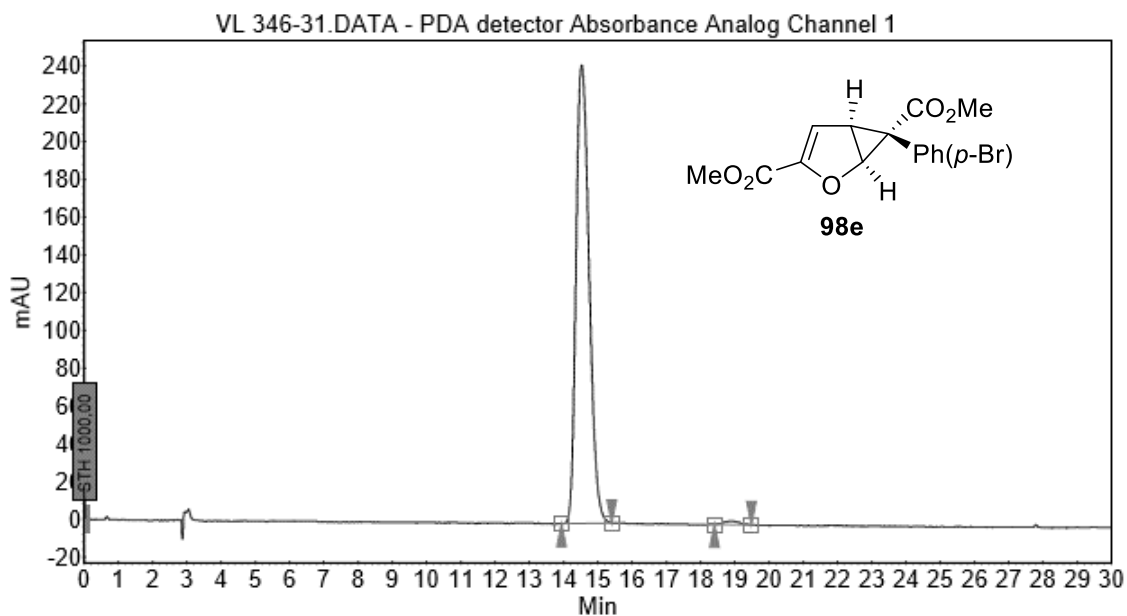
### Peak Results :

Index	Name	Time [Min]	Quantity [% Area]	Height [mAU]	Area [mAU.Min]	Area % [%]
1	UNKNOWN	13.50	97.59	542.7	238.6	97.589
2	UNKNOWN	18.48	2.41	12.5	5.9	2.411
Total			100.00	555.2	244.5	100.000



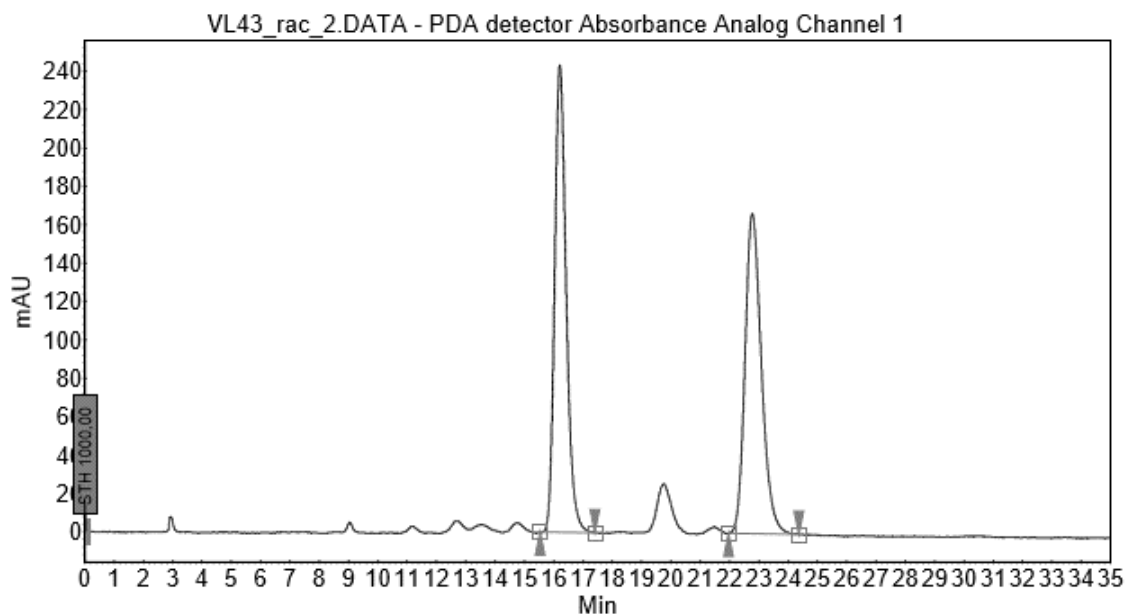
### Peak Results :

Index	Name	Time [Min]	Quantity [% Area]	Height [mAU]	Area [mAU.Min]	Area % [%]
1	UNKNOWN	14.44	45.97	378.5	216.3	45.970
2	UNKNOWN	18.54	54.03	361.3	254.2	54.030
Total			100.00	739.8	470.5	100.000



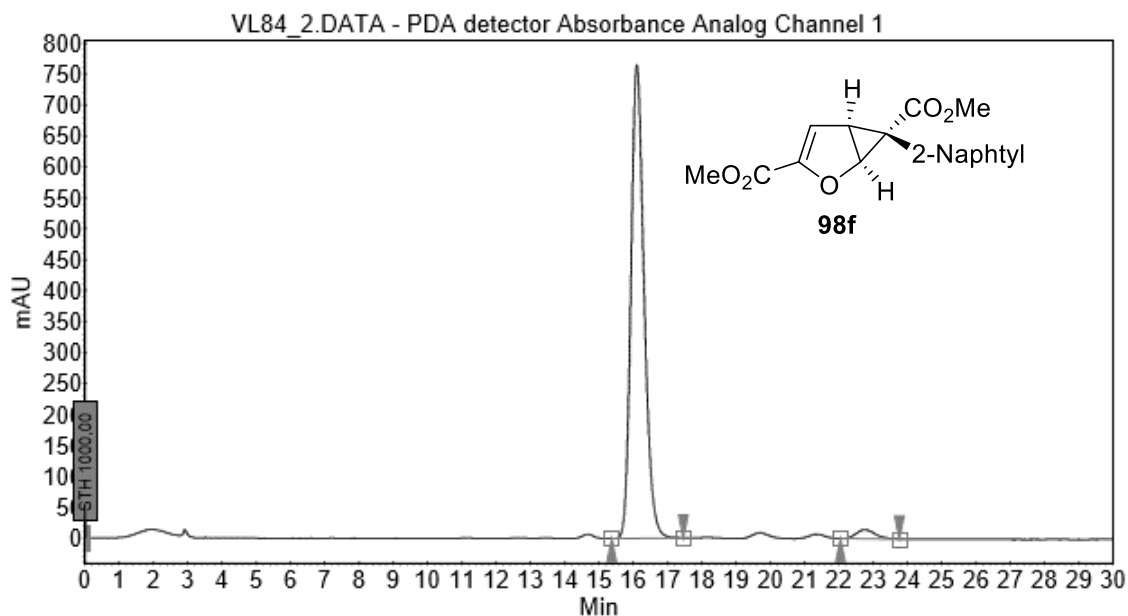
### Peak Results :

Index	Name	Time [Min]	Quantity [% Area]	Height [mAU]	Area [mAU.Min]	Area % [%]
2	UNKNOWN	14.53	99.14	242.8	107.5	99.138
1	UNKNOWN	18.91	0.86	1.9	0.9	0.862
Total			100.00	244.7	108.5	100.000



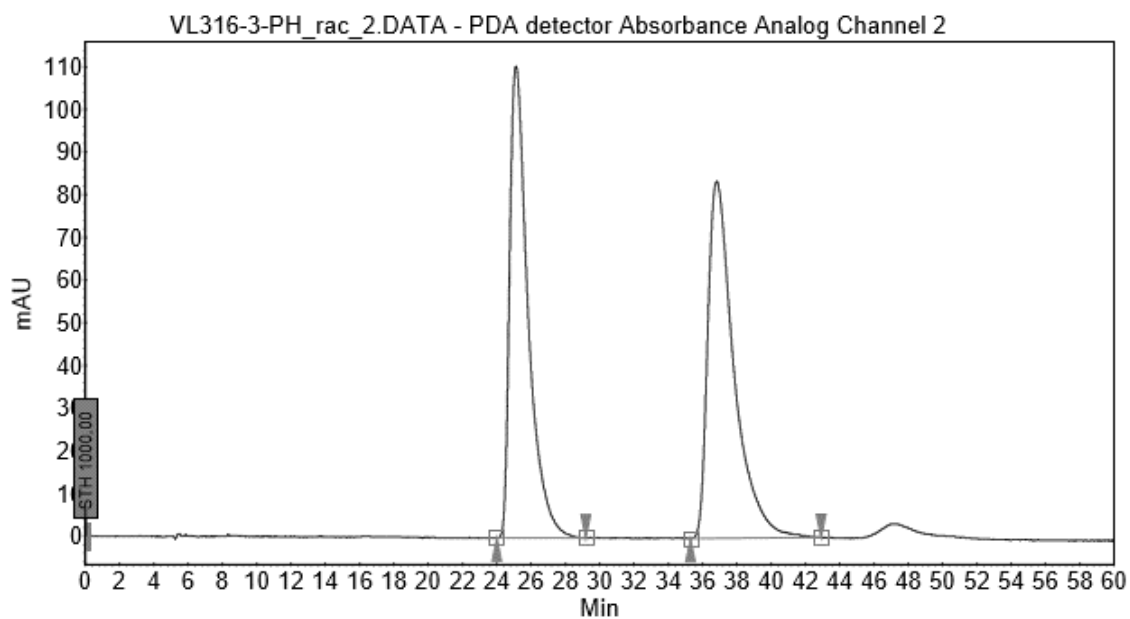
### Peak Results :

Index	Name	Time [Min]	Quantity [% Area]	Height [mAU]	Area [mAU.Min]	Area % [%]
1	UNKNOWN	16.21	50.65	243.6	111.2	50.651
2	UNKNOWN	22.78	49.35	166.7	108.4	49.349
Total			100.00	410.3	219.6	100.000



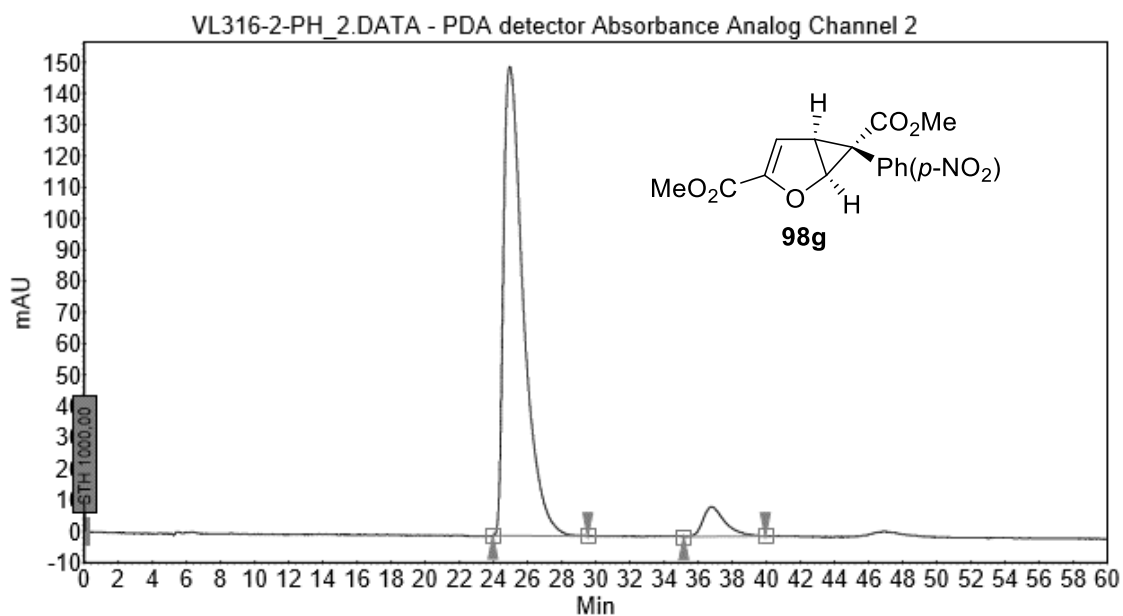
### Peak Results :

Index	Name	Time [Min]	Quantity [% Area]	Height [mAU]	Area [mAU.Min]	Area % [%]
1	UNKNOWN	16.11	97.25	766.0	340.4	97.249
2	UNKNOWN	22.77	2.75	14.8	9.6	2.751
Total			100.00	780.8	350.0	100.000



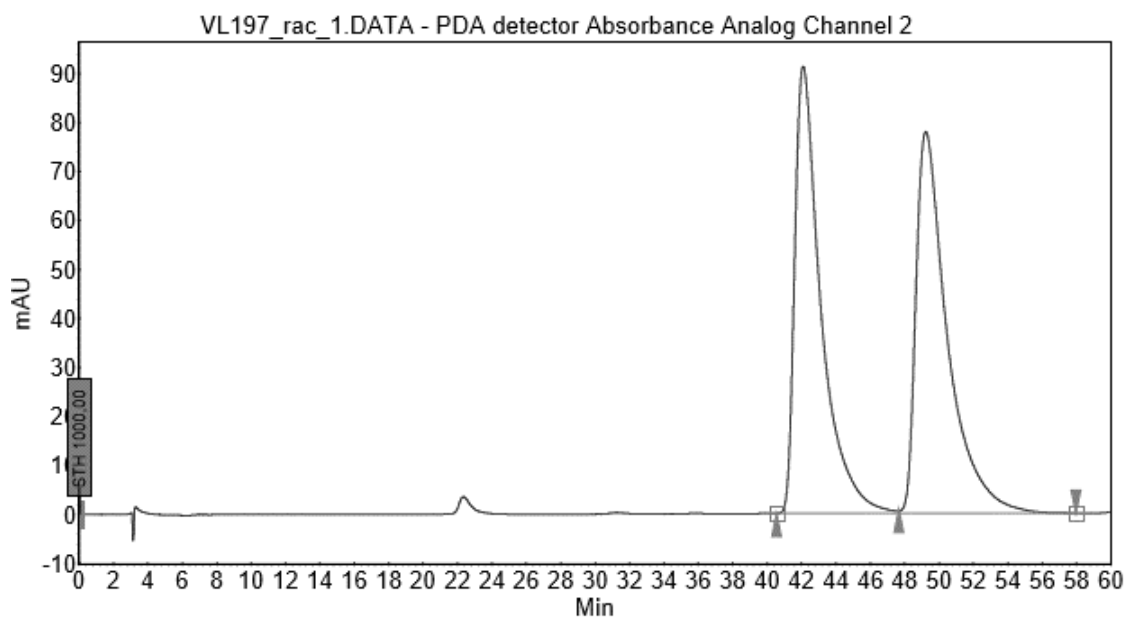
### Peak Results :

Index	Name	Time [Min]	Quantity [% Area]	Height [mAU]	Area [mAU.Min]	Area % [%]
1	UNKNOWN	25.12	48.21	110.6	137.7	48.207
2	UNKNOWN	36.83	51.79	83.6	147.9	51.793
Total			100.00	194.2	285.6	100.000



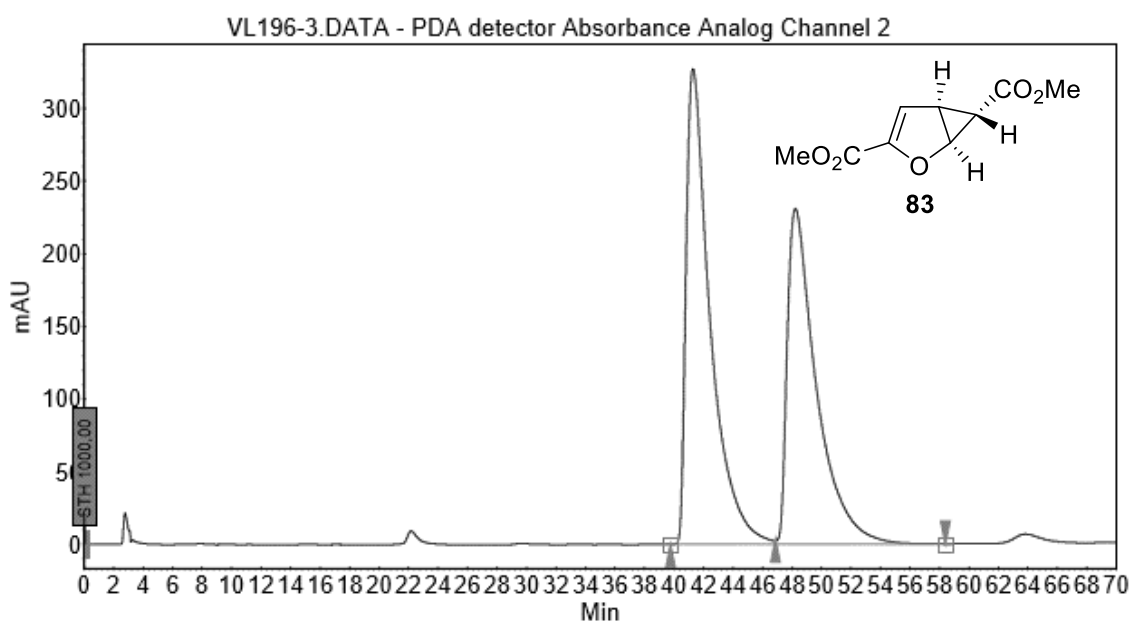
### Peak Results :

Index	Name	Time [Min]	Quantity [% Area]	Height [mAU]	Area [mAU.Min]	Area % [%]
1	UNKNOWN	24.96	93.51	150.1	203.2	93.505
2	UNKNOWN	36.80	6.49	9.4	14.1	6.495
Total			100.00	159.6	217.3	100.000



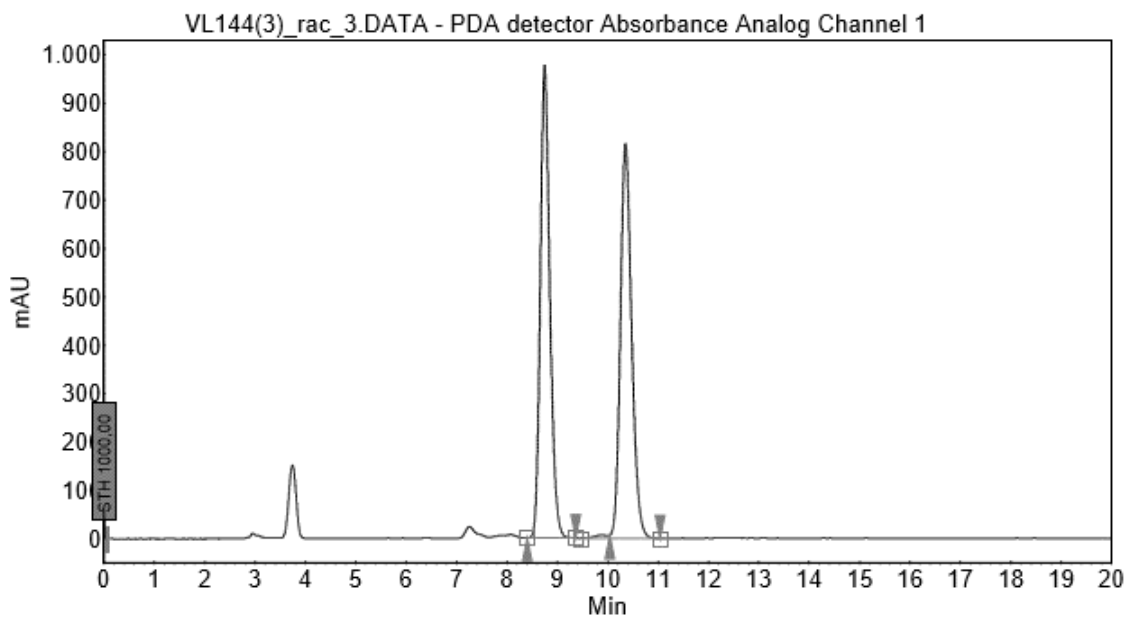
**Peak Results :**

Index	Name	Time [Min]	Quantity [% Area]	Height [mAU]	Area [mAU.Min]	Area % [%]
1	UNKNOWN	42.10	49.38	91.4	161.2	49.379
2	UNKNOWN	49.23	50.62	77.9	165.3	50.621
Total			100.00	169.3	326.6	100.000



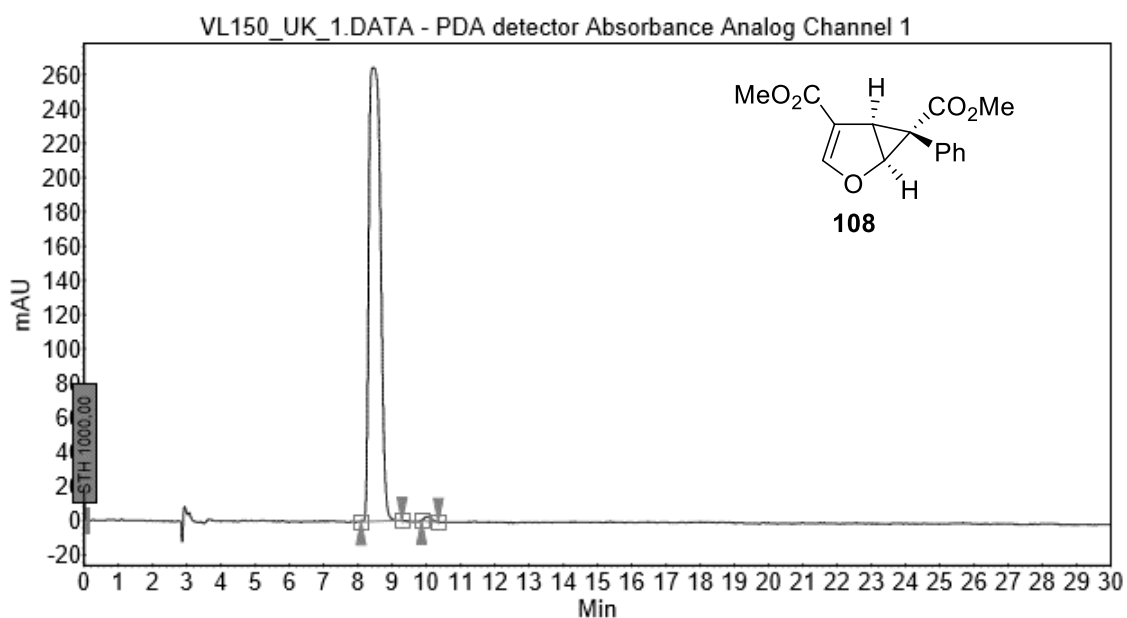
**Peak Results :**

Index	Name	Time [Min]	Quantity [% Area]	Height [mAU]	Area [mAU.Min]	Area % [%]
1	UNKNOWN	41.29	53.95	327.2	618.8	53.946
2	UNKNOWN	48.23	46.05	230.8	528.2	46.054
Total			100.00	558.0	1147.0	100.000



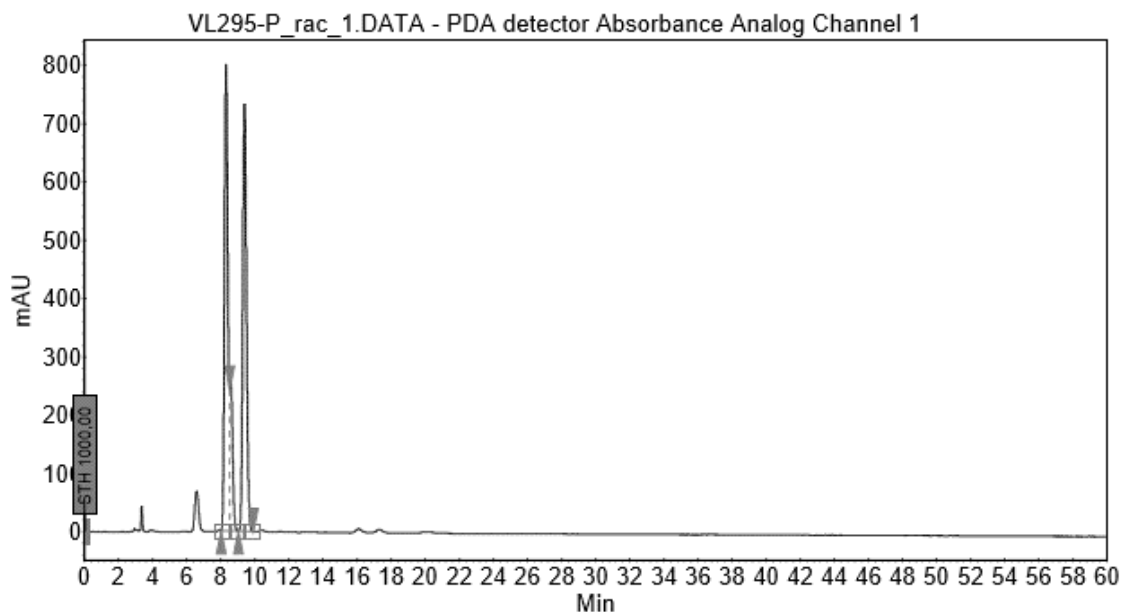
### Peak Results :

Index	Name	Time [Min]	Quantity [% Area]	Height [mAU]	Area [mAU.Min]	Area % [%]
1	UNKNOWN	8.75	50.37	978.3	214.5	50.370
2	UNKNOWN	10.35	49.63	816.0	211.3	49.630
Total			100.00	1794.3	425.8	100.000



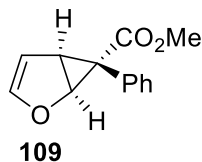
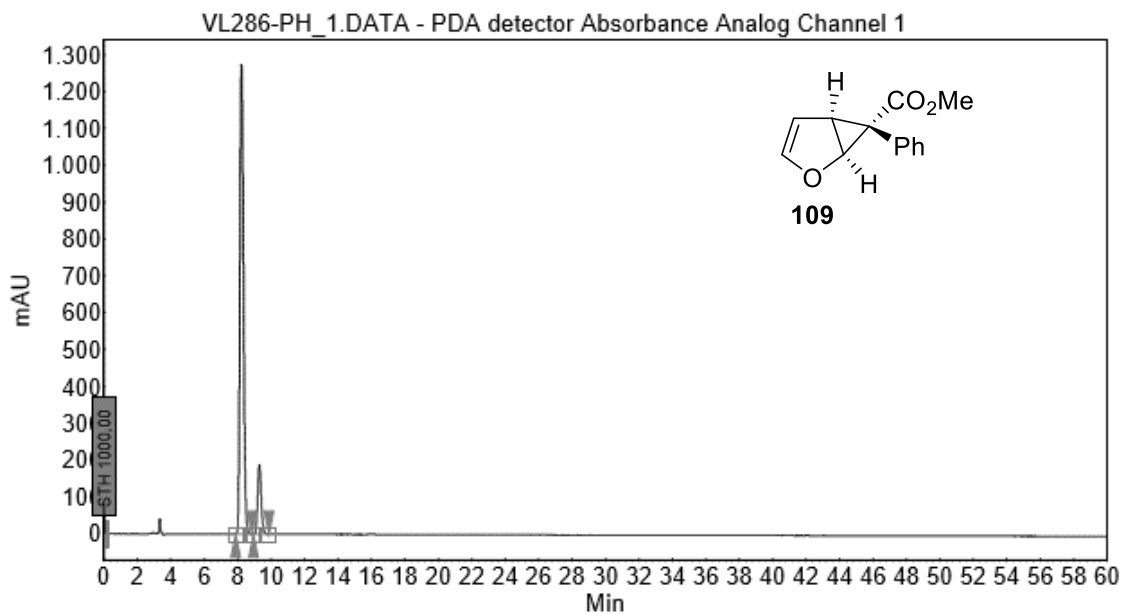
### Peak Results :

Index	Name	Time [Min]	Quantity [% Area]	Height [mAU]	Area [mAU.Min]	Area % [%]
1	UNKNOWN	8.46	99.39	264.7	104.1	99.388
2	UNKNOWN	10.03	0.61	2.7	0.6	0.612
Total			100.00	267.5	104.7	100.000



### Peak Results :

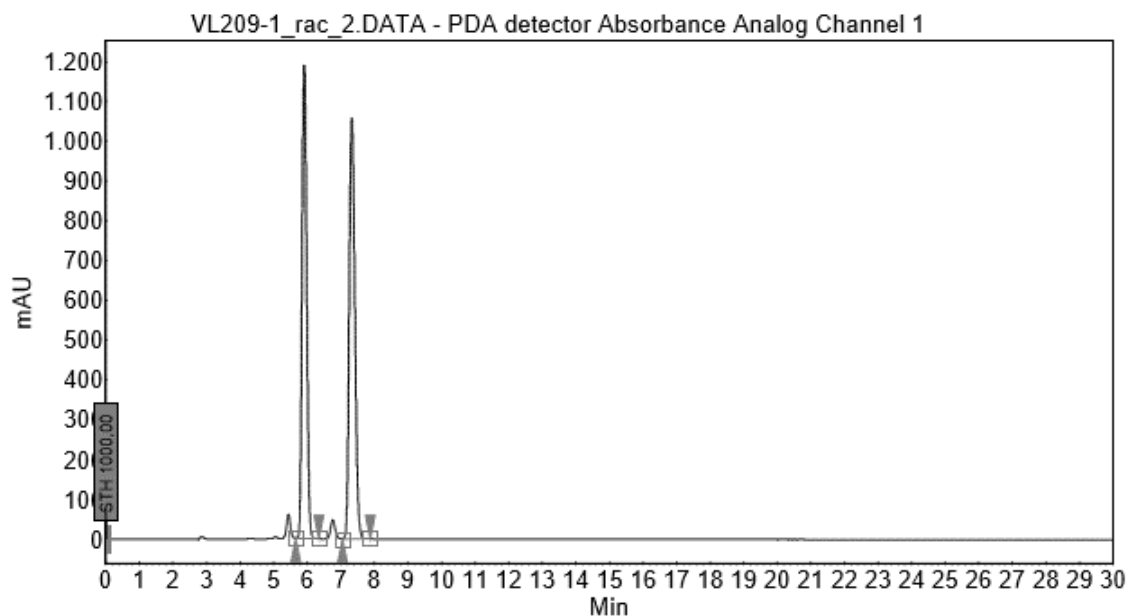
Index	Name	Time [Min]	Quantity [% Area]	Height [mAU]	Area [mAU.Min]	Area % [%]
1	UNKNOWN	8.31	49.86	800.5	184.2	49.858
2	UNKNOWN	9.39	50.14	733.3	185.3	50.142
Total			100.00	1533.8	369.5	100.000



### Peak Results :

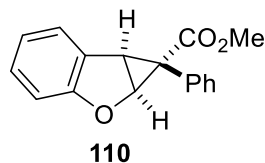
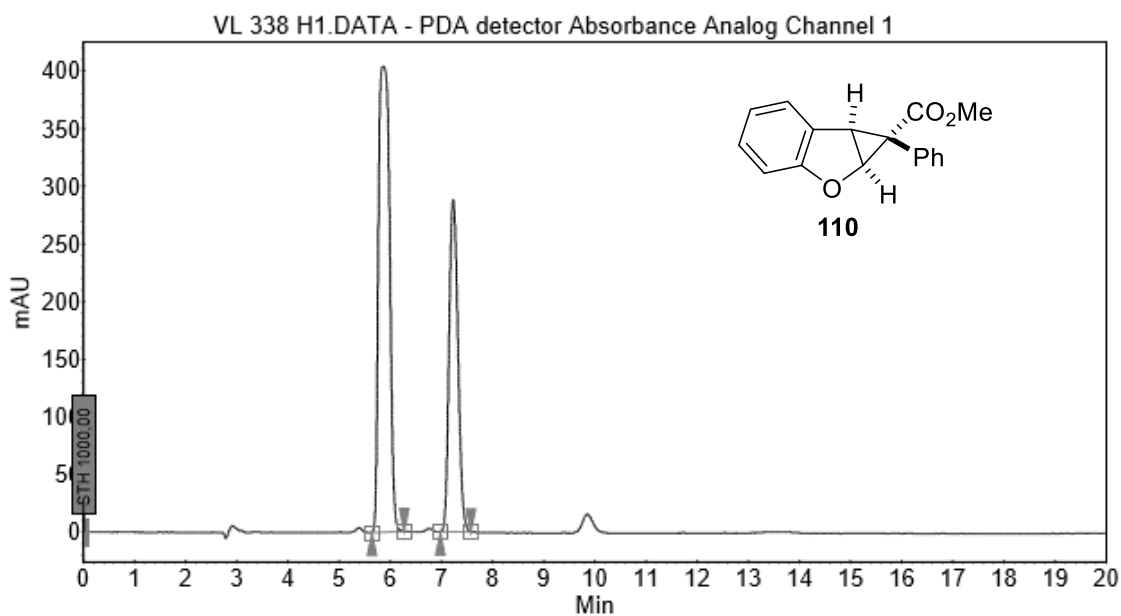
Index	Name	Time [Min]	Quantity [% Area]	Height [mAU]	Area [mAU.Min]	Area % [%]
1	UNKNOWN	8.22	87.05	1275.1	309.0	87.055
2	UNKNOWN	9.29	12.95	188.9	45.9	12.945
Total			100.00	1464.0	354.9	100.000





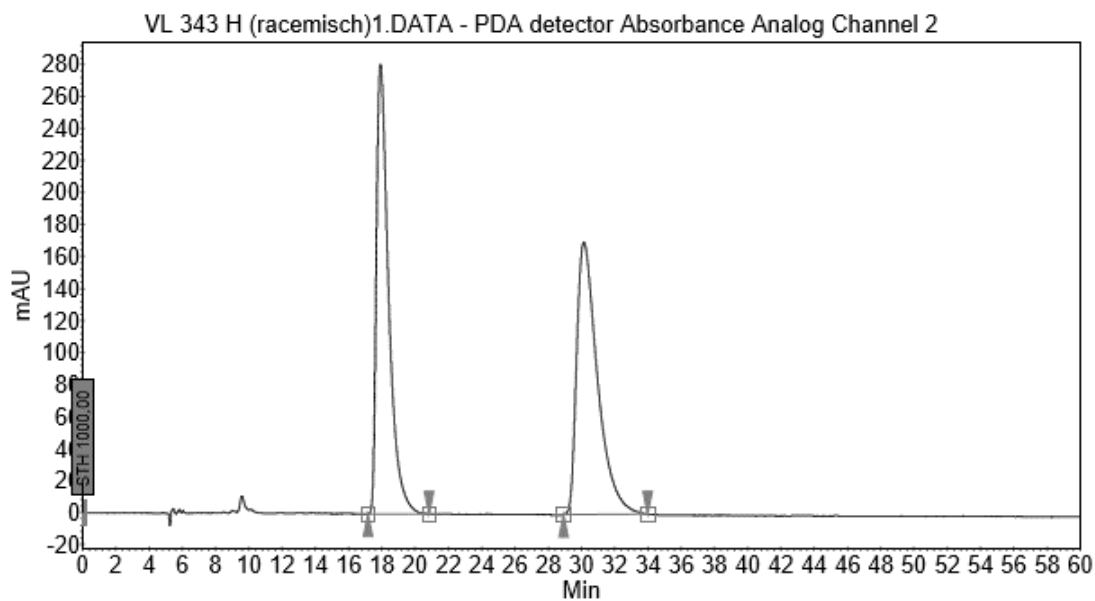
### Peak Results :

Index	Name	Time [Min]	Quantity [% Area]	Height [mAU]	Area [mAU.Min]	Area % [%]
1	UNKNOWN	5.91	48.02	1190.6	190.7	48.018
2	UNKNOWN	7.33	51.98	1058.3	206.5	51.982
Total			100.00	2248.8	397.2	100.000



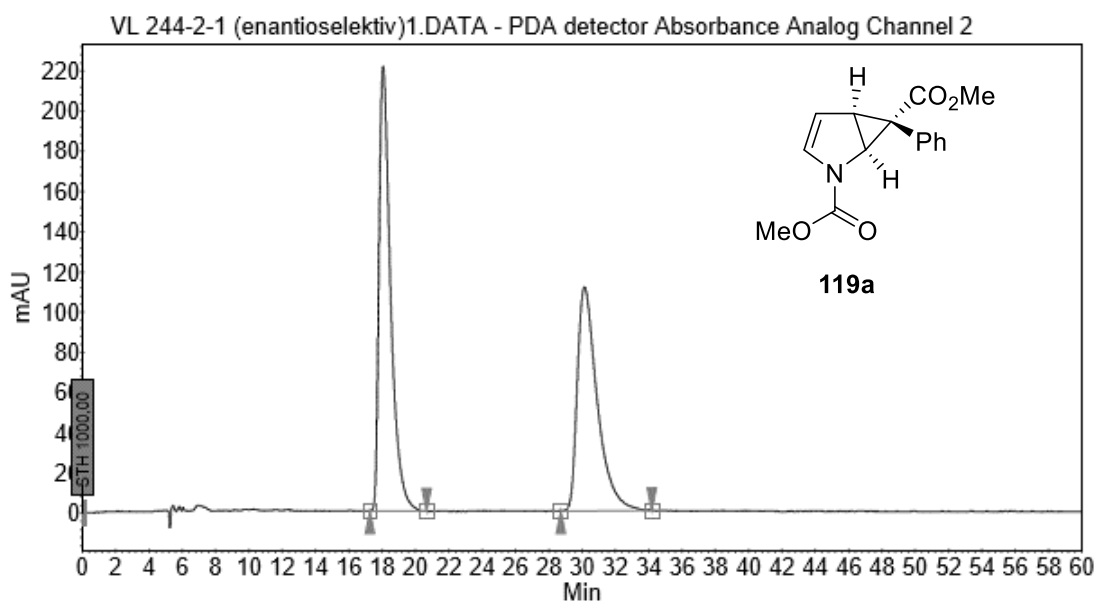
### Peak Results :

Index	Name	Time [Min]	Quantity [% Area]	Height [mAU]	Area [mAU.Min]	Area % [%]
1	UNKNOWN	5.86	63.65	403.8	101.4	63.646
2	UNKNOWN	7.23	36.35	288.0	57.9	36.354
Total			100.00	691.8	159.3	100.000



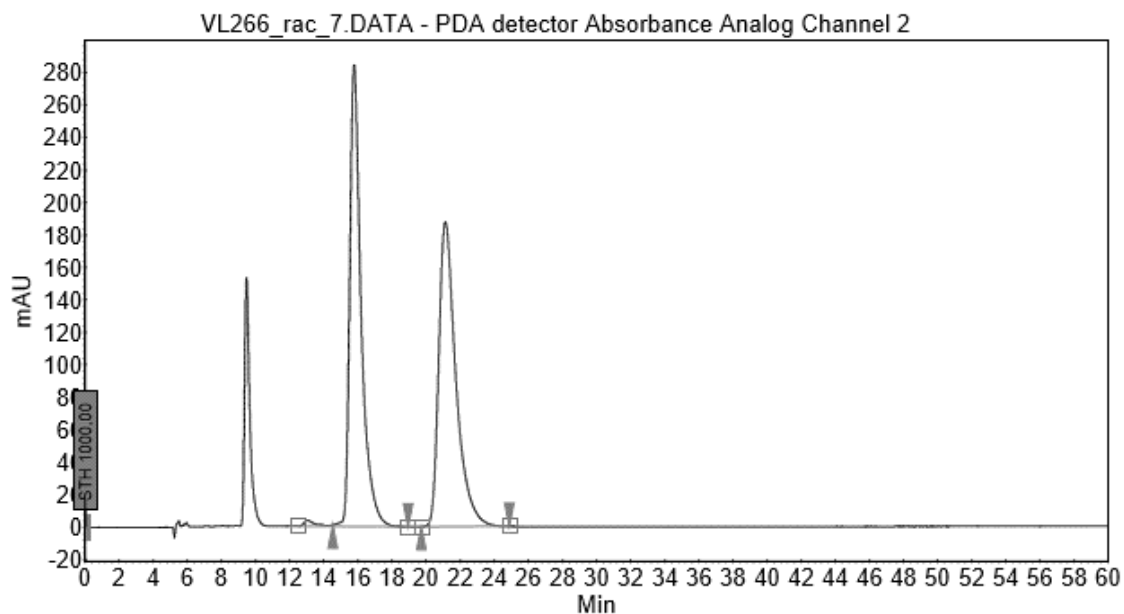
### Peak Results :

Index	Name	Time [Min]	Quantity [% Area]	Height [mAU]	Area [mAU.Min]	Area % [%]
1	UNKNOWN	17.92	49.28	280.7	240.1	49.284
2	UNKNOWN	30.15	50.72	170.3	247.1	50.716
Total			100.00	451.0	487.2	100.000



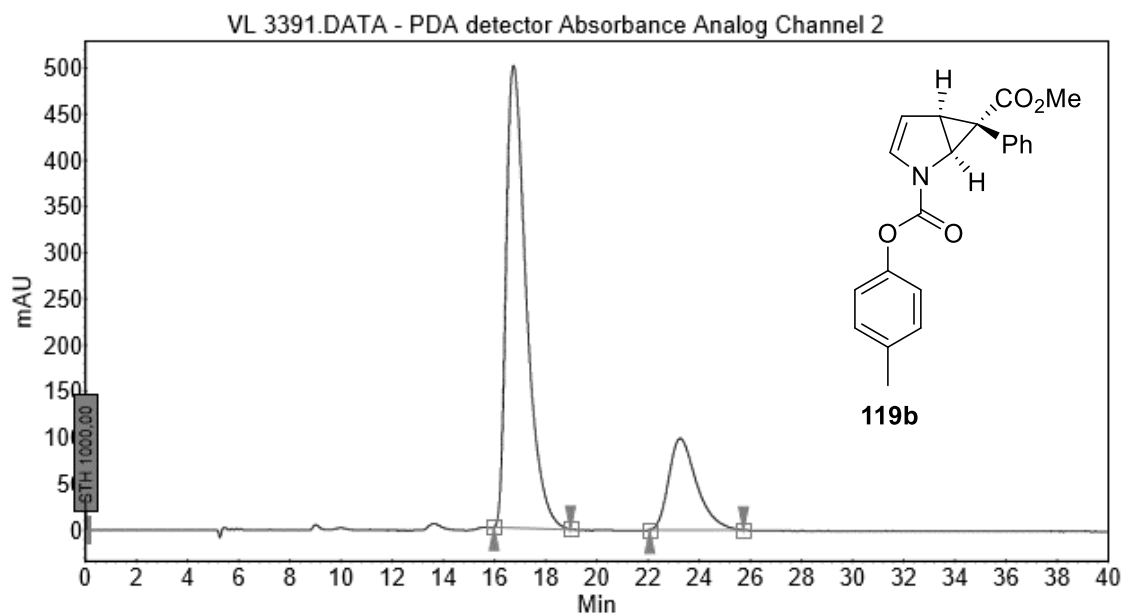
### Peak Results :

Index	Name	Time [Min]	Quantity [% Area]	Height [mAU]	Area [mAU.Min]	Area % [%]
1	UNKNOWN	18.05	53.71	221.2	178.3	53.707
2	UNKNOWN	30.14	46.29	111.4	153.7	46.293
Total			100.00	332.6	332.0	100.000



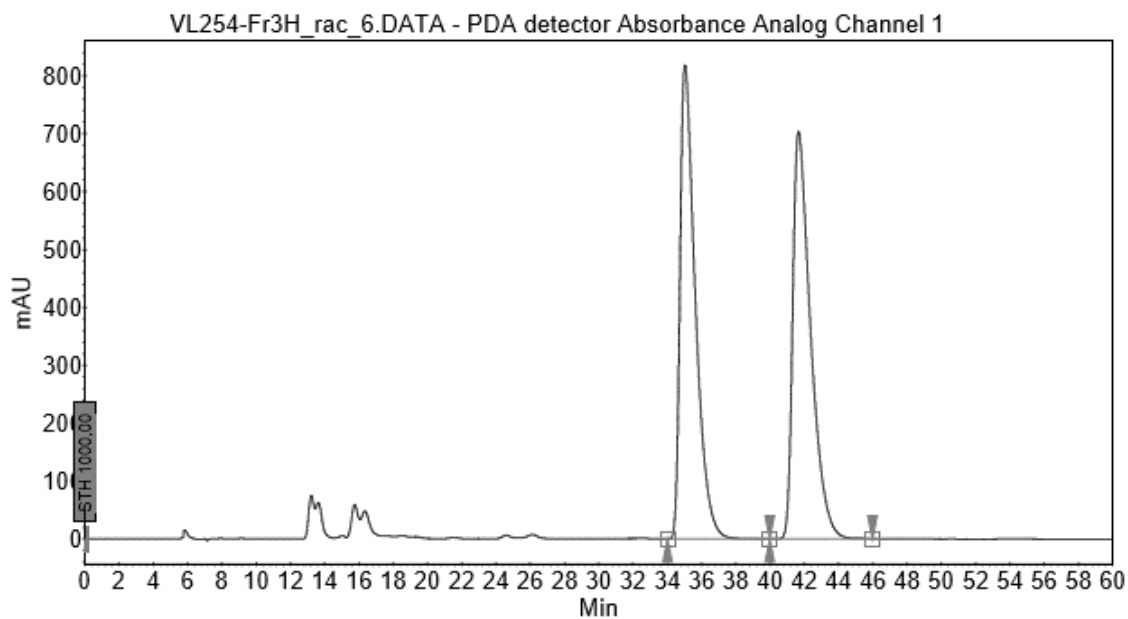
### Peak Results :

Index	Name	Time [Min]	Quantity [% Area]	Height [mAU]	Area [mAU Min]	Area % [%]
1	UNKNOWN	15.78	50.21	284.6	219.8	50.207
2	UNKNOWN	21.13	49.79	187.8	218.0	49.793
Total			100.00	472.4	437.7	100.000



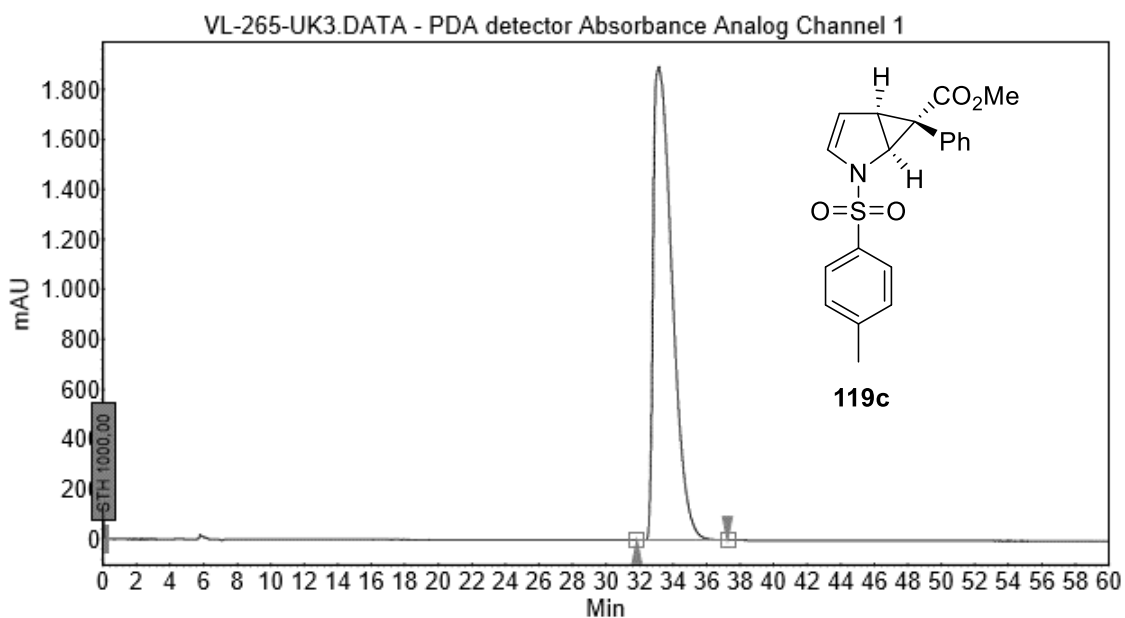
### Peak Results :

Index	Name	Time [Min]	Quantity [% Area]	Height [mAU]	Area [mAU Min]	Area % [%]
1	UNKNOWN	16.74	78.45	500.5	457.0	78.453
2	UNKNOWN	23.26	21.55	99.2	125.5	21.547
Total			100.00	599.6	582.5	100.000



### Peak Results :

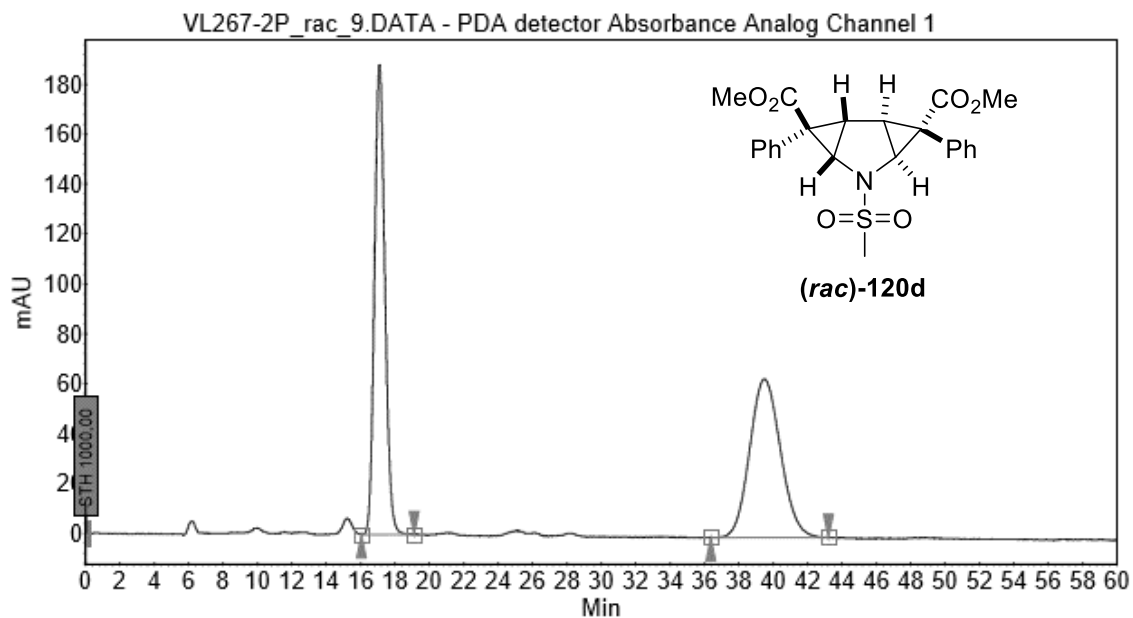
Index	Name	Time [Min]	Quantity [% Area]	Height [mAU]	Area [mAU.Min]	Area % [%]
1	UNKNOWN	35,04	49,97	819,2	846,5	49,971
2	UNKNOWN	41,66	50,03	704,2	847,4	50,029
Total			100,00	1523,5	1693,9	100,000



### Peak Results :

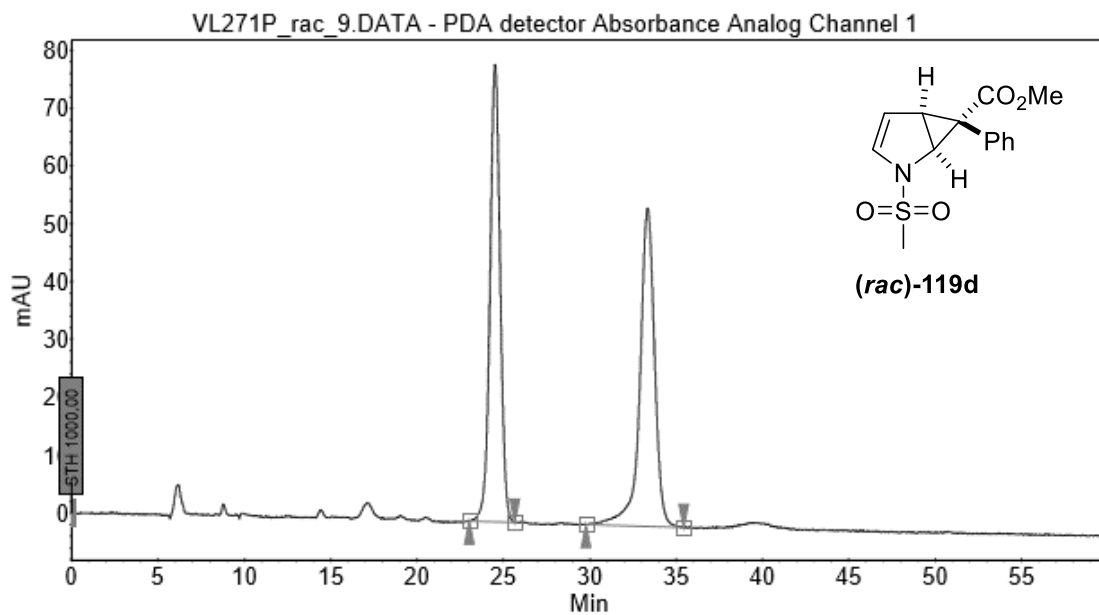
Index	Name	Time [Min]	Quantity [% Area]	Height [mAU]	Area [mAU.Min]	Area % [%]
1	UNKNOWN	33,16	100,00	1896,7	2472,8	100,000
Total			100,00	1896,7	2472,8	100,000

It was not feasible to separate **119d** and **120d**. Therefore, determination of the enantiomeric excess of **120d** was performed with a mixture of **119d** and **120d** and analytical HPLC was carried out for racemic **119d** as well as racemic **120d**.



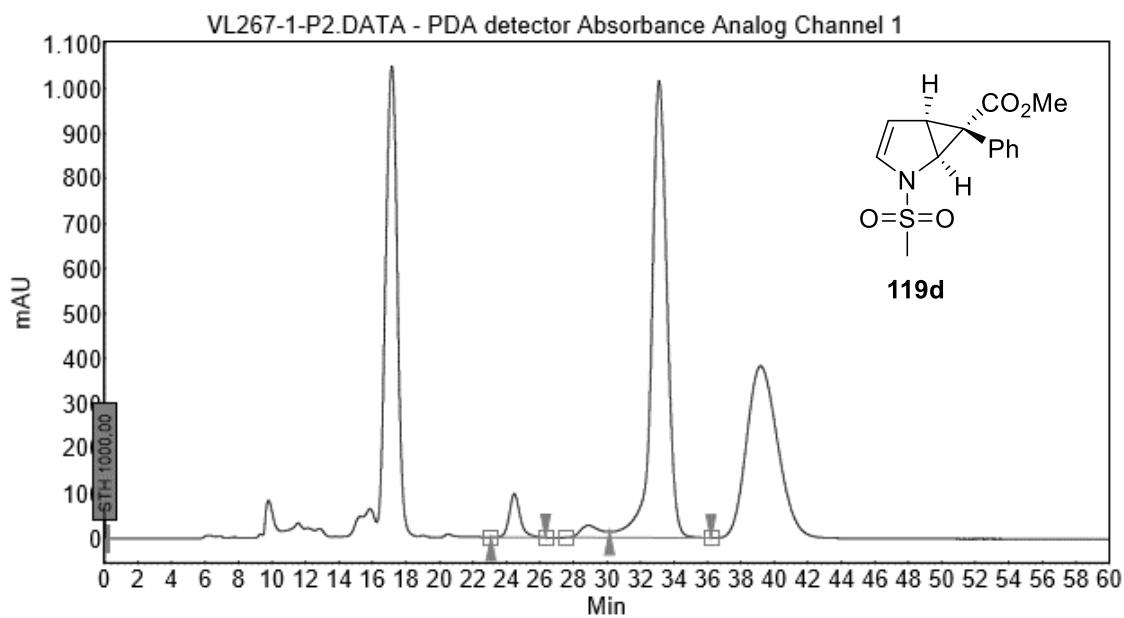
### Peak Results :

Index	Name	Time [Min]	Quantity [% Area]	Height [mAU]	Area [mAU.Min]	Area % [%]
1	UNKNOWN	17.10	49.93	188.5	132.5	49.934
2	UNKNOWN	39.52	50.07	63.7	132.8	50.066
Total			100.00	252.2	265.3	100.000



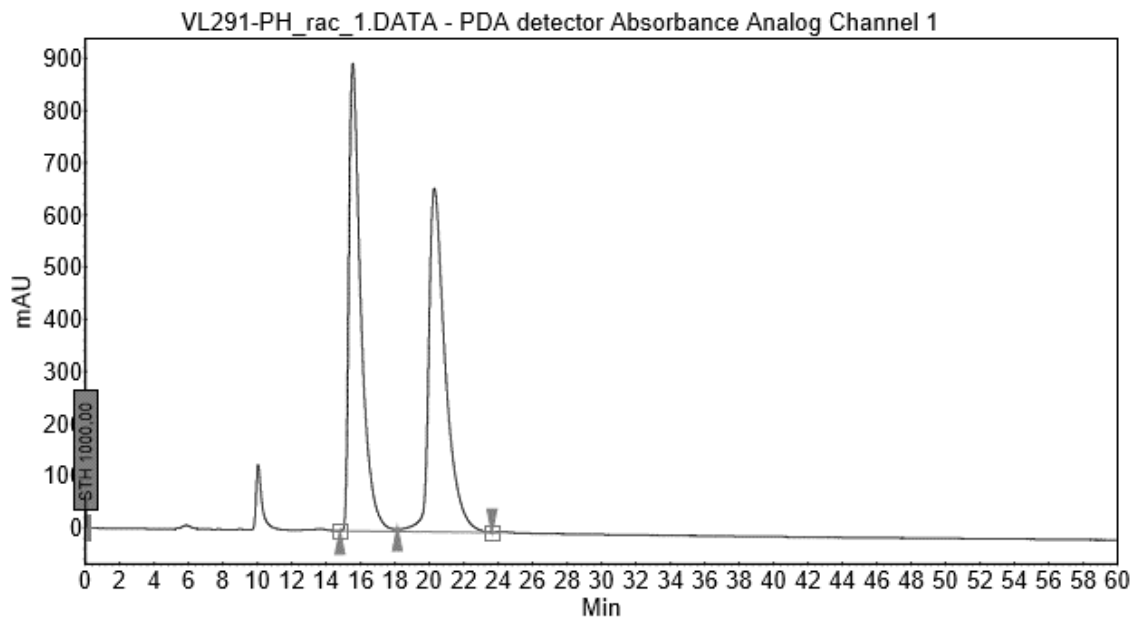
### Peak Results :

Index	Name	Time [Min]	Quantity [% Area]	Height [mAU]	Area [mAU.Min]	Area % [%]
1	UNKNOWN	24.52	49,61	79,2	53,9	49,612
2	UNKNOWN	33,35	50,39	55,0	54,8	50,388
Total			100,00	134,2	108,7	100,000



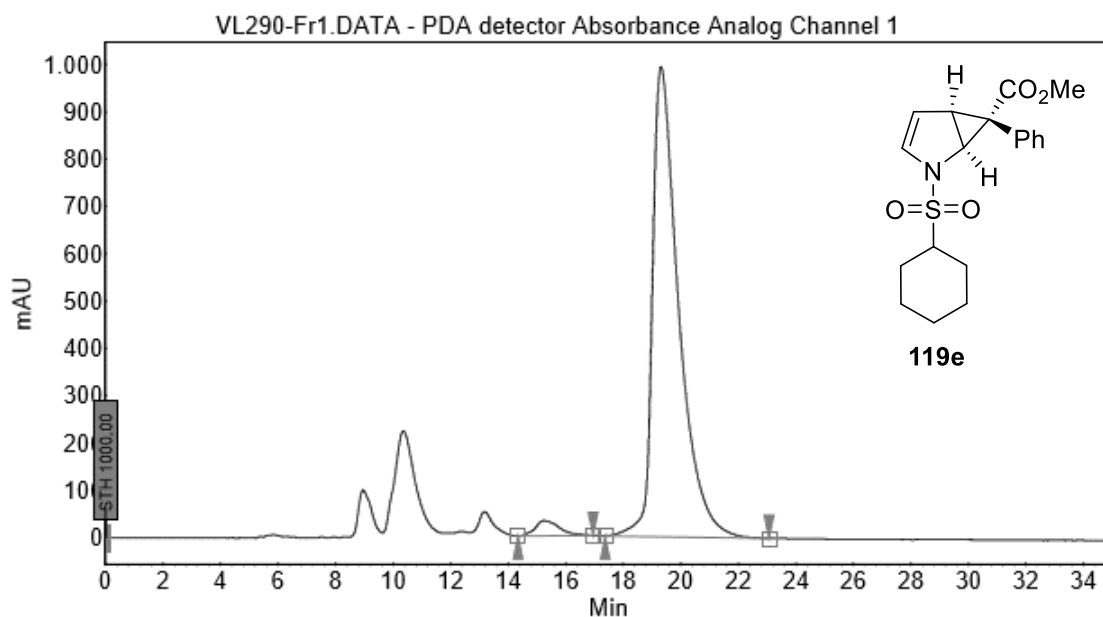
### Peak Results :

Index	Name	Time [Min]	Quantity [% Area]	Height [mAU]	Area [mAU.Min]	Area % [%]
1	UNKNOWN	24,47	6,40	97,6	74,7	6,404
2	UNKNOWN	33,12	93,60	1016,8	1091,3	93,596
Total			100,00	1114,4	1166,0	100,000



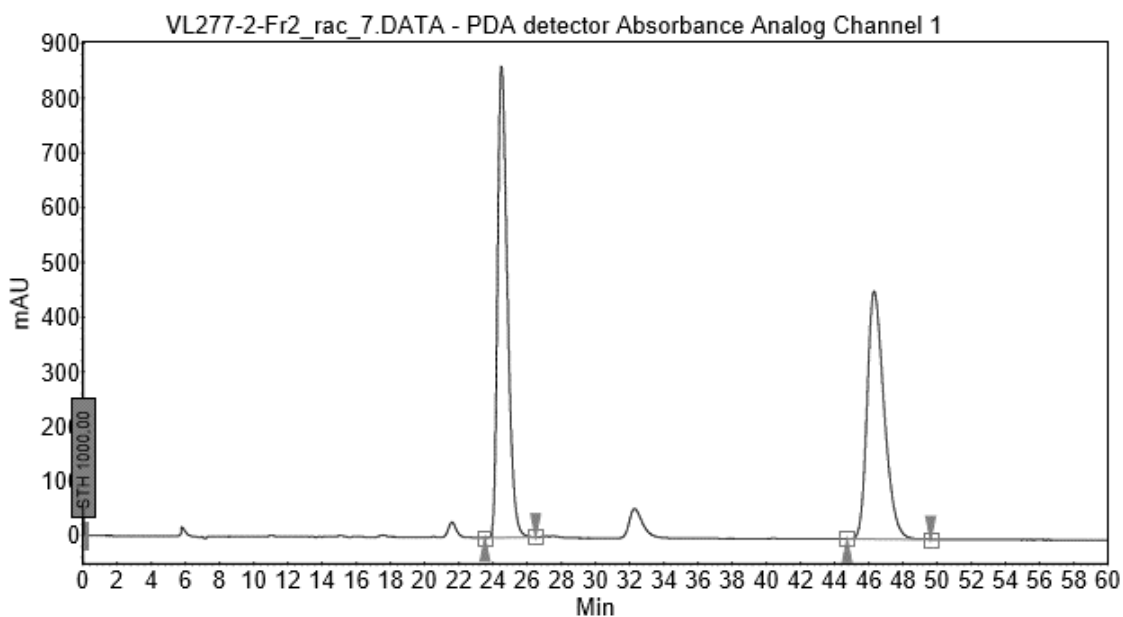
### Peak Results :

Index	Name	Time [Min]	Quantity [% Area]	Height [mAU]	Area [mAU.Min]	Area % [%]
1	UNKNOWN	15.55	49.58	896.6	722.9	49.581
2	UNKNOWN	20.29	50.42	658.6	735.1	50.419
Total			100.00	1555.2	1457.9	100.000



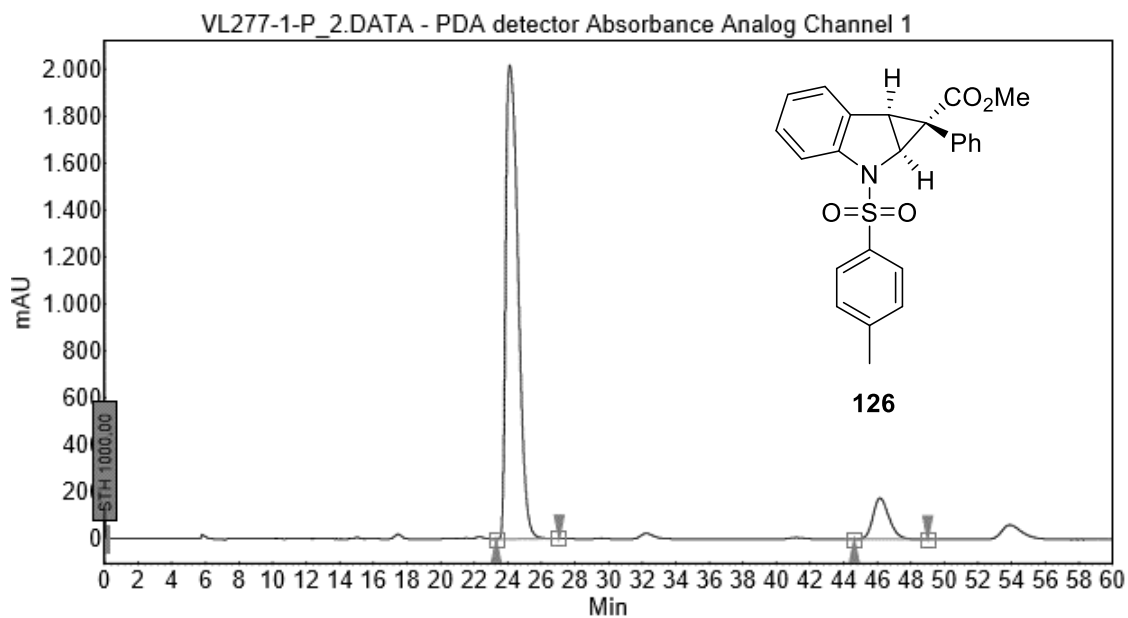
### Peak Results :

Index	Name	Time [Min]	Quantity [% Area]	Height [mAU]	Area [mAU.Min]	Area % [%]
1	UNKNOWN	15.24	2.98	32.7	32.2	2.981
2	UNKNOWN	19.31	97.02	994.2	1049.0	97.019
Total			100.00	1026.9	1081.3	100.000



### Peak Results :

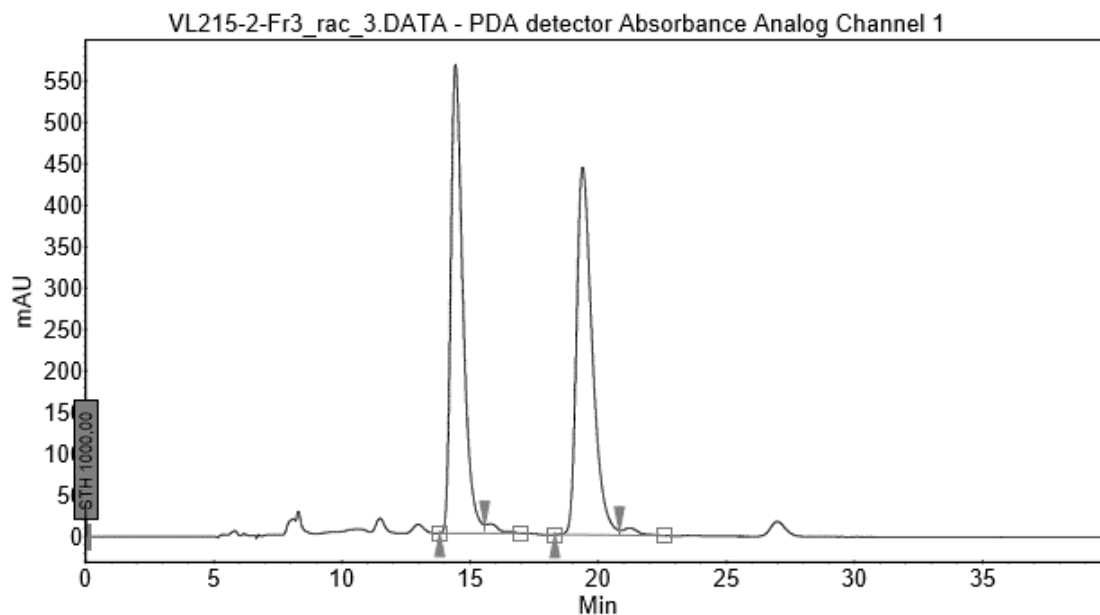
Index	Name	Time [Min]	Quantity [% Area]	Height [mAU]	Area [mAU.Min]	Area % [%]
1	UNKNOWN	24.50	52.48	862.7	576.3	52.485
2	UNKNOWN	46.31	47.52	453.8	521.7	47.515
Total			100.00	1316.5	1098.0	100.000



### Peak Results :

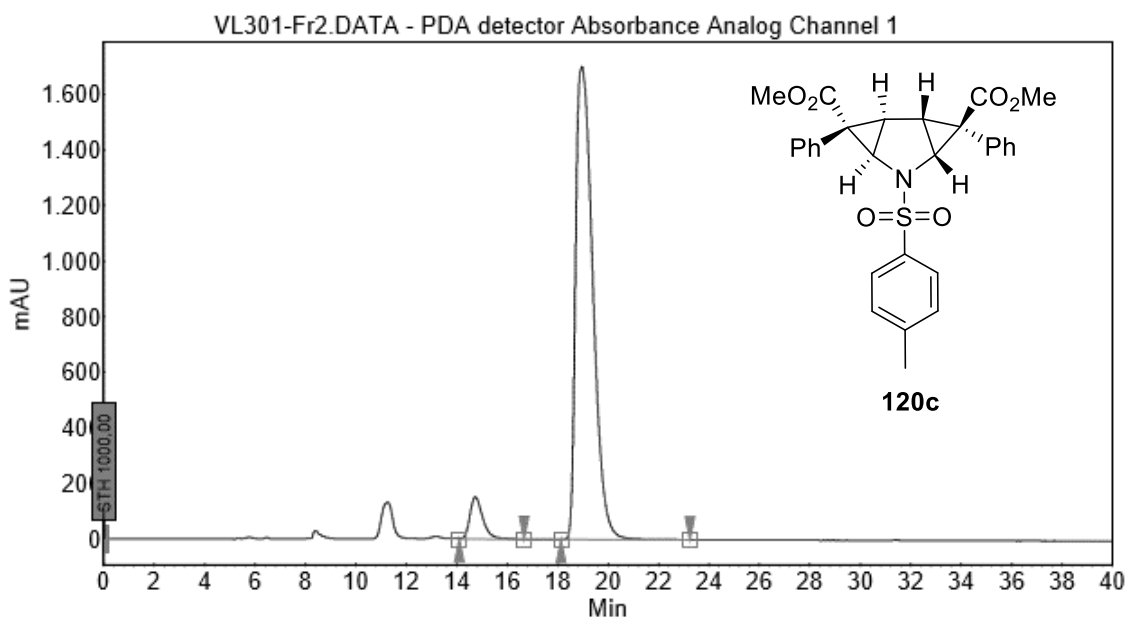
Index	Name	Time [Min]	Quantity [% Area]	Height [mAU]	Area [mAU.Min]	Area % [%]
1	UNKNOWN	24.13	89.81	2019.0	1722.7	89.809
2	UNKNOWN	46.16	10.19	175.0	195.5	10.191
Total			100.00	2194.0	1918.1	100.000





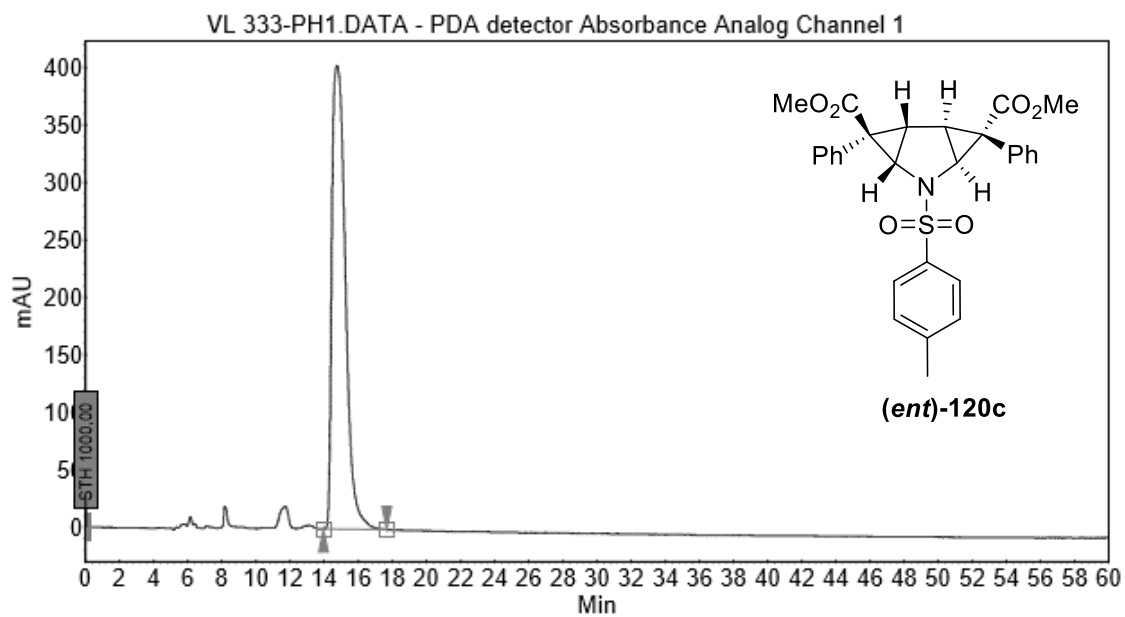
### Peak Results :

Index	Name	Time [Min]	Quantity [% Area]	Height [mAU]	Area [mAU.Min]	Area % [%]
1	UNKNOWN	14.43	49.62	565.9	310.5	49.617
2	UNKNOWN	19.39	50.38	443.8	315.3	50.383
Total			100.00	1009.7	625.9	100.000



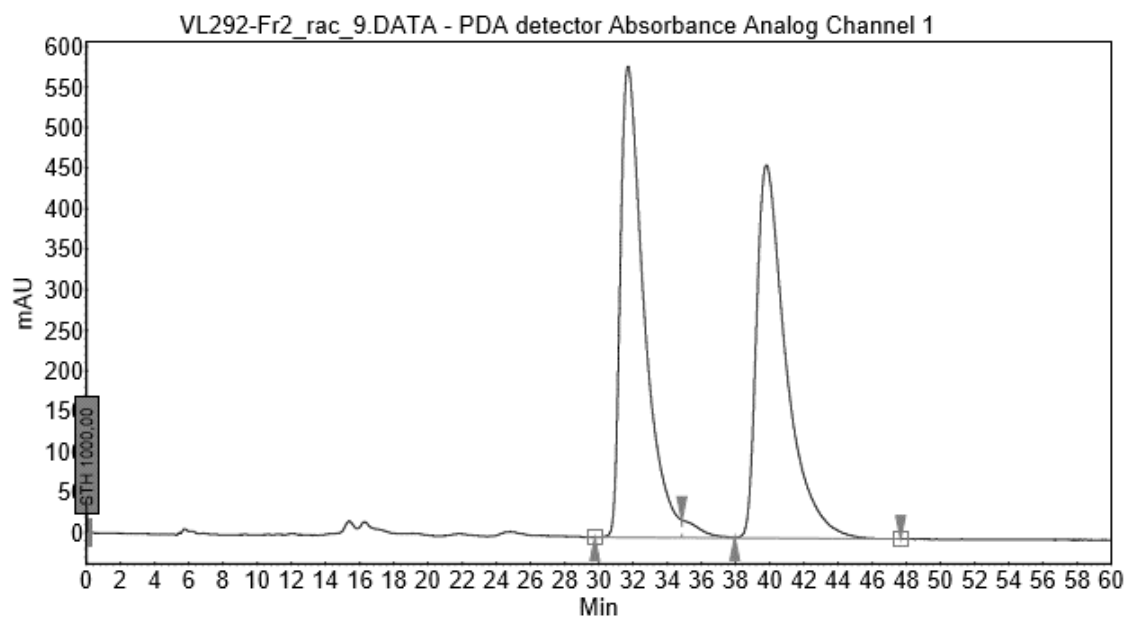
### Peak Results :

Index	Name	Time [Min]	Quantity [% Area]	Height [mAU]	Area [mAU.Min]	Area % [%]
1	UNKNOWN	14.73	6.17	151.0	88.4	6.175
2	UNKNOWN	18.97	93.83	1704.5	1342.9	93.825
Total			100.00	1855.5	1431.3	100.000



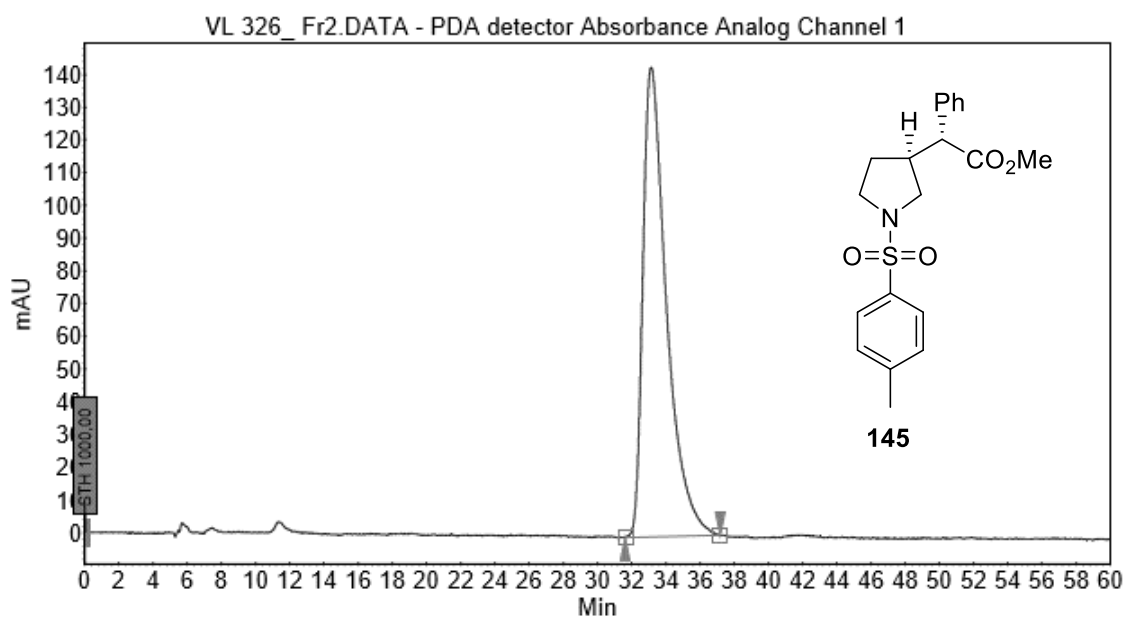
### Peak Results :

Index	Name	Time [Min]	Quantity [% Area]	Height [mAU]	Area [mAU.Min]	Area % [%]
1	UNKNOWN	14.75	100.00	403.7	370.8	100.000
Total			100.00	403.7	370.8	100.000



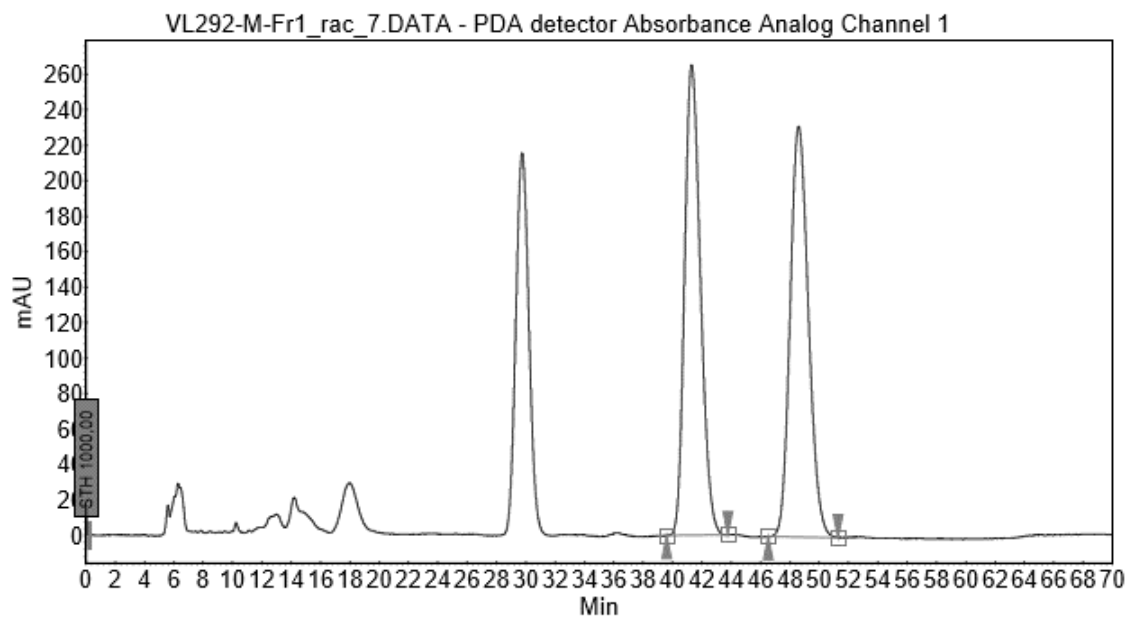
### Peak Results :

Index	Name	Time [Min]	Quantity [% Area]	Height [mAU]	Area [mAU.Min]	Area % [%]
1	UNKNOWN	31.72	50,23	582,0	931,7	50,229
2	UNKNOWN	39,80	49,77	461,0	923,2	49,771
Total			100,00	1043,0	1854,8	100,000



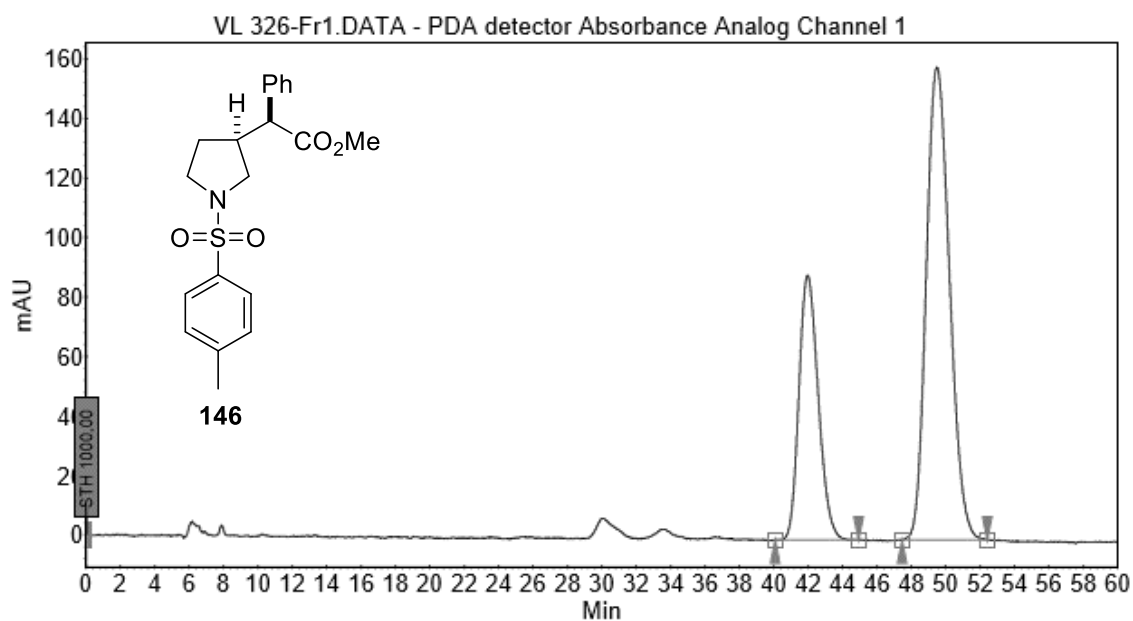
### Peak Results :

Index	Name	Time [Min]	Quantity [% Area]	Height [mAU]	Area [mAU.Min]	Area % [%]
1	UNKNOWN	33,14	100,00	143,4	229,7	100,000
Total			100,00	143,4	229,7	100,000



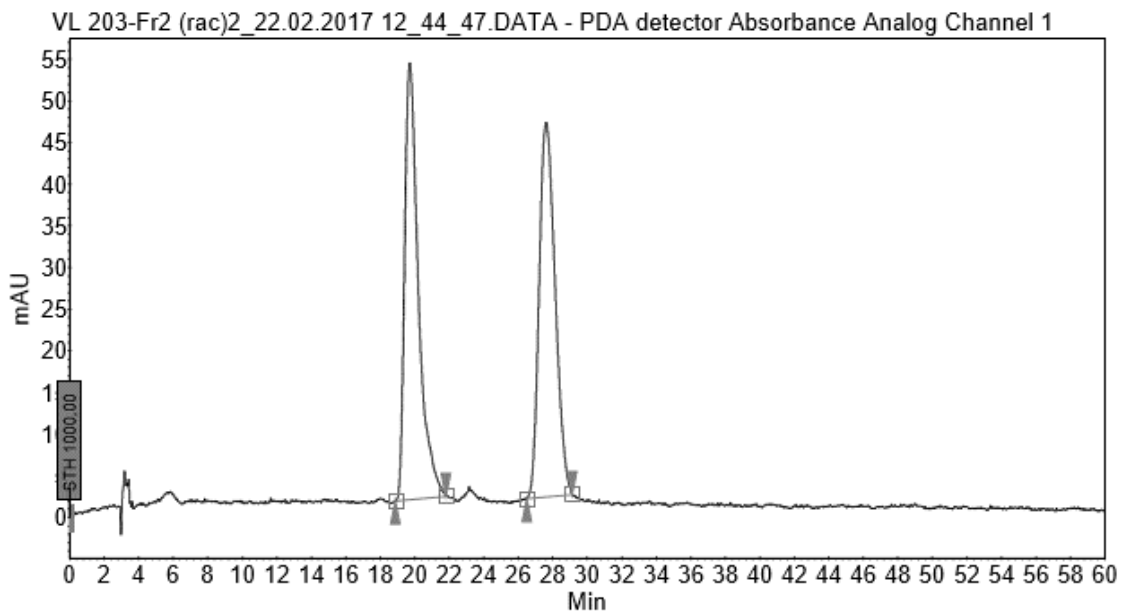
### Peak Results :

Index	Name	Time [Min]	Quantity [% Area]	Height [mAU]	Area [mAU.Min]	Area % [%]
1	UNKNOWN	41.31	49.82	265.2	332.0	49.822
2	UNKNOWN	48.59	50.18	231.7	334.4	50.178
Total			100.00	496.9	666.4	100.000



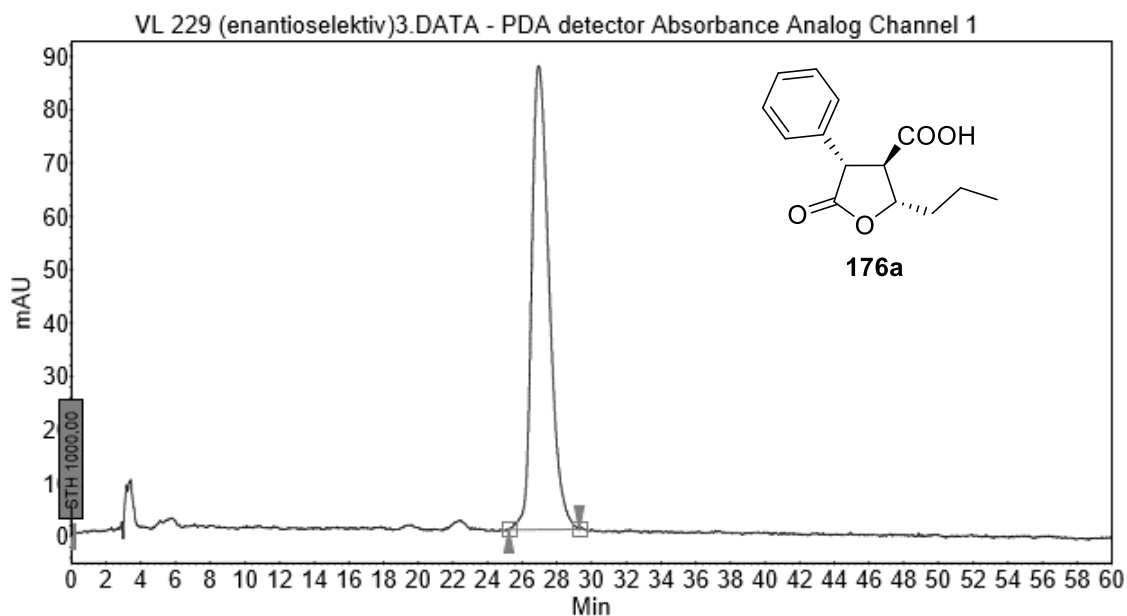
### Peak Results :

Index	Name	Time [Min]	Quantity [% Area]	Height [mAU]	Area [mAU.Min]	Area % [%]
1	UNKNOWN	41.96	31.67	89.0	115.7	31.672
2	UNKNOWN	49.49	68.33	159.0	249.5	68.328
Total			100.00	248.1	365.2	100.000



### Peak Results :

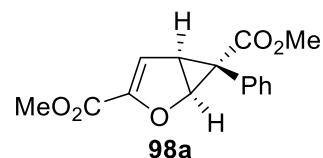
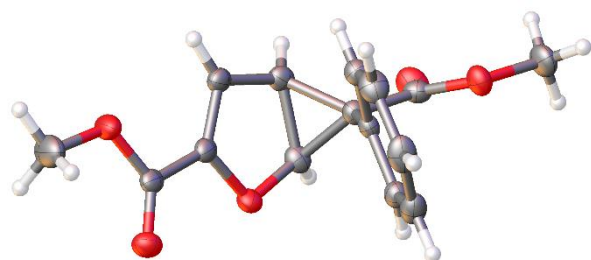
Index	Name	Time [Min]	Quantity [% Area]	Height [mAU]	Area [mAU.Min]	Area % [%]
1	UNKNOWN	19.71	50.06	52.4	48.2	50.056
2	UNKNOWN	27.62	49.94	44.9	48.1	49.944
Total			100.00	97.3	96.4	100.000



### Peak Results :

Index	Name	Time [Min]	Quantity [% Area]	Height [mAU]	Area [mAU.Min]	Area % [%]
1	UNKNOWN	26.94	100.00	87.0	101.5	100.000
Total			100.00	87.0	101.5	100.000

## 3 X-ray crystallography data

**Table 1.** Crystal data and structure refinement for **98a**.

Identification code	N053
Empirical formula	C <sub>15</sub> H <sub>14</sub> O <sub>5</sub>
Formula weight	274.26
Temperature/K	123.01(10)
Crystal system	monoclinic
Space group	P2 <sub>1</sub>
a/Å	9.82867(19)
b/Å	6.11703(12)
c/Å	11.6406(2)
α/°	90.00
β/°	100.4716(19)
γ/°	90.00
Volume/Å <sup>3</sup>	688.20(2)
Z	2
ρ <sub>calc</sub> /mg/mm <sup>3</sup>	1.324
m/mm <sup>-1</sup>	0.836
F(000)	288.0
Crystal size/mm <sup>3</sup>	0.3063 × 0.1966 × 0.0822
Radiation	CuKα (λ = 1.54184)
2θ range for data collection	7.72 to 128.36°
Index ranges	-11 ≤ h ≤ 11, -7 ≤ k ≤ 6, -13 ≤ l ≤ 13
Reflections collected	14187
Independent reflections	2224 [R <sub>int</sub> = 0.0329, R <sub>sigma</sub> = 0.0171]
Data/restraints/parameters	2224/1/183
Goodness-of-fit on F <sup>2</sup>	1.151
Final R indexes [I ≥ 2σ (I)]	R <sub>1</sub> = 0.0264, wR <sub>2</sub> = 0.0763

Final R indexes [all data]	$R_1 = 0.0268$ , $wR_2 = 0.0768$
Largest diff. peak/hole / $e \text{ \AA}^{-3}$	0.23/-0.26
Flack parameter	-0.07(15)

**Table 2.** Fractional Atomic Coordinates ( $\times 10^4$ ) and Equivalent Isotropic Displacement Parameters ( $\text{\AA}^2 \times 10^3$ ) for **98a**.  $U_{\text{eq}}$  is defined as 1/3 of the trace of the orthogonalized  $U_{\text{II}}$  tensor.

Atom	$x$	$y$	$z$	$U(\text{eq})$
O1	9747.2(9)	6201.8(16)	6023.9(8)	23.9(2)
O3	5667.2(10)	2859.1(18)	6751.6(8)	28.0(3)
O5	12918.2(10)	5455.7(18)	8012.8(10)	33.2(3)
O4	11998.5(10)	8580.6(19)	7196.4(9)	29.9(3)
O2	6438.6(11)	1719(2)	5150.6(9)	34.8(3)
C5	7939.9(14)	3788(2)	6593.8(12)	21.3(3)
C10	7994.7(13)	5105(2)	7683.5(11)	20.0(3)
C11	7486.6(15)	7231(2)	7598.0(13)	24.9(3)
C15	8514.1(15)	4251(3)	8784.0(12)	24.9(3)
C13	7969.6(16)	7591(3)	9682.3(14)	34.7(4)
C1	10776.4(14)	5220(3)	6824.6(12)	22.6(3)
C8	11933.7(14)	6641(3)	7344.0(12)	22.9(3)
C12	7462.4(15)	8464(3)	8589.9(14)	30.9(4)
C2	10556.4(14)	3115(2)	7013.0(12)	23.6(3)
C14	8497.4(15)	5492(3)	9776.1(13)	32.5(4)
C3	9208.3(15)	2498(3)	6320.4(12)	24.8(3)
C9	14147.9(17)	6652(4)	8524.1(18)	47.7(5)
C4	8741.2(15)	4558(3)	5665.6(12)	24.6(3)
C6	6623.6(14)	2689(2)	6075.5(12)	24.1(3)
C7	4347.4(16)	1842(3)	6297.6(15)	35.7(4)

**Table 3.** Anisotropic Displacement Parameters ( $\text{\AA}^2 \times 10^3$ ) for **98a**. The Anisotropic displacement factor exponent takes the form:  $-2\pi^2[h^2a^*U_{11}+2hka^*b^*U_{12}+\dots]$ .

Atom	$U_{11}$	$U_{22}$	$U_{33}$	$U_{23}$	$U_{13}$	$U_{12}$
O1	24.7(5)	25.2(6)	22.6(5)	4.9(4)	6.1(4)	-0.7(4)
O3	23.0(5)	29.7(6)	31.0(5)	-4.1(5)	4.5(4)	-7.3(5)
O5	22.7(5)	30.1(7)	44.0(6)	11.6(5)	-0.9(4)	-1.8(4)

O4	34.3(6)	22.3(7)	33.4(6)	0.7(5)	6.9(4)	-0.7(4)
O2	39.6(6)	37.7(7)	26.6(5)	-9.3(5)	4.9(4)	-10.3(5)
C5	23.1(7)	21.0(8)	20.2(7)	-1.8(6)	5.5(5)	-1.3(6)
C10	17.8(6)	21.6(8)	21.5(7)	-1.7(5)	5.9(5)	-3.9(5)
C11	22.0(7)	25.3(9)	27.5(7)	-1.4(6)	4.8(6)	-2.1(6)
C15	24.6(7)	26.1(8)	24.1(7)	-0.1(6)	4.7(5)	-1.7(6)
C13	32.8(8)	40.1(10)	32.2(8)	-17.5(8)	8.7(6)	-5.1(7)
C1	21.9(7)	25.7(8)	22.2(7)	3.5(6)	9.6(5)	3.3(6)
C8	24.3(7)	24.7(10)	22.1(7)	3.1(6)	10.8(6)	2.6(6)
C12	25.8(7)	26.0(8)	41.4(9)	-9.9(7)	7.2(6)	-1.8(6)
C2	23.9(7)	22.3(9)	26.6(7)	1.4(6)	9.8(5)	4.3(6)
C14	32.9(8)	43.4(10)	20.7(7)	-2.2(6)	3.4(6)	-3.7(7)
C3	28.7(8)	21.5(8)	26.3(7)	-2.8(6)	10.7(6)	0.6(6)
C9	27.0(8)	45.4(11)	65.2(12)	12.7(10)	-6.1(8)	-7.6(9)
C4	26.8(7)	27.4(8)	20.4(6)	-2.1(6)	6.5(5)	-2.6(6)
C6	29.1(7)	19.7(7)	23.1(7)	1.6(6)	3.9(6)	-0.6(6)
C7	25.1(8)	34.8(9)	45.5(9)	-2.5(7)	1.6(7)	-10.8(7)

**Table 4.** Bond Lengths for **98a**.

Atom	Atom	Length/Å	Atom	Atom	Length/Å
O1	C1	1.3821(17)	C5	C6	1.4854(19)
O1	C4	1.4189(18)	C10	C11	1.390(2)
O3	C6	1.3352(17)	C10	C15	1.391(2)
O3	C7	1.4490(17)	C11	C12	1.383(2)
O5	C8	1.3396(18)	C15	C14	1.385(2)
O5	C9	1.446(2)	C13	C12	1.386(2)
O4	C8	1.202(2)	C13	C14	1.381(3)
O2	C6	1.2134(18)	C1	C8	1.472(2)
C5	C10	1.4954(19)	C1	C2	1.330(2)
C5	C3	1.5562(19)	C2	C3	1.469(2)
C5	C4	1.5228(19)	C3	C4	1.500(2)

**Table 5.** Bond Angles for **98a**.

Atom	Atom	Atom	Angle/°	Atom	Atom	Atom	Angle/°
C1	O1	C4	106.01(11)	C2	C1	C8	129.85(14)



C6	O3	C7	115.53(11)	O5	C8	C1	109.97(13)
C8	O5	C9	115.25(13)	O4	C8	O5	124.47(14)
C10	C5	C3	122.67(11)	O4	C8	C1	125.56(13)
C10	C5	C4	119.46(12)	C11	C12	C13	119.88(16)
C4	C5	C3	58.31(10)	C1	C2	C3	108.38(13)
C6	C5	C10	118.88(11)	C13	C14	C15	120.31(15)
C6	C5	C3	111.01(12)	C2	C3	C5	115.70(12)
C6	C5	C4	112.11(11)	C2	C3	C4	103.03(12)
C11	C10	C5	119.09(13)	C4	C3	C5	59.73(9)
C11	C10	C15	118.93(14)	O1	C4	C5	115.67(11)
C15	C10	C5	121.97(14)	O1	C4	C3	108.25(11)
C12	C11	C10	120.71(15)	C3	C4	C5	61.96(10)
C14	C15	C10	120.28(15)	O3	C6	C5	112.31(11)
C14	C13	C12	119.86(15)	O2	C6	O3	123.58(13)
O1	C1	C8	115.89(12)	O2	C6	C5	124.10(13)
C2	C1	O1	114.25(13)				

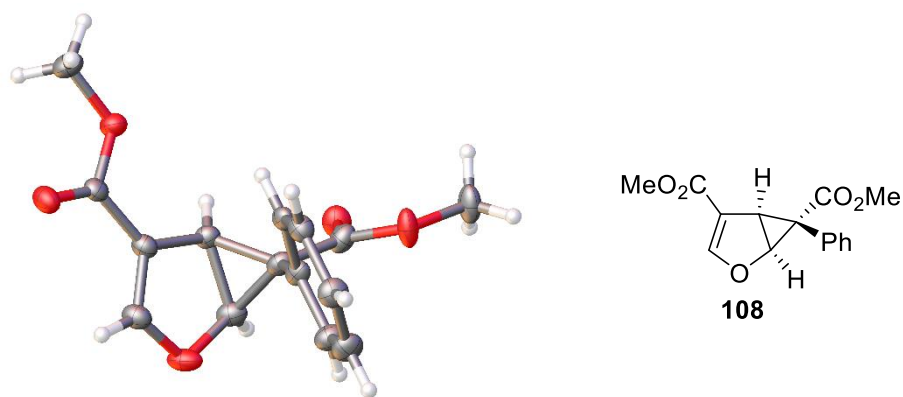
**Table 6.** Torsion Angles for **98a**.

<b>A</b>	<b>B</b>	<b>C</b>	<b>D</b>	<b>Angle/°</b>	<b>A</b>	<b>B</b>	<b>C</b>	<b>D</b>	<b>Angle/°</b>
O1	C1	C8	O5	-174.02(11)	C2	C3	C4	C5	-112.36(12)
O1	C1	C8	O4	5.95(19)	C14	C13	C12	C11	0.0(2)
O1	C1	C2	C3	-2.44(16)	C3	C5	C10	C11	131.53(14)
C5	C10	C11	C12	177.05(13)	C3	C5	C10	C15	-49.8(2)
C5	C10	C15	C14	-177.43(13)	C3	C5	C4	O1	-97.91(13)
C5	C3	C4	O1	109.94(12)	C3	C5	C6	O3	144.15(12)
C10	C5	C3	C2	-16.4(2)	C3	C5	C6	O2	-35.0(2)
C10	C5	C3	C4	-106.90(15)	C9	O5	C8	O4	-3.1(2)
C10	C5	C4	O1	14.41(19)	C9	O5	C8	C1	176.82(13)
C10	C5	C4	C3	112.33(14)	C4	O1	C1	C8	-178.70(10)
C10	C5	C6	O3	-6.56(19)	C4	O1	C1	C2	0.81(15)
C10	C5	C6	O2	174.33(13)	C4	C5	C10	C11	62.29(17)
C10	C11	C12	C13	1.1(2)	C4	C5	C10	C15	-119.02(15)
C10	C15	C14	C13	-0.2(2)	C4	C5	C3	C2	90.50(14)
C11	C10	C15	C14	1.3(2)	C4	C5	C6	O3	-152.68(12)
C15	C10	C11	C12	-1.7(2)	C4	C5	C6	O2	28.2(2)
C1	O1	C4	C5	68.13(14)	C6	C5	C10	C11	-81.33(17)

C1	O1	C4	C3	1.13(14)	C6	C5	C10	C15	97.36(16)
C1	C2	C3	C5	-59.56(16)	C6	C5	C3	C2	-165.80(12)
C1	C2	C3	C4	2.87(15)	C6	C5	C3	C4	103.69(13)
C8	C1	C2	C3	176.99(12)	C6	C5	C4	O1	160.32(12)
C12	C13	C14	C15	-0.4(2)	C6	C5	C4	C3	-101.77(13)
C2	C1	C8	O5	6.56(19)	C7	O3	C6	O2	-1.5(2)
C2	C1	C8	O4	-173.47(15)	C7	O3	C6	C5	179.43(14)
C2	C3	C4	O1	-2.41(14)					

**Table 7.** Hydrogen Atom Coordinates ( $\text{\AA} \times 10^4$ ) and Isotropic Displacement Parameters ( $\text{\AA}^2 \times 10^3$ ) for **98a**.

Atom	<i>x</i>	<i>y</i>	<i>z</i>	U(eq)
H11	7159	7831	6866	30
H15	8874	2842	8853	30
H13	7955	8416	10351	42
H12	7106	9876	8524	37
H2	11154	2191	7500	28
H14	8843	4910	10509	39
H3	9083	1076	5928	30
H9A	14534	7346	7917	72
H9B	14814	5662	8948	72
H9C	13912	7744	9047	72
H4	8306	4463	4840	30
H7A	3896	2631	5622	54
H7B	3777	1867	6885	54
H7C	4495	356	6085	54

**Table 1.** Crystal data and structure refinement for **108**.

Identification code	Q072
Empirical formula	C <sub>15</sub> H <sub>14</sub> O <sub>5</sub>
Formula weight	274.26
Temperature/K	123.00(10)
Crystal system	monoclinic
Space group	C2
a/Å	16.4819(2)
b/Å	5.77330(10)
c/Å	14.4387(2)
α/°	90
β/°	106.4900(10)
γ/°	90
Volume/Å <sup>3</sup>	1317.40(3)
Z	4
ρ <sub>calc</sub> /mg/mm <sup>3</sup>	1.383
m/mm <sup>-1</sup>	0.874
F(000)	576.0
Crystal size/mm <sup>3</sup>	0.209 × 0.089 × 0.059
Radiation	CuKα (λ = 1.54184)
2θ range for data collection	11.198 to 147.04°
Index ranges	-20 ≤ h ≤ 20, -6 ≤ k ≤ 7, -17 ≤ l ≤ 17
Reflections collected	19381
Independent reflections	2593 [R <sub>int</sub> = 0.0373, R <sub>sigma</sub> = 0.0183]
Data/restraints/parameters	2593/217/233
Goodness-of-fit on F <sup>2</sup>	1.047
Final R indexes [I ≥ 2σ (I)]	R <sub>1</sub> = 0.0287, wR <sub>2</sub> = 0.0738

Final R indexes [all data]	$R_1 = 0.0302$ , $wR_2 = 0.0751$
Largest diff. peak/hole / $e \text{ \AA}^{-3}$	0.14/-0.16
Flack parameter	0.03(8)

**Table 2.** Fractional Atomic Coordinates ( $\times 10^4$ ) and Equivalent Isotropic Displacement Parameters ( $\text{\AA}^2 \times 10^3$ ) for **108**.  $U_{\text{eq}}$  is defined as 1/3 of the trace of the orthogonalized  $U_{\text{II}}$  tensor.

Atom	$x$	$y$	$z$	$U(\text{eq})$
O5	8505.1(8)	2891(3)	9218.3(9)	25.8(3)
O4	8198.8(9)	5857(3)	10077.7(9)	29.6(3)
O2	7391.5(8)	2988(3)	5573.1(9)	30.4(3)
O3	7229.1(9)	8871(3)	7299.9(10)	30.8(3)
O1	6022(8)	2837(13)	5436(8)	29.8(14)
C14	8174.1(11)	4976(4)	9310.8(13)	21.9(4)
C13	7484.0(12)	8181(4)	8239.4(14)	26.5(4)
C3	6816.0(11)	4808(4)	6730.6(13)	23.6(4)
C2	6789.5(11)	3334(4)	5871.2(13)	27.1(4)
C4	6015(3)	4772(10)	7059(4)	22.3(11)
C9	5348(3)	6216(9)	6596(4)	28.5(10)
C8	4603(3)	6191(10)	6866(4)	31.6(10)
C7	4525(3)	4723(10)	7598(4)	30.1(11)
C6	5192(5)	3279(10)	8061(4)	25.7(11)
C5	5937(4)	3304(11)	7791(5)	21.5(10)
C12	7799.6(11)	6035(4)	8366.1(13)	22.4(4)
C11	7727.0(11)	5011(4)	7404.5(13)	22.1(4)
C10	7353.5(12)	6967(4)	6728.2(14)	26.2(4)
C15	8905.8(13)	1711(4)	10114.2(14)	30.7(4)
C1	5918(6)	1582(13)	4535(6)	34.8(15)
C4A	6077(2)	4988(8)	7130(3)	23.2(10)
C9A	5530(2)	6870(7)	6911(3)	26.9(9)
C8A	4806(2)	6909(7)	7222(3)	31.3(9)
C7A	4629(3)	5066(8)	7754(3)	29.2(9)
C6A	5176(4)	3184(7)	7973(4)	26.4(10)
C5A	5900(4)	3145(7)	7662(4)	24.6(10)
O1A	6016(9)	2133(17)	5492(10)	32.7(18)
C1A	5949(7)	683(16)	4660(7)	36.0(17)

**Table 3.** Anisotropic Displacement Parameters ( $\text{\AA}^2 \times 10^3$ ) for **108**. The Anisotropic displacement factor exponent takes the form:  $-2\pi^2[h^2a^2U_{11}+2hka^*b^*U_{12}+\dots]$ .

Atom	U <sub>11</sub>	U <sub>22</sub>	U <sub>33</sub>	U <sub>23</sub>	U <sub>13</sub>	U <sub>12</sub>
O5	29.8(6)	23.5(7)	24.0(6)	1.8(6)	7.2(5)	4.5(6)
O4	40.8(8)	24.3(7)	24.8(7)	-2.8(6)	10.9(6)	-2.3(6)
O2	26.9(6)	37.4(8)	30.6(7)	-6.3(6)	14.0(5)	1.6(6)
O3	44.3(8)	22.3(7)	31.5(7)	6.8(6)	19.8(6)	9.2(6)
O1	25.3(18)	40(4)	25.4(18)	-12(3)	8.9(13)	-1(3)
C14	22.4(8)	18.4(9)	25.8(9)	-0.5(8)	8.5(6)	-2.8(7)
C13	34.1(9)	21.7(10)	27.8(9)	-0.6(8)	15.3(7)	1.6(8)
C3	22.2(8)	27.8(10)	22.5(9)	3.4(8)	8.9(7)	7.0(8)
C2	23.7(9)	37.3(12)	20.4(8)	1.3(8)	6.3(7)	4.6(8)
C4	23.4(18)	26(2)	18.8(18)	-3.2(17)	8.2(17)	6.1(17)
C9	28.6(19)	32(2)	27(2)	5.6(18)	10.7(17)	5.8(17)
C8	25.8(19)	35(2)	35(2)	0.9(18)	10.4(16)	8.8(17)
C7	26.8(19)	35(2)	32.4(19)	0.9(18)	14.6(17)	1.5(17)
C6	29.1(19)	27(2)	23.2(19)	-2.8(18)	11.6(17)	-2.3(19)
C5	26.0(18)	20.3(19)	18.4(18)	-4.7(16)	6.8(15)	2.5(17)
C12	25.6(9)	20.3(9)	23.7(9)	-0.9(7)	10.9(7)	0.2(7)
C11	22.4(8)	22.9(9)	22.4(8)	-0.2(8)	8.8(6)	3.5(7)
C10	29.8(9)	26.2(10)	26.4(9)	4.0(8)	13.9(7)	7.3(8)
C15	32.7(10)	31.3(12)	27.3(9)	8.2(9)	7.2(7)	6.6(9)
C1	27.6(18)	45(4)	31(2)	-16(3)	6.3(17)	2(3)
C4A	22.5(16)	25.5(18)	21.6(17)	1.0(16)	6.5(15)	2.0(15)
C9A	25.1(16)	26.6(19)	31.3(19)	6.0(16)	11.6(14)	3.4(14)
C8A	25.8(17)	31(2)	39(2)	3.6(17)	11.8(15)	7.5(15)
C7A	26.2(16)	33.9(19)	30.7(17)	-2.2(16)	13.3(14)	1.5(15)
C6A	30.7(17)	26.4(18)	23.6(16)	0.4(16)	10.1(15)	-3.5(16)
C5A	26.3(16)	23.8(17)	22.9(18)	-1.4(16)	6.0(14)	3.2(16)
O1A	22(2)	48(5)	29(3)	-20(4)	8.1(17)	-8(4)
C1A	29(2)	50(5)	28(3)	-19(3)	8(2)	-4(4)

**Table 4.** Bond Lengths for **108**.

Atom	Atom	Length/Å	Atom	Atom	Length/Å
O5	C14	1.344(2)	C4	C9	1.3900
O5	C15	1.445(2)	C4	C5	1.3900
O4	C14	1.208(2)	C9	C8	1.3900
O2	C2	1.205(2)	C8	C7	1.3900
O3	C13	1.361(2)	C7	C6	1.3900
O3	C10	1.424(2)	C6	C5	1.3900
O1	C2	1.275(12)	C12	C11	1.482(2)
O1	C1	1.456(10)	C11	C10	1.506(3)
C14	C12	1.462(2)	C4A	C9A	1.3900
C13	C12	1.336(3)	C4A	C5A	1.3900
C3	C2	1.495(3)	C9A	C8A	1.3900
C3	C4	1.524(5)	C8A	C7A	1.3900
C3	C11	1.544(2)	C7A	C6A	1.3900
C3	C10	1.530(3)	C6A	C5A	1.3900
C3	C4A	1.492(4)	O1A	C1A	1.443(12)
C2	O1A	1.418(13)			

**Table 5.** Bond Angles for **108**.

Atom	Atom	Atom	Angle/°	Atom	Atom	Atom	Angle/°
C14	O5	C15	115.38(15)	C8	C9	C4	120.0
C13	O3	C10	107.29(15)	C9	C8	C7	120.0
C2	O1	C1	113.6(8)	C6	C7	C8	120.0
O5	C14	C12	110.94(15)	C5	C6	C7	120.0
O4	C14	O5	123.98(18)	C6	C5	C4	120.0
O4	C14	C12	125.07(19)	C14	C12	C11	127.42(18)
C12	C13	O3	113.95(17)	C13	C12	C14	124.07(17)
C2	C3	C4	115.2(3)	C13	C12	C11	108.48(17)
C2	C3	C11	111.11(15)	C12	C11	C3	115.20(15)
C2	C3	C10	110.03(16)	C12	C11	C10	102.58(16)
C4	C3	C11	125.3(2)	C10	C11	C3	60.18(13)
C4	C3	C10	124.4(3)	O3	C10	C3	116.68(15)
C10	C3	C11	58.65(12)	O3	C10	C11	107.63(15)
C4A	C3	C2	121.7(2)	C11	C10	C3	61.17(12)
C4A	C3	C11	120.4(2)	C9A	C4A	C3	120.9(3)

C4A	C3	C10	118.8(2)	C9A	C4A	C5A	120.0
O2	C2	O1	126.1(6)	C5A	C4A	C3	118.8(3)
O2	C2	C3	123.90(17)	C4A	C9A	C8A	120.0
O2	C2	O1A	121.5(6)	C7A	C8A	C9A	120.0
O1	C2	C3	109.1(5)	C8A	C7A	C6A	120.0
O1A	C2	C3	114.2(6)	C7A	C6A	C5A	120.0
C9	C4	C3	118.6(4)	C6A	C5A	C4A	120.0
C9	C4	C5	120.0	C2	O1A	C1A	116.9(10)
C5	C4	C3	121.4(4)				

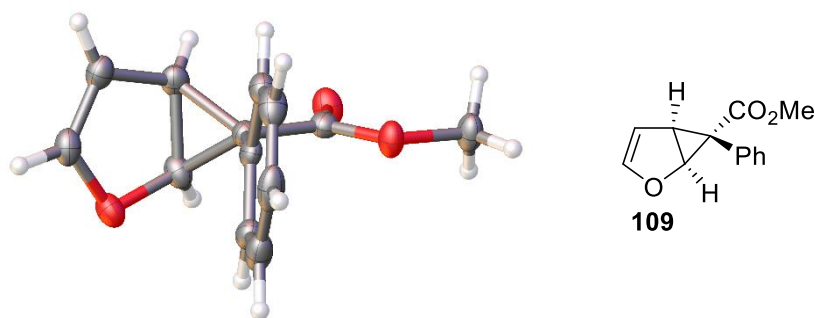
**Table 6.** Hydrogen Atom Coordinates ( $\text{\AA} \times 10^4$ ) and Isotropic Displacement Parameters ( $\text{\AA}^2 \times 10^3$ ) for **108**.

Atom	x	y	z	U(eq)
H13	7442.29	9119.07	8747.63	32
H9	5400.51	7197.89	6105.5	34
H8	4156.85	7156.59	6556.04	38
H7	4026.16	4705.96	7779.05	36
H6	5139.12	2296.59	8551.53	31
H5	6382.79	2337.84	8101	26
H11	8183.61	4055.31	7297.4	26
H10	7567.05	7260.81	6171.13	31
H15A	9131.84	259.22	9977.81	46
H15B	8496.12	1435.46	10459.91	46
H15C	9355.48	2653.67	10500.02	46
H1A	6038.54	2597.19	4064.47	52
H1B	5346.39	1031.3	4301.57	52
H1C	6300.15	290.09	4645.07	52
H9A	5648.15	8102.56	6555.32	32
H8A	4439.61	8168.26	7075.45	38
H7A	4144.3	5092.71	7962.11	35
H6A	5057.54	1951.47	8328.65	32
H5A	6266.09	1885.74	7808.54	29
H1AA	5363.51	454.18	4319.79	54
H1AB	6209.95	-787.72	4865.91	54
H1AC	6230.26	1418.26	4239.79	54

**Table 7.** Atomic Occupancy for **108**.

<b>Atom</b>	<b>Occupancy</b>	<b>Atom</b>	<b>Occupancy</b>	<b>Atom</b>	<b>Occupancy</b>
O1	0.545(7)	C4	0.455(7)	C9	0.455(7)
H9	0.455(7)	C8	0.455(7)	H8	0.455(7)
C7	0.455(7)	H7	0.455(7)	C6	0.455(7)
H6	0.455(7)	C5	0.455(7)	H5	0.455(7)
C1	0.545(7)	H1A	0.545(7)	H1B	0.545(7)
H1C	0.545(7)	C4A	0.545(7)	C9A	0.545(7)
H9A	0.545(7)	C8A	0.545(7)	H8A	0.545(7)
C7A	0.545(7)	H7A	0.545(7)	C6A	0.545(7)
H6A	0.545(7)	C5A	0.545(7)	H5A	0.545(7)
O1A	0.455(7)	C1A	0.455(7)	H1AA	0.455(7)
H1AB	0.455(7)	H1AC	0.455(7)		



**Table 1.** Crystal data and structure refinement for **109**.

Identification code	Q075_1
Empirical formula	C <sub>13</sub> H <sub>12</sub> O <sub>3</sub>
Formula weight	216.23
Temperature/K	122.99(10)
Crystal system	orthorhombic
Space group	P2 <sub>1</sub> 2 <sub>1</sub> 2 <sub>1</sub>
a/Å	8.1779(2)
b/Å	8.8079(2)
c/Å	15.2085(3)
α/°	90
β/°	90
γ/°	90
Volume/Å <sup>3</sup>	1095.47(4)
Z	4
ρ <sub>calc</sub> /mg/mm <sup>3</sup>	1.311
m/mm <sup>-1</sup>	0.763
F(000)	456.0
Crystal size/mm <sup>3</sup>	0.352 × 0.232 × 0.177
Radiation	CuKα (λ = 1.54184)
2θ range for data collection	11.61 to 133.062°
Index ranges	-9 ≤ h ≤ 9, -10 ≤ k ≤ 10, -18 ≤ l ≤ 17
Reflections collected	13735
Independent reflections	1920 [R <sub>int</sub> = 0.0326, R <sub>sigma</sub> = 0.0158]
Data/restraints/parameters	1920/0/194
Goodness-of-fit on F <sup>2</sup>	1.078
Final R indexes [I ≥ 2σ (I)]	R <sub>1</sub> = 0.0240, wR <sub>2</sub> = 0.0600
Final R indexes [all data]	R <sub>1</sub> = 0.0258, wR <sub>2</sub> = 0.0611
Largest diff. peak/hole / e Å <sup>-3</sup>	0.13/-0.10

Flack parameter -0.10(8)

**Table 2.** Fractional Atomic Coordinates ( $\times 10^4$ ) and Equivalent Isotropic Displacement Parameters ( $\text{\AA}^2 \times 10^3$ ) for **109**.  $U_{\text{eq}}$  is defined as 1/3 of the trace of the orthogonalized  $U_{\text{II}}$  tensor.

Atom	x	y	z	U(eq)
O1	3317.8(14)	5228.3(14)	6069.1(8)	27.7(3)
O3	7930.6(15)	7286.3(14)	7452.0(7)	29.1(3)
O2	2919.3(14)	7464.7(15)	6740.1(8)	30.3(3)
C2	5645(2)	6689(2)	6399.0(11)	22.0(4)
C3	6260(2)	7491(2)	7229.7(11)	25.4(4)
C7	6619.7(19)	5474.4(19)	5955.4(11)	21.3(4)
C1	3834(2)	6529.1(19)	6425.7(11)	22.3(4)
C5	7924(2)	8659(2)	6190.0(12)	27.0(4)
C8	6833(2)	5494(2)	5046.3(11)	25.8(4)
C4	6177(2)	8387(2)	6394.1(12)	25.4(4)
C12	7243(2)	4268(2)	6438.1(13)	26.1(4)
C6	8828(2)	7994(2)	6798.6(12)	28.2(4)
C10	8255(2)	3102(2)	5114.4(14)	36.4(5)
C9	7637(2)	4306(2)	4630.9(13)	33.3(5)
C11	8055(2)	3084(2)	6020.5(14)	33.3(4)
C13	1557(2)	4998(2)	6089.3(15)	31.3(4)

**Table 3.** Anisotropic Displacement Parameters ( $\text{\AA}^2 \times 10^3$ ) for **109**. The Anisotropic displacement factor exponent takes the form:  $-2\pi^2[h^2a^*U_{11}+2hka^*b^*U_{12}+\dots]$ .

Atom	U <sub>11</sub>	U <sub>22</sub>	U <sub>33</sub>	U <sub>23</sub>	U <sub>13</sub>	U <sub>12</sub>
O1	17.7(6)	26.5(6)	39.1(7)	-5.5(5)	0.9(5)	-1.1(5)
O3	21.2(6)	37.6(7)	28.5(6)	-3.2(5)	-3.7(5)	1.0(6)
O2	21.6(6)	34.3(7)	34.9(6)	-9.8(6)	1.1(5)	3.3(6)
C2	20.9(8)	23.0(8)	22.0(8)	0.3(7)	-0.4(7)	0.4(7)
C3	18.6(8)	32.3(9)	25.3(8)	-5.4(8)	-0.5(7)	2.1(7)
C7	16.0(8)	22.6(8)	25.3(8)	-0.1(7)	1.7(7)	-4.6(7)
C1	23.2(8)	24.2(9)	19.6(7)	1.3(7)	-0.2(7)	0.9(7)
C5	24.6(9)	22.5(9)	34.0(9)	-3.0(7)	2.6(8)	-1.9(7)
C8	21.8(9)	28.7(10)	27.0(9)	-2.2(7)	-0.1(7)	-3.4(8)
C4	22.5(9)	20.9(8)	32.9(9)	-1.8(7)	-2.2(7)	2.8(7)

C12	21.6(8)	24.3(9)	32.2(9)	2.4(8)	-1.1(7)	-2.8(7)
C6	21.4(9)	28.4(9)	34.7(9)	-8.2(8)	1.1(8)	-2.2(7)
C10	23.4(10)	27.1(10)	58.7(13)	-16.4(9)	4.4(9)	-2.5(8)
C9	27.4(10)	40.6(11)	31.9(11)	-11.6(8)	5.4(8)	-7.7(8)
C11	23.3(9)	22.4(9)	54.3(12)	-1.5(9)	-3.3(9)	-1.3(7)
C13	18.2(9)	28.1(10)	47.6(12)	-3.3(9)	-0.4(8)	-1.4(8)

**Table 4.** Bond Lengths for **109**.

Atom	Atom	Length/Å	Atom	Atom	Length/Å
O1	C1	1.336(2)	C3	C4	1.498(3)
O1	C13	1.454(2)	C7	C8	1.394(2)
O3	C3	1.419(2)	C7	C12	1.388(2)
O3	C6	1.384(2)	C5	C4	1.481(2)
O2	C1	1.211(2)	C5	C6	1.321(3)
C2	C3	1.533(2)	C8	C9	1.388(3)
C2	C7	1.495(2)	C12	C11	1.390(3)
C2	C1	1.489(2)	C10	C9	1.386(3)
C2	C4	1.558(2)	C10	C11	1.388(3)

**Table 5.** Bond Angles for **109**.

Atom	Atom	Atom	Angle/°	Atom	Atom	Atom	Angle/°
C1	O1	C13	115.07(14)	O1	C1	C2	112.59(14)
C6	O3	C3	106.38(13)	O2	C1	O1	123.29(16)
C3	C2	C4	57.96(12)	O2	C1	C2	124.12(16)
C7	C2	C3	121.79(14)	C6	C5	C4	108.73(16)
C7	C2	C4	122.41(14)	C9	C8	C7	120.09(18)
C1	C2	C3	110.36(14)	C3	C4	C2	60.17(12)
C1	C2	C7	118.38(14)	C5	C4	C2	115.19(15)
C1	C2	C4	111.64(14)	C5	C4	C3	102.66(14)
O3	C3	C2	117.00(14)	C7	C12	C11	120.54(18)
O3	C3	C4	108.24(14)	C5	C6	O3	113.96(16)
C4	C3	C2	61.88(11)	C9	C10	C11	119.51(18)
C8	C7	C2	120.37(16)	C10	C9	C8	120.54(18)
C12	C7	C2	120.31(15)	C10	C11	C12	120.09(18)

---

C12    C7    C8    119.22(16)

---



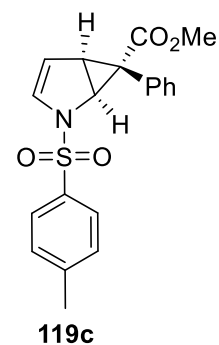
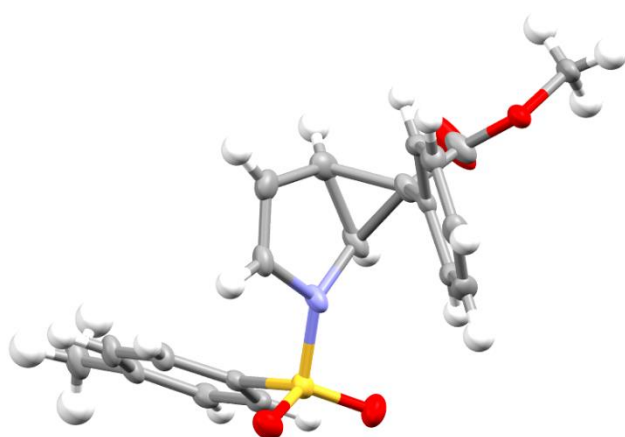
---

**Table 6.** Hydrogen Atom Coordinates ( $\text{\AA}\times 10^4$ ) and Isotropic Displacement Parameters ( $\text{\AA}^2\times 10^3$ ) for **109**.

---

Atom	<i>x</i>	<i>y</i>	<i>z</i>	<b>U(eq)</b>
H3	5550(20)	7610(20)	7748(13)	25(5)
H8	6380(30)	6330(20)	4697(13)	29(5)
H4	5390(30)	9120(20)	6269(12)	27(5)
H6	10030(30)	7910(20)	6865(12)	30(5)
H13A	1030(30)	5740(30)	5709(15)	42(6)
H13B	1180(20)	5090(20)	6704(14)	29(5)
H12	7090(30)	4220(20)	7076(14)	32(5)
H5	8340(30)	9200(20)	5692(14)	32(5)
H11	8460(30)	2210(30)	6364(14)	44(6)
H13C	1360(30)	3980(30)	5855(15)	45(6)
H9	7730(30)	4320(20)	4005(15)	38(6)
H10	8800(30)	2270(30)	4826(14)	43(6)

---


**Table 1.** Crystal data and structure refinement for **119c**.

Identification code	P039
Empirical formula	C <sub>20</sub> H <sub>19</sub> NO <sub>4</sub> S
Formula weight	369.42
Temperature/K	123.00(10)
Crystal system	orthorhombic
Space group	P2 <sub>1</sub> 2 <sub>1</sub> 2 <sub>1</sub>
a/Å	8.25344(9)
b/Å	9.76016(12)
c/Å	22.2332(2)
α/°	90
β/°	90
γ/°	90
Volume/Å <sup>3</sup>	1790.99(4)
Z	4
ρ <sub>calc</sub> /mm <sup>3</sup>	1.370
m/mm <sup>-1</sup>	1.825
F(000)	776.0
Crystal size/mm <sup>3</sup>	0.234 × 0.196 × 0.172
Radiation	CuKα (λ = 1.54184)
2θ range for data collection	7.954 to 146.656°
Index ranges	-9 ≤ h ≤ 10, -11 ≤ k ≤ 10, -26 ≤ l ≤ 27
Reflections collected	10156
Independent reflections	3499 [R <sub>int</sub> = 0.0270, R <sub>sigma</sub> = 0.0266]

Data/restraints/parameters	3499/0/237
Goodness-of-fit on $F^2$	1.062
Final R indexes [ $I \geq 2\sigma(I)$ ]	$R_1 = 0.0315$ , $wR_2 = 0.0801$
Final R indexes [all data]	$R_1 = 0.0327$ , $wR_2 = 0.0812$
Largest diff. peak/hole / $e \text{ \AA}^{-3}$	0.22/-0.41
Flack parameter	0.006(7)

**Table 2.** Fractional Atomic Coordinates ( $\times 10^4$ ) and Equivalent Isotropic Displacement Parameters ( $\text{\AA}^2 \times 10^3$ ) for **119c**.  $U_{\text{eq}}$  is defined as 1/3 of the trace of the orthogonalized  $U_{\text{ij}}$  tensor.

Atom	$x$	$y$	$z$	$U(\text{eq})$
S1	3264.8(7)	6036.8(6)	6443.6(3)	20.37(15)
O4	2942(2)	528.9(17)	5169.7(7)	20.4(4)
O2	2098(2)	6160(2)	5970.5(8)	30.3(4)
O1	2843(2)	6329.4(19)	7053.5(8)	28.3(4)
N1	3840(3)	4428(2)	6448.1(9)	20.8(4)
C4	4976(3)	7762(2)	5714.5(10)	21.0(5)
O3	4567(4)	2194(3)	4856.0(9)	71.1(10)
C3	6339(3)	8522(2)	5563(1)	22.2(5)
C11	2974(3)	403(2)	6626.2(10)	18.8(5)
C12	1961(3)	-126(3)	7063.8(10)	22.5(5)
C2	7704(3)	8546(2)	5930.9(10)	21.8(5)
C15	1172(3)	2297(3)	6483.1(11)	22.2(5)
C6	6301(3)	7060(3)	6634.9(10)	21.8(5)
C5	4972(3)	7025(2)	6250.7(10)	17.7(5)
C17	5668(3)	2815(3)	6732.5(12)	26.6(5)
C18	4745(3)	3846(3)	6926.2(11)	23.5(5)
C7	7656(3)	7811(3)	6472.9(11)	24.6(5)
C13	561(3)	572(3)	7223.8(11)	26.1(5)
C20	3103(3)	-79(3)	4577.5(10)	24.5(5)
C8	4250(3)	3698(3)	5902(1)	24.3(5)
C10	2585(3)	1619(2)	6330.3(10)	16.7(5)
C9	3730(3)	2202(3)	5876.3(10)	21.4(5)
C1	9210(3)	9306(3)	5744.0(12)	32.3(6)
C16	5461(3)	2619(3)	6079.2(12)	26.6(6)
C14	174(3)	1780(3)	6935.1(12)	27.2(6)

C19                    3781(4)                    1674(3)                    5248.1(11)                    29.5(6)

**Table 3.** Anisotropic Displacement Parameters ( $\text{\AA}^2 \times 10^3$ ) for **119c**. The Anisotropic displacement factor exponent takes the form:  $-2\pi^2[h^2a^{*2}U_{11}+2hka^*b^*U_{12}+\dots]$ .

Atom	U <sub>11</sub>	U <sub>22</sub>	U <sub>33</sub>	U <sub>23</sub>	U <sub>13</sub>	U <sub>12</sub>
S1	20.6(3)	18.6(3)	21.9(3)	-0.6(2)	-0.4(2)	-3.5(2)
O4	23.0(9)	16.8(8)	21.5(8)	-4.1(6)	-1.0(6)	-0.8(7)
O2	23.8(9)	32.3(10)	35(1)	3.8(8)	-8.2(7)	-4.9(8)
O1	27.9(9)	28.9(10)	28.1(9)	-4.0(7)	8.7(7)	-4.8(8)
N1	32.1(10)	15.6(10)	14.6(8)	0.5(8)	-2.2(8)	-6.0(8)
C4	23.9(11)	18.6(12)	20.6(11)	-0.8(9)	-2.1(9)	3.7(10)
O3	140(3)	44.0(15)	28.9(11)	-13.7(10)	38.3(14)	-53.2(17)
C3	30.2(13)	17.6(13)	18.8(11)	2.6(9)	1.0(9)	0.7(10)
C11	18.2(11)	15.5(11)	22.8(11)	0.5(9)	1.4(9)	0.2(9)
C12	25.7(13)	21.2(12)	20.7(11)	4.2(9)	0.0(9)	-3.9(10)
C2	30.7(12)	16.5(12)	18.1(11)	-2.1(9)	0.8(9)	-6.4(10)
C15	20.6(11)	15.9(11)	30.1(12)	-0.6(10)	-6.6(10)	-0.5(9)
C6	28.4(13)	19.0(12)	17.9(10)	2.4(9)	-2.0(9)	-4.8(10)
C5	20.9(11)	12.8(11)	19.5(10)	-2.1(8)	2.1(9)	-0.8(9)
C17	20.0(12)	26.0(14)	33.8(13)	4.5(11)	-4(1)	-7.7(11)
C18	27.8(12)	22.8(12)	19.9(11)	2.4(10)	-5.6(9)	-10.1(11)
C7	27.7(12)	27.0(12)	19.1(11)	-1.0(11)	-4.7(10)	-8.5(10)
C13	24.7(12)	31.8(14)	22.0(11)	-2.9(11)	6.2(10)	-9.1(11)
C20	28.2(13)	22.0(12)	23.1(11)	-8.2(9)	-5.7(10)	3.8(11)
C8	37.9(14)	17.6(13)	17.3(10)	-0.7(9)	3(1)	-11.5(11)
C10	19.8(10)	15.0(11)	15.2(10)	-2.2(8)	-1.1(8)	-4.5(9)
C9	29.1(13)	16.8(12)	18.2(11)	1.1(9)	2.7(9)	-8.6(10)
C1	36.5(14)	35.6(16)	24.8(12)	-0.1(11)	0.1(11)	-18.2(12)
C16	22.9(12)	23.1(14)	33.9(14)	-0.9(11)	8.3(10)	-8.2(10)
C14	16.4(11)	29.2(14)	35.9(14)	-7.7(11)	3.8(10)	-0.3(10)
C19	48.0(16)	19.3(13)	21.1(12)	-1.5(10)	4.6(11)	-8.3(12)

**Table 4.** Bond Lengths for **119c**.

Atom	Atom	Length/ $\text{\AA}$	Atom	Atom	Length/ $\text{\AA}$
S1	O2	1.4314(18)	C2	C7	1.403(3)

S1	O1	1.4287(18)	C2	C1	1.506(3)
S1	N1	1.641(2)	C15	C10	1.383(3)
S1	C5	1.761(2)	C15	C14	1.394(4)
O4	C20	1.450(3)	C6	C5	1.390(3)
O4	C19	1.326(3)	C6	C7	1.385(3)
N1	C18	1.418(3)	C17	C18	1.334(4)
N1	C8	1.448(3)	C17	C16	1.475(4)
C4	C3	1.388(3)	C13	C14	1.380(4)
C4	C5	1.392(3)	C8	C9	1.523(3)
O3	C19	1.200(3)	C8	C16	1.505(4)
C3	C2	1.393(3)	C10	C9	1.495(3)
C11	C12	1.383(3)	C9	C16	1.553(3)
C11	C10	1.394(3)	C9	C19	1.489(3)
C12	C13	1.388(4)			

**Table 5.** Bond Angles for **119c**.

Atom	Atom	Atom	Angle/°	Atom	Atom	Atom	Angle/°
O2	S1	N1	106.26(11)	C17	C18	N1	111.2(2)
O2	S1	C5	108.26(11)	C6	C7	C2	121.1(2)
O1	S1	O2	121.08(12)	C14	C13	C12	119.6(2)
O1	S1	N1	104.84(11)	N1	C8	C9	115.94(19)
O1	S1	C5	108.48(11)	N1	C8	C16	106.3(2)
N1	S1	C5	107.12(11)	C16	C8	C9	61.69(17)
C19	O4	C20	114.58(19)	C11	C10	C9	119.8(2)
C18	N1	S1	122.71(17)	C15	C10	C11	119.0(2)
C18	N1	C8	108.0(2)	C15	C10	C9	121.2(2)
C8	N1	S1	122.23(16)	C8	C9	C16	58.57(17)
C3	C4	C5	119.1(2)	C10	C9	C8	121.1(2)
C4	C3	C2	121.5(2)	C10	C9	C16	119.0(2)
C12	C11	C10	120.7(2)	C19	C9	C8	111.02(19)
C11	C12	C13	120.0(2)	C19	C9	C10	121.3(2)
C3	C2	C7	118.2(2)	C19	C9	C16	109.7(2)
C3	C2	C1	120.9(2)	C17	C16	C8	104.1(2)
C7	C2	C1	120.8(2)	C17	C16	C9	115.3(2)
C10	C15	C14	120.2(2)	C8	C16	C9	59.74(17)
C7	C6	C5	119.4(2)	C13	C14	C15	120.5(2)



C4	C5	S1	119.59(18)	O4	C19	C9	113.6(2)
C6	C5	S1	119.66(18)	O3	C19	O4	122.9(2)
C6	C5	C4	120.7(2)	O3	C19	C9	123.4(2)
C18	C17	C16	110.5(2)				

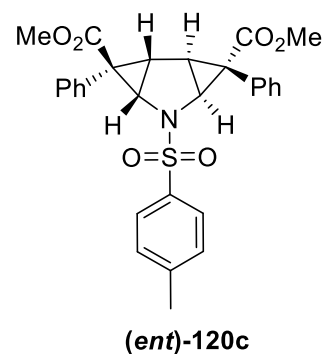
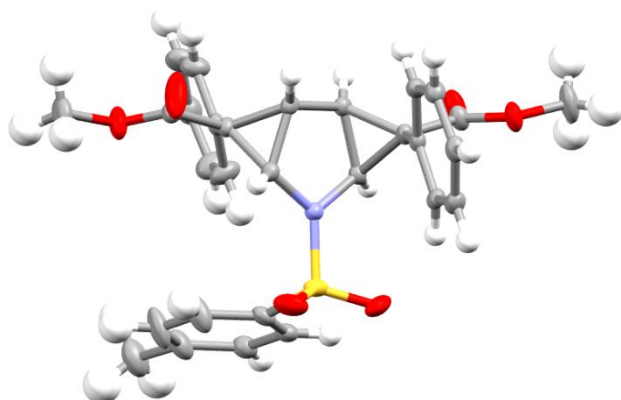
**Table 6.** Torsion Angles for **119c**.

A	B	C	D	Angle/°	A	B	C	D	Angle/°
S1	N1	C18	C17	-151.63(19)	C5	S1	N1	C18	77.2(2)
S1	N1	C8	C9	-142.41(19)	C5	S1	N1	C8	-69.8(2)
S1	N1	C8	C16	151.63(17)	C5	C4	C3	C2	0.9(4)
O2	S1	N1	C18	-167.27(19)	C5	C6	C7	C2	0.6(4)
O2	S1	N1	C8	45.7(2)	C18	N1	C8	C9	66.4(3)
O2	S1	C5	C4	1.0(2)	C18	N1	C8	C16	0.4(3)
O2	S1	C5	C6	-178.98(19)	C18	C17	C16	C8	-0.2(3)
O1	S1	N1	C18	-37.9(2)	C18	C17	C16	C9	-63.1(3)
O1	S1	N1	C8	175.04(19)	C7	C6	C5	S1	178.30(19)
O1	S1	C5	C4	-132.14(19)	C7	C6	C5	C4	-1.7(4)
O1	S1	C5	C6	47.9(2)	C20	O4	C19	O3	2.4(4)
N1	S1	C5	C4	115.19(19)	C20	O4	C19	C9	-174.2(2)
N1	S1	C5	C6	-64.8(2)	C8	N1	C18	C17	-0.6(3)
N1	C8	C9	C10	11.9(3)	C8	C9	C16	C17	92.1(3)
N1	C8	C9	C16	-95.3(2)	C8	C9	C19	O4	-162.6(2)
N1	C8	C9	C19	163.9(2)	C8	C9	C19	O3	20.8(4)
N1	C8	C16	C17	-0.1(3)	C10	C11	C12	C13	-1.7(4)
N1	C8	C16	C9	111.1(2)	C10	C15	C14	C13	-1.6(4)
C4	C3	C2	C7	-1.9(4)	C10	C9	C16	C17	-18.6(3)
C4	C3	C2	C1	176.3(2)	C10	C9	C16	C8	-110.7(2)
C3	C4	C5	S1	-179.08(18)	C10	C9	C19	O4	-10.7(4)
C3	C4	C5	C6	0.9(4)	C10	C9	C19	O3	172.7(3)
C3	C2	C7	C6	1.1(4)	C9	C8	C16	C17	-111.3(2)
C11	C12	C13	C14	1.3(4)	C1	C2	C7	C6	-177.1(2)
C11	C10	C9	C8	-129.9(2)	C16	C17	C18	N1	0.5(3)
C11	C10	C9	C16	-61.1(3)	C16	C8	C9	C10	107.2(2)
C11	C10	C9	C19	81.0(3)	C16	C8	C9	C19	-100.9(2)
C12	C11	C10	C15	0.4(3)	C16	C9	C19	O4	134.5(2)
C12	C11	C10	C9	177.6(2)	C16	C9	C19	O3	-42.1(4)

C12	C13	C14	C15	0.3(4)	C14	C15	C10	C11	1.3(3)
C15	C10	C9	C8	47.2(3)	C14	C15	C10	C9	-175.9(2)
C15	C10	C9	C16	116.0(3)	C19	C9	C16	C17	-164.7(2)
C15	C10	C9	C19	-101.9(3)	C19	C9	C16	C8	103.2(2)

**Table 7.** Hydrogen Atom Coordinates ( $\text{\AA}\times 10^4$ ) and Isotropic Displacement Parameters ( $\text{\AA}^2\times 10^3$ ) for **119c**.

Atom	<i>x</i>	<i>y</i>	<i>z</i>	U(eq)
H4	4079	7746	5461	25
H3	6339	9026	5208	27
H11	3925	-56	6528	23
H12	2218	-951	7251	27
H15	887	3099	6284	27
H6	6279	6585	6997	26
H17	6347	2293	6975	32
H18	4700	4144	7323	28
H7	8550	7827	6728	29
H13	-111	229	7524	31
H20A	2803	581	4277	37
H20B	2406	-864	4548	37
H20C	4206	-356	4515	37
H8	4404	4210	5527	29
H1A	9694	8854	5405	48
H1B	9965	9321	6072	48
H1C	8931	10228	5635	48
H16	6399	2426	5822	32
H14	-761	2252	7043	33




---

**Table 1.** Crystal data and structure refinement for *(ent)*-120c.
 

---

Identification code	P197
Empirical formula	C <sub>29</sub> H <sub>27</sub> NO <sub>6</sub> S
Formula weight	517.57
Temperature/K	123.04(10)
Crystal system	triclinic
Space group	P1
a/Å	8.8134(2)
b/Å	11.4422(3)
c/Å	13.9834(3)
α/°	106.922(2)
β/°	103.296(2)
γ/°	96.903(2)
Volume/Å <sup>3</sup>	1286.14(6)
Z	2
ρ <sub>calc</sub> /mm <sup>3</sup>	1.336
m/mm <sup>-1</sup>	1.492
F(000)	544.0
Crystal size/mm <sup>3</sup>	0.203 × 0.065 × 0.059
Radiation	Cu Kα (λ = 1.54184)
2θ range for data collection	6.88 to 147.02°
Index ranges	-10 ≤ h ≤ 10, -14 ≤ k ≤ 14, -17 ≤ l ≤ 17
Reflections collected	33167
Independent reflections	9686 [R <sub>int</sub> = 0.0326, R <sub>sigma</sub> = 0.0280]
Data/restraints/parameters	9686/3/673

Goodness-of-fit on $F^2$	1.037
Final R indexes [ $I \geq 2\sigma(I)$ ]	$R_1 = 0.0319$ , $wR_2 = 0.0821$
Final R indexes [all data]	$R_1 = 0.0334$ , $wR_2 = 0.0835$
Largest diff. peak/hole / $e \text{ \AA}^{-3}$	0.22/-0.25
Flack parameter	-0.009(8)

**Table 2.** Fractional Atomic Coordinates ( $\times 10^4$ ) and Equivalent Isotropic Displacement Parameters ( $\text{\AA}^2 \times 10^3$ ) for (*ent*)-**120c**.  $U_{eq}$  is defined as 1/3 of the trace of the orthogonalized  $U_{ij}$  tensor.

Atom	x	y	z	U(eq)
S2	4261.5(7)	3280.3(5)	4081.9(4)	22.37(14)
S1	8643.4(8)	9792.2(6)	8155.1(5)	28.41(15)
O9	1741(2)	4461.8(18)	524.4(15)	28.0(4)
O3	7781(2)	6614.4(18)	4297.5(14)	26.0(4)
O10	3635(3)	3356(2)	248.7(18)	39.3(5)
O4	5670(3)	7434(2)	3810.4(14)	31.1(4)
O7	4730(2)	4474.7(17)	3990.8(16)	31.2(5)
O8	3279(2)	3115(2)	4736.5(15)	34.9(5)
O5	8272(2)	5615(2)	9311.2(16)	32.9(5)
O6	5762(2)	5828(2)	8751.4(15)	31.6(4)
O1	9801(3)	10159(2)	7671.7(19)	41.1(5)
O2	9096(3)	9765(2)	9196.9(16)	39.7(5)
O12	2476(2)	-1809.8(19)	2476.2(18)	34.4(5)
N00E	3336(2)	2362.7(18)	2906.8(15)	18.3(4)
N00F	7704(3)	8380.6(19)	7422.8(16)	21.1(4)
C21	4721(3)	7666(2)	5579.1(17)	16.8(4)
O11	203(3)	-1142(2)	2188(3)	56.7(8)
C42	3988(3)	-281(2)	1663.8(19)	20.2(5)
C31	7413(3)	3249(2)	4342.3(19)	23.5(5)
C22	3361(3)	6807(2)	5444.8(18)	19.5(5)
C50	644(3)	3253(2)	1699.9(18)	17.3(5)
C51	836(3)	4236(2)	2614.2(19)	19.6(5)
C56	2564(3)	3582(2)	636(2)	23.3(5)
C23	1939(3)	7184(2)	5485(2)	24.1(5)
C40	2219(3)	1217(2)	2652.9(18)	17.5(5)

C33	8676(4)	1656(3)	4815(2)	34.8(7)
C54	-2213(3)	3031(2)	1353(2)	23.5(5)
C32	8733(3)	2712(3)	4519(2)	27.6(6)
C12	9282(3)	6237(3)	7796.9(19)	22.0(5)
C53	-2009(3)	4041(2)	2244(2)	23.7(5)
C11	7677(3)	6398(2)	7925.4(18)	21.1(5)
C39	1472(3)	750(2)	1503.4(18)	18.2(5)
C52	-478(3)	4631(2)	2880(2)	23.6(5)
C27	6654(3)	7048(2)	4472.6(18)	20.1(5)
C9	6967(3)	6431(2)	6067.8(17)	16.7(5)
C38	2345(3)	1588(2)	1068.2(18)	18.1(5)
C49	2044(3)	2923(2)	1322.8(18)	18.3(5)
C18	6914(3)	7511(2)	7807.9(18)	20.6(5)
C37	3492(3)	2601(2)	1972.9(18)	16.9(5)
C19	7111(3)	5908(3)	8690(2)	23.8(5)
C10	6353(3)	6292(2)	6955.0(18)	18.3(5)
C20	6250(3)	7266(2)	5488.5(17)	16.3(5)
C13	9428(3)	5075(3)	7188(2)	28.8(6)
C26	4614(3)	8913(2)	5752(2)	23.0(5)
C8	7810(3)	7760(2)	6390.1(18)	17.5(5)
C24	1839(3)	8427(3)	5643(2)	26.9(6)
C41	2520(3)	-24(2)	1989.2(18)	19.1(5)
C55	-892(3)	2642(2)	1084.2(19)	21.3(5)
C4	4851(5)	12129(3)	7884(2)	40.8(8)
C43	5522(4)	395(3)	2163(2)	34.1(6)
C30	6004(3)	2726(3)	4469.9(19)	24.7(5)
C47	3786(3)	-1303(3)	770(2)	31.0(6)
C17	10614(3)	7198(3)	8241(2)	30.4(6)
C14	10881(4)	4863(4)	7043(2)	39.8(8)
C25	3180(3)	9291(2)	5775(2)	28.3(6)
C46	5068(4)	-1655(3)	432(2)	35.8(7)
C1	7232(4)	10754(3)	8099(2)	30.3(6)
C48	1580(3)	-1056(2)	2202(2)	23.6(5)
C44	6806(4)	52(3)	1812(3)	37.5(7)
C2	7327(5)	11612(3)	7587(3)	39.6(7)
C58	1685(4)	-2805(3)	2747(3)	39.3(7)
C45	6593(4)	-976(3)	958(2)	32.4(6)

C15	12195(4)	5817(4)	7480(3)	44.1(9)
C6	6010(4)	10618(3)	8560(2)	37.3(7)
C3	6133(5)	12287(3)	7484(3)	43.4(8)
C5	4833(5)	11301(3)	8440(3)	43.3(8)
C16	12061(4)	6986(4)	8068(3)	41.8(8)
C57	2198(4)	5169(3)	-108(3)	43.0(8)
C35	5914(4)	1675(4)	4780(3)	43.5(8)
C28	6040(5)	7304(4)	2831(3)	49.2(10)
C34	7243(4)	1152(4)	4939(3)	49.1(10)
C29	7822(4)	5184(4)	10111(3)	44.9(9)
C36	10089(4)	1044(4)	4972(3)	48.2(9)
C7	3519(5)	12822(4)	7720(3)	54.4(10)

**Table 3.** Anisotropic Displacement Parameters ( $\text{\AA}^2 \times 10^3$ ) for (*ent*)-**120c**. The Anisotropic displacement factor exponent takes the form:  $-2\pi^2[h^2a^*U_{11}+2hka^*b^*U_{12}+\dots]$ .

Atom	U <sub>11</sub>	U <sub>22</sub>	U <sub>33</sub>	U <sub>23</sub>	U <sub>13</sub>	U <sub>12</sub>
S2	18.6(3)	25.2(3)	17.7(3)	0.2(2)	2.4(2)	6.1(2)
S1	28.7(4)	23.2(3)	23.4(3)	-2.1(2)	1.5(3)	4.6(3)
O9	33.0(11)	31.7(10)	34.9(10)	23.2(9)	18.1(9)	16.9(8)
O3	23.5(10)	38.3(10)	22.4(9)	11.0(8)	11.4(7)	16.7(8)
O10	43.0(13)	52.1(13)	50.8(13)	36.1(11)	32.2(11)	28.4(10)
O4	37.2(12)	48.2(12)	21.4(9)	19.2(8)	14.1(8)	27.6(10)
O7	24.9(10)	18.3(9)	37.2(11)	-2.9(8)	-1.1(8)	4.3(8)
O8	24.6(11)	52.3(13)	21.7(9)	1.8(9)	8.0(8)	8.8(9)
O5	25.1(10)	57.5(13)	31(1)	30.9(10)	10.7(8)	16.6(9)
O6	22.7(10)	51.8(12)	31.4(10)	23.3(9)	13.2(8)	13.8(9)
O1	32.0(12)	29.7(11)	49.6(13)	-1.1(9)	11.3(10)	-2.8(9)
O2	44.5(13)	36.2(11)	22.4(10)	-3.9(8)	-6.8(9)	14(1)
O12	28.6(11)	32.4(10)	54.0(13)	30.3(10)	11.8(9)	9.3(8)
N00E	18.8(10)	16.8(9)	17.7(9)	5.0(7)	3.0(8)	3.6(8)
N00F	22.0(11)	22.3(10)	16.6(9)	3.0(8)	4.3(8)	5.7(8)
C21	14.7(11)	23.0(11)	13.6(10)	6.5(9)	3.2(8)	7.1(9)
O11	26.7(12)	52.2(15)	116(2)	59.0(16)	23.6(14)	12.5(10)
C42	20.2(12)	18.6(11)	25.1(12)	11.4(10)	5.3(10)	7.2(9)
C31	23.1(13)	25.6(12)	17.8(11)	4.2(9)	2.1(10)	3.8(10)

C22	20.1(12)	19.4(11)	18.6(11)	6.4(9)	3.2(9)	5.8(9)
C50	18.0(12)	16.6(10)	20.5(11)	8.7(9)	7.3(9)	4.9(9)
C51	20.6(12)	15.3(11)	22.8(11)	6.2(9)	6.4(9)	2.5(9)
C56	23.9(13)	28.4(13)	25.5(12)	14.4(10)	11.4(10)	11.7(10)
C23	14.8(12)	30.2(13)	29.1(13)	13.0(11)	5.6(10)	4.7(10)
C40	15.1(11)	16.6(11)	20.8(11)	5.6(9)	5.2(9)	3.9(9)
C33	29.2(16)	51.5(18)	35.0(15)	25.6(14)	11.0(12)	17.8(14)
C54	18.6(12)	24.7(12)	27.7(12)	10.6(10)	5.2(10)	3.7(10)
C32	23.3(14)	33.3(14)	25.0(12)	9.1(11)	5.4(10)	5.7(11)
C12	16.3(12)	37.5(14)	17.2(11)	14.9(10)	3.8(9)	10.7(10)
C53	21.1(13)	26.0(13)	31.8(13)	14.4(11)	13.2(11)	9.9(10)
C11	17.3(12)	30.1(13)	18.7(11)	10.7(10)	5.3(9)	8.1(10)
C39	14.9(12)	15.8(11)	22.4(11)	4.9(9)	3.0(9)	5.3(9)
C52	27.8(14)	19.7(11)	25.1(12)	6.3(10)	11.3(10)	7.2(10)
C27	20.6(13)	22.2(11)	17.8(11)	7.0(9)	4.9(9)	5.3(10)
C9	15.5(11)	19.0(11)	15.6(10)	4.4(9)	4.5(9)	6.7(9)
C38	18.2(12)	17.9(11)	19.1(11)	5.9(9)	5.1(9)	7.5(9)
C49	20.4(12)	17.9(11)	19.2(11)	7.4(9)	7.2(9)	7.3(9)
C18	17.3(12)	28.5(12)	17.8(11)	8.1(10)	5.7(9)	8.2(10)
C37	15.5(12)	17.6(11)	19.3(11)	7.2(9)	5.7(9)	5.9(9)
C19	22.1(14)	30.7(13)	21.1(12)	10.3(10)	6.5(10)	9.5(10)
C10	13.2(11)	24.0(12)	18.7(11)	7.5(9)	4.1(9)	7.3(9)
C20	15.2(11)	18.2(10)	15.2(10)	5.0(9)	3.5(9)	4.3(9)
C13	24.3(14)	41.8(15)	24.2(13)	13.4(11)	6.0(11)	17.1(12)
C26	20.0(13)	20.2(11)	29.7(13)	8.1(10)	7.7(10)	6.4(10)
C8	16.1(12)	19.9(11)	15.8(10)	3.9(9)	4.6(9)	5.8(9)
C24	18.9(13)	35.3(14)	36.1(14)	16.8(12)	13.6(11)	16.9(11)
C41	17.9(12)	16.4(11)	22.0(11)	6.5(9)	2.7(9)	4.4(9)
C55	23.4(13)	19.1(11)	19.9(11)	5.2(9)	4(1)	5.5(10)
C4	57(2)	29.0(15)	29.0(15)	0.3(12)	3.9(14)	20.4(15)
C43	24.6(15)	26.1(13)	40.1(16)	-4.1(12)	6.8(12)	4.8(11)
C30	23.1(13)	32.6(14)	16.9(11)	8.1(10)	2.2(10)	7.1(11)
C47	22.4(14)	38.8(16)	24.7(13)	3.0(11)	3.1(11)	5.2(12)
C17	21.0(13)	43.6(16)	26.9(13)	16.0(12)	1.3(11)	6.3(12)
C14	33.5(17)	70(2)	25.4(14)	18.3(14)	10.4(12)	34.1(16)
C25	28.0(14)	23.5(13)	37.6(15)	11.1(11)	11.9(12)	13.2(11)
C46	35.7(17)	41.8(16)	25.9(13)	2.6(12)	9.0(12)	13.1(13)

C1	40.0(17)	23.4(13)	21.5(12)	-0.5(10)	5.0(11)	10.8(12)
C48	20.1(13)	20.6(11)	28.8(13)	8.8(10)	3.3(10)	3.8(10)
C44	20.7(14)	34.4(15)	50.0(18)	3.5(13)	9.2(13)	5.1(12)
C2	48(2)	26.2(14)	40.8(17)	8.0(13)	10.7(14)	4.3(13)
C58	39.2(18)	36.0(16)	51.6(19)	30.0(15)	11.7(14)	4.2(13)
C45	26.5(15)	39.3(16)	37.6(15)	15.2(12)	13.1(12)	14.4(12)
C15	22.9(15)	94(3)	33.1(15)	34.7(17)	15.1(12)	27.6(17)
C6	53(2)	36.9(16)	29.9(14)	11.9(12)	17.9(14)	24.1(14)
C3	58(2)	25.9(14)	44.0(17)	11.9(13)	7.8(16)	11.0(14)
C5	58(2)	42.2(17)	36.4(16)	10.0(13)	21.7(16)	27.1(16)
C16	16.1(14)	71(2)	39.8(16)	29.1(16)	0.3(12)	3.3(14)
C57	50(2)	50.8(19)	58(2)	43.6(17)	29.7(17)	26.9(16)
C35	30.7(17)	66(2)	56(2)	45.2(19)	19.5(15)	17.2(16)
C28	62(2)	86(3)	27.9(15)	34.5(17)	28.1(16)	50(2)
C34	41(2)	69(2)	68(2)	57(2)	23.0(18)	22.7(18)
C29	40.2(19)	74(2)	38.1(17)	39.7(17)	13.9(14)	17.0(17)
C36	41(2)	63(2)	60(2)	38.8(19)	17.8(17)	26.4(17)
C7	69(3)	45.0(19)	45.9(19)	8.6(16)	7.9(18)	32.4(19)

---

**Table 4.** Bond Lengths for (*ent*)-120c.

Atom	Atom	Length/Å	Atom	Atom	Length/Å
S2	O7	1.430(2)	C33	C34	1.393(5)
S2	O8	1.432(2)	C33	C36	1.504(4)
S2	N00E	1.625(2)	C54	C53	1.389(4)
S2	C30	1.763(3)	C54	C55	1.386(4)
S1	O1	1.433(2)	C12	C11	1.492(4)
S1	O2	1.430(2)	C12	C13	1.394(4)
S1	N00F	1.634(2)	C12	C17	1.389(4)
S1	C1	1.760(3)	C53	C52	1.395(4)
O9	C56	1.333(3)	C11	C18	1.543(4)
O9	C57	1.449(3)	C11	C19	1.494(3)
O3	C27	1.205(3)	C11	C10	1.536(3)
O10	C56	1.209(3)	C39	C38	1.503(3)
O4	C27	1.329(3)	C39	C41	1.535(3)
O4	C28	1.450(3)	C27	C20	1.502(3)
O5	C19	1.325(3)	C9	C10	1.504(3)



O5	C29	1.459(3)	C9	C20	1.526(3)
O6	C19	1.206(3)	C9	C8	1.497(3)
O12	C48	1.316(3)	C38	C49	1.535(3)
O12	C58	1.452(3)	C38	C37	1.497(3)
N00E	C40	1.439(3)	C49	C37	1.538(3)
N00E	C37	1.442(3)	C18	C10	1.486(3)
N00F	C18	1.444(3)	C20	C8	1.550(3)
N00F	C8	1.442(3)	C13	C14	1.380(4)
C21	C22	1.394(3)	C26	C25	1.388(4)
C21	C20	1.495(3)	C24	C25	1.386(4)
C21	C26	1.395(3)	C41	C48	1.500(3)
O11	C48	1.201(4)	C4	C3	1.385(5)
C42	C41	1.500(4)	C4	C5	1.391(5)
C42	C43	1.383(4)	C4	C7	1.506(5)
C42	C47	1.399(4)	C43	C44	1.388(4)
C31	C32	1.385(4)	C30	C35	1.392(4)
C31	C30	1.384(4)	C47	C46	1.380(4)
C22	C23	1.381(4)	C17	C16	1.388(5)
C50	C51	1.395(3)	C14	C15	1.374(5)
C50	C49	1.496(3)	C46	C45	1.383(4)
C50	C55	1.395(3)	C1	C2	1.378(4)
C51	C52	1.382(4)	C1	C6	1.392(4)
C56	C49	1.498(3)	C44	C45	1.367(4)
C23	C24	1.392(4)	C2	C3	1.384(5)
C40	C39	1.494(3)	C15	C16	1.386(6)
C40	C41	1.545(3)	C6	C5	1.380(5)
C33	C32	1.385(4)	C35	C34	1.380(5)

**Table 5.** Bond Angles for (*ent*)-**120c**.

Atom	Atom	Atom	Angle/°	Atom	Atom	Atom	Angle/°
O7	S2	O8	121.33(14)	C37	C38	C39	107.19(19)
O7	S2	N00E	105.72(11)	C37	C38	C49	60.95(15)
O7	S2	C30	107.75(12)	C50	C49	C56	117.5(2)
O8	S2	N00E	107.32(12)	C50	C49	C38	121.23(19)
O8	S2	C30	107.56(13)	C50	C49	C37	124.02(19)

N00E	S2	C30	106.27(12)	C56	C49	C38	112.5(2)
O1	S1	N00F	106.67(12)	C56	C49	C37	109.7(2)
O1	S1	C1	107.89(15)	C38	C49	C37	58.32(15)
O2	S1	O1	121.51(15)	N00F	C18	C11	118.2(2)
O2	S1	N00F	106.16(12)	N00F	C18	C10	107.9(2)
O2	S1	C1	107.26(14)	C10	C18	C11	60.94(16)
N00F	S1	C1	106.49(13)	N00E	C37	C38	107.41(18)
C56	O9	C57	115.9(2)	N00E	C37	C49	116.9(2)
C27	O4	C28	115.2(2)	C38	C37	C49	60.73(15)
C19	O5	C29	115.3(2)	O5	C19	C11	112.2(2)
C48	O12	C58	115.7(2)	O6	C19	O5	124.2(2)
C40	N00E	S2	124.84(16)	O6	C19	C11	123.5(2)
C40	N00E	C37	110.57(18)	C9	C10	C11	113.4(2)
C37	N00E	S2	124.58(16)	C18	C10	C11	61.36(17)
C18	N00F	S1	123.26(17)	C18	C10	C9	106.9(2)
C8	N00F	S1	125.04(17)	C21	C20	C27	118.9(2)
C8	N00F	C18	110.65(19)	C21	C20	C9	122.2(2)
C22	C21	C20	121.4(2)	C21	C20	C8	122.9(2)
C22	C21	C26	118.6(2)	C27	C20	C9	111.1(2)
C26	C21	C20	119.9(2)	C27	C20	C8	108.9(2)
C43	C42	C41	126.3(2)	C9	C20	C8	58.26(14)
C43	C42	C47	116.9(3)	C14	C13	C12	120.9(3)
C47	C42	C41	116.9(2)	C25	C26	C21	120.8(2)
C30	C31	C32	119.5(2)	N00F	C8	C9	107.40(19)
C23	C22	C21	120.7(2)	N00F	C8	C20	118.2(2)
C51	C50	C49	121.1(2)	C9	C8	C20	60.07(15)
C55	C50	C51	119.0(2)	C25	C24	C23	119.7(3)
C55	C50	C49	119.6(2)	C42	C41	C40	128.7(2)
C52	C51	C50	120.2(2)	C42	C41	C39	120.0(2)
O9	C56	C49	112.3(2)	C39	C41	C40	58.02(15)
O10	C56	O9	124.2(2)	C48	C41	C42	116.7(2)
O10	C56	C49	123.4(2)	C48	C41	C40	107.2(2)
C22	C23	C24	120.3(2)	C48	C41	C39	113.0(2)
N00E	C40	C39	108.08(18)	C54	C55	C50	120.8(2)
N00E	C40	C41	120.1(2)	C3	C4	C5	117.7(3)
C39	C40	C41	60.68(15)	C3	C4	C7	121.4(3)
C32	C33	C34	117.7(3)	C5	C4	C7	120.9(4)

C32	C33	C36	121.7(3)	C42	C43	C44	121.5(3)
C34	C33	C36	120.5(3)	C31	C30	S2	119.4(2)
C55	C54	C53	119.7(2)	C31	C30	C35	120.4(3)
C33	C32	C31	121.5(3)	C35	C30	S2	119.8(2)
C13	C12	C11	118.0(2)	C46	C47	C42	121.5(3)
C17	C12	C11	122.8(3)	C16	C17	C12	119.6(3)
C17	C12	C13	119.2(3)	C15	C14	C13	119.8(3)
C54	C53	C52	119.7(2)	C24	C25	C26	119.9(2)
C12	C11	C18	124.5(2)	C47	C46	C45	120.4(3)
C12	C11	C19	118.1(2)	C2	C1	S1	120.1(3)
C12	C11	C10	118.0(2)	C2	C1	C6	120.8(3)
C19	C11	C18	110.3(2)	C6	C1	S1	119.1(2)
C19	C11	C10	114.1(2)	O12	C48	C41	111.7(2)
C10	C11	C18	57.70(16)	O11	C48	O12	123.9(2)
C40	C39	C38	106.30(19)	O11	C48	C41	124.3(3)
C40	C39	C41	61.30(16)	C45	C44	C43	120.8(3)
C38	C39	C41	113.3(2)	C1	C2	C3	118.9(3)
C51	C52	C53	120.4(2)	C44	C45	C46	118.9(3)
O3	C27	O4	124.1(2)	C14	C15	C16	120.0(3)
O3	C27	C20	123.5(2)	C5	C6	C1	118.9(3)
O4	C27	C20	112.4(2)	C2	C3	C4	122.0(3)
C10	C9	C20	117.7(2)	C6	C5	C4	121.7(3)
C8	C9	C10	106.96(19)	C15	C16	C17	120.5(3)
C8	C9	C20	61.68(15)	C34	C35	C30	118.8(3)
C39	C38	C49	115.8(2)	C35	C34	C33	122.0(3)

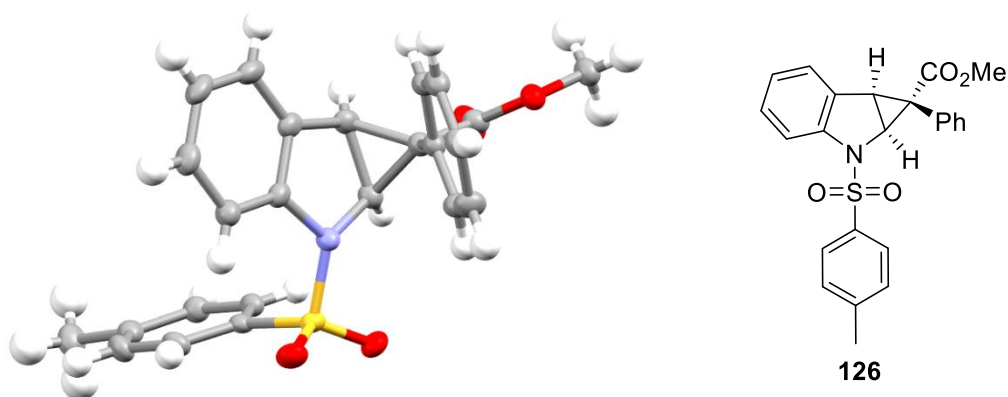
**Table 6.** Hydrogen Atom Coordinates ( $\text{\AA} \times 10^4$ ) and Isotropic Displacement Parameters ( $\text{\AA}^2 \times 10^3$ ) for *(ent)*-120c.

Atom	<i>x</i>	<i>y</i>	<i>z</i>	U(eq)
H31	7472.81	3954.15	4139.45	28
H22	3411.35	5971.59	5326.69	23
H51	1852.08	4627.72	3046.25	24
H23	1045.12	6604.59	5406.92	29
H40	1527.15	1179.92	3105.13	21
H54	-3230.98	2616.4	938.31	28

H32	9679.92	3069.29	4437.64	33
H53	-2889.26	4322.48	2416.43	28
H39	318.78	446.55	1218.86	22
H52	-341.22	5293.67	3486.06	28
H9	7448.85	5770.3	5706.92	20
H38	2673.38	1220.65	441.11	22
H18	6208.54	7798.48	8237.07	25
H37	4555.17	2886.54	1922.56	20
H10	5288.24	5800.82	6817.51	22
H13	8535.24	4433.75	6875.47	35
H26	5514.08	9499.11	5852.23	28
H8	8818.22	7937.53	6226.24	21
H24	876.22	8677.2	5658.76	32
H55	-1030.54	1967.32	486.33	26
H43	5696.5	1096.26	2746.47	41
H47	2765.44	-1755.31	395.46	37
H17	10536.84	7977.45	8651.42	37
H14	10970.63	4077.6	6650.33	48
H25	3119.65	10123.13	5880.27	34
H46	4904.72	-2352.13	-152.55	43
H44	7822.99	527.21	2161.12	45
H2	8179.14	11735.77	7315.65	48
H58A	937.8	-3394.76	2132.97	59
H58B	1131.32	-2461.52	3245.78	59
H58C	2461.22	-3217.51	3041.41	59
H45	7459.71	-1214.67	735.57	39
H15	13174.38	5677.82	7380.98	53
H6	5986.35	10076.28	8941.52	45
H3	6191.95	12864.31	7136.98	52
H5	4006.64	11204.92	8739.01	52
H16	12947.99	7633.63	8348.36	50
H57A	1956.98	4629.47	-815.64	65
H57B	3319.75	5512.21	151.42	65
H57C	1621.13	5832.33	-78.08	65
H35	4974.48	1330.43	4878.04	52
H28A	5852.07	6435.02	2432.14	74
H28B	7136.89	7673.74	2964.63	74

H28C	5375.03	7715.5	2447.73	74
H34	7180.63	441.56	5134.21	59
H29A	6957.89	4475.3	9787.62	67
H29B	7495.8	5841.15	10573.7	67
H29C	8716.29	4951.48	10496.81	67
H36A	9927.85	303.22	4387.14	72
H36B	10209.07	828.08	5595.4	72
H36C	11030.64	1610.15	5033.52	72
H7A	3796.43	13625.84	8251.26	82
H7B	2563.84	12356.8	7755.29	82
H7C	3347.32	12926.71	7049.06	82

---

**Table 1.** Crystal data and structure refinement for **126**.

Identification code	P047
Empirical formula	C <sub>24</sub> H <sub>21</sub> NO <sub>4</sub> S
Formula weight	419.48
Temperature/K	123.01(10)
Crystal system	orthorhombic
Space group	P2 <sub>1</sub> 2 <sub>1</sub> 2 <sub>1</sub>
a/Å	8.61361(8)
b/Å	12.18576(11)
c/Å	19.50535(15)
α/°	90
β/°	90
γ/°	90
Volume/Å <sup>3</sup>	2047.35(3)
Z	4
ρ <sub>calc</sub> /mm <sup>3</sup>	1.361
m/mm <sup>-1</sup>	1.667
F(000)	880.0
Crystal size/mm <sup>3</sup>	0.362 × 0.267 × 0.215
Radiation	CuKα (λ = 1.54184)
2θ range for data collection	8.556 to 147.946°
Index ranges	-10 ≤ h ≤ 9, -14 ≤ k ≤ 12, -24 ≤ l ≤ 21
Reflections collected	12042

Independent reflections	4071 [ $R_{\text{int}} = 0.0238$ , $R_{\text{sigma}} = 0.0206$ ]
Data/restraints/parameters	4071/0/273
Goodness-of-fit on $F^2$	1.048
Final R indexes [ $I \geq 2\sigma(I)$ ]	$R_1 = 0.0260$ , $wR_2 = 0.0677$
Final R indexes [all data]	$R_1 = 0.0263$ , $wR_2 = 0.0678$
Largest diff. peak/hole / $e \text{ \AA}^{-3}$	0.13/-0.33
Flack parameter	-0.012(6)

**Table 2.** Fractional Atomic Coordinates ( $\times 10^4$ ) and Equivalent Isotropic Displacement Parameters ( $\text{\AA}^2 \times 10^3$ ) for **126**.  $U_{\text{eq}}$  is defined as 1/3 of the trace of the orthogonalized  $U_{\text{ij}}$  tensor.

Atom	<i>x</i>	<i>y</i>	<i>z</i>	$U(\text{eq})$
S001	4935.0(5)	5917.7(3)	2835.4(2)	21.17(11)
O1	3717.5(16)	5891.1(12)	2335.1(6)	28.0(3)
O4	-636.3(15)	3427.3(11)	3836.1(6)	24.5(3)
O2	5419.9(17)	6935.1(10)	3131.1(7)	29.3(3)
O3	977.1(18)	2702.7(13)	3056.0(8)	37.3(4)
N1	4293.2(18)	5152.7(13)	3471.7(7)	21.9(3)
C5	6582(2)	5257.3(14)	2494.4(8)	20.4(3)
C4	6388(2)	4346.6(14)	2071.2(9)	22.5(3)
C13	1553(2)	4826.8(14)	4387.9(9)	20.6(3)
C14	1208(2)	5912.3(16)	4234.9(9)	26.0(4)
C8	5160(2)	4921.6(15)	4079.4(8)	22.7(4)
C9	4708(2)	3903.3(15)	4339.6(9)	24.8(4)
C3	7682(2)	3861.2(16)	1779.4(9)	26.1(4)
C17	1127(2)	5206.1(16)	5589.4(9)	26.3(4)
C10	3537(2)	3398.7(15)	3886.9(9)	24.7(4)
C6	8045(2)	5661.2(16)	2639.2(9)	26.6(4)
C18	1511(2)	4481.7(15)	5070.5(9)	23.6(4)
C12	1969(2)	4023.1(15)	3838.9(9)	22.2(3)
C15	834(3)	6642.2(16)	4757.4(10)	31.0(4)
C11	3282(2)	4225.6(15)	3329.9(9)	22.9(4)
C2	9169(2)	4272.9(16)	1901.0(9)	26.7(4)
C7	9331(2)	5166.5(17)	2340.1(10)	29.7(4)
C20	5347(2)	3523.2(17)	4950.1(10)	30.8(4)
C23	6268(2)	5563.6(17)	4400.7(9)	27.4(4)
C19	739(2)	3322.3(15)	3529.4(9)	24.3(4)

C24	-1841(2)	2719.4(18)	3560.2(10)	30.0(4)
C16	793(2)	6290.8(16)	5435.8(10)	29.2(4)
C21	6456(3)	4155(2)	5277.2(10)	36.5(5)
C22	6919(2)	5152(2)	5004.1(10)	34.1(5)
C1	10561(3)	3781(2)	1551.0(11)	37.4(5)

**Table 3.** Anisotropic Displacement Parameters ( $\text{\AA}^2 \times 10^3$ ) for **126**. The Anisotropic displacement factor exponent takes the form:  $-2\pi^2[h^2a^*^2U_{11}+2hka^*b^*U_{12}+\dots]$ .

Atom	$U_{11}$	$U_{22}$	$U_{33}$	$U_{23}$	$U_{13}$	$U_{12}$
S001	26.4(2)	19.13(19)	17.97(18)	1.70(14)	0.23(15)	2.61(17)
O1	30.4(7)	32.0(7)	21.6(6)	2.6(5)	-3.3(5)	6.8(6)
O4	23.9(6)	28.6(7)	20.8(6)	-2.1(5)	2.6(5)	-1.1(5)
O2	40.5(8)	19.3(6)	28.0(6)	-1.5(5)	0.6(6)	2.0(5)
O3	36.3(8)	38.7(8)	37.1(8)	-19.0(6)	12.3(6)	-8.7(6)
N1	23.2(7)	26.4(7)	16.2(6)	0.3(6)	0.0(6)	-1.6(6)
C5	25.0(9)	20.2(8)	16.0(7)	3.2(6)	3.1(6)	-0.7(7)
C4	23.7(8)	24.8(8)	18.9(8)	0.7(6)	-1.1(6)	-2.6(7)
C13	21.1(8)	22.3(8)	18.3(7)	-2.1(6)	1.5(6)	-0.5(7)
C14	32.7(10)	25.3(9)	20.2(8)	-0.3(7)	1.6(7)	1.4(8)
C8	21.8(9)	28.0(9)	18.4(7)	-0.3(6)	1.5(7)	6.3(7)
C9	24.1(9)	27.2(9)	23.1(8)	1.4(7)	4.6(7)	8.5(7)
C3	30.1(9)	27.3(9)	20.8(8)	-3.0(7)	0.7(7)	0.6(7)
C17	26.9(9)	33.7(10)	18.4(7)	-2.5(7)	0.7(7)	-3.3(8)
C10	26.8(9)	20.7(9)	26.4(8)	-1.3(7)	5.8(7)	3.7(7)
C6	31.6(10)	25.1(9)	23.1(8)	-1.6(7)	1.9(7)	-8.1(7)
C18	23.9(9)	25.0(9)	21.7(8)	1.0(7)	1.9(7)	0.2(7)
C12	24.0(8)	22.4(8)	20.2(7)	-1.4(7)	2.9(6)	1.1(7)
C15	41.9(12)	21.5(9)	29.5(9)	-3.1(7)	3.9(8)	3.2(8)
C11	24.9(8)	24.0(9)	19.7(7)	-2.5(7)	3.0(6)	-1.0(7)
C2	27.2(9)	32.5(10)	20.5(8)	4.4(7)	3.3(7)	0.6(8)
C7	25.9(9)	34.8(10)	28.3(9)	0.6(8)	2.4(8)	-7.5(8)
C20	32.3(11)	32.9(10)	27.0(9)	8.5(8)	6.3(8)	12.2(8)
C23	26.2(9)	33.2(10)	22.9(8)	0.2(7)	-0.1(7)	0.6(8)
C19	27.7(9)	23.1(8)	22.1(8)	-1.0(7)	5.1(7)	-0.7(7)
C24	27(1)	36.1(10)	26.8(9)	-0.5(8)	-0.4(7)	-6.2(8)
C16	33.1(10)	30.3(10)	24.2(8)	-9.2(7)	5.1(8)	-2.4(8)



C21	34.0(11)	50.4(13)	25.1(9)	7.5(9)	-1.6(8)	15.3(10)
C22	28.1(10)	48.3(12)	26.0(9)	-3.2(9)	-4.8(8)	3.9(9)
C1	29.7(10)	53.3(13)	29.3(9)	-3.5(9)	5.9(8)	2.7(9)

**Table 4.** Bond Lengths for **126**.

Atom	Atom	Length/Å	Atom	Atom	Length/Å
S001	O1	1.4330(13)	C8	C23	1.384(3)
S001	O2	1.4296(13)	C9	C10	1.475(3)
S001	N1	1.6478(15)	C9	C20	1.391(3)
S001	C5	1.7616(18)	C3	C2	1.396(3)
O4	C19	1.333(2)	C17	C18	1.383(3)
O4	C24	1.453(2)	C17	C16	1.385(3)
O3	C19	1.210(2)	C10	C12	1.553(2)
N1	C8	1.429(2)	C10	C11	1.498(3)
N1	C11	1.453(2)	C6	C7	1.389(3)
C5	C4	1.393(2)	C12	C11	1.525(2)
C5	C6	1.382(3)	C12	C19	1.489(3)
C4	C3	1.384(3)	C15	C16	1.391(3)
C13	C14	1.388(3)	C2	C7	1.392(3)
C13	C18	1.397(2)	C2	C1	1.504(3)
C13	C12	1.495(2)	C20	C21	1.383(3)
C14	C15	1.391(3)	C23	C22	1.397(3)
C8	C9	1.396(3)	C21	C22	1.385(3)

**Table 5.** Bond Angles for **126**.

Atom	Atom	Atom	Angle/°	Atom	Atom	Atom	Angle/°
O1	S001	N1	104.75(8)	C9	C10	C11	104.72(15)
O1	S001	C5	108.78(8)	C11	C10	C12	59.95(12)
O2	S001	O1	120.54(8)	C5	C6	C7	119.11(17)
O2	S001	N1	106.55(8)	C17	C18	C13	120.76(17)
O2	S001	C5	108.25(9)	C13	C12	C10	119.10(15)
N1	S001	C5	107.23(8)	C13	C12	C11	122.56(16)
C19	O4	C24	114.30(14)	C11	C12	C10	58.23(12)
C8	N1	S001	124.12(13)	C19	C12	C13	119.72(15)

C8	N1	C11	108.54(14)	C19	C12	C10	111.24(15)
C11	N1	S001	119.84(11)	C19	C12	C11	110.89(14)
C4	C5	S001	119.42(14)	C14	C15	C16	120.39(18)
C6	C5	S001	119.64(14)	N1	C11	C10	107.27(15)
C6	C5	C4	120.93(17)	N1	C11	C12	116.51(15)
C3	C4	C5	119.19(17)	C10	C11	C12	61.82(12)
C14	C13	C18	119.10(16)	C3	C2	C1	120.75(18)
C14	C13	C12	121.44(16)	C7	C2	C3	118.50(18)
C18	C13	C12	119.46(16)	C7	C2	C1	120.73(18)
C13	C14	C15	120.11(17)	C6	C7	C2	121.20(18)
C9	C8	N1	109.32(16)	C21	C20	C9	118.89(19)
C23	C8	N1	128.64(17)	C8	C23	C22	117.08(19)
C23	C8	C9	122.02(16)	O4	C19	C12	113.28(15)
C8	C9	C10	110.10(15)	O3	C19	O4	123.57(18)
C20	C9	C8	119.77(19)	O3	C19	C12	123.13(17)
C20	C9	C10	130.12(18)	C17	C16	C15	119.61(17)
C4	C3	C2	121.02(17)	C20	C21	C22	120.63(18)
C18	C17	C16	120.02(17)	C21	C22	C23	121.6(2)
C9	C10	C12	115.25(15)				

**Table 6.** Torsion Angles for **126**.

<b>A</b>	<b>B</b>	<b>C</b>	<b>D</b>	<b>Angle/°</b>	<b>A</b>	<b>B</b>	<b>C</b>	<b>D</b>	<b>Angle/°</b>
S001	N1	C8	C9	-151.21(13)	C8	C9	C20	C21	-1.8(3)
S001	N1	C8	C23	29.9(3)	C8	C23	C22	C21	-1.3(3)
S001	N1	C11	C10	151.79(12)	C9	C8	C23	C22	-0.3(3)
S001	N1	C11	C12	-141.63(14)	C9	C10	C12	C13	-19.4(2)
S001	C5	C4	C3	177.08(13)	C9	C10	C12	C11	92.96(17)
S001	C5	C6	C7	-176.86(14)	C9	C10	C12	C19	-164.96(15)
O1	S001	N1	C8	178.08(14)	C9	C10	C11	N1	0.38(18)
O1	S001	N1	C11	31.82(15)	C9	C10	C11	C12	-110.95(15)
O1	S001	C5	C4	-35.98(16)	C9	C20	C21	C22	0.3(3)
O1	S001	C5	C6	142.79(14)	C3	C2	C7	C6	-1.7(3)
O2	S001	N1	C8	-53.13(16)	C10	C9	C20	C21	179.23(18)
O2	S001	N1	C11	160.61(14)	C10	C12	C11	N1	-96.27(17)
O2	S001	C5	C4	-168.61(13)	C10	C12	C19	O4	139.34(15)
O2	S001	C5	C6	10.16(16)	C10	C12	C19	O3	-39.2(2)

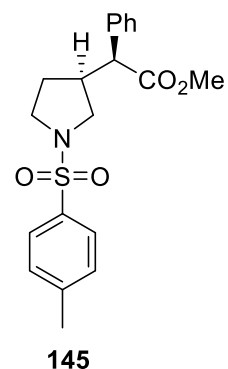
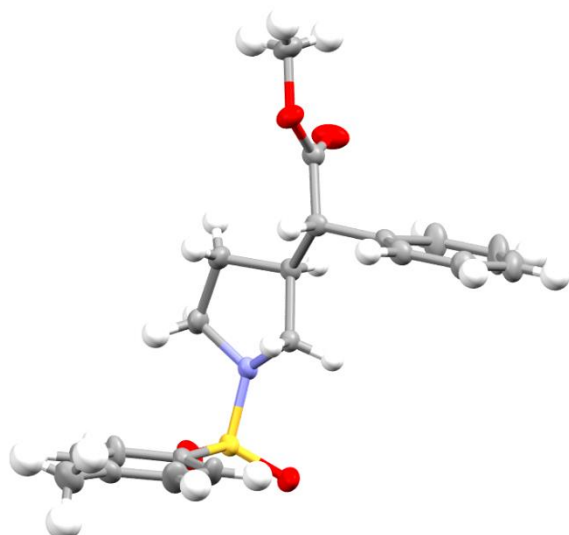
N1	S001	C5	C4	76.79(15)	C6	C5	C4	C3	-1.7(3)
N1	S001	C5	C6	-104.44(15)	C18	C13	C14	C15	0.2(3)
N1	C8	C9	C10	2.03(19)	C18	C13	C12	C10	-56.3(2)
N1	C8	C9	C20	-177.15(16)	C18	C13	C12	C11	-125.25(19)
N1	C8	C23	C22	178.46(18)	C18	C13	C12	C19	86.4(2)
C5	S001	N1	C8	62.61(16)	C18	C17	C16	C15	0.6(3)
C5	S001	N1	C11	-83.65(15)	C12	C13	C14	C15	-179.64(18)
C5	C4	C3	C2	-0.2(3)	C12	C13	C18	C17	-179.84(17)
C5	C6	C7	C2	-0.2(3)	C12	C10	C11	N1	111.33(16)
C4	C5	C6	C7	1.9(3)	C11	N1	C8	C9	-1.75(19)
C4	C3	C2	C7	1.9(3)	C11	N1	C8	C23	179.38(18)
C4	C3	C2	C1	-176.53(18)	C11	C10	C12	C13	-112.32(18)
C13	C14	C15	C16	-0.3(3)	C11	C10	C12	C19	102.08(16)
C13	C12	C11	N1	10.2(2)	C11	C12	C19	O4	-157.81(15)
C13	C12	C11	C10	106.46(19)	C11	C12	C19	O3	23.7(3)
C13	C12	C19	O4	-6.0(2)	C20	C9	C10	C12	114.3(2)
C13	C12	C19	O3	175.49(18)	C20	C9	C10	C11	177.60(18)
C14	C13	C18	C17	0.3(3)	C20	C21	C22	C23	1.3(3)
C14	C13	C12	C10	123.57(19)	C23	C8	C9	C10	-179.01(16)
C14	C13	C12	C11	54.6(3)	C23	C8	C9	C20	1.8(3)
C14	C13	C12	C19	-93.8(2)	C19	C12	C11	N1	161.04(15)
C14	C15	C16	C17	-0.1(3)	C19	C12	C11	C10	-102.70(16)
C8	N1	C11	C10	0.80(19)	C24	O4	C19	O3	0.8(3)
C8	N1	C11	C12	67.38(19)	C24	O4	C19	C12	-177.71(15)
C8	C9	C10	C12	-64.82(19)	C16	C17	C18	C13	-0.7(3)
C8	C9	C10	C11	-1.47(19)	C1	C2	C7	C6	176.75(19)

**Table 7.** Hydrogen Atom Coordinates ( $\text{\AA}\times 10^4$ ) and Isotropic Displacement Parameters ( $\text{\AA}^2\times 10^3$ ) for **126**.

Atom	x	y	z	U(eq)
H4	5402	4068	1986	27
H14	1228	6152	3782	31
H3	7559	3251	1498	31
H17	1092	4965	6042	32
H10	3589	2615	3778	30
H6	8167	6256	2933	32

H18	1745	3756	5177	28
H15	609	7370	4653	37
H11	3165	3972	2856	27
H7	10317	5437	2435	36
H20	5034	2855	5135	37
H23	6565	6240	4223	33
H24A	-1990	2881	3083	45
H24B	-2793	2844	3804	45
H24C	-1536	1966	3611	45
H16	544	6781	5784	35
H21	6896	3908	5685	44
H22	7682	5556	5228	41
H1A	10521	2996	1589	56
H1B	11491	4047	1765	56
H1C	10560	3987	1076	56

---




---

**Table 1.** Crystal data and structure refinement for **145**.
 

---

Identification code	P056
Empirical formula	C <sub>20</sub> H <sub>23</sub> NO <sub>4</sub> S
Formula weight	373.45
Temperature/K	123.00(10)
Crystal system	triclinic
Space group	P1
a/Å	5.7954(2)
b/Å	8.1636(4)
c/Å	10.5823(3)
α/°	78.116(4)
β/°	87.172(3)
γ/°	74.207(4)
Volume/Å <sup>3</sup>	471.42(4)
Z	1
ρ <sub>calc</sub> /mg/mm <sup>3</sup>	1.315
m/mm <sup>-1</sup>	1.733
F(000)	198.0
Crystal size/mm <sup>3</sup>	0.611 × 0.159 × 0.085
Radiation	CuKα (λ = 1.54184)
2θ range for data collection	8.538 to 153.528°
Index ranges	-7 ≤ h ≤ 7, -10 ≤ k ≤ 10, -13 ≤ l ≤ 13
Reflections collected	12493
Independent reflections	3552 [R <sub>int</sub> = 0.0297, R <sub>sigma</sub> = 0.0241]
Data/restraints/parameters	3552/3/237

Goodness-of-fit on $F^2$	1.127
Final R indexes [ $I \geq 2\sigma(I)$ ]	$R_1 = 0.0526$ , $wR_2 = 0.1464$
Final R indexes [all data]	$R_1 = 0.0530$ , $wR_2 = 0.1485$
Largest diff. peak/hole / $e \text{ \AA}^{-3}$	0.25/-0.48
Flack parameter	0.02(2)

**Table 2.** Fractional Atomic Coordinates ( $\times 10^4$ ) and Equivalent Isotropic Displacement Parameters ( $\text{\AA}^2 \times 10^3$ ) for **145**.  $U_{\text{eq}}$  is defined as 1/3 of the trace of the orthogonalized  $U_{\text{ij}}$  tensor.

Atom	$x$	$y$	$z$	$U(\text{eq})$
S1	1890.3(9)	3042.2(8)	6268.6(6)	24.5(3)
O4	8893(5)	9014(4)	3573(3)	28.3(6)
O1	1815(6)	2040(4)	5315(3)	34.8(7)
O2	-218(5)	3644(5)	6997(3)	34.2(7)
O3	5171(5)	9863(4)	2744(3)	38.8(8)
N1	2612(5)	4782(4)	5516(3)	20.8(6)
C12	7005(6)	6801(5)	3586(3)	21.3(7)
C19	6847(6)	8743(5)	3250(3)	23.5(7)
C8	4688(6)	4642(5)	4648(3)	20.2(6)
C4	4219(7)	2145(6)	8594(3)	28.9(8)
C16	8574(8)	4746(7)	101(4)	35.0(9)
C14	9688(7)	4877(5)	2231(4)	26.3(8)
C5	4242(7)	1843(5)	7350(3)	25.4(8)
C2	8128(8)	102(5)	9013(4)	28.9(8)
C6	6204(9)	677(6)	6924(4)	34.5(9)
C9	4676(6)	6551(5)	4233(3)	19.9(7)
C15	10215(8)	4214(6)	1111(4)	33.3(9)
C13	7523(6)	6079(5)	2356(3)	22.2(7)
C20	9031(8)	10806(6)	3241(4)	33.3(9)
C11	2393(8)	6220(5)	6205(4)	28.8(8)
C3	6148(8)	1272(6)	9419(4)	31.8(9)
C10	4170(7)	7189(5)	5514(4)	26.0(8)
C7	8121(9)	-170(6)	7758(4)	37.7(10)
C18	5889(7)	6605(7)	1336(4)	36(1)
C1	10225(9)	-808(7)	9898(5)	40.2(10)
C17	6408(8)	5941(8)	224(4)	41.6(11)

**Table 3.** Anisotropic Displacement Parameters ( $\text{\AA}^2 \times 10^3$ ) for **145**. The Anisotropic displacement factor exponent takes the form:  $-2\pi^2[h^2a^*U_{11}+2hka^*b^*U_{12}+\dots]$ .

Atom	U <sub>11</sub>	U <sub>22</sub>	U <sub>33</sub>	U <sub>23</sub>	U <sub>13</sub>	U <sub>12</sub>
S1	26.7(4)	31.0(5)	18.3(4)	-2.3(3)	-2.9(3)	-13.1(4)
O4	25.4(13)	23.0(14)	36.9(14)	-6.8(11)	-8.5(11)	-5.2(11)
O1	49.4(18)	38.4(17)	23.9(13)	-5.2(11)	-8.1(12)	-23.0(15)
O2	22.3(13)	50.5(19)	27.4(13)	-0.9(12)	1.1(11)	-11.2(13)
O3	24.0(14)	26.4(15)	59(2)	6.4(13)	-9.7(13)	-3.7(12)
N1	20.8(14)	21.5(15)	18.4(12)	-4.1(11)	1.4(10)	-3.3(12)
C12	15.8(14)	20.4(17)	24.6(17)	-2.5(13)	-3.1(12)	-0.7(13)
C19	22.3(17)	23.8(18)	23.1(15)	-3.3(13)	-0.9(13)	-4.9(14)
C8	17.9(15)	22.0(16)	20.3(15)	-5.6(12)	0.7(12)	-3.7(13)
C4	22.3(17)	40(2)	18.0(16)	-4.5(15)	-3.0(13)	1.2(16)
C16	33(2)	47(3)	26.7(18)	-13.6(17)	4.6(16)	-10.0(19)
C14	21.5(17)	28.3(19)	26.0(17)	-1.9(14)	-1.9(13)	-3.5(15)
C5	33(2)	27.7(19)	19.2(16)	-4.3(13)	1.5(13)	-15.0(17)
C2	31(2)	22.1(19)	28.1(19)	2.5(14)	-2.8(15)	-3.8(16)
C6	53(3)	24(2)	24.3(18)	-10.0(15)	-1.4(17)	-3.8(19)
C9	15.7(15)	20.3(17)	20.5(15)	-2.1(12)	-2.6(12)	-0.5(13)
C15	28.7(19)	34(2)	34(2)	-9.2(17)	4.0(16)	-1.6(17)
C13	21.1(16)	23.6(17)	21.1(16)	-1.5(13)	-0.3(12)	-6.9(14)
C20	36(2)	24(2)	42(2)	-8.8(16)	-5.8(17)	-9.0(17)
C11	34(2)	29(2)	24.7(17)	-11.7(15)	5.9(15)	-7.4(16)
C3	34(2)	40(2)	18.3(16)	-4.8(15)	-1.9(15)	-4.9(18)
C10	30.1(19)	23.3(19)	26.3(17)	-9.9(14)	2.0(14)	-6.5(16)
C7	44(3)	24(2)	35(2)	-7.4(16)	-3.0(18)	9.0(18)
C18	19.0(18)	54(3)	28.8(19)	-11.6(19)	-4.3(15)	3.1(18)
C1	37(2)	39(2)	36(2)	3.2(18)	-6.9(18)	-0.6(19)
C17	27(2)	69(3)	27(2)	-17(2)	-7.4(16)	-2(2)

**Table 4.** Bond Lengths for **145**.

Atom	Atom	Length/ $\text{\AA}$	Atom	Atom	Length/ $\text{\AA}$
S1	O1	1.433(3)	C4	C3	1.388(5)
S1	O2	1.437(3)	C16	C15	1.386(6)

S1	N1	1.628(3)	C16	C17	1.384(7)
S1	C5	1.758(4)	C14	C15	1.389(6)
O4	C19	1.336(4)	C14	C13	1.386(6)
O4	C20	1.456(5)	C5	C6	1.393(6)
O3	C19	1.197(5)	C2	C3	1.392(6)
N1	C8	1.471(4)	C2	C7	1.391(6)
N1	C11	1.479(5)	C2	C1	1.497(6)
C12	C19	1.530(5)	C6	C7	1.386(6)
C12	C9	1.527(5)	C9	C10	1.537(5)
C12	C13	1.521(5)	C13	C18	1.391(5)
C8	C9	1.528(5)	C11	C10	1.533(5)
C4	C5	1.388(5)	C18	C17	1.381(6)

**Table 5.** Bond Angles for **145**.

Atom	Atom	Atom	Angle/°	Atom	Atom	Atom	Angle/°
O1	S1	O2	120.12(19)	C4	C5	S1	120.1(3)
O1	S1	N1	106.63(16)	C4	C5	C6	120.2(4)
O1	S1	C5	107.64(19)	C6	C5	S1	119.6(3)
O2	S1	N1	105.74(18)	C3	C2	C1	120.7(4)
O2	S1	C5	108.78(17)	C7	C2	C3	118.2(4)
N1	S1	C5	107.29(16)	C7	C2	C1	121.1(4)
C19	O4	C20	115.7(3)	C7	C6	C5	119.1(4)
C8	N1	S1	120.3(2)	C12	C9	C8	113.1(3)
C8	N1	C11	110.4(3)	C12	C9	C10	114.1(3)
C11	N1	S1	118.8(2)	C8	C9	C10	101.9(3)
C9	C12	C19	109.0(3)	C16	C15	C14	120.3(4)
C13	C12	C19	108.4(3)	C14	C13	C12	119.6(3)
C13	C12	C9	113.0(3)	C14	C13	C18	118.6(4)
O4	C19	C12	110.0(3)	C18	C13	C12	121.8(3)
O3	C19	O4	124.4(4)	N1	C11	C10	104.0(3)
O3	C19	C12	125.6(3)	C4	C3	C2	120.9(4)
N1	C8	C9	100.7(3)	C11	C10	C9	104.2(3)
C5	C4	C3	119.9(4)	C6	C7	C2	121.7(4)
C17	C16	C15	119.1(4)	C17	C18	C13	120.7(4)
C13	C14	C15	120.7(3)	C18	C17	C16	120.5(4)



**Table 6.** Torsion Angles for **145**.

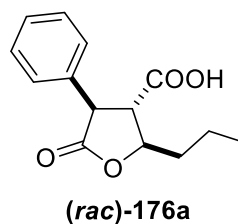
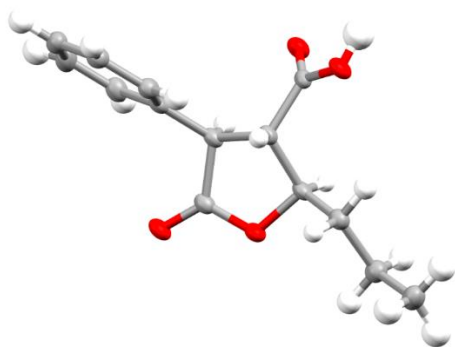
<b>A</b>	<b>B</b>	<b>C</b>	<b>D</b>	<b>Angle/°</b>	<b>A</b>	<b>B</b>	<b>C</b>	<b>D</b>	<b>Angle/°</b>
S1	N1	C8	C9	-178.1(2)	C5	S1	N1	C11	-76.1(3)
S1	N1	C11	C10	155.6(3)	C5	C4	C3	C2	0.6(6)
S1	C5	C6	C7	175.5(3)	C5	C6	C7	C2	0.6(7)
O1	S1	N1	C8	-49.8(3)	C9	C12	C19	O4	135.7(3)
O1	S1	N1	C11	168.8(3)	C9	C12	C19	O3	-46.0(5)
O1	S1	C5	C4	-156.4(3)	C9	C12	C13	C14	-124.7(3)
O1	S1	C5	C6	28.0(4)	C9	C12	C13	C18	56.0(5)
O2	S1	N1	C8	-178.7(2)	C15	C16	C17	C18	0.4(8)
O2	S1	N1	C11	39.9(3)	C15	C14	C13	C12	-179.2(4)
O2	S1	C5	C4	-24.8(4)	C15	C14	C13	C18	0.0(6)
O2	S1	C5	C6	159.6(3)	C13	C12	C19	O4	-100.9(3)
N1	S1	C5	C4	89.1(3)	C13	C12	C19	O3	77.4(5)
N1	S1	C5	C6	-86.4(3)	C13	C12	C9	C8	61.3(4)
N1	C8	C9	C12	165.5(3)	C13	C12	C9	C10	177.2(3)
N1	C8	C9	C10	42.5(3)	C13	C14	C15	C16	-0.1(6)
N1	C11	C10	C9	16.9(4)	C13	C18	C17	C16	-0.4(8)
C12	C9	C10	C11	-159.3(3)	C20	O4	C19	O3	-1.5(6)
C12	C13	C18	C17	179.5(4)	C20	O4	C19	C12	176.9(3)
C19	C12	C9	C8	-178.1(3)	C11	N1	C8	C9	-33.8(3)
C19	C12	C9	C10	-62.2(4)	C3	C4	C5	S1	-176.1(3)
C19	C12	C13	C14	114.3(4)	C3	C4	C5	C6	-0.5(6)
C19	C12	C13	C18	-65.0(4)	C3	C2	C7	C6	-0.5(7)
C8	N1	C11	C10	10.7(4)	C7	C2	C3	C4	-0.1(7)
C8	C9	C10	C11	-37.1(4)	C1	C2	C3	C4	178.8(4)
C4	C5	C6	C7	-0.1(6)	C1	C2	C7	C6	-179.3(4)
C14	C13	C18	C17	0.2(7)	C17	C16	C15	C14	-0.1(7)
C5	S1	N1	C8	65.3(3)					

**Table 7.** Hydrogen Atom Coordinates ( $\text{\AA} \times 10^4$ ) and Isotropic Displacement Parameters ( $\text{\AA}^2 \times 10^3$ ) for **145**.

<b>Atom</b>	<b>x</b>	<b>y</b>	<b>z</b>	<b>U(eq)</b>
-------------	----------	----------	----------	--------------

H12	8336	6217	4195	26
H8A	4462	4151	3918	24
H8B	6159	3951	5100	24
H4	2913	2930	8875	35
H16	8924	4305	-650	42
H14	10800	4511	2904	32
H6	6227	469	6091	41
H9	3332	7156	3635	24
H15	11675	3410	1039	40
H20A	8398	11321	2386	50
H20B	10673	10831	3272	50
H20C	8111	11449	3846	50
H11A	2818	5777	7110	35
H11B	773	6975	6139	35
H3	6117	1472	10255	38
H10A	5630	6902	6018	31
H10B	3470	8436	5360	31
H7	9439	-941	7472	45
H18	4431	7414	1403	43
H1A	10172	-205	10592	60
H1B	11686	-826	9426	60
H1C	10161	-1979	10243	60
H17	5292	6301	-447	50

---


**Table 1.** Crystal data and structure refinement for *(rac)*-176a.

Identification code	P165
Empirical formula	C <sub>14</sub> H <sub>16</sub> O <sub>4</sub>
Formula weight	248.27
Temperature/K	123.00(10)
Crystal system	monoclinic
Space group	P2 <sub>1</sub> /c
a/Å	8.22602(16)
b/Å	15.4712(3)
c/Å	10.0483(2)
α/°	90
β/°	103.364(2)
γ/°	90
Volume/Å <sup>3</sup>	1244.17(4)
Z	4
ρ <sub>calc</sub> /mg/mm <sup>3</sup>	1.325
m/mm <sup>-1</sup>	0.799
F(000)	528.0
Crystal size/mm <sup>3</sup>	0.141 × 0.094 × 0.059
Radiation	CuKα (λ = 1.54184)
2θ range for data collection	10.704 to 146.872°
Index ranges	-10 ≤ h ≤ 10, -18 ≤ k ≤ 18, -12 ≤ l ≤ 12
Reflections collected	15266
Independent reflections	2480 [R <sub>int</sub> = 0.0269, R <sub>sigma</sub> = 0.0157]
Data/restraints/parameters	2480/0/228
Goodness-of-fit on F <sup>2</sup>	1.040
Final R indexes [I >= 2σ (I)]	R <sub>1</sub> = 0.0305, wR <sub>2</sub> = 0.0753

Final R indexes [all data]  $R_1 = 0.0350$ ,  $wR_2 = 0.0787$   
 Largest diff. peak/hole /  $e \text{ \AA}^{-3}$  0.24/-0.16

**Table 2.** Fractional Atomic Coordinates ( $\times 10^4$ ) and Equivalent Isotropic Displacement Parameters ( $\text{\AA}^2 \times 10^3$ ) for (*rac*)-**176a**.  $U_{eq}$  is defined as 1/3 of the trace of the orthogonalized  $U_{ij}$  tensor.

Atom	x	y	z	U(eq)
O1	9085.8(9)	5013.7(5)	3192.9(8)	25.2(2)
O3	5195.2(10)	5984.4(6)	5015.0(8)	27.0(2)
O2	11040.9(9)	6009.7(6)	3920.8(9)	28.1(2)
O4	3727.4(10)	5727.1(6)	2881.5(9)	27.1(2)
C7	8329.4(13)	7232.9(7)	4127.9(11)	21.5(2)
C14	5133.2(13)	5861.1(7)	3821.5(12)	20.6(2)
C8	7495.5(14)	7736.4(8)	3033.1(12)	24.0(2)
C6	8178.2(13)	6259.7(7)	4140.8(11)	21.4(2)
C4	7269.0(13)	4903.6(7)	3070.1(12)	22.5(2)
C13	9601.4(13)	5777.1(7)	3749.5(11)	22.5(2)
C3	6527.1(14)	4462.6(8)	1728.7(12)	24.8(2)
C12	9344.6(15)	7642.3(8)	5254.0(12)	27.9(3)
C5	6656.8(13)	5834.3(7)	3215.3(11)	20.8(2)
C10	8669.0(16)	9030.7(8)	4198.1(13)	29.5(3)
C9	7668.9(15)	8630.4(8)	3070.6(12)	27.0(3)
C11	9512.8(16)	8534.0(9)	5288.0(13)	32.5(3)
C2	7060.4(16)	3520.9(8)	1670.6(13)	28.8(3)
C1	6247.9(19)	3099.0(9)	310.6(14)	34.8(3)

**Table 3.** Anisotropic Displacement Parameters ( $\text{\AA}^2 \times 10^3$ ) for (*rac*)-**176a**. The Anisotropic displacement factor exponent takes the form:  $-2\pi^2[h^2a^{*2}U_{11}+2hka^*b^*U_{12}+\dots]$ .

Atom	U <sub>11</sub>	U <sub>22</sub>	U <sub>33</sub>	U <sub>23</sub>	U <sub>13</sub>	U <sub>12</sub>
O1	15.4(4)	28.0(4)	32.3(4)	0.1(3)	5.6(3)	2.4(3)
O3	19.4(4)	35.4(5)	26.5(4)	-0.4(3)	6.2(3)	-1.1(3)
O2	13.8(4)	37.5(5)	32.3(5)	0.7(4)	4.2(3)	0.4(3)
O4	13.3(4)	39.0(5)	28.2(4)	-0.9(3)	3.1(3)	-0.5(3)
C7	14.3(5)	27.1(6)	24.2(5)	0.1(4)	6.4(4)	0.4(4)

C14	15.3(5)	17.9(5)	27.8(6)	2.6(4)	3.2(4)	0.8(4)
C8	19.0(5)	27.4(6)	23.8(6)	-1.6(4)	1.4(4)	0.7(4)
C6	14.1(5)	27.1(6)	22.5(5)	2.9(4)	3.3(4)	0.8(4)
C4	14.1(5)	26.1(6)	27.5(6)	3.7(4)	5.3(4)	2.0(4)
C13	16.4(5)	27.7(6)	22.7(5)	5.0(4)	2.8(4)	2.4(4)
C3	20.3(5)	26.9(6)	26.7(6)	1.7(5)	4.5(4)	0.8(4)
C12	23.3(6)	34.9(7)	23.5(6)	2.8(5)	1.5(5)	-2.1(5)
C5	14.9(5)	23.9(5)	22.8(5)	2.1(4)	2.8(4)	0.4(4)
C10	29.8(6)	26.4(6)	33.5(6)	-3.4(5)	10.0(5)	-2.7(5)
C9	24.6(6)	28.4(6)	27.9(6)	1.9(5)	5.6(5)	2.2(5)
C11	31.0(6)	35.9(7)	29.0(6)	-5.7(5)	3.8(5)	-8.2(5)
C2	30.0(6)	25.9(6)	30.8(6)	0.9(5)	7.4(5)	0.7(5)
C1	38.8(7)	30.7(7)	35.9(7)	-5.0(5)	10.9(6)	-3.9(5)

**Table 4.** Bond Lengths for (*rac*)-**176a**.

Atom	Atom	Length/Å	Atom	Atom	Length/Å
O1	C4	1.4808(13)	C6	C13	1.5151(15)
O1	C13	1.3334(14)	C6	C5	1.5252(15)
O3	C14	1.2038(14)	C4	C3	1.5082(16)
O2	C13	1.2113(14)	C4	C5	1.5433(15)
O4	C14	1.3295(14)	C3	C2	1.5266(17)
C7	C8	1.3923(16)	C12	C11	1.3861(18)
C7	C6	1.5111(16)	C10	C9	1.3831(18)
C7	C12	1.3936(16)	C10	C11	1.3858(19)
C14	C5	1.5154(15)	C2	C1	1.5225(18)
C8	C9	1.3902(17)			

**Table 5.** Bond Angles for (*rac*)-**176a**.

Atom	Atom	Atom	Angle/°	Atom	Atom	Atom	Angle/°
C13	O1	C4	110.73(8)	C3	C4	C5	115.66(9)
C8	C7	C6	122.53(10)	O1	C13	C6	110.82(9)
C8	C7	C12	118.72(11)	O2	C13	O1	121.91(10)

C12	C7	C6	118.75(10)	O2	C13	C6	127.26(11)
O3	C14	O4	124.20(10)	C4	C3	C2	113.92(10)
O3	C14	C5	123.80(10)	C11	C12	C7	120.67(11)
O4	C14	C5	112.00(10)	C14	C5	C6	112.42(9)
C9	C8	C7	120.43(11)	C14	C5	C4	112.44(9)
C7	C6	C13	114.76(9)	C6	C5	C4	102.74(8)
C7	C6	C5	118.83(9)	C9	C10	C11	119.57(12)
C13	C6	C5	101.74(9)	C10	C9	C8	120.37(11)
O1	C4	C3	108.58(9)	C10	C11	C12	120.23(12)
O1	C4	C5	103.29(8)	C1	C2	C3	111.90(11)

**Table 6.** Torsion Angles for (*rac*)-**176a**.

A	B	C	D	Angle/°	A	B	C	D	Angle/°
O1	C4	C3	C2	69.06(12)	C4	O1	C13	O2	-178.52(10)
O1	C4	C5	C14	-151.19(9)	C4	O1	C13	C6	2.98(12)
O1	C4	C5	C6	-30.10(10)	C4	C3	C2	C1	178.67(10)
O3	C14	C5	C6	-18.63(15)	C13	O1	C4	C3	140.76(9)
O3	C14	C5	C4	96.74(13)	C13	O1	C4	C5	17.47(11)
O4	C14	C5	C6	161.75(9)	C13	C6	C5	C14	152.21(9)
O4	C14	C5	C4	-82.88(11)	C13	C6	C5	C4	31.10(10)
C7	C8	C9	C10	-0.17(18)	C3	C4	C5	C14	90.34(12)
C7	C6	C13	O1	-151.93(9)	C3	C4	C5	C6	-148.57(9)
C7	C6	C13	O2	29.67(16)	C12	C7	C8	C9	-0.35(16)
C7	C6	C5	C14	-80.73(12)	C12	C7	C6	C13	-81.28(13)
C7	C6	C5	C4	158.16(9)	C12	C7	C6	C5	158.08(10)
C7	C12	C11	C10	0.02(19)	C5	C6	C13	O1	-22.27(12)
C8	C7	C6	C13	98.61(12)	C5	C6	C13	O2	159.33(11)
C8	C7	C6	C5	-22.03(15)	C5	C4	C3	C2	-175.44(10)
C8	C7	C12	C11	0.42(17)	C9	C10	C11	C12	-0.54(19)
C6	C7	C8	C9	179.76(10)	C11	C10	C9	C8	0.62(19)
C6	C7	C12	C11	-179.68(11)					

**Table 7.** Hydrogen Atom Coordinates ( $\text{\AA} \times 10^4$ ) and Isotropic Displacement Parameters ( $\text{\AA}^2 \times 10^3$ ) for (*rac*)-**176a**.

<b>Atom</b>	<b><i>x</i></b>	<b><i>y</i></b>	<b><i>z</i></b>	<b>U(eq)</b>
H5	6378(16)	6092(8)	2330(14)	21(3)
H4A	7151(15)	4550(8)	3857(13)	18(3)
H3A	6831(16)	4786(9)	983(14)	22(3)
H6	8220(17)	6067(9)	5071(15)	27(3)
H3B	5302(18)	4496(9)	1609(14)	29(3)
H8	6781(18)	7481(10)	2232(15)	33(4)
H10	8773(18)	9664(11)	4209(15)	36(4)
H2A	6774(19)	3200(10)	2435(16)	35(4)
H12	9923(19)	7297(10)	6013(16)	36(4)
H2B	8300(20)	3497(10)	1836(15)	34(4)
H9	7055(18)	8969(10)	2313(16)	33(4)
H1A	5000(20)	3099(11)	167(16)	42(4)
H1B	6530(20)	3426(11)	-432(18)	46(4)
H4	2880(20)	5767(12)	3302(19)	54(5)
H11	10270(20)	8799(11)	6077(17)	45(4)
H1C	6630(20)	2496(12)	267(17)	48(5)

---





#### 4. Curriculum vitae

Verena Lehner

##### *Personal data*

---

Date and place of birth:	22.03.1989 in Viechtach
Marital status	unmarried
Nationality	German
Email	verena.lehner.1@web.de

##### *Education*

---

11/2013 – 09/2017	<b>PhD Thesis</b> at the University of Regensburg under supervision of Prof. Dr. Oliver Reiser <i>“Rh(II)-catalyzed Cyclopropanation of Aromatic Heterocycles and its Application to the Total Synthesis of Natural Product Derivatives”</i>
01/2014 – 04/2014	<b>Research stay</b> with Prof. Dr. Huw M. L Davies (Emory University, Atlanta, USA)
09/2013	<b>Graduation:</b> Master of Science in Chemistry
01/2013 – 09/2013	<b>Master Thesis</b> at the University of Regensburg under supervision of Prof. Dr. Oliver Reiser <i>“A new strategy for the synthesis of 3,4,5-trisubstituted <math>\gamma</math>-Butyrolactones”</i>
10/2011-12/2012	<b>Advanced studies</b> in Organic Chemistry, University of Regensburg
09/2011	<b>Graduation:</b> Bachelor of Science in Chemistry
10/2008 – 09/2011	Studies in Chemistry, University of Regensburg
03/2011 – 06/2011	Bachelor Thesis at the University of Regensburg under supervision of Prof. Dr. Oliver Reiser <i>“Studien zu einer neuen Totalsynthese von Xanthatin”</i>
09/1999 – 06/2008	Abitur (A-levels), Dominicus-von-Linprun Gymnasium, Viechtach, <i>High school Certificate equivalent</i>

***Professional References***

---

Prof. Dr. Oliver Reiser  
Institut für Organische Chemie  
Universität Regensburg, Universitätsstr. 31  
93053 Regensburg, Germany  
oliver.reiser@ur.de

Prof. Dr. Huw M. L. Davies  
Department of Chemistry  
Emory University, 1515 Dickey Drive  
Atlanta, Georgia 30322, United States  
hmdavie@emory.edu

***List of publications***

---

- 1) Lehner, V.; Davies, H. M. L.; Reiser, O. *Rh(II)-Catalyzed Cyclopropanation of Furans and Its Application to the Total Synthesis of Natural Product Derivatives*. *Org. Lett.* **2017** (accepted)
- 2) Lehner, V.; Fu, J.; Davies, H. M. L.; Reiser, O. *Rh(II)-Catalyzed Monocyclopropanation of Pyrroles and its Application to the Synthesis of a Homo- $\beta$ -proline Analog*. Manuscript in preparation.

***Conferences***

---

- 1) GDCh-Wissenschaftsforum Chemie, Dresden, Germany, **2015**  
*A new strategy for the synthesis of 3,4,5-trisubstituted  $\gamma$ -butyrolactones*  
Lehner, V.; Reiser, O.
- 2) 6<sup>th</sup> EUCHEMS Chemistry Congress, Sevilla, Spain, **2016**  
*Studies towards the synthesis of homo- $\beta$ -proline derivatives*  
Lehner, V.; Pils, L. K. A.; Davies, H. M. L.; Reiser, O.

## G. Acknowledgments – Danksagung

Bedanken möchte ich mich zunächst sehr herzlich bei meinem Doktorvater Prof. Dr. Oliver Reiser für die freundliche Aufnahme in seinen Arbeitskreis, die Überlassung des interessanten und abwechslungsreichen Themas, die Unterstützung und hilfreichen Diskussionen während der gesamten Arbeit sowie die Ermöglichung meines Auslandsaufenthaltes.

Bei Prof. Dr. Huw Davies sowie allen Mitarbeitern möchte ich mich für die herzliche Aufnahme, die zahlreichen Diskussionen zum Thema Cyclopropanierung und die Unterstützung mit den gemeinsamen Publikationen bedanken.

Prof. Dr. Jörg Heilmann, Prof. Dr. Antje Bäumner und ihren Mitarbeitern danke ich für die biologischen Messungen der Paraconsäure Derivate.

Für die geduldige Hilfe bei allen chemischen und technischen Problemen möchte ich mich ganz besonders bei Dr. Peter Kreitmeier bedanken. Antje Weigert möchte ich sehr herzlich für die Unterstützung in allen organisatorischen Fragen und die außeruniversitären Unternehmungen danken.

Für die synthetische Hilfestellung bedanke ich mich bei Roxane Harteis, Helena Konkell, Brigitte Eichenseer und Klaus Döring. Den Mitarbeitern der zentralen Analytik möchte ich für die zahlreichen Messungen und die Unterstützung bei der Auswertung danken.

Allen aktuellen und ehemaligen Mitarbeitern des Ak Reisers danke ich für die angenehme Arbeitsatmosphäre und die interessanten, fachlichen Diskussionen.

Bei meinen Laborkollegen Dr. Andreas Bergmann, Martin Hofmann, Matthias Gnahn und Carina Sonnleitner möchte ich für die schöne Zeit im „Power“Labor danken. Danke Andi, von dir konnte ich schon in meiner Bachelorarbeit vieles lernen (insbesondere Säulen und richtiges Putzen) und danke Martin, dass du mich stets ermutigt hast meine Probleme selbständig zu lösen (Google).

Mein ganz besonderer Dank gilt Matthias Gnahn für den grenzenlosen Enthusiasmus beim gemeinsamen Spektren auswerten, die gute Unterhaltung während den zahlreichen Säulenmarathons und die interessanten Naturstoffdiskussionen. Mit dir war es nie langweilig!

Für die moralische Unterstützung während der Schreibphase möchte ich Thomas Ertl sehr herzlich danken. Danke dafür, dass du so geduldig auf zahlreiche: ich habe mal eine Frage, geantwortet hast, mit dir hat das Schreiben Spaß gemacht.

Für das sorgfältige Korrekturlesen dieser Arbeit gebührt Matthias Gnahn, Thomas Föll, Saerom Park, Sabine Kerres, Dr. Andreas Bergmann, Benjamin Kastl und Martin Hofmann mein herzlichster Dank.

Meinen Freunden und aktuellen bzw. ehemaligen Arbeitskollegen Matze, Martin, Thomas (Ertl), Thomas (Rawner), Bergmeister, Easy, Michi, Dobi, Saerom, Corina, Christian (Faderl), Roxy, Lisa, Bedameister, Paul, Sabine (Möhle), Lu, Berni und Nanaji danke ich sehr herzlich für die tolle Zeit am Arbeitskreis und die zahlreichen Unternehmungen in und außerhalb der Universität. Besonders möchte ich hierbei Benni und Sabine danken. Danke dafür, dass ich mit

euch Burglengenfeld kennenlernen durfte (incl. Deglgrube) und dass ihr immer für die nötige Ablenkung gesorgt habt.

Meinen Bacheloranten und Forschungspraktikanten Carina Sonnleitner, Matthias Schmalzbauer, Florian Ostler, Nikolai Wurzer, Verena Streitferdt und Peter Ehrnsberger danke ich für ihre Unterstützung bei der Laborarbeit und die zahlreichen Säulen.

Meinen Freunden Maria, Raissa, Christoph und Michaela, meinen Mitbewohnern Adrian und Christian, sowie dem ganzen Apostelkellerteam (besonders Andi, Anna, Yvei, Arjeta und Caro) danke ich für die stete Aufmunterung und die tolle Zeit, die wir zusammen hatten.

Zum Schluss möchte ich mich bei meiner Familie bedanken. Danke für die Unterstützung während meines gesamtem Studiums, ohne euch wäre das alles nicht möglich gewesen.

## **H. Declaration**

Herewith I declare that this present PhD thesis is a presentation of my original work prepared single-handed. Wherever contributions from others are involved, all of them are marked clearly, with reference to the literature, license and acknowledgement of collaborative research.

Verena Lehner

Regensburg, 17.08.17